

# INNATE IMMUNE RESPONSE TO RESPIRATORY VIRUSES

**Satwik Kar**

Thesis Submitted for the Degree

Doctor of Philosophy

September 2014

**Supervisors:**

**Dr Martha Triantafilou**

**Prof. Kathy Triantafilou**



*To Martha this be given....*

## Acknowledgement

I am immensely thankful for all the support and guidance provided by Dr Martha Triantafilou and Professor Kathy Triantafilou, for their continuous selfless contributions and for making this project a success. I will always be indebted to them for sharing their valuable knowledge and providing years of excellent teaching.

I would like to thank Mr Christopher Ward for being a great colleague and an amazing friend who has always been there for me in every good and bad times.

I would also like to thank my beloved lab-mates Robin Olden, Dilan Eryilmazlar, Florentia Loizou for making my time in the laboratory fun and memorable. Many Thanks to Dr Gareth Evans for helping me with my work.

I will always be grateful for all the love and support from Ms Asya Choudry and Mrs Swati Kar.

\*\*\*

## ABSTRACT

The innate immune system has a variety of ways of recognizing infection from pathogens such as viruses and bacteria. One of its first lines of defence is to detect Pattern Associated Molecular Patterns (PAMPs) using Pattern Recognition Receptors (PRRs) such as the Toll-Like Receptors (TLRs), the RIG-Like Helicases (RLHs) and the Nod-Like Receptors (NLRs). These receptors recognize certain molecular structures from the pathogens and lead to first line of defence which includes increased cytokines and IFNs.

This study delineate the human body's innate immune responses to human respiratory viruses such as HRV (Human Rhinovirus), RSV (Respiratory Syncytial Virus) and IAV (Influenza A virus). *In Vitro* experiments carried out on various kinds of lung tissues suggest that respiratory disease pathogenesis is related to inflammatory mediators including interleukins and cytokines produced by the host's innate immune system.

Virus induced respiratory tract infection are known to trigger bronchiolitis, wheezing and acute asthma exacerbations, as a result of inflammation of lung tissues and excessive release of pro-inflammatory cytokines such as IL-1 $\beta$ . This study identifies that intracellular macromolecular complexes called inflammasomes assemble as a result of viral trigger. Inflammasomes convert the inactive forms of the pro-inflammatory cytokines to their active forms. Although the exact mechanism of activations of these complexes was unknown. This study identified that Virus encoded proteins such as the 2B protein of HRV, the SH protein from RSV and the Influenza M2 which are also termed viroporins can activate the inflammasome by causing ion imbalance (across cells membranes and organelles). Thus providing a trigger for inflammasome assemblage.

Drugs which act as ion channel blockers have been shown to block viroporin activity and hence reduce IL-1 $\beta$  production. Therefore in the future the use of ion inhibitors could be a possible therapeutic intervention in order to reduce lung inflammation and prevent associated respiratory disease such as COPD and Asthma.

# CONTENTS

<b>CHAPTER 1. INTRODUCTION</b>	<b>1</b>
1.1 Respiratory Viruses and Disease	2
1.1.1 ssRNA viruses	4
1.1.1.1 Human Rhinoviruses (HRV)	5
1.1.1.2 Influenza Virus (H3N2)	6
1.1.1.3 Respiratory Syncytial Virus (RSV)	8
1.2 Innate Immunity and Toll-like Receptors	9
1.2.1 Toll-like Receptors	10
1.2.2 Toll-like Receptor Structure	10
1.2.3 Toll-like Receptor Signalling Pathways	11
1.2.4 Virus Recognition by Toll-like Receptors	15
1.3 Innate Immunity and RIG-I-like Receptors	17
1.3.1 RIG-I, MDA5, and LGP2 Structures	17
1.3.2 CARDs and RLR Dimerisation	19
1.3.2.1 IPS1	20
1.3.3 Host Response to Viral Infection	21

1.4 NALPs in Innate Immunity	28
1.5 Inflammasomes	29
1.5.1 Structure and function	30
1.5.2 Mechanism of Activation	31
1.5.3 Types of Inflammasome	36
1.5.3.1 NLRP 1	36
1.5.3.2 NLRP 3	37
1.5.3.3 NLRC 5	38
1.5.3.4 AIM2	39
1.5.4 Virus recognition by Inflammasomes	40
1.6 Viroporins	44
1.6.1 Viroporins as Channel Proteins	45
1.6.2 Viroporin 2B	47
1.6.3 Viroporin M2	48
1.6.4 Viroporin SH	49
1.6.5 Other Viroporins	50
1.7 Aims and Hypothesis	51
<b>CHAPTER 2: MATERIALS AND METHODS</b>	<b>53</b>
2.1 Materials	53
2.1.1 Chemicals	53
2.1.2 Plasmid	53
2.1.3 List of Antibodies	55
2.1.4 RNA Interference	56
2.2 Tissue Culture	57

2.2.1 Cell Lines	57
2.2.1.1 A549 Cell Line	57
2.2.1.2 BES Cell Line	57
2.2.1.3 Human Primary Cells	58
2.2.1.4 HEK-Blue IFN- $\alpha$ / $\beta$ Cells	58
2.2.2 Thawing Cells	59
2.2.3 Propagating Cells	59
2.2.3.1 Adherent Cell Lines	60
2.2.4 Freezing Cells	60
2.3 Virus Culture	61
2.3.1 Propagating viruses	61
2.3.2 Purifying Viruses using a Sucrose Density Gradient	62
2.3.3 Isolating Single-Stranded RNA from Purified HRV	62
2.4 Immunofluorescence	63
2.4.1 Direct Immunofluorescence	63
2.4.2 Indirect Immunofluorescence	64
2.5 Flow Cytometry	65
2.5.1 Principles of Flow Cytometry	66



2.6 Determining PRR Expression Levels	67
2.7 Phospho-I $\kappa$ B, IRF3 and Caspase-1 Detection	68
2.7.1 SDS-PAGE	68
2.7.1.1 Continuous SDS-PAGE	68
2.7.1.2 Discontinuous SDS-PAGE	68
2.7.2 Western Blot	69
2.7.2.1 Probing membranes with antibodies.	70
2.7.3 Stripping and Reprobing Membranes	71
2.8 Immunoprecipitation	71
2.9 Confocal Microscopy	73

2.10 Plasmid DNA	75
2.10.1 Plasmid DNA Preparation	75
2.10.1.1 Transformation	75
2.10.1.2 DNA Isolation	75
2.10.1.3 Agarose Gel Electrophoresis	76
2.10.2 Silencing	77
2.10.2.1 Ttransfection Procedure	77
2.11 Cytometric Bead Array	79
2.12 Statistical Analysis	80
<b>CHAPTER 3: INNATE IMMUNE RESPONSE TO HUMAN RHINOVIRUS (HRV5, HRV14, HRV58)</b>	<b>81</b>
3.1 Introduction	82
3.2 Results	82
3.2.1 PRR Expression Levels	84

3.2.1.1	PRR expression of A549 cells upon HRV14 infection	84
3.2.1.2	PRR expression of A549 cells upon HRV58 infection	87
3.2.2	Signalling Detection upon Infection with HRV	89
3.2.2.1	Signalling detection in HRV5 infected cells	89
3.2.2.2	Signalling detection in HRV14 infected cells	91
3.2.2.3	Signalling detection in HRV58 infected cells	92
3.2.3	IFN- $\beta$ and IL1 $\beta$ Production of HRV infected Cells	93
3.2.4	HRV5 ssRNA stimulations	96
3.2.4.1	Isolating ssRNA	97
3.2.4.2	ssRNA stimulations and PRR expression levels	97
3.2.4.3	Cytokine secretions	101
3.2.5	RLR Dimerization	106
3.2.5.1	MDA5 and LGP2 dimerisation	107
3.2.5.2	MDA5 homotypic associations	109
3.2.5.3	RIG-I – LGP2 dimerisations	111
3.2.5.4	LGP-2 homotypic associations	112
3.2.5.5	RIG-I homotypic associations	113
3.2.5.6	RIG-I and MDA5 under reducing conditions	114
3.3	Conclusion	115
<b>CHAPTER 4:</b>	<b>Inflammasome activation in HRV infection</b>	<b>117</b>
4.1	Introduction	118
4.2	Results	119
4.2.1	HRV infection induces inflammasome activation	119
4.2.2	2B ion channel protein triggers inflammasome activation	122
4.2.3	2B protein changes the calcium homeostasis in the cell	125

4.2.4 Calcium inhibitors block rhinovirus induced inflammasome activation	126
4.2.5 2B localises with NLRC5 and NLRP3 in the golgi	130
4.3 Discussion	135
<b>CHAPTER 5: Human Respiratory Syncytial virus</b>	
5.1 Introduction	140
5.2 Results	141
5.2.1 RSV infection activates the NLRP3 inflammasome	141
5.2.1.1 RSV triggers pro-IL1beta secretion	141
5.2.1.2 TLR signalling is required for inflammasome activation	143
5.2.1.3 SH mediated mechanism of inflammasome activation	146
5.2.2 SH Interactions	152
5.3 Discussion	158
<b>CHAPTER 6: INNATE IMMUNE RESPONSE TO</b>	
6.1 Introduction	163
6.2 Results	164
6.2.1 BBB Expression Levels in IAV infection	164
6.2.2 Innate Immune responses to IAV	167

6.2.3 IFN- $\beta$ and IL1 $\beta$ Production	167
6.2.4 H3N2 activates the Inflammasome	169
6.2.4.1 NLRP3 Inflammasome activation	170
6.2.5 Effects of different Inhibitors in IAV infection	171
6.3 Discussion	173
<b>CHAPTER 7: DISCUSSION</b>	<b>179</b>
<b>REFERENCES</b>	<b>182</b>

**CHAPTER 1**  
**INTRODUCTION**

## **1.1 Respiratory Viruses and Disease**

Viral infection of the lower respiratory tract causes severe illness and disease in people from infants to the elderly. Prevention of lower respiratory tract infection (LRTI) is not yet available for most viral infections, apart from the readily available influenza vaccine. Hence understanding the basis of pathological mechanisms of such viral infections causing LRTI, is needed to develop novel and effective therapeutic approaches. In this study we attempt to gain an insight into the human body's anti-viral innate immune response. After viral recognition, airway epithelial cells and other immune cells produce a vast range of mediators that include innate interferons and proinflammatory cytokines. These play a crucial role in controlling the effects of the viral invasion and controlling inflammation and disease pathogenesis.

LRTI most commonly leads to different kinds of disease including bronchiolitis and pneumonia. Asthma exacerbations and Chronic Obstructive Pulmonary Disease (COPD) are other debilitating effects of respiratory viral infections. Respiratory viruses commonly infect the airway epithelial cells (AECs) and also resident mucosal immune cells like the macrophages and dendritic cells (DCs) (Schwarze and Mackenzie 2013). The majority of the viruses causing such maladies are ssRNA viruses; major examples are Influenza virus, Respiratory Syncytial virus (RSV), Rhinoviruses, Parainfluenza viruses and Human Metapneumovirus. During the virus's replication cycle, double stranded RNA intermediates get recognised by a plethora of Pattern Recognition Receptors (PRRs). Some of them are the Toll Like Receptors (TLRs) and the RIG-like helicases (RLRs). For instance TLR3 is endosomal and recognises viral invasion, so does RIG-I and MDA-5 which are present in the cytoplasm of the cell. All these PRRs that are upregulated in the airway epithelial cells (AECs) promote a downstream signalling cascade that activates the NF $\kappa$ B transcription complex and eventual production of

interferons. A type-I interferon called the IFN- $\beta$  is secreted in an autocrine fashion enhancing its own production. It also promotes the production of IFN- $\alpha$  and (type-III) IFN- $\lambda$  in AECs and innate immune cells (Vareille et al. 2011). The function of these interferons (IFNs) is to induce antiviral genes in AECs causing programmed cell death in infected cells. It also causes the activation of natural killer cells to combat infection. Recent studies show that the lack of IFN response in virus infected AECs in patients suffering from pre-existing lung disease (COPD and Cystic Fibrosis) results in an increased viral load. This causes an increase in proinflammatory stimuli and potential lung and airway inflammation (Contoli et al. 2006). Therapies that enhance type I/III responses will prove beneficial for patients suffering from pulmonary disease caused by viruses, such an effect is observed in *in vitro* studies using macrolide azithromycin (Gielen et al. 2010, Vareille et al. 2011).

The airway epithelium acts as a physical barrier to pathogens entering the body through air-borne routes, acting as a defensive interface between the environment and the body. Each cells are attached to each other through cell-cell junctions including tight junctions (TJs), adherens junctions (AJs) and gap junctions (Roche et al. 1993). This forms an impermeable and defensive structure to invading pathogens at the same time allowing maintenance of ionic gradients. On top of this epithelium that acts as a physical barrier, sits a layer of mucous that allows the exchange of gasses, water and soluble nutrients. This is the second layer of barrier and is not hostile or permeable to most pathogens. About 90% of inhaled pathogens and viruses are cleared by the mucociliary escalator. These pathogens and particles are trapped in the mucous in the bronchioles and transported to the trachea, and most of the time is expelled. This transportation is feasible due to the beating action of the cilia that are present on the surface of the lung epithelium (Voynow and Rubin 2009). The mucus contains antimicrobial substances such as



lysozymes and defensins. It also contains cytokines and antioxidant proteins, to name just a few of the 200 different kinds of proteins present taking part in preventing pathogen entry (Voynow and Rubin 2009).

In spite of all the defence mechanism the body provides, occasionally pathogens gain entry into bronchial and alveolar cells and establish themselves, continuing viral replication and causing an infection. In such cases the body's own immune system (the innate immunity) responds in several ways to eliminate the virus, which is the scope of this study.

### **1.1.1 ssRNA viruses**

Single stranded RNA viruses can be generally categorised under: positive stranded RNA viruses and negative stranded RNA viruses and they do not have a DNA phase. Examples of plus stranded RNA viruses are poliovirus, rhinovirus (picornaviridae), togaviruses, flaviviruses etc. Examples of negative-stranded RNA viruses include influenza virus (orthomyxoviridae), measles virus, mumps virus etc.

In order to replicate viruses have clever strategies. RNA viruses replicate via an RNA intermediate. This requires an enzyme called the RNA-dependent RNA-polymerase in order to successfully replicate their viral genome, which is the strand of RNA. Due to the absence of suitable enzymes in the eukaryotic cells, the RNA viruses code for RNA-dependent RNA polymerase. In plus stranded RNA viruses, the virion (genomic) RNA functions as an mRNA because of their similarity in structure and function. Immediately after infection of a eukaryotic cell, the mRNA is translated. However on the other hand, negative stranded RNA genome is negative sense (hence the name), which means that the RNA is complimentary to the mRNA. Before translation occurs the formation of a plus-sense mRNA is needed. Apart from needing to code RNA-dependent RNA polymerase,

these RNA viruses need to package it in the virion so that mRNAs can be made after host cell infection (Hunt, April 26, 2010 ).

### 1.1.1.1 Human Rhinoviruses (HRV)

Human Rhinoviruses (HRV) belongs to the family of viruses called Picornaviridae and the genus Enterovirus, and are the major causative agents of common cold. They also play a major role in asthmatic exacerbations, cystic fibrosis and chronic obstructive pulmonary disease (COPD) (Gern 2010). Like other Picornaviruses they also contain 60 copies each of four capsid proteins, VP1, VP2, VP3, and the small myristoylated VP4. These are arranged on an icosahedral lattice.

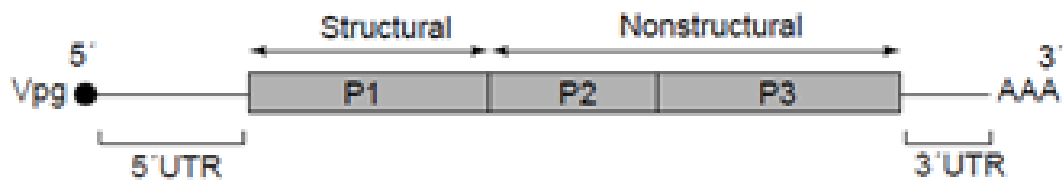


**Figure 1.1 Picornavirus Genome.** Schematic representation showing the coding regions for structural and non-structural proteins, the 5' and 3' untranslated regions (5'UTR; 3'UTR) and the genome-linked protein Vpg (Modified from (Andino et al. 1999) ).

The particle is 30nm across. The genome of the virus consists of a positive sense single stranded RNA molecule which is 7100 bases long. In its 3' end the RNA has a poly-(A) tail which is 70-150 bases long and the 5' end carries a covalently linked peptide (VPg) (Ahlquist and Kaesberg 1979, Nair and Panicali 1976). The 5' region is non-translational and is approximately 650 bases long and is involved in cap-independent translation initiation and RNA replication (Rohll et al. 1994) (Harutyunyan et al. 2013).

The life cycle of Picornaviruses share a common pathway. After entering the cell, the genomic RNA acts as an mRNA which acts as a template for the synthesis of a very large peptide molecule. This molecule is proteolytically cleaved and mature viral proteins are

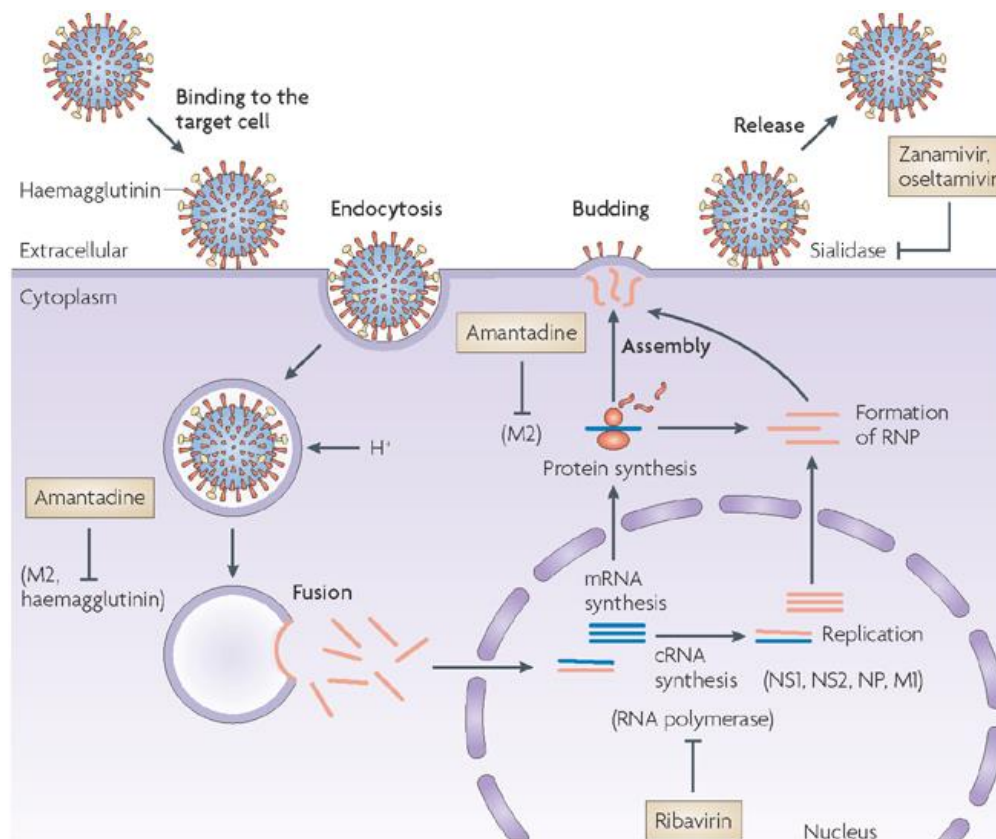
formed. The viral RNA molecule is amplified in a two-step process. Firstly a complementary negative strand of the RNA is synthesised and secondly new molecules of positive strand RNA is made using this negative template as a reference (Gamarnik et al. 2000). A RNA-dependent RNA polymerase catalyses the synthesis of both the negative and positive stranded RNA (Dasgupta et al. 1979, Flanagan and Baltimore 1977). Viral proteins are essential for RNA replication such as *cis*-acting elements (present in the viral genome), proteins (Andino et al. 1999, Barton et al. 1995, Blyn et al. 1997, Gamarnik and Andino 1996, Jackson and Kaminski 1995) from the host cell and cell membrane structures. Paul et al have discovered that a primer dependent enzyme (3D pol) directly uridylylated the viral protein Vpg, and the resultant protein acts as a primer for the initiation process (Harutyunyan et al. 2013). It is however not clear how amplification of a single RNA molecule into thousands of copies are made.

Initiation of picornavirus translation begins in a cap-independent manner and is promoted by an internal ribosome entry mechanism. A RNA segment of the 5' UTR is needed for this process. There is a vast amount of knowledge that has been gathered over the years about translation mechanism (Andino et al. 1999, Belsham and Sonenberg 1996), but the molecular details of the mechanism is still unclear.

#### **1.1.1.2 Influenza A Virus (IAV)**

Influenza A virus belongs to the Orthomyxoviridae family of viruses. It is an enveloped virus that contains a negative strand RNA genome which is segmented. The viral genome encodes for 11 different viral genes which it utilises to infect cells and create more viral progeny and eventually subvert the host cell machinery. Influenza virus come in a number of shapes but the most abundant ones are spherical. The viral proteins HA, NA and M2 (a viroporin) are abundantly found in the viral envelope which is found in the lipid bilayer (lipid bilayer is obtained from the host cell membrane) (Fields, B.N. 2007)(Samji 2009).

The following four stages will briefly describe the influenza life cycle. It starts with the entry of the virus into the host cell. Then the vRNPs enter the nucleus of the host cell. Following this the viral genome goes through transcription and replication, and the export of the vRNPs occur from the nucleus. Assembly and budding occurs at the host cell plasma membrane. The following diagram provides a schematic representation of the Influenza A life cycle.



Nature Reviews | Drug Discovery

**Figure 1.2. Schematic diagram showing the influenza life cycle.** Influenza A surface protein consists of M2 ion channel protein, lectin haemagglutinin and sialidase an enzyme. The virus uses haemagglutinin to adhere itself to the target host cell. Following this, endocytosis and fusion occurs. Host cell machinery starts producing viral components. Subsequent viral protein synthesis and particle assembly in the host cell prepares the virion progeny for the budding process to exit the host cell. (von Itzstein 2007). Diagram obtained from: (von Itzstein 2007).

### **1.1.1.3 Respiratory Syncytial Virus (RSV)**

Human Respiratory Syncytial Virus (RSV) causes respiratory tract infections in infants which most of the time results in complications like bronchiolitis and pneumonia and even death. The virus is classified under the genus pneumovirus (also includes bovine RSV and mouse pneumonia virus). The family of this virus is *Paramyxoviridae*. RSV consists of 10 genes and studies have identified the conserved mRNA termini, intergenic sequences, and coding regions for each of these genes (Barik 1992, Stec et al. 1991) The RSV genome consists of a non-segmented negative stranded RNA; the RNA being about 15,221 nucleotides (nt) long. The gene order is 3'(leader)-1C-1B-N-P-MSH- G-F-22K-L-(trailer)5'; alternative names of some genes are NS1 (1C), NS2 (1B), 1A (SH), and M2 (22K)(Barik 1992). The 10 RSV proteins have all been identified and most of them are virion components. The most abundant among these are the 1C and the 1B which appear to be non-structural (Fernie and Gerin 1982, Peebles and Levine 1979, Pringle et al. 1981, Wunner and Pringle 1976). The viral RNA is contained in the nucleocapsid core. The N,P and L proteins are also found in the nucleocapsid core (Mittmann et al. 2002). Although still debatable, it is vastly believed that the nucleocapsid of the RSV is the transcription complex of the virus and this encodes for an RNA-dependent RNA polymerase activity (Barik 1992). Proteins are present in the functional Ribonucleoprotein Complex (RNP) the functions of which are not characterised yet. Figure 1.3 represents a schematic diagram of the RSV genome.

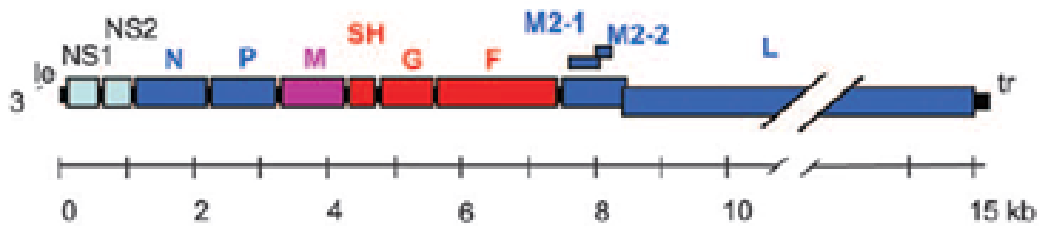


**Figure 1.3 RSV Genome.** The negative-sense RNA genome (strain A2) is depicted 3' to 5' showing the extragenic 3' leader (le) and 5' trailer (tr) regions and the intervening 10 viral genes (rectangles) that are each expressed as a separate mRNA . M2-1 and M2-2 are overlapping open reading frames of the M2 mRNA. The M2 and L genes overlap slightly, and L is expressed by polymerase backtracking. Diagram and legend obtained from (Collins and Graham 2008).

## 1.2 Innate Immunity and Toll-like Receptors

The innate immune system is essential in recognising microbial pathogens that invade the body. This recognition is possible due to the presence of germline-encoded pattern-recognition receptors (PRRs) which identifies molecular patterns present on the pathogen itself; these are called pathogen-associated molecular pattern (PAMPs) (Janeway 1989). A series of signalling cascade is generated after PRR recognises PAMPs and this forms the basis of the first line of host defence that is necessary for killing the invading microbes. Additionally the adaptive immune response is also triggered off by PRR signalling as a result of dendritic cell (DC) maturation.

The first PRR to be identified was the Toll Like Receptors (TLRs) which are also the most characterised and recognise a wide scale of PAMPs (Akira 2003, Beutler 2009, Hoffmann 2003, Medzhitov 2007). To date there has been 10 and 12 TLRs identified in human and mouse respectively.

### 1.2.1 Toll-like Receptors

Each TLR detects different PAMPs derived from bacteria, viruses, mycobacteria, fungi and parasites. PAMPs derived from these pathogens include lipoproteins (identified by TLR1, TLR2 and TLR6), double stranded RNA (dsRNA) which is recognised by TLR3.

Bacterial lipopolysaccharide (LPS) by TLR4, flagellin by TLR5, single-stranded (ss) RNA by TLR7 and TLR8; DNA by TLR9 are few other common examples (Akira et al. 2006). The following table gives a brief overview of TLRs recognising PAMPs.

Species	PAMPs	TLR Usage	PRRs Involved in Recognition
Bacteria, mycobacteria	LPS	TLR4	
	lipoproteins, LTA, PGN, lipoarabinomannan	TLR2/1, TLR2/6	NOD1, NOD2, NALP3, NALP1
	flagellin	TLR5	IPAF, NAIP5
	DNA	TLR9	AIM2
	RNA	TLR7	NALP3
Viruses	DNA	TLR9	AIM2, DAI, IFI16
	RNA	TLR3, TLR7, TLR8	RIG-I, MDA5, NALP3
	structural protein	TLR2, TLR4	
Fungus	zymosan, $\beta$ -glucan	TLR2, TLR6	Dectin-1, NALP3
	Mannan	TLR2, TLR4	
	DNA	TLR9	
	RNA	TLR7	
Parasites	tGPI-mutin ( <i>Trypanosoma</i> )	TLR2	
	glycoinositolphospholipids ( <i>Trypanosoma</i> )	TLR4	
	DNA	TLR9	
	hemozoin ( <i>Plasmodium</i> )	TLR9	NALP3
	profilin-like molecule ( <i>Toxoplasma gondii</i> )	TLR11	

**Table 1. Detection of PAMPs by TLRs and other PRRs.**

### 1.2.2 Toll-like Receptor Structure

TLRs fall under the category of type I transmembrane proteins. The extracellular domain contains a leucine rich repeat (LRR), composed of 19-25 tandem copies of the “xLxxLxLxx” motif, 24-29 amino acids in length, in a horseshoe-like structure (Akira et al. 2006, Jin and Lee 2008). This mediate PAMP recognition. TLRs also contain a transmembrane region and cytosolic Toll-IL-1 receptor (TIR) domains that activate downstream signalling pathways.

TLRs can be found both on the cell surface and intracellular compartments. All TLRs have the capability to form either homodimers or heterodimers through their TIR domains which triggers downstream signalling. Often an additional protein might be required by a TLR to be bound to them for activation. For example MD2 is a protein that binds TLR4 strongly on the cell surface. TLR4 is responsible for recognising LPS and triggering a downstream signalling cascade (Shimazu et al. 1999) involved in the LPS recognition by TLR4 are CD14 and LPS binding protein (LBP) (Kitchens 2000). Examples of TLR

heterodimerization can be seen in the case of TLR2 when it binds to TLR1 and TLR6 including non-TLR receptors like CD36 and Dectin-1. These bindings to various proteins help recognise TLR2 ligand (Gantner et al. 2003, Hoebe et al. 2005). Crystal structures of a few TLRs have been elucidated, such as TLR1, TLR2 (Jin and Lee 2008), TLR3, TLR4 (Kim et al. 2007) and TLR6 (Kang J. Y. et al. 2009). Vastly TLRs can be categorised under intracellular and extracellular members as shown in the following figure.

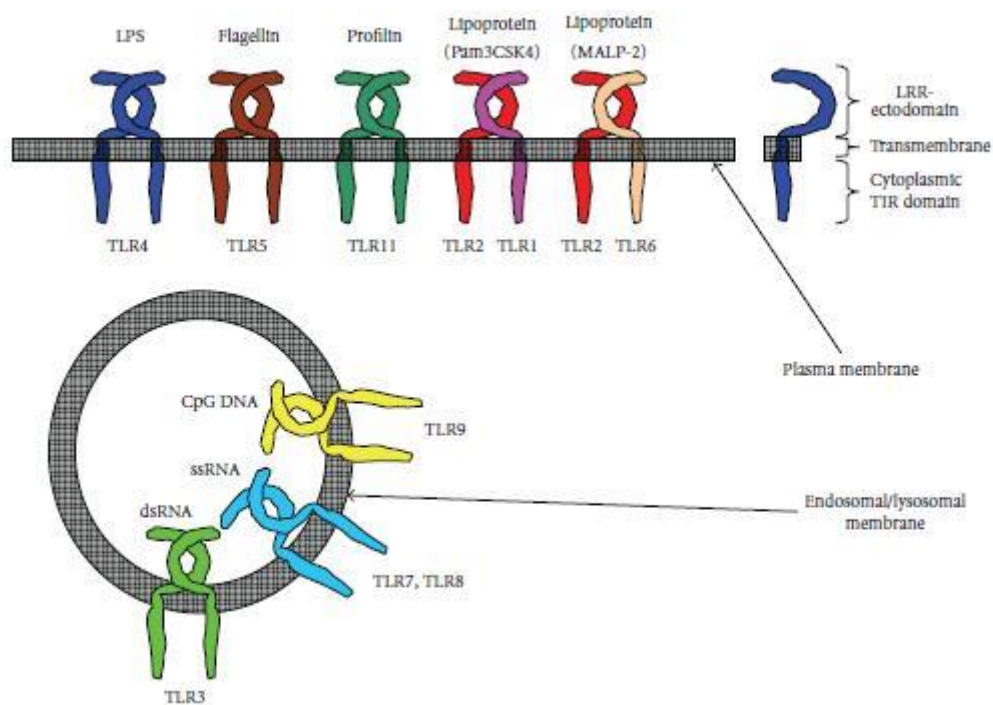


**Figure 1.4 TLR localisation.** TLR1, TLR2, TLR4, TLR5, TLR6, and TLR11 recognise their ligands on the cell surface, whilst TLR3, TLR7, TLR8, and TLR9 are located intracellularly, in endosomes and lysosomes (Yamamoto and Takeda 2010).

### 1.2.3 Toll-like Receptor Signalling Pathways

TLR signalling can be broadly classified into two categories depending on the adaptor molecule each TLR utilises. Most of TLR signalling is MyD88 dependent (except TLR3)



and in some cases it is Trif dependent (TLR3 and TLR4). MyD88 (Myeloid differentiation primary response gene 88) is a member of the family of adapter molecules containing a cytoplasmic TIR domain. Other similar adaptor molecules include TIRAP (TIR-containing adaptor protein, also known as Mal; MyD88-adaptor like), TRIF (TIR-domain-containing adapter-inducing IFN- $\beta$ ), and TRAM (TRIF-related adaptor molecule). TLRs contain a TIR domain which recruits specific adaptors (containing TIR-domain) which results in the signalling specificity for the TLRs (Yamamoto and Takeda 2010).

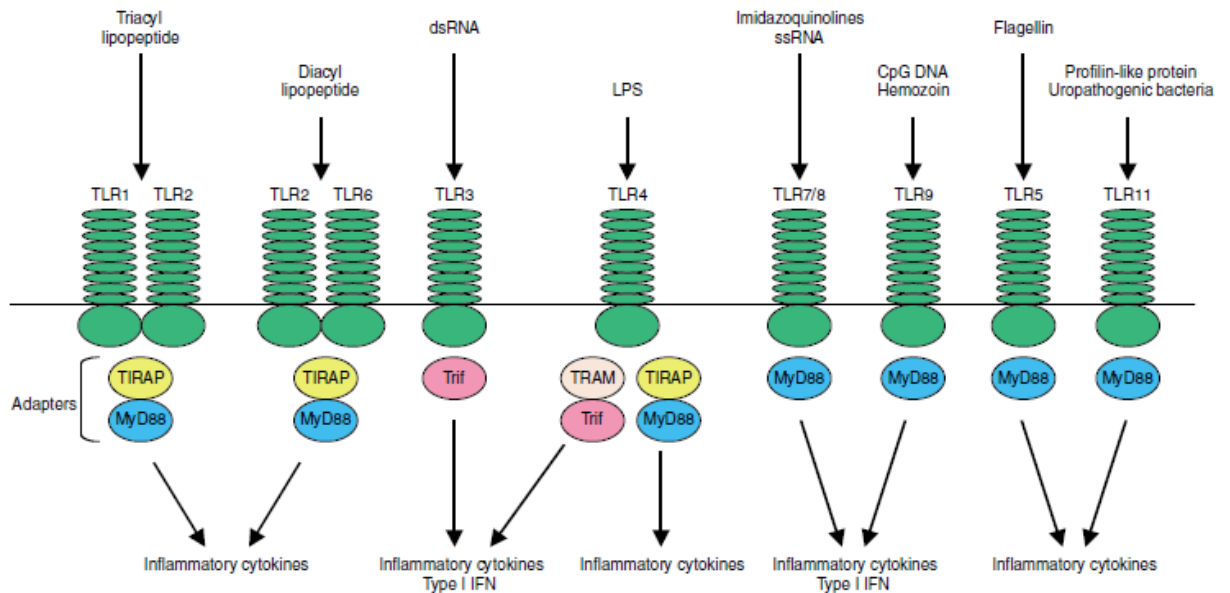


**Figure 1.5 Innate Immune response to TLRs.** Different TLRs represented along with their respective PAMPs. Apart from TLR3 all other TLRs utilize the adapter molecule MyD88. TLR3 uses only Trif whereas TLR4 uses Trif, TRAM, TRAP and MyD88. Eventual release of inflammatory cytokines is observed in all cases and Type I IFN in some cases.

The activation of NF- $\kappa$ B and AP-1 is a primary outcome of TLR activation which results in the induction of inflammatory pathways and production of Interferons. TLRs utilise

their extracellular leucine-rich repeats for recognising pathogens whereas the transmembrane and cytoplasmic Toll/interleukin-1 receptor (TIR) domains is needed for downstream signal transduction. Activation of all TLRs results in an eventual triggering of inflammatory pathway and activation of the nuclear factor (NF)- $\kappa$ B which is a dimeric transcription factor and activating protein-1 (AP-1). NF- $\kappa$ B contains two subunits, p65 and p50 and is a heterodimer in most cell types. The inactive form of this protein complex is found in the cytoplasm of unstimulated cells interacting with inhibitor of NF- $\kappa$ B (I $\kappa$ B) proteins. Phosphorylation of I $\kappa$ B occurs (at serine residues) as a result of TLR stimulation by its ligands. Phosphorylation is sequestered by the IKK complex which consists of IKK alpha and IKK  $\beta$  protein kinases and a regulatory molecule, IKK gamma/Nemo. As a result of this I $\kappa$ B is targeted for degradation and ubiquitination by the 26s proteasome. NF- $\kappa$ B is then released in the nucleus and acts as a transcription factor (Akira et al. 2006, Kawai and Akira 2010, Takeda and Akira 2004, Yamamoto and Akira 2004, Yamamoto and Takeda 2010)

All TLRs apart from TLR3 utilises MyD88 which is a master adaptor molecule. It is also used by by all IL-1R family members (Akira et al. 2006). The TIR domain is essential for the binding of MyD88 and Mal/TIRAP and causes selective participation of TLR2 and TLR4 mediated MyD88 signalling (Yamamoto and Takeda 2010). The adaptor molecule interacts with IL-1R-associated kinase (IRAK) 4, through homophilic interactions of its death domains. IRAK4, via IRAK1, regulates the activity of tumour necrosis factor (TNF) receptor-associated factor (TRAF) 6, a RING finger-containing E3 ligase, which is involved in lysine 63 (K63)-linked ubiquitination-mediated signalling. TRAF6, catalysed by the E2 ubiquitin conjugating enzyme complex Ubc13 and UEV1A, activates the TAK1 – TABs complex (Akira 2009, Akira et al. 2006). This complex activates the IKK (I $\kappa$ B

kinase) complex of NEMO (NF- $\kappa$ B essential modulator), IKK- $\alpha$ , and IKK- $\beta$ , which in turn phosphorylates I $\kappa$ B, tabbing it for ubiquitination and targeting it to the proteasome for degradation, thereby releasing NF- $\kappa$ B and allowing it to translocate to the nucleus (Karin and Ben-Neriah 2000).

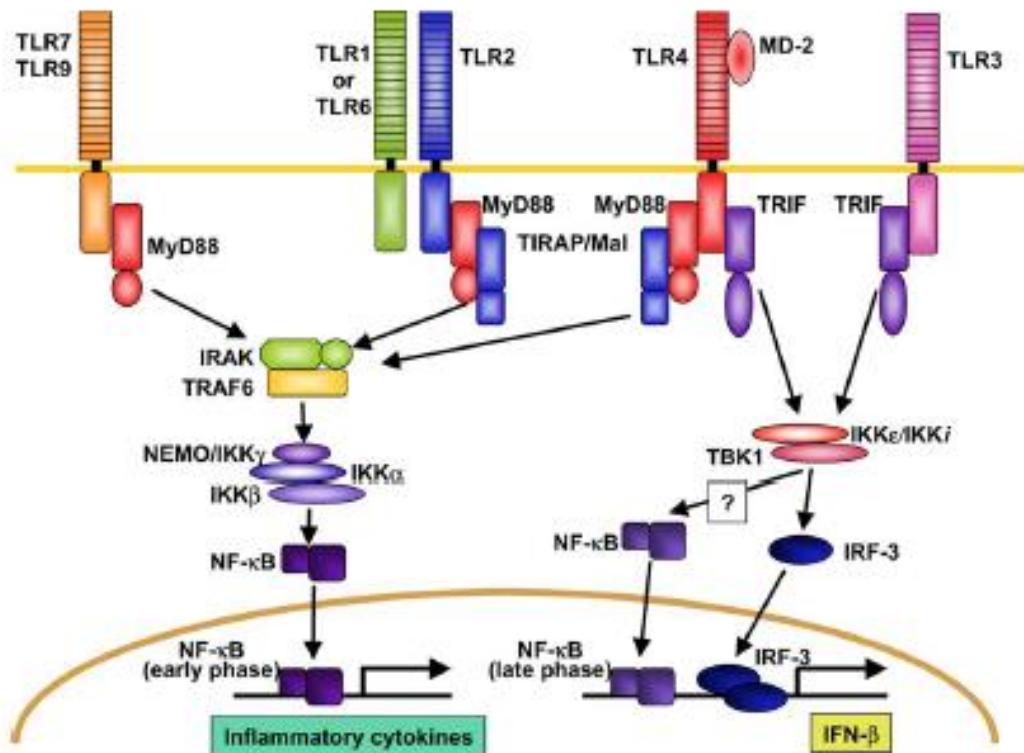


**Figure 1.6 Visualization of the MyD88 dependent and TRIF dependent TLR signalling pathway.** TIR containing adaptor molecule MyD88 is essential for downstream signalling for the secretion of inflammatory cytokines through TLR signalling. Also shown is the MyD88 independent pathway leading to IRF3 activation via IKK $\epsilon$ /IKK $\iota$ . Another TIR containing adaptor molecule TRIF mediates the MyD88-independent pathway (Takeda and Akira 2004).

The other TLR activated downstream pathway is MyD88-independent, which means the adaptor molecule Trif is utilised by TLRs instead of MyD88. This also activates NF- $\kappa$ B

and AP-1. The only TLRs participating in such a signalling cascade is TLR3 and TLR4. TLR3 uses the TIR domain to bind itself to TRIF however TRAM is required for TLR4 downstream TRIF-dependent signalling (Yamamoto and Takeda 2010). TRIF signals to TRAF3, which activates the IKK complex of TRAF-associated NF- $\kappa$ B activator (TANK)-binding kinase 1 (TBK1) and IKK $\epsilon$ . This complex activates the signal-dependent phosphorylation of IRF3 and IRF7, causing homo- or heterodimerization, nuclear translocation, and assembly onto the IFN- $\beta$  enhancer, assisted by CBP/p300 (CREB binding protein) (Fitzgerald et al. 2003, Sharma et al. 2003).

Depending on the pathway used the transcription factors NF- $\kappa$ B, ATF2-c-Jun, MAPKs, IRF3, or IRF7 are activated, resulting in the upregulation of Type I IFNs. This causes inflammation and other physiological defence mechanisms are triggered (Yamamoto and Takeda 2010).

#### **1.2.4 Virus Recognition by Toll-like Receptors**

Different kinds of Pathogen Associated Molecular Patterns (PAMPs) are recognised by TLRs which are a type-I integral membrane glycoprotein (Akira 2009, Akira et al. 2006). Primary human airway epithelial cell lines express 10 different kinds of TLRs (TLR1-TLR10) (Muir et al. 2004, Sha et al. 2004). TLRs play a crucial role in the initiation of immune responses in the respiratory epithelium, producing mitogen activated protein (MAP) kinases, and many other transcription factors such as interferon regulatory factor 3 (IRF3), and IRF7 causing the release of numerous proinflammatory cytokines such as type I ( $\alpha$  and  $\beta$ ) and type III ( $\gamma$ ) IFNs (Iwamura and Nakayama 2008).

A TLR subfamily which is found in the endosomes of the airway epitheliums consisting of TLR3, TLR7, TLR8, and TLR9 recognise viral nucleic acids which causes the

induction of type I IFNs. For instance TLR3 recognises infections by Human Rhinoviruses, RSV (Groskreutz et al. 2006) and Influenza virus (Guillot et al. 2005). TLR7, TLR8, and TLR9 recognize double-stranded RNA (dsRNA), single-stranded RNA (ssRNA), and CpG DNA, respectively (Kawai and Akira 2008). MyD88 is an essential adapter molecule utilised by TLR7 and TLR9 for the activation of NF- $\kappa$  B and IRF7 which in turn leads to the release of proinflammatory cytokines and (Kawai and Akira 2007) type I interferons (Greene and McElvaney 2005), however only a very few studies have investigated the role of TLR7,8 or 9 in respiratory virus infections. Adenoviral vectors interact with TLR9 and TLR7 is known to interact with Influenza virus, in dendritic cells (DCs) (Lund et al. 2004, Reibman et al. 2003) however it is still unknown whether these observations are relevant in airway epithelial cells. Intracellular TLRs and TLR3 are known to recognise viruses whereas the extracellular TLRs (such as TLRs 2,4 and 6) recognise bacterial products. These bacteria recognising TLRs may also be involved in virus recognition and innate immune sensing by the airway epitheliums. We learn that RSV fusion protein and TLR4 interactions which results in a MyD88 dependent signalling cascade and inducing immune response in airway epithelium (Boukhvalova et al. 2006, Haeberle et al. 2002) A newer study describes the interactions of TLR2 and TLR6 with RSV (Vareille et al. 2011).

### **1.3 Innate Immunity and RIG-I-like Receptors**

Apart from the very well-known PRRs such as the Toll Like Receptors, there are other PRRs that has been recently discovered which are TLR independent. These include the retinoic acid inducible gene-I (RIG-I)-like receptor (RLR) family. This family has three known member and they are: RIG-I (also known as DDX58) (Yoneyama et al. 2005), melanoma differentiation-associated gene 5 (MDA5, also known as IFIH1 or Helicard)(Kang D. C. et al. 2002) and laboratory of genetics and physiology 2 (LGP2, also known as DHX58) (Rothenfusser et al. 2005).

#### **1.3.1 RIG-I, MDA5, and LGP2 Structures**

RIG-I and MDA-5 are proteins that are homologous in nature. They are 925 aa and 1025 aa long respectively and are known to be upregulated after they are able to detect cytoplasmic viral RNA during viral replication (Wilkins and Gale 2010). They belong to the family of helicases, superfamily 2 (SF2). Both the proteins have seven conserved 'helicase motifs' that helps to mediate binding of ATP and nucleic acid (Gorbalenya et al. 1988). RIG-I is associated with F-actin and is hence found to localize at the cytoskeleton of the cell whereas MDA-5 is found to be distributed throughout the cytosol (Mukherjee et al. 2009).

A N-terminal region and a caspase activation and recruitment domain (CARDs) is a common feature in both RIG-I and MDA-5. They also contain a central SF2 type DExD/H-box RNA helicase domain, and a C-terminal repressor domain (RD) (Takeuchi and Akira 2007). LGP2, which is the third RLR as mentioned before is 678 amino acids long and contains a DExD/H-box RNA helicase domain (which shows 31% and 41% amino acid identities to the RNA helicase domains of RIG-I and MDA5, respectively) and a C-terminal RD, but lacks any CARDs (Yoneyama et al. 2005).

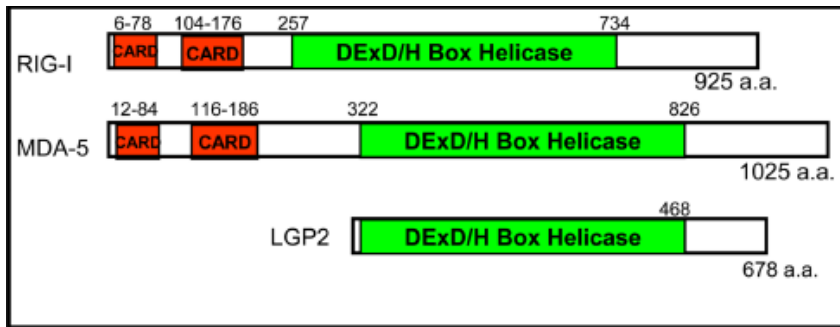


**Fig 1.7 Structural Diagrams of RLR showing their functional domains** (Wilkins and Gale 2010).

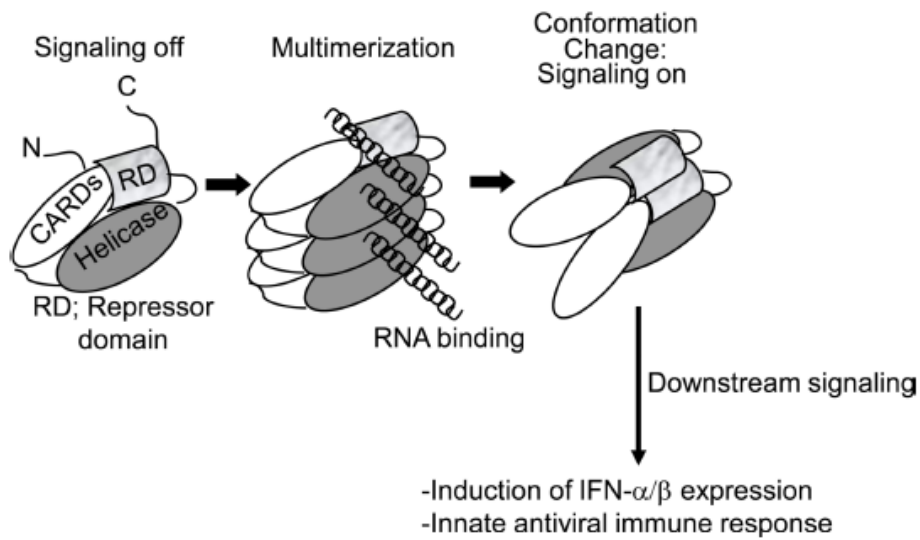


**Figure 1.8 Representation of RIG-I activation through a 3-step model.** Left: monomer in resting form. Centre: Dimer when bound to RNA ligand. Right: Final activated form. Shown above are the positions of CARDs, Repressor Domain (RD) and helicase domain. RIG-I -ligand interaction cause a conformational change resulting in downstream signalling of innate antiviral immunity (Wilkins and Gale 2010).

### **1.3.2 CARDS and RLR Dimerisation**

CARDs belong to the pro-apoptotic death domain family and contains death domains, death effector domains and pyrin domains. They also have six antiparallel alpha helices. They are known to have homophilic interactions (CARD-CARD interactions) that promotes cell death pathway and eventually triggering off a downstream signalling that activates IRF3/7 and NF $\kappa$ B. ATPase activity is a valiant feature of the internal DExD/H-box RNA helicase domain, activated upon ligand binding. This feature is of no use for RNA binding however plays a role in downstream signalling (Takahasi et al. 2008, Yoneyama et al. 2005).

RIG-I in its C-terminal Repressor Domain (RD) contains a zinc binding site that plays an important role in controlling IFN mediated IFN responses (Saito et al. 2007). It has been proven that RIG-I uses its C-terminal RD to bind itself to uncapped 5'-triphosphate single-stranded RNA (5'-pppRNA). This is feasible due to the presence of an invariant lysine residue that helps with interacting with phosphate. RIG-I has an active (open) and an inactive (closed) state. The RD represses the CARD and the helicase domain in its inactive state. Upon viral RNA binding to the RD, RIG-I is converted to its active state following a conformational change. The active state of RIG-I is a dimerised state that promotes a downstream signalling via CARDs. RIG-I only constitutively activates downstream signalling without the presence of the RD. Overexpression of RD causes inhibition of antiviral response (Cui et al. 2008). The following model (figure 1.10) represents the activation of RIG-I by 5'-pppRNA resulting in ligand induced dimer formation of RD.



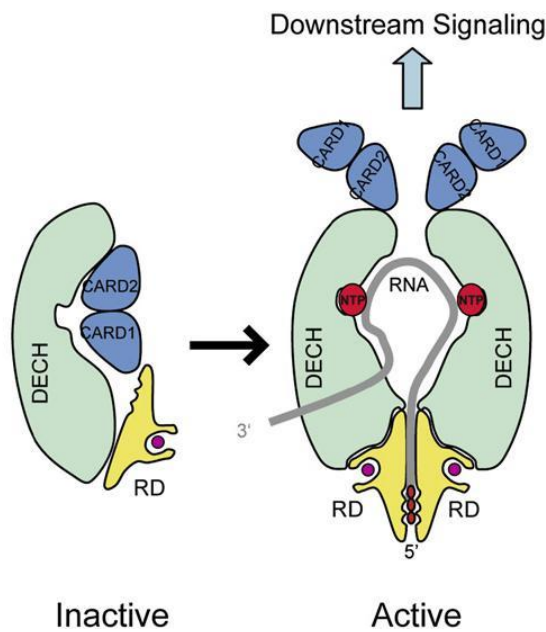


**Figure 1.9 Proposed model for activation of RIG-I and dimer formation after 5'-triphosphate RNA binding** (grey with red phosphates). CARDs and the helicase domains are repressed by the RD in the active state of RIG-I. Binding of 5'-triphosphate RNA induces a conformational change, resulting in the dimerization of RIG-I and activation of downstream signalling (Cui et al. 2008).

### 1.3.2.1 IPS-1

Post viral-ligand binding both RIG-I and MDA-5 takes part in a downstream signalling using their CARDs that eventually directly activates IRF3/7 and indirectly NF- $\kappa$ B. An intermediate protein is involved in the signal transduction called IFN- $\beta$  Promoter Stimulator 1(IPS-1) (find Kawai 2005). It is also known as MAVS (Mitochondrial Antiviral Signalling Protein) (Seth et al. 2005), VISA (Virus Induced Signalling Adaptor)(Xu et al. 2005) and Cardif (CARD adaptor inducing IFN- $\beta$ ) (Meylan et al. 2005). IPS-1 plays as an adapter protein for both RIG-I and MDA-5 signalling eventually resulting in effective anti-viral response against a variety of RNA viruses (Kumar et al. 2006, Sun et al. 2006). The length of IPS-1 is 540 amino acids which is found on the outer membrane of the mitochondria. It is anchored there with a short hydrophobic C-terminal

region (Seth et al. 2005). Although fixed there, during viral infection it moves into a detergent-resistant mitochondrial fraction. We get a link between mitochondrial function and viral infection from the location of IPS-1 (Hiscott et al. 2006). Structural elucidation of IPS-1 led us to discover the following: a N-terminal CARD-like domain (CLD), homologous to the CARDS of RIG-I and MDA5, a proline-rich region, and a C-terminal effector domain. Crystal structure of N-terminal CLD of IPS-1 has been determined to 2.1 Angstrom resolution. The structure is very typical of the death domain superfamily consisting of a six-helix bundle.

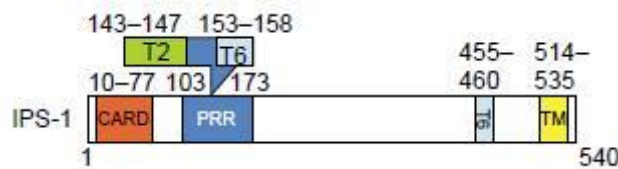


**Figure 1.10 Schematic diagram of IPS-1.** The position of each significant area is shown. TRAF3 not shown. Abbreviations: T2, TRAF2 binding motif; T6, TRAF6 binding motif; PRR, proline-rich region; TM, mitochondrial transmembrane domain. Amino acid positions are indicated (Johnson and Gale 2006).

### 1.3.3 Host Response to Viral Infection

RNA acts as a ligand to RIG-I and MDA-5 leading to their activation involving interactions with IPS-1 via CARD-CARD binding. In the process it recruits downstream signalling molecule as seen in figure 1.11. Molecules involved in such signal transduction often belong to the TRAF family. For example; IPS-1 contains a TRAF-interacting motif to which TRAF3 binds directly. TRAF2 and TRAF6 binds to IPS-1 in the same manner (Oganesyanyan et al. 2006, Saha et al. 2006, Xu et al. 2005). The TRAF proteins signals downstream that eventually activates transcription factors IRF3/7 and NF- $\kappa$ B.

The first signalling pathway occurs through the canonical IKK complex composed of IKK- $\alpha$  and IKK- $\beta$  along with its regulatory subunit NEMO. I $\kappa$ B is phosphorylated by this complex. Phospho-I $\kappa$ B then acts as an inhibitor of NF- $\kappa$ B on serines 32 and 36; following this ubiquitination of Phospho-I $\kappa$ B occurs and results in its targeted degradation in the proteasome. NF $\kappa$ B is released as a result and translocates to the nucleus (Karin and Ben-Neriah 2000). The second pathway is non-canonical and involves the complex IKK which consists of TBK1 and IKK $\epsilon$ . IRF3 and IRF7 are phosphorylated by this complex and causes homo-dimerisations or heterodimerisation. The IRFs then translocate to the nucleus and acts as transcription factors and assemble to the IFN- $\beta$  enhancer, assisted by CBP/p300 (Fitzgerald et al. 2003). IRFs are also known to be activated by NEMO (Zhao et al. 2007).

TRAF3 is important in recruiting both the IKK complexes through its IPS-1 interactions whilst TRAF2 and 6 essentially activates NF- $\kappa$ B.

Transcriptional upregulation of type I IFNs is the most significant outcome of transcription factors IRF3/7 and NF- $\kappa$ B after reaching the nucleus. IFNs then signal through the IFN- $\alpha/\beta$  receptor and the Jak-STAT pathway. This causes interferon stimulated gene expression (ISG) which triggers off apoptosis of infected cells. ISG expressions results in innate immune response by inhibiting viral infection. They are also known to trigger adaptive immune response (Lei et al. 2009, Yoneyama and Fujita 2009). The RLR signalling pathway described is pasteurised in the following diagram (Figure 1.11).

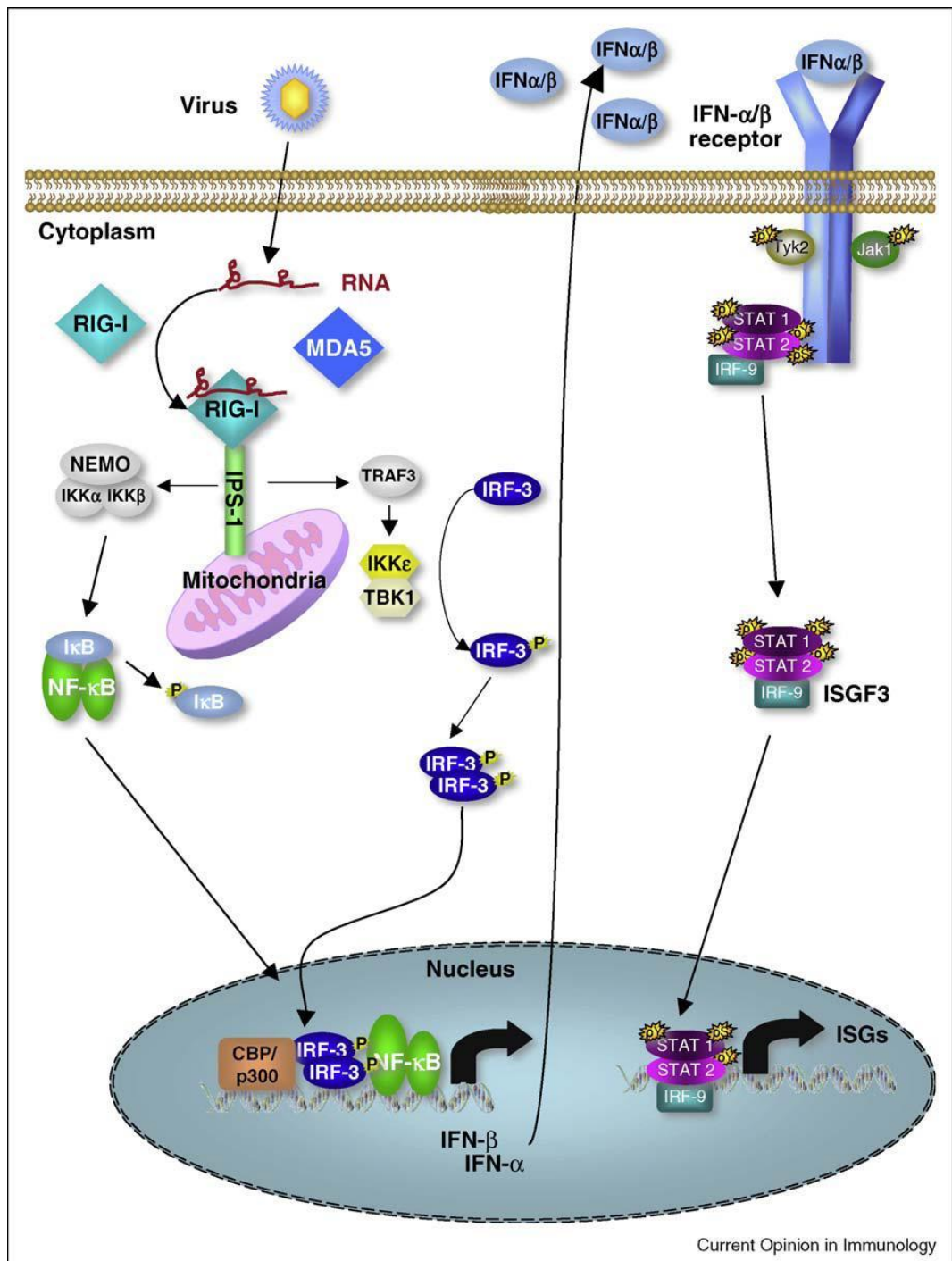
















**Figure 1.11 The RLR signalling pathway.** Viral RNA binds to RIG-I followed by downstream signalling IRF3 and NF- $\kappa$ B that induces the production of IFN- $\alpha/\beta$  from a virus infected cell. IFN- $\alpha/\beta$  binds to the IFN- $\alpha/\beta$  receptors and signals through the Jak-STAT pathway driving interferon stimulated gene (ISG). This results in antiviral innate immune response (Wilkins and Gale 2010).

### **RLR Ligands**

The innate immune response to different viral pathogens vary greatly by different RLRs; RIG-I and MDA-5 being no different. Although they are very similar structurally their preference for viral recognition is different. The cause for this is thought to be due to amino acid sequences of the DExD/H-box RNA helicase domains of RIG-I and MDA5 which are 35% identical which is very little. This genetic diversity allows them to prefer different specifications for distinct RNA conformations (Kato et al. 2006, Loo et al. 2008).

### **RIG-I Ligands**

Both positive and negative stranded viruses are detected by RIG-I. These viruses include HCV, RSV and some related paramyxoviruses. RIG-I also detects VSV and Influenza A viruses (Kato et al. 2008, Loo et al. 2008). Reoviruses, WNV and Dengue viruses are all detected by both RIG-I and MDA-5 (Fredericksen and Gale 2006) as well as measles virus (Ikegame et al. 2010). RIG-I detects the uncapped 5'-ppp RNA (Hornung et al. 2006). This is how RIG-I distinguishes from self and non-self (viral) RNA. Host RNA is always capped or post-translationally modified removing the 5'triphosphate. This is why RIG-I is not activated by the host RNA. RIG-I detects both dsRNA (Yoneyama et al. 2004) and 5'-ppp ssRNA (Pichlmair et al. 2006). Although this is the case, some form of double-strandedness may be required (Schmidt et al. 2009). RIG-I can also recognise particular sequences or motifs within viral RNA, such as uridine and adenosine-rich 3'-sequences in 5'-ppp ssRNA (found within HCV and other viruses (Saito et al. 2008, Uzri and Gehrke 2009) or short double-stranded blunt-end 5'-pppRNA (Schlee and Hartmann 2010).

Name	Length (nt)	Structure (source)		5'	3'
GFP2	24	ds and ss 3pRNA (phage polymerase IVT)		3p	OH
Lamin A/C	50–1,000	ds 3pRNA, 5' and 3' blunt end (phage polymerase IVT)		3p	OH
VSV	11,000	ss 3pRNA (VSV genomic RNA)		3p	OH
Tri-GFPs	24	ss 3pRNA (phage polymerase IVT)		3p	OH
SAD ΔPLp	11,900	ss 3pRNA (Rabies genomic RNA)		3p	OH
Tri-G-AC-U	31	ss 3pRNA (phage polymerase IVT)		3p	OH
Flu vRNA	890–2,341	ss 3pRNA (Influenza A genomic RNA, 8 segments)		3p	OH
RNaseL fragments	<200	ss and dsRNA, 5'- or 3'-overhangs (digestion of cellular RNA with RNaseL)		OH	1p
pppRVL	58	ss 3pRNA (phage polymerase IVT)		3p	OH
pppVSVL	60	ss 3pRNA (phage polymerase IVT)		3p	OH
ppp-shRNA-luc3	22+24 loop	sh 3pRNA, 2-nt 3'-overhang (phage polymerase IVT)		3p	OH
PU/UC	105	ss 3pRNA (phage polymerase IVT)		3p	OH
Short poly I:C	300	ds 1pRNA, 2-nt 3'-overhang (digestion of poly I:C with RNase III)		1p	OH
PolyAU	(20–?)	ds 3pRNA, generated <i>in vivo</i> by transcription of transfected DNA poly(dAdT) by cellular RNA polymerase III		3p	OH

**Table 2. Table showing putative RIG-I ligands which are generated by enzymatic polymerization or cleavage.** The RNA molecules shown in the table are not molecularly defined (Schlee and Hartmann 2010).

The host endonuclease RNAase L produces cleavage products during a viral infection, these are known to be recognised by RIG-I and hence RLR mediated antiviral response is amplified (Malathi et al. 2007). Short dsRNA products/ viral transcripts (less than 1kb length) are also recognised by RIG-I (Kato et al. 2008). It is still a matter of debate as to what exactly the RIG-I ligand is. Suggestions include negative stranded viral RNA

genome which are generated during the viral replication cycle; this being the major actor for RIG-I upregulation and antiviral response. Other types of RNA products are not responsible for RIG-I activation and an eventual IFN induction (Rehwinkel 2010, Rehwinkel and Reis e Sousa 2010).

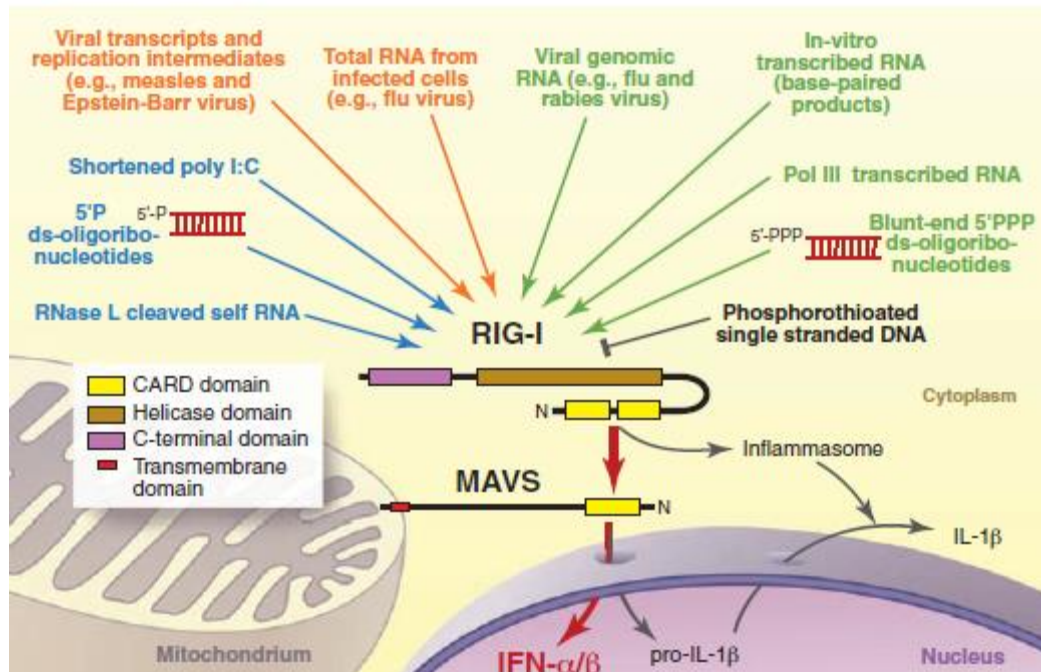


**Fig 1.12 Diagram showing putative RIG-I ligands. Variety of RNA agonists trigger RIG-I expression.** Green arrows show 5'PPP-bearing RNAs. RNAs without 5'PPP are shown in blue. Orange arrows show RNA which may have different 5'end characteristics. Antagonists shown in black arrow. Activated RIG-I promotes the induction of interferons and other pro-inflammatory cytokines via MAV (red bold arrow). Eventual release of IL-1β after inflammasome activation (Rehwinkel and Reis e Sousa 2010).

### **MDA5 Ligands**

MDA5 mostly is known to detect Picornaviridae. Most common ones are Human Rhinovirus (HRV), encephalomyocarditis virus (EMCV) and Theiler's virus. The viral genome contains a VPg region at its 5' end which is detected by MDA5. As we have discussed before that the 5' triphosphate is essential for RIG-I recognition; the VPg region blocks this and doesn't allow RIG-I recognition and allows MDA5 binding (Kato et al. 2006, Pichlmair et al. 2006). Upregulation of MDA5 is also noticed in infections by reoviruses (Loo et al. 2008), flaviviruses (Fredericksen and Gale 2006), paramixoviruses and norovirus (McCartney et al. 2008). It has been observed that mice in the absence of MDA5-IPS1 pathway have increased mortality post CBV3 infection; it is believed that this is due to the importance of MDA5 and IPS1 pathway mediating Type 1 IFN responses (Huhn et al. 2010, Wang Q. et al. 2009). MDA5 is required for Poly I:C-induced IFN production (Kato et al. 2006, Loo et al. 2008). MDA5 prefers binding to long dsRNA products (greater than 1-2kb in length) whilst RIG-I detects short dsRNA (Kato et al. 2008).

### **LGP2 Ligands**

*In Vitro* studies show that, LGP2 negatively regulates RIG-I and MDA5 and also MDA5 mediated antiviral response. LGP2 when produced in excess causes inhibition of IRF3 and NF- $\kappa$ B production, post viral infection (Rothenfusser et al. 2005). A plausible explanation of how it happens is that LGP2 isolates away dsRNA from RIG-I and MDA5 and hence prevents the activation of an antiviral signal (Saito et al. 2007). Other studies say that using its RD, LGP2 is able to prevent RIG-I dimerisation and its interaction with IPS-1 (Komuro and Horvath 2006). Other possibilities include; that LGP2 competes with IKK $\epsilon$  for recruitment to IPS-1. The RD of LGP2 binds to dsRNA in a more stronger



manner than does MDA5; structural analyses has revealed (Li et al. 2009, Pippig et al. 2009, Takahasi et al. 2009). However, in vivo analyses on the contrary shows us that LGP-2 acts as positive regulator of antiviral response mediated through RIG-I and MDA5. This functions through its ATPase domain (Satoh et al. 2010, Venkataraman et al. 2007).

#### **1.4 NALPs in Innate Immunity**

NALPS- These are cytoplasmic proteins that have been implicated in the activation of Caspase-1 by TLRs as a response to pathogenic invasion into a cell. They are similar in structure to APAF-1 (apoptotic protease-activating factor-1) that is known to activate Caspase-9. NALP1 forms a large multiprotein complex that has the ability to activate Caspase-1, and is referred to as the inflammasome (Tschopp et al. 2003).

The successful completion of the human genome sequence has shown us that TLRs are not the only PRRs that contain LRRs (Leucine Rich Repeats). This family of proteins was named CATERPILLER. They have no TIR domain unlike the TLRs, but contain three distinct domain. Some of these domains are called NACHT domain, Caspase recruitment domain (CARD) or the pyrin domain (PYD) (Tschopp et al. 2003)

In this study we focus on only one of the sub-families called the NALPs, details of its structure and function of a few member are discussed in the following chapter (1.5 Inflammasomes). Below in a diagram showing the typical domains of the NLR subfamilies (NLRPs, NAIPs, NLRCs and CIITA).

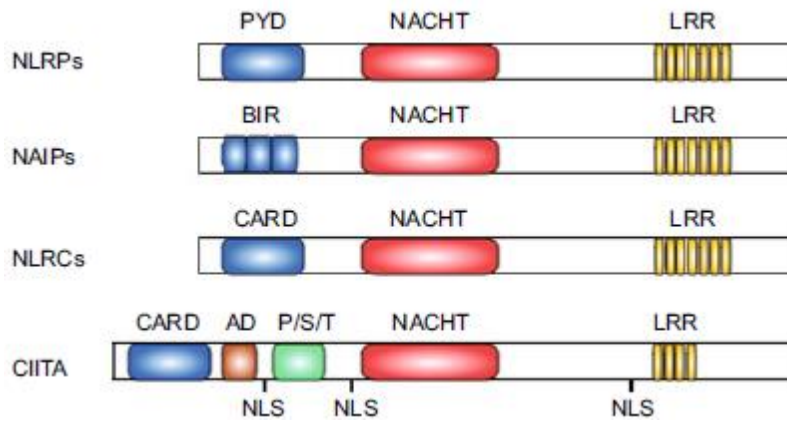


**Diagram 1.13** The typical domains of the NLR subfamilies (NLRPs, NAIPs, NLRCs and CIITA) are shown. Diagram obtained from (Yao and Qian 2013)

### 1.5 Inflammasomes

Cellular infection and stress are causative agents for activating molecular platforms called the Inflammasome which are responsible for the production and maturation of proinflammatory cytokines such as Interleukin 1- $\beta$  and IL-18 which when released from the cell causes potential inflammation. Inflammasomes form large multimeric structures which come together when each of the component are overexpressed in the cytosol (Martinon et al. 2002). An activated inflammasome in turn activates Caspase-1 which cleaves pro IL-1 $\beta$  into IL-1 $\beta$  which is then secreted from the cells. It is believed that this process is analogous to the formation of an apoptosome as a response to apoptotic stimuli. Strikingly nuclear magnetic resonance spectroscopy (NMR) reveals structural similarities between an inflammasome and an apoptosome. (Faustin et al. 2007). *In vitro* studies tell us that a sufficient subset of NLRs can activate the inflammasome. NLRP1,2,3,6,12, NLRC4 and NOD2 when overexpressed with caspase-1 and ASC ectopically, facilitates the activation of caspase-1 and IL-1 $\beta$  processing (Davis et al. 2011, Martinon et al. 2002). The physiological role of most inflammasomes are still unclear, only a minority of these

protein have known characteristics and function, such as the NLRP3, NLRC4 and NAIP5. It is not very clear if at all the other NLRs have a role in inflammasome assembly. A structurally unrelated inflammasome known as the AIM2 (absent in Melanoma 2) sheds some light on inflammasome assemblage (Davis et al. 2011).

### **1.5.1 Structure and function**

The NLR and PYHIN family proteins can form inflammasomes. The NLR protein has three domains, a C-terminal leucine-rich repeat (LRR) domain, an intermediate nucleotide binding and oligomerization domain (NOD, also called NACHT domain), and a N terminal pyrin (PYD), caspase activation and recruitment domain (CARD) or a baculovirus inhibitor of apoptosis repeat domain (BIR). The LRR domains of these proteins are hypothesized to interact with putative ligands and play a role in autoregulation of these proteins. The NACHT domain can bind to ribonucleotides, which regulates the self-oligomerization and inflammasome assembly (Latz 2010, Martinon et al. 2002).

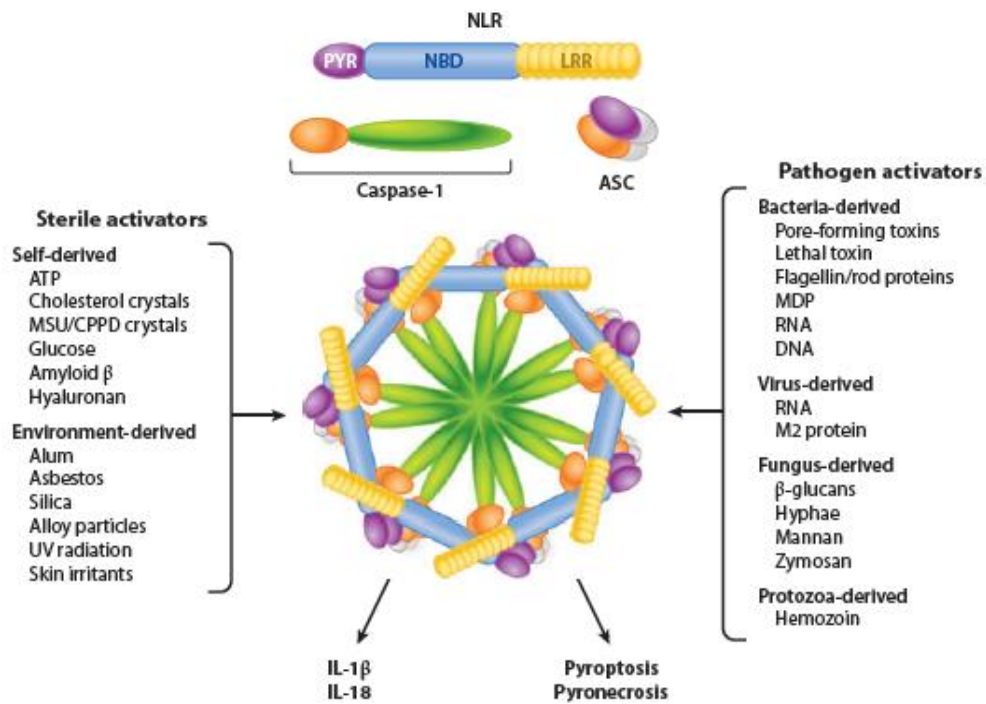


**Fig 1.14 Schematic Diagram of an Inflammasome and its activators.** The NLRs, ASC and Caspase-1 assemble to form the penta- or heptameric structure called the inflammasome resulting in the maturation of IL-1 $\beta$  and IL-18 as well as inflammatory cell death, by either pyroptosis or pyronecrosis. The two categories of inflammasome activators are sterile activators (host and environmental derived products) and pathogen-associated activators (PAMPs from bacteria, virus, fungus and protozoa) (Davis et al. 2011).

### 1.5.2 Mechanism of Activation

As a result of infection or injuries a multi-protein complex called the inflammasome is activated by Caspase-1, in the cytoplasm of the cell. Caspase-1 cleaves the pro-forms of interleukin-1 cytokine family members making them active and to be secreted from the cells. The IL-1 family is heavily involved in many pro-inflammatory activities and plays

a role in inflammatory disease pathogenesis. Although there are a few ligands discovered for NLRP1, IPAF, and AIM2 inflammasomes, not much is known about mechanisms of NLRP3 inflammasome activation. Various different molecular entities have been held responsible for the activation of NLRP3 inflammasome, such as extracellular ATP, pore forming toxins or viroporins, crystals and many others. New research suggest that NLRP3 activation is made possible indirectly by host factors that are generated in response to NLRP3 triggers (Latz 2010).

How the inflammasome is actually activated is still unclear, however there are different proposed models of activation. In these models the whole picture of a signal transduction pathways is not yet deciphered. Because of the presence of various different kinds of PAMPs, DAMPs and pathogens that activate the inflammasome, it is possible that multiple pathways exist.

“In addition, the transcriptional upregulation of limiting factors such as pro-IL1 $\beta$  and -IL18, which constitute signal 1, is a prerequisite for inflammasome activation. In addition to induced transcription of genes encoding procytokines, activation of NLRP3 transcription is also induced by NF- $\kappa$ B activators such as TLR ligands. Three models have been put forth to explain mechanisms of inflammasome activation.” (Davis et al. 2011)

Model 1 proposes the idea that NLRP3 inflammasome is activated by ROS (Reactive Oxygen Species) which is generated by PAMPs and DAMPs. It has been observed that many NLRP3-specific agonists induce the formation of ROS and when reactive oxygen compounds like Hydrogen Peroxide were added, it resulted in the formation and activation of NLRP3 inflammasome. Although there are different biological pathway that can activate ROS but not all of them has the ability to activate inflammasome. Additionally is ROS is inhibited it can cause NLRP3 inflammasome activation to be

suppressed (Meissner et al. 2008). It is still not clear where ROS is generated. A recent paper published tells us that, a protein called thioredoxin-interacting protein (TXNIP which is a redox sensitive protein) is involved in the pathway where ROS activates the inflammasome (Zhou et al. 2010). This is still highly controversial. So, in general the detailed mechanism by which ROS activates inflammasome need further clarification.

The second model of inflammasome activation involves formation of pores on the plasma membrane that is initiated either by P2X7 receptors or by pore forming toxins. These pore forming toxins also facilitate K<sup>+</sup> efflux and possibly the influx of small DAMPs or PAMPs. One of the definite causes for the initiation of inflammasome activation is K<sup>+</sup> efflux. All the three NLR inflammasome seems to be inhibited by hyperosmotic K<sup>+</sup> levels during lysis.

The lysosomal rupture model serves as our third model of inflammasome activation. Inflammasomes are believed to be activated due to the lysosomal damage, specifically due to Cathepsin B leakage. Pharmacologically if cathepsin B is inhibited, a drastic inhibition of inflammasome activation is noticed even in response to DAMP stimulation. Partial impairment of inflammasome activation is observed in mice deficient in cathepsin B; when they are treated with NLRP3 agonists. In vivo studies suggest that deficiency of either cathepsin B or L is a cause for decrease in inflammasome activation in response to cholesterol crystals. It is yet to be understood whether or not these pathways work independently or in concert in stimulation-dependent contexts (Davis et al. 2011).

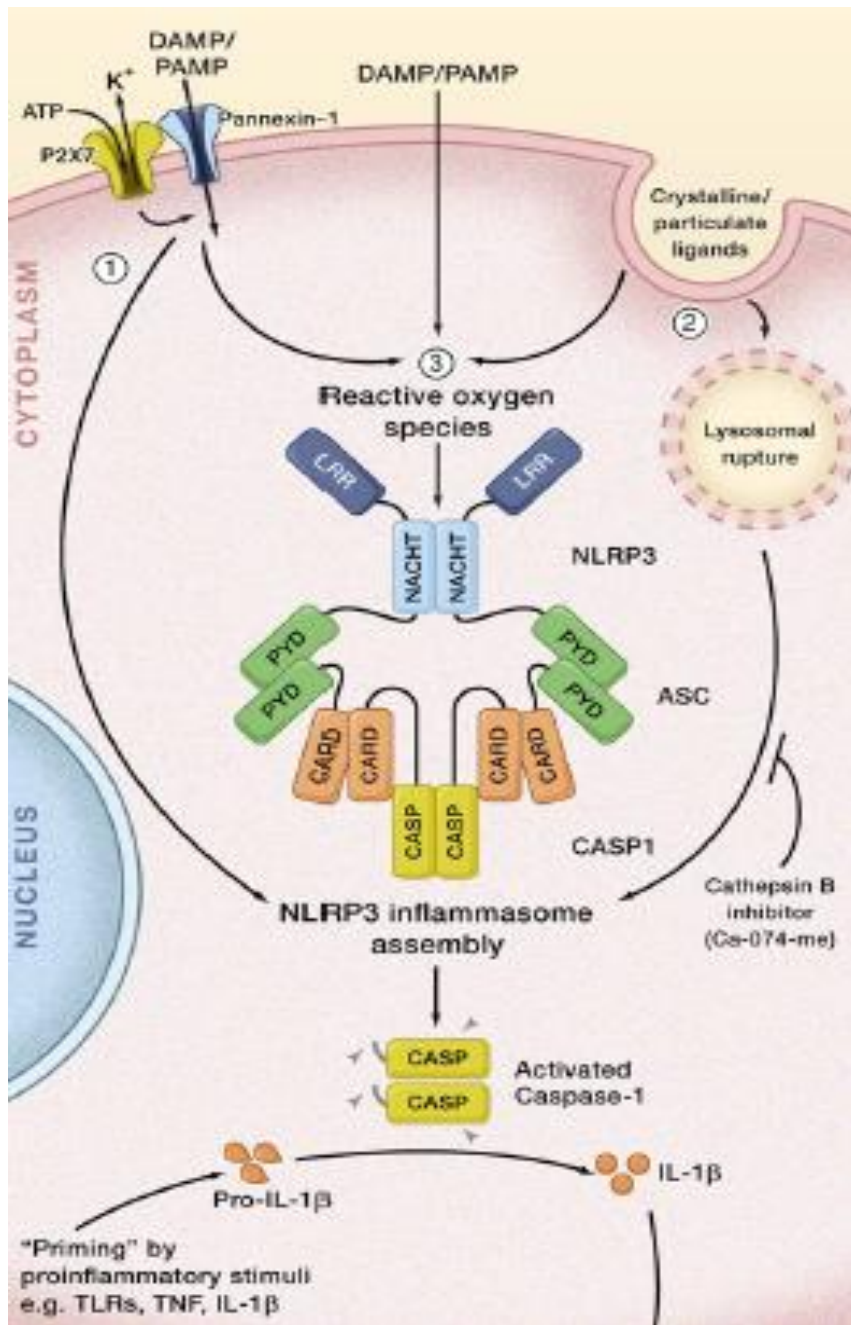


**Fig 1.15 NLRP3 inflammasome activation.** A suggested three way model of NLRP3 inflammasome activation detailed above. 1) ATP acts as a NLRP3 agonist triggering the formation of pores by the Pannexin-1 hemichannel which allows NLRP3 agonists to enter the cytosol and directly engage NLRP3. 2) Lysosomal rupture initiated by crystalline particles that are engulfed. Cytoplasmic lysosomal contents are sensed by NLRP3 by via cathepsin- B-dependent processing of a direct NLRP3 ligand. 3) Production of Reactive Oxygen Species (ROS) is triggered by PAMPs and DAMPs (including ATP, crystals). ROS in turn activates the NLRP3 inflammasome complex formation. Eventually clustering of Caspase-1 induces autoactivation results in secretion of pro-inflammatory cytokines (Schroder and Tschopp 2010).

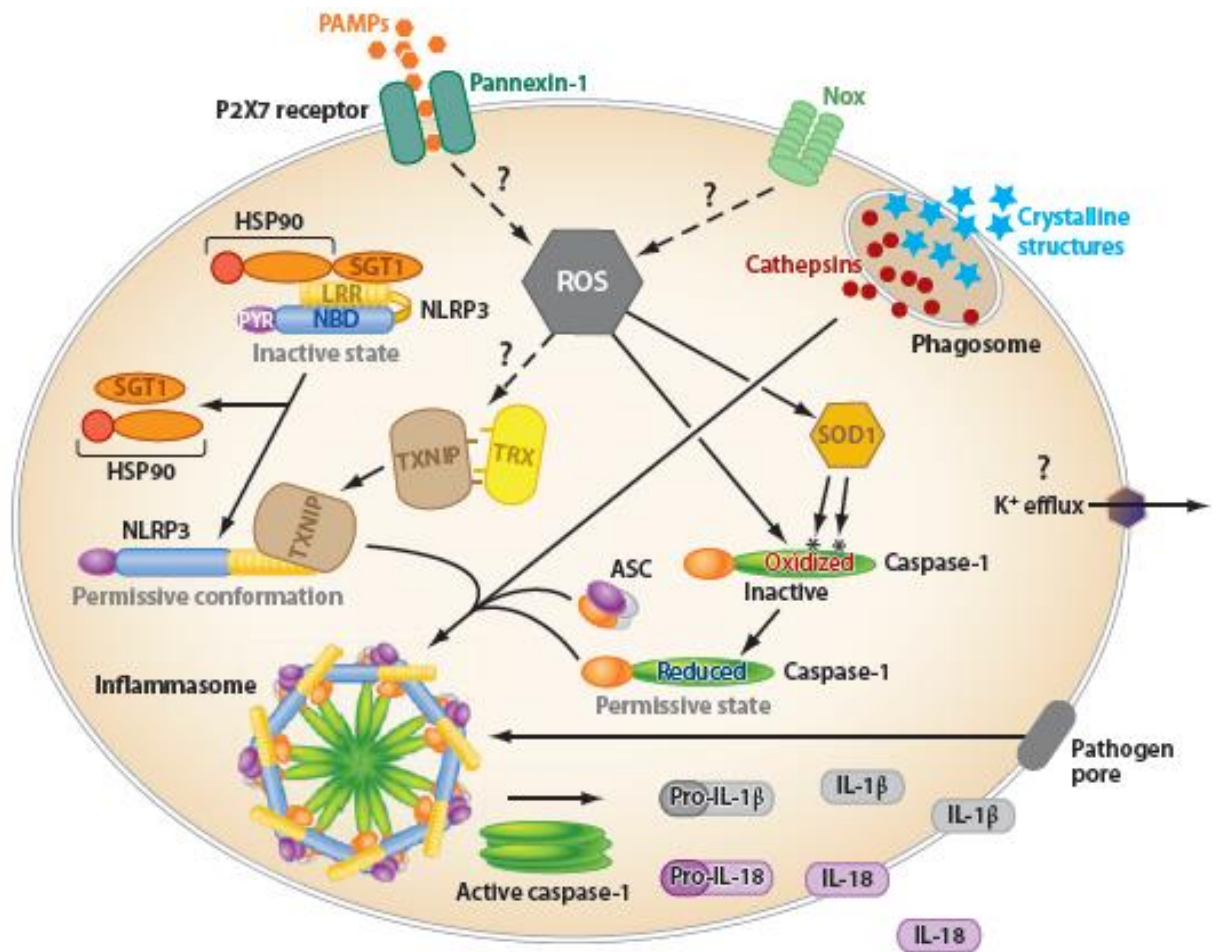


**Fig 1.16 Model of Inflammasome Activation.** Combination of a series of signals results in inflammasome activation. The models put forth above suggests that a wide variety of biological molecule which indirectly activates inflammasomes rather than a direct receptor-ligand pairing.

As we have explained before, the inflammasome needs 2 signals for its activation (namely signal 1 and 2). Studies by Shimada et al refers to the signal 1 as the primary cause of NFκB production and signal 2 being mitochondrial apoptosis, culmination of both of which causes the NLRP3 inflammasome to be activated. This results in the secretion of IL 1 β. In this case the secondary signal activator is claimed to be oxidised mitochondrial DNA (mtDNA) released into the cytosol due to ATP induced mitochondrial dysfunction and apoptosis. MtDNA binds to NLRP3 in the cytosol causing its activation. An antiapoptotic protein called Bcl2 inversely regulates mitochondrial dysfunction and preventing NLRP3 inflammasome activation. MtDNA is believed to directly interact and



activate NLRP3 inflammasome. We know this from experiments showing that macrophages that lack mtDNA had very little production of IL-1 $\beta$ , although it went through apoptosis. Oxidized nucleoside 8-OH-dG has a drastic inhibiting effect on the inflammasome-oxidised mtDNA binding. Shimada and group infers that oxidized mtDNA which is released during programmed cell death causes the NLRP3 inflammasome to be activated. This provides us with a clue in deducing the apoptosis-inflammasome activation signal. (Shimada et al.).

### **1.5.3 Types of Inflammasome**

#### **1.5.3.1 NLRP 1**

Expression levels of NALP1 are comparatively lot less in a cell than NLRP3 or NLRC4, and is generally found in adaptive immune cell and non-hematopoietic tissues. Human NLRP1 gene encodes an N-terminal CARD domain, a central NACHT, LRR, FIIND, and a C-terminal CARD. This structural layout is unique to NLRP1 (Davis et al. 2011). NLRP1 forms a macromolecular complex after interacting with Caspase-1 and -5 and also possible with ASC, in cell free lysates (Martinon et al. 2002). This complex promotes the processing of IL-1 $\beta$ /IL-18 and also pyroptosis. NLRP1 also interacts with caspase-2 and 9 triggering the formation of an apoptosome eventually resulting in cell death (Hlaing et al. 2001). Because it hasn't been possible yet to obtain Nlrp1  $-/-$  mouse model much of its physiological relevance and mechanism of interaction is still unknown (Davis et al. 2011).

Experiments on murine models suggests that NLRP1 may be involved in the sensing of the bacterial toxin LT which is one of the major virulence factor from the bacteria *Bacillus anthracis*.

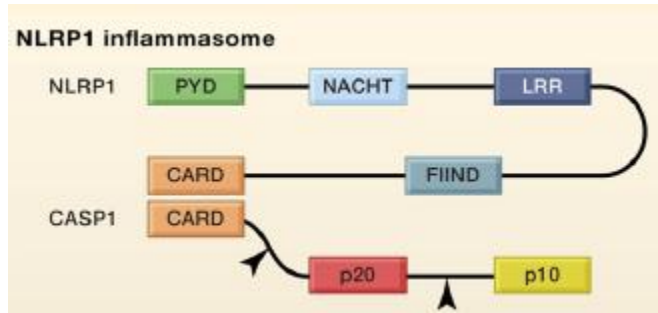


**Fig 1.17 Minimal model for NLRP1 inflammasome.** Depicted above in an unoligomerized inflammasome complex. Domains: CARD, caspase recruitment domain; LRR, leucin rich repeats; NACHT, nucleotide-binding and oligomerization domain; PYD, pyrin domain, FIIND, domain with function to find; HIN, HIN-200/IF120x domain (Schroder and Tschopp 2010).

### 1.5.3.2 NLRP 3

Also known as cryopyrin or NALP3, has been shown to be expressed in myeloid cells and its upregulation is observed when macrophages are stimulated with PAMPs. (O'Connor et al. 2003). The NLRP3 gene encodes for proteins that has an N-terminal pyrin domain, a central NBD domain and C-terminal LRR domain (Hoffman et al. 2001). NALP 3 does not contain a caspase recruitment domain (CARD) and cannot recruit procaspase-1 unless the adaptor molecule ASC is present. A pyrin domain is responsible for NLRP3s interaction with ASC. NLRP3 although interacts with CARD8 the role of which is not understood yet (Allen et al. 2009). NLRP3 also activates caspase-1 in the presence of ASC (Agostini et al. 2004). Programmed inflammatory cell death and secretion of IL-1 $\beta$ /IL-18 are some of the obvious consequences of NLRP3 inflammasome activation.

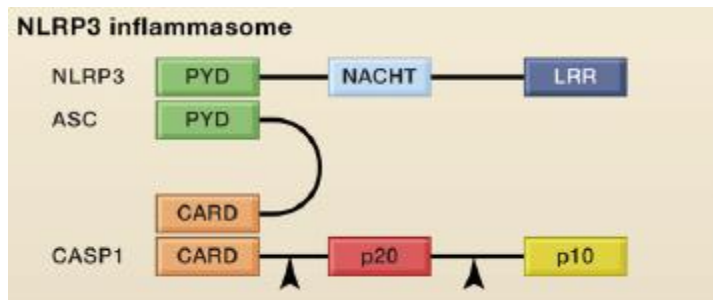


**Fig 1.18. Minimal model for NLRP3 inflammasome.** Depicted above in an unoligomerized inflammasome complex. Domains: CARD, caspase recruitment domain; LRR, leucin rich repeats; NACHT, nucleotide-binding and oligomerization domain; PYD, pyrin domain (Schroder and Tschopp 2010).

### 1.5.3.3 NLRC 5

The NOD like receptors (NLRs) are receptors found intracellularly, and NLRC5 is the largest among them and is widely expressed. It has been recently identified to regulate immune responses. NLRC5 is induced by interferons during a pathogenic invasion and is also known to be a master regulator of major histocompatibility complex (MHC) class I genes (Yao and Qian 2013).

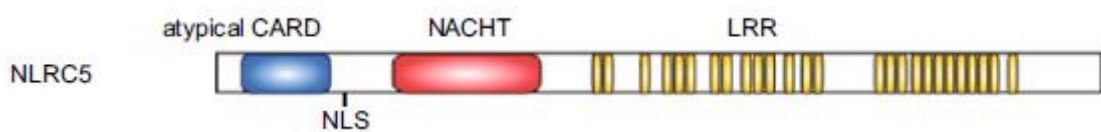


**Figure 1.19 Structural Domain of NLRC5.** NLRC5 has typical tripartite domains including the N-terminal atypical caspase activation and recruitment domain (CARD), the centrally located NACHT (named after NAIP, CIITA, HET-E, and TP-1 proteins) and multiple leucine rich repeats (LRRs) at the C-terminal. Obtained from (Yao and Qian 2013).

A subgroup of NLRs can form an inflammasome complexes and NLRC5 is one of them facilitating conversion of pro-caspase 1 into caspase-1 and a production of IL-1 $\beta$  and IL-18 (Tschopp et al. 2003). Although the exact mechanism of how the NLRC5

inflammasome works is not understood, it is associated with the NLRP3 inflammasomes and the activators of both are similar. NLRC5 is predominantly found in hematopoietic cells and inflammasome study has not been conducted. However RNAi experiments suggests that knocking down NLRC5 abrogates the production of pro-inflammatory cytokines such as IL-1 $\beta$  and IL-18 and also Caspase-1, in response to bacterial infections, PAMPs, DAMPs and also viruses. Colocalization of NLRP3 and NLRC5 is also observed in a few studies (Triantafilou et al. 2013a). Together they are known to activate inflammasome in Bronchial cells in response to HRV infection (Triantafilou et al. 2013a)

#### 1.5.3.4 AIM 2

AIM2 [also known as PYHIN4], belong to the HIN-200 family member which is a double stranded DNA (ds DNA) sensors that induces IL-1 $\beta$  maturation through activating Caspase-1, which is a common characteristics of inflammasomal activity (Tschopp et al. 2003). AIM2 is the first member which does not belong to the NLR family but forms an inflammasome scaffold. “oligomerization of the complex is suggested to be mediated not by a central oligomerization domain within the inflammasome scaffold protein (as for the NLR NACHT domain) but by clustering upon multiple binding sites in the ligand, dsDNA, to which AIM2 binds via its C-terminal HIN domain (Tschopp2011) (Bürek et al., 2009; Fernandes- Alnemri et al., 2009; Hornung et al., 2009).”

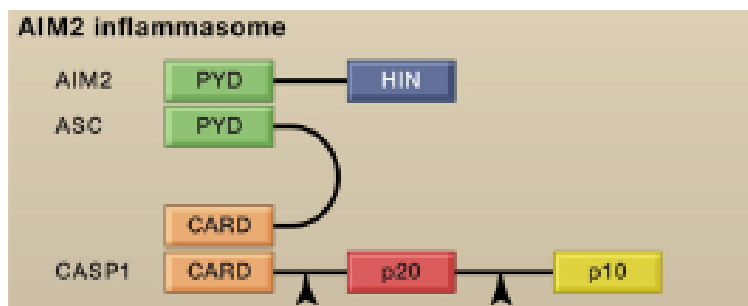


**Fig 1.20 Minimal model for AIM2 inflammasome.** Depicted above in an unoligomerized inflammasome complex. Domains: CARD, caspase recruitment domain; PYD, pyrin domain.

The AIM2 inflammasome consists of AIM2, Caspase-1, ASC as well as a PYD domain which interacts with the ASC homotypically; PYD-PYD interaction. The ASC CARD domain recruits procaspase-1 to the complex. In other inflammasomes, once its autoactivated, caspase-1 directs the maturation of proinflammatory cytokines and their secretion (IL-1 $\beta$  and IL-18). The AIM2 inflammasome is activated by dsDNA from viruses, bacteria or the host itself (Hornung et al., 2009; Muruve et al., 2008) (tschopp2011). The physiological relevance of AIM2 needs further study and investigation, currently its known to predominantly act as a cytosolic DNA virus sensor.

#### **1.5.4 Virus recognition by Inflammasomes**

Three distinct inflammasome complexes are known at present to be involved in antiviral immunity. They are the NLRP3 inflammasome (Allen et al. 2009, Kanneganti 2010), the RIG-I inflammasome (Poeck et al. 2010) and the AIM2 (Burckstummer et al. 2009, Hornung et al. 2009) inflammasome. The link between these three inflammasomes and the pro-form of caspase-1 is the 22kDa adaptor protein called the apoptosis-associated speck-like protein that contains a CARD (ASC). As mentioned before the activated caspase-1 cleaves pro-IL-1 $\beta$  and pro-IL-18 into biologically active IL-1 $\beta$  and IL-18. After secretion of these active cytokines from the cells a series of biological effects take place that includes inflammation and infection associated autoimmune processes. The following table shows a list of viruses that activates Caspase-1 and induces IL-1 $\beta$  and IL-18 production.

NLR or inflammasome component (alternative name)	Signalling pathways activated during viral infection	Viruses recognized	Viral PAMP recognized
NLRP3	Inflammasome	Influenza virus, Sendai virus, adenovirus, vaccinia virus and encephalomyocarditis virus	RNA
RIG-I	MAVS and inflammasome	Vesicular stomatitis virus, hepatitis C virus, Japanese encephalitis virus, rabies virus, measles virus, respiratory syncytial virus, influenza virus and Sendai virus	5'-triphosphate single-stranded RNA
AIM2	Inflammasome	Vaccinia virus and mouse cytomegalovirus	Cytosolic DNA
NOD2 (NLRC2)	MAVS and OAS2	Respiratory syncytial virus, influenza A virus, parainfluenza virus 3 and vesicular stomatitis virus	Single-stranded RNA
NLRX1	MAVS	Sendai virus and Sindbis virus	Exact sensing capacity is unknown
NLRC5	RIG-I, MDA5 and NF-κB	Sendai virus, vesicular stomatitis virus and cytomegalovirus	Poly(I:C)

**Table 3 Inflammasomes and their corresponding NLRs that are involved in recognising viral infection** (Kanneganti 2010). AIM2, Absent in melanoma 2; MAVS, mitochondrial antiviral signalling protein; MDA5, melanoma differentiation-associated antigen 5; NLRP3, NLR family PYD containing protein 3; NLRX1, NLR family member X1 protein; OAS2, 2'-5'-oligoadenylate synthetase type 2; poly(I:C), polyinosinic-polycytidylic acid; RIG-I, retinoic acid inducible gene-I.

The following is a short summary of how the intracellular sensors of the innate immune system works when it comes to viral recognition and an eventual activation of inflammasomes causing the release of pro-inflammatory cytokines. PAMPs, also known as pathogen associated molecular patterns after recognising the presence of pathogens (virus in this case) activates the NOD-like receptors (NLRs). This in most cases mean that the inflammasome complex is formed and its assemblage, which has an eventual outcome of pro-inflammatory cytokine production, thereby amplifying antiviral response.

NLRP3 and AIM2 in the presence of PAMPs oligomerize and recruit the adapter protein ASC which has a caspase recruitment domain (CARD). The CARD of both ASC and pro-

caspase-1 binds to each other activating caspase-1 and results in the cleavage of pro-IL1 $\beta$  and pro-IL-18 into IL-1 $\beta$  and IL-18 respectively (Kanneganti 2010).

The RNA helicase domain of RIG-I senses single stranded RNA (ssRNA) through the 5'triphosphate moiety of the RNA strand of the viral genome. Signalling occurs through the N-terminal CARD domain of RIG-I which interacts with the CARD domain of the adapter molecule mitochondrial antiviral signalling protein (MAVS). This is followed by interferon (IFN) response factor 3 (IRF3) and IRF7 to be phosphorylated and activated. These in turn, turns on the transcription of type I IFN (IFN $\alpha/\beta$ ) genes (Kanneganti 2010).

RIG-I also regulates IL-1 $\beta$  production transcriptionally and post-translationally following recognition of 5'-triphosphate double-stranded (ds) RNA. Whereas RIG-I-triggered transcription of pro-IL-1 $\beta$  depends on nuclear factor- $\kappa$ B (NF- $\kappa$ B) activation and is mediated by MAVS, inflammasome formation, caspase-1 activation, and IL-1 $\beta$  and IL-18 production in response to RIG-I activation involve ASC. The NLRs NOD2, NLR family member X1 (NLRX1) and NLR family CARD-containing protein 5 (NLRC5) associate with MAVS. Whereas NOD2 mediates the induction of type I IFNs, NLRX1 and NLRC5 inhibit RIG-I–MAVS interactions and thereby negatively regulate type I IFN production. LRR, leucine-rich repeat; MAPK, mitogen-activated protein kinase; MYD88, myeloid differentiation primary-response protein 88; RIPK2, receptor-interacting serine-threonine protein kinase 2; ROS, reactive oxygen species; TLR, Toll-like receptor; TNF, tumour necrosis factor; TRIF, TIR-domain-containing adaptor protein inducing IFN $\beta$  (Kanneganti 2010).

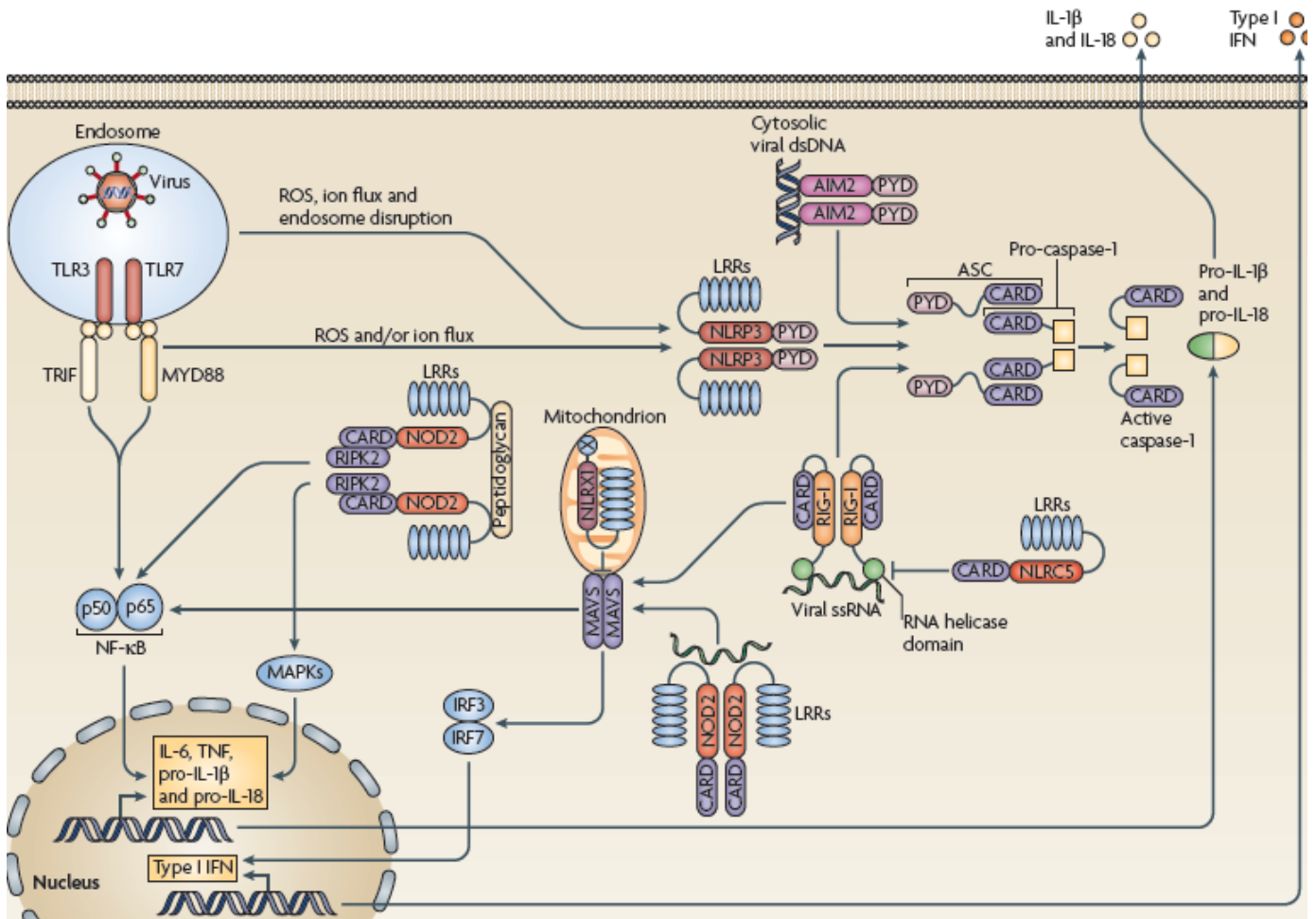


Figure 1.21 Innate immune response to viruses by intracellular sensors.



## **1.6 Viroporins**

Viral Ion channels also generally known as Viroporins are short peptide chains containing 50-120 amino acids and play a very important role in the regulation of cellular processes and also viral entry into the cell as well as assembly of the virions. These small proteins also modulate and change the electrochemical balance in cell compartments of the host cell (Wang K. et al. 2011). There are several features of viroporins that they have in common including their small size and their hydrophobic nature, membrane permeabilization being a very typical trait which occurs when they oligomerize. Their main role is to participate in virus assembly and release of viruses from infected cells. If a viroporin encoding gene is deleted from the viral genome, there is a drastic reduction of viral pathogenicity and the formation of viral progeny. This gives a clear idea of its functions (Gonzalez and Carrasco 2003).

General features of viroporins include a highly hydrophobic domain able to form an amphipathic alpha-helix. The component proteins are inserted into the membrane and they oligomerize to form a hydrophilic pore. The hydrophobic 'aa' residues face the lipid bilayer and the hydrophilic residues form a part of the pore. There are many other additional features of viroporins which make them unique, such as an additional hydrophobic region interacting with the membrane. Potentially this can cause the membrane to be disorganised. Sometimes the viroporin may have a stretch of 'detergent like acting' basic aa. These factors may cause membranes to destabilize (Gonzalez and Carrasco 2003).

### 1.6.1 Viroporins as Channel Proteins

The virus encoded ion channel, viroporins represent only one factor taking part in the cascade of interactions between virus and cells, which leads to the virus entering the cell, replication and make profound changes in membrane permeability (Ciampor 2003). As the name suggests, viroporins forms pores in cell membranes and internal organelles enhancing membrane permeability which is noted in several virus-cell system. There are a couple of different modes of membrane ‘leakiness’ observed which have been distinguished according to the time of infection. During viral entry, early membrane modification occurs independent of gene expression since these alterations are caused by the virion’s components (Gonzalez and Carrasco 2003). During the course of the infection many different viral products have the capacity to affect the cell membrane. Viroporins are one of them which are responsible, at least to some extent for causing membrane leakiness that happens late in infection (Gonzalez and Carrasco 2003).

Virus family	Viroporin	AA residues
Picornaviridae	Poliovirus 2B	97
	Coxsackievirus 2B	99
	Poliovirus 3A	87
Togaviridae	SFV 6K	60
	Sindbis virus 6K	55
	Ross River virus 6K	62
	HIV-1 Vpu	81
Paramyxoviridae	HRSV SH	64
Orthomyxoviridae	Influenza A virus M2	97
Reoviridae	ARV p10	98
Flaviviridae	HCV p7	63
Phycodnaviridae	PBCV-1 Kcv	94
Rhabdoviridae	BEFV alpha 10p	88

**Table 4 List of viroporins along with the length of their amino acid residues** (Gonzalez and Carrasco 2003).

Narrowly speaking, the fact that different kinds of viral proteins are able to modify membrane permeability, defines the activity of a viroporin. Some viral glycoproteins have an architectural advantage in the formation of a physical pore when they oligomerize. In theory, peptides may fuse together to form a physical viral glycoprotein pore that acts in conjugate with transmembrane domains. When inserted, the fusion peptide would create a pore in the virion membrane. More so, domains adjacent to the transmembrane region could be replaced by the pore forming glycoproteins, while other viruses may have no viroporin activity.

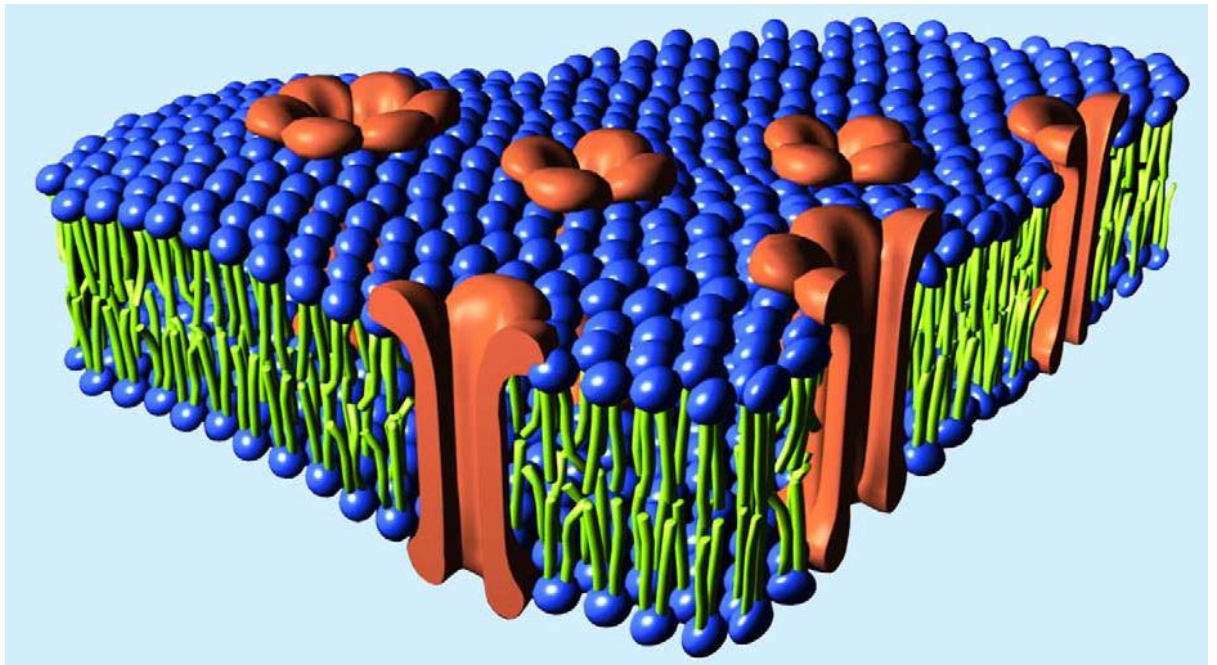


**Fig 1.22 Schematic presentation of the pore formation by viroporins (Gonzalez and Carrasco 2003)**

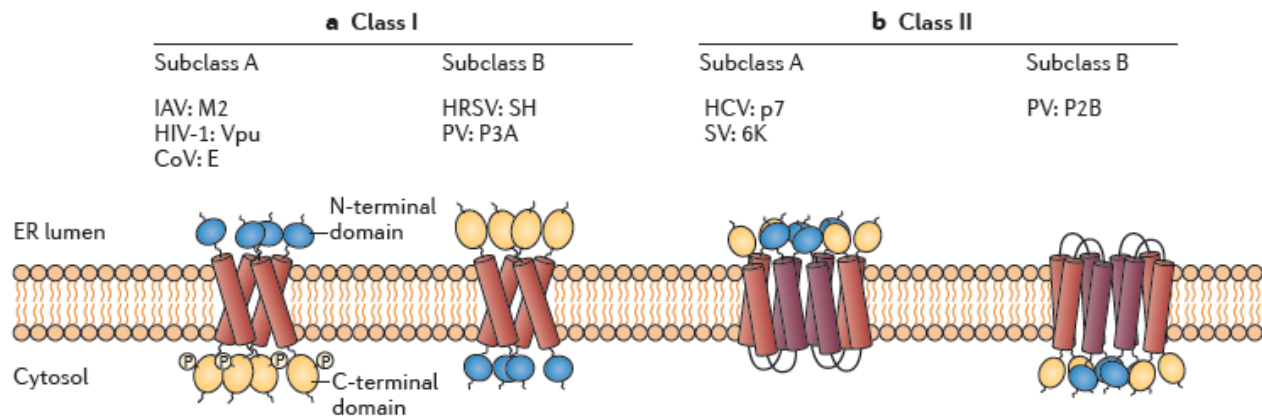


**Fig 1.23 Viroporin classification** depending on the number of transmembrane domains they contain and the membrane topology of the monomers. a) Class I viroporins are characterised by its single membrane-spanning domain. There are proteins inserted inside the membranes that differentiates between the A and B subclasses. Class IA has proteins with luminal amino terminus and cytosolic carboxyl terminus whereas class IB has an opposite orientation. b) Class II viroporins have transmembrane helix-turn-helix hairpin motifs. In subclass A both the N and C terminals of the proteins are luminal whereas in subclass B the N and C terminals are facing the cytosol. (Nieva et al. 2012).

### 1.6.2 Viroporin 2B

It has been demonstrated by (Ito et al. 2012) that the Encephalomyocarditis virus (EMCV) which is a positive strand RNA virus of the Picornaviridae family activates the NLRP3 inflammasome in mouse dendritic cells and macrophages. When macrophages were infected with live EMCV or they were transfected with EMCV virions, a robust expression of Type I interferons was noticed. But this failed to produce any IL-1 $\beta$ . However, when the EMCV viroporin 2B was transfected into lipopolysaccharide primed macrophages, NLRP3 inflammasome activation is prominent. In un-transfected cell or transfected cells (with protein 2A and 2C, which are non-structural), NLRP3 is found to be uniformly distributed throughout the cytoplasm. In transfected cells however with the viroporin 2B, NLRP3 is observed to co-localize in the perinuclear space (Ito et al. 2012). A similar observation is made with the Influenza M2 viroporin (Pinto et al. 1992).

Elevation of the intracellular  $\text{Ca}^{2+}$  level is a very typical characteristic effect caused by the picornaviridae 2B, but not mitochondrial reactive oxygen species and lysosomal cathepsin B, was important in EMCV-induced NLRP3 inflammasome activation (Ito et al. 2012). Virus induced IL-1 $\beta$  secretions were not reduced even after chelation of extracellular Calcium. These results indicate and confirm that, like many other viroporins and specially Picornaviridae 2B has the capacity to independently activate the NLRP3 inflammasome resulting in the production of IL-1 $\beta$  subtraction and potential inflammation (Gonzalez and Carrasco 2003, Ito et al. 2012, Madan et al. 2010).

Triantafilou and group (2013) demonstrates that the Rhinovirus 2B viroporin acts in a very similar way. NLRP3 in untransfected bronchial epithelial cells (BES) is found generously scattered around the cytosol but co-localizes to the Golgi and ER upon 2B transfection. The same happens for NLRC5. Subsequently the NLRP3 and NLRC5 inflammasomes are activated resulting in the production of IL-1 $\beta$ . Rhinovirus 2B also causes  $\text{Ca}^{2+}$  reduction in these organelles thus disturbing the intracellular calcium homeostasis. The NLRP3 and NLRC5 act in a cooperative manner during the inflammasome assembly by sensing intracellular  $\text{Ca}^{2+}$  fluxes and trigger IL1 $\beta$  secretion. These results reveal for the first time that human rhinovirus infection in primary bronchial cells triggers inflammasome activation (Triantafilou et al. 2013a). This study has been described in details in later chapters which is also the main scope this research.

### **1.6.3 Viroporin M2**

The M2 protein is encoded from a small part of the Influenza virus RNA genome (Lamb and Pinto 1997). Another protein called the M1 is encoded by this RNA fragment although the synthesis of these proteins occur in different mRNAs, generated by differential splicing. The M2 protein is 96 amino acid long and is classed under a type III integral membrane phosphoprotein. It's structurally divided into three regions: a 23

residue fragment which is extracellular, a transmembrane domain which is 19 amino acid long. The cytoplasmic tail is composed of 54 residues (Lamb and Pinto 1997). The M2 protein homo-oligomerises and is active in its tetrameric form. Studies in the *Xenopus laevis* oocyte led us to elucidate the functionality of the M2 protein (Pinto et al. 1992).

#### **1.6.4 Viroporin SH**

The RSV genome contains a negative stranded RNA of about the size of ~15kb transcribing 11 proteins and three membrane proteins. One of these membrane proteins is the SH which is categorised as a viroporin. The other two membrane proteins are the F and G which are essential for viral entry, attachment and fusion. However it is less clear as to what part the SH protein plays, since RSV that lacks SH (RSV $\Delta$ SH) is still viable (Krusat and Streckert 1997) and also forms syncytia (Collins and Mottet 1993). The SH protein is 64 aa long in RSV subgroup A and is 65 aa long in RSV subgroup B. It is a type II integral membrane protein with an extracellular facing C terminus and an  $\alpha$ -helical trans-membrane domain (TM), with a very highly conserved sequence (Gan et al. 2012). The RSV SH protein co-localises at the membranes of the Golgi complex and the ER in an infected cell. It is also found in the plasma membrane (Rixon et al. 2004). There are several forms of the SH viroporin that it exists in, e.g. full length truncated form (4.5kDa), and a post translationally modified form. The most prevalent form is the full length unmodified form (Collins and Mottet 1993). The RSV small hydrophobic protein has been classified as a viroporin which alters membrane permeability displaying properties of a cation-selective ion channel.

Studies have shown that SH plays an essential role in triggering signal 2 leading to caspase 1 production and inflammasome activation (Triantafilou et al. 2013b)

### **1.6.5 Other Viroporins**

Apart from the viroporins that are described above, there are many other examples of such which have received very less attention. The typical viroporin structure matches or have very high resemblance to a lot of other animal virus proteins. Sometimes they have been even found to have the membrane permealization property that a classical viroporin structure suggests. Such an example is of the p7 (small hydrophobic protein) resembling the alphavirus 6K, encoded by a species of Flaviviridae family. P7 from the Human hepatitis C virus (HCV) associates with intracellular compartments of the secretory pathways. Some has been also found to localize in the plasma membrane {Harada, 2000}. P7 forms a hexamer functioning as a Calcium channel in black lipid membranes. Algae virus encodes a potassium channel protein corresponds to Kcv protein from *Paramecium bursaria chlorella virus* (PBCV-1). Kcv localizes more at the ER and less in the Golgi and forms a two membrane spanning domains linked by 44 amino acids.

## 1.7 Aims and Hypothesis

Viruses and bacteria elicit a very strong innate immune response once they are detected by the plethora of germ line encoded proteins which are a part of the innate immune system. One of its first lines of defence is to detect Pathogen Associated Molecular Patterns (PAMPs) using Pattern Recognition Receptors (PRRs) such as the Toll-Like Receptors (TLRs), the RIG-Like Helicases (RLHs) and the Nod-Like Receptors (NLRs). These receptors recognize certain molecular structures from the pathogens and lead to first line of defence which induces increased cytokines and IFNs.

The aim of this study is to delineate how the innate immune system responds to viral invasion such as HRV (Human Rhinovirus), RSV (Respiratory Syncytial Virus) and IAV (Influenza A virus). Inflammatory mediators such as interleukins and cytokines which are secreted as a result of these invading viral pathogens are responsible for disease pathogenesis and lung injury. *In vivo* experiments carried on various kinds of lung tissue for this study suggests the same and sheds light on cellular mechanisms that cause lung inflammation. This study aims to understand and identify intracellular macromolecular complexes called inflammasomes that is known to assemble as a result of viral trigger. Inflammasomes convert the inactive forms of the pro-inflammatory cytokines to their active forms. Although the exact mechanism of activations of these complexes was unknown and finding the trigger is one of the scopes of this study. Here, we aim to identify that virus encoded proteins such as the 2B protein of HRV, the SH protein from RSV and the Influenza M2 which are also termed viroporins can activate the inflammasome by causing ion imbalance (across cells membranes and organelles) thus providing a trigger for inflammasome assembly and an eventual release of inflammatory cytokines.



There is emerging evidence that points towards the fact that ion flux can act as trigger to the activation of inflammasomes and a subsequent release of IL-1 $\beta$ . When this happens in the lungs due to respiratory viral infections, disease pathogenesis progresses to developing lung disease such as COPD, Asthma and wheezing etc. This study hypothesises that viroporins such as the HRV- 2B, RSV- SH protein and the M2 protein of the Influenza virus are responsible for the changes in the intracellular ion homeostasis (such as Na<sup>+</sup> and K<sup>+</sup> and also Ca<sup>2+</sup>) that modulates inflammasome activation and cell death in the lung. We propose therapeutic interventions; that by blocking these ion channels using drugs, we inhibit inflammasome assemblage that proves beneficial in terms of drastic reduction in lung inflammation. By inhibiting the activity of electrogenic pumps (for example the Na<sup>+</sup>/K<sup>+</sup>/ATPase and Ca<sup>2+</sup> transport pumps) using drugs such as Adamantyls and Verapamil etc. respectively (*in vitro*) we demonstrate the potential of using these drugs to combat lung disease in the near future.

## **CHAPTER 2**

### **MATERIALS AND METHODS**

## **2.1 Materials**

### **2.1.1 Chemicals**

All fine chemicals were obtained from Sigma (UK).

### **2.1.2 Plasmid**

pEF1alpha-Myc Vector was purchased from Clontech. The 2B coding sequences for HRV14

were amplified and cloned into p2B-myc construct using *Sal*I and *Bam*HI restriction sites as

described in de Jong et al.

The ER targeted construct p2B-Flag-KKAA and the Golgi targeted p2B-Flag-AAAA were

constructed using a forward primer containing a *Bam*HI restriction site ( 5'-  
gggggggggattcatcgccaccgtcagcaagggcgaggag-3') and a reverse primer containing a stop  
codon, a *Not*I restriction site and a sequence encoding either the AAAAAAKKAA or the  
AAAAAAAAAAA tag 5'-

ggggggggcgggccgcttacgccgcttcttagctgaggctgccgcgccctgtacagctcgtccatgcc-3' and 5'-

ggggggggcgggccgcttacgccgagcagcagctgaggctgccgcgccctgtacagctcgtccatgcc-3',

respectively).

The PCR product was cloned into p2B-Flag as described in de Jong et al.

### 2.1.3 List of Antibodies

- 2B Mouse Polyclonal IgG, purchased from Santa Cruz Biotechnology
- Caspase-1 (P-10) Rabbit Polyclonal IgG, purchased from Santa Cruz Biotechnology sc-515
- IRF-3 (FL-425) Rabbit Polyclonal IgG, purchased from Santa Cruz Biotechnology sc-9082. 65
- LGP2 Goat pAb to DHX58, purchased from Abcam ab82151.
- LGP2 (H-159) Rabbit Polyclonal IgG, purchased from Santa Cruz Biotechnology sc-134667.
- MDA5 (C-16) Goat Polyclonal IgG, purchased from Santa Cruz Biotechnology sc-48031.
- MDA5 (H-61) Rabbit Polyclonal IgG, purchased from Santa Cruz Biotechnology sc-134513.
- NALP1 Mouse Polyclonal IgG, purchased from Santa Cruz Biotechnology sc-
- NLRP3 Rabbit Polyclonal IgG, purchased from Santa Cruz Biotechnology sc-
- Phospho-I $\kappa$ B $\alpha$  (Ser32) (14D4) Rabbit mAb, purchased from Cell Signaling Technology #2859L.
- Rabbit Anti-Goat Polyclonal Immunoglobulins FITC, purchased from DAKO F0250.
- RIG-I (C-15) Goat Polyclonal IgG, purchased from Santa Cruz Biotechnology sc-48929 .
- RIG-I (H-300) Rabbit Polyclonal IgG, purchased from Santa Cruz Biotechnology sc-98911.
- Streptavidin-HRP conjugate, purchased from Amersham Biosciences 1058765.

- Swine Anti-Rabbit Polyclonal Immunoglobulins FITC, purchased from DAKO F0205.
- Swine Anti-Rabbit Polyclonal Immunoglobulins HRP, purchased from DAKO P0217.
- TLR2 Goat Polyclonal IgG, purchased from Santa Cruz Biotechnology sc-8690
- TLR3 Rabbit Polyclonal IgG, purchased from Santa Cruz Biotechnology sc-10740
- TLR4 Goat Polyclonal IgG, purchased from Santa Cruz Biotechnology sc-8694
- TLR7 Goat Polyclonal IgG, purchased from Santa Cruz Biotechnology sc-
- TLR8 Goat Polyclonal IgG, purchased from Santa Cruz Biotechnology sc-

#### **2.1.4 RNA interference**

RNA interference was used in order to silence the NLRC4, NLRC5, NLRP1, NLRP3 genes. Different pshRNA clones were generated using the psh7SK vector from Invitrogen the most efficient was against the sequence: for NLRP3 GGAAGTGGACTGCGAGAAGTT, for NLRC5, GAACCTGTGGAGCTGTCTTGT and GCAACAGCATCTGCGTGTC, for NLRC4, GGATGCTGCTAGAGGGATCAT and GACAACCTGGGCTCCTCTGTAA for NLRP1, GAAGGAGGAGCTGAAGGAGTT and GGCCTGATTATGTGGAGGAGA.

For TLR4 GCCAGGAGAACTACGTGTGAA and for TLR2 GTCAATTCAGAACGTAAGTCA.

Cells ( $1 \times 10^5$ ) were seeded in six well plates and transfected with 0.5  $\mu$ g of pshRNA for either NLRC4, NLRC5, NLRP1, NLRP3, TLR2, TLR4 or scrambled shRNA as a control using Lipofectamine 2000® (Invitrogen). After 48h the level of silencing was determined

by western blotting. Transfections with the specific shRNAs resulted in an approximately 80% decrease in receptor expression as determined by western blotting whereas transfection of cells with the scrambled shRNA did not show any decrease in the specific gene expression.

## **2.2 Tissue Culture**

The following basic tissue culture technique was used throughout the project. All Tissue Culture (TC) was performed in a Microflow Class 2 laminar flow hood in a sterile environment. To clean work surfaces and equipments, aqueous solution of Virkon was used, in order to maintain and ensure sterility. Lab coat, disposable gloves and overshoes were worn at all times. 25 cm<sup>2</sup> Nuclon® TM Surface flasks and Nunc Falcon tubes were used throughout.

### **2.2.1 Cell Lines**

#### **2.2.1.1 A549 Human Cell Line**

A549 (adenocarcinomic human alveolar basal epithelial cells) cell line (ECACC – European Collection of Animal Cell Cultures), maintained in 1g/L Glucose Dulbecco's Modified Eagle's Medium (DMEM), containing GlutaMAX, 10% heat-inactivated Foetal Calf Serum (FCS), and 1% non-essential amino acids (Invitrogen (UK)).

#### **2.2.1.2 BES Human cell line**

Bronchial Epithelial Spheroids (BES) cell line (ECACC – European Collection of Animal Cell Cultures), maintained in 1g/L Glucose Dulbecco's Modified Eagle's Medium

(DMEM), containing GlutaMAX, 10% heat-inactivated Foetal Calf Serum (FCS), and 1% non-essential amino acids (Invitrogen (UK)).

### **2.2.1.3 Human Primary cells**

Human Primary Bronchial Epithelial cells were isolated from the surface epithelium bronchi of three healthy donors and obtained from TCS cell works, UK. The cells were cryopreserved at passage 2 and were cultured and propagated for up to 14 doublings before senescence. The bronchial epithelial cells stained positive for cytokeratin. They were grown in T25 ECM-coated flasks in 5% CO<sub>2</sub> and 37°C using the Airway epithelial cell medium provided by TCS.

### **2.2.1.4 HEK-Blue IFN- $\alpha$ / $\beta$ Cells**

HEK-Blue IFN- $\alpha$ / $\beta$  cells were purchased from Invivogen USA and maintained in DMEM, 4.5 g/l glucose, 2-4 mM L-glutamine, 10% (v/v) fetal bovine serum, 50  $\mu$ g/ml penicillin, 50  $\mu$ g/ml streptomycin, 100  $\mu$ g/ml Normocin.

The way that these cells work to detect human type I interferon production is by monitoring the activation of the ISG3 pathway. This is a HEK293 cell line which has been transfected with human STAT2 and IRF9 genes in order to obtain fully active human STAT2 and IRF9 genes. These cells were again transfected with a SEAP reporter gene. This gene is under the control of IFN- $\alpha$ / $\beta$  inducible ISG54 promoter. When the HEK-Blue IFN- $\alpha$ / $\beta$  cells are stimulated by IFN- $\alpha$  or IFN- $\beta$ , the JAK/STAT/ISGF3 is activated.

This results in the subsequent production of SEAP. The amount of SEAP in the supernatant is measured by QUANTI-Blue™.

QUANTI-Blue™ is a colorimetric enzyme assay developed to determine any alkaline phosphatase activity (AP) in a biological sample, such as supernatants of cell cultures. In particular, QUANTI-Blue™ provides an easy and rapid mean to detect and quantify secreted embryonic alkaline phosphatase (SEAP), a reporter widely used for in vitro and in vivo analytical studies.

In the presence of alkaline phosphatase, the colour of QUANTI-Blue™ changes from pink to purple/blue. The intensity of the blue hue reflects the activity of AP. The levels of AP can be determined qualitatively with the naked eye or quantitatively using a spectrophotometer at 620-655 nm. <http://www.invivogen.com/quant-blue> .

### **2.2.2 Thawing Cells**

Vials of cells that were stored in liquid Nitrogen were carefully removed. 10ml of their appropriate growth medium were added as soon as they were fully defrosted and transferred to a 15 ml Falcon tube. This was then centrifuged at 1200 rpm for 5 mins at room temperature (RT). Then the supernatant was aspirated off. 5ml of growth medium was added to the cells and resuspended carefully before transferring to a flask to be incubated at 37° C, 5% CO<sub>2</sub>.

### **2.2.3 Propagating Cells**

Cells having a limited lifespan in culture. Thus they need to be propagated in order to ensure their survival and continual growth. Foetal Calf Serum (FCS; growth factor) and



fresh growth medium provides nutritional environment and viable condition for the cells to grow in. MEM non-essential amino acids (Sigma) is also used providing nutrition to the cells. Cells need propagating when they become confluent (covering 90% of the base of the flask). It involves splitting down their total number allowing enough space for the cells to grow in and eventually reach confluency. This way certain cell lines can be maintained indefinitely. Although after a certain number of passages the overall quality of the cell line decreases.

#### **2.2.3.1 Adherent Cell Lines**

The first step is to remove the supernatant from the flask. The cell layer was washed with 2ml of 1X PBS to remove any dead cells or cell debris. 2mls of trypsin (A serine protease that hydrolyses the proteins that adhere the cells to the bottom of the flask) was added into the flask and incubated for 4 mins (or until the cells could be tapped off the bottom of the flask). Equal amounts of growth medium was added (2ml) to neutralize the trypsin. The cells were then split evenly into separate flasks , and fresh medium was added (to a total of 5 ml). Flasks containing cells were now incubated at 37°C,5% CO<sub>2</sub>. In some cases cell lines are required to be just maintained rather than propagating. The process is the same, instead of neutralizing the trypsin, 1ml of trypsin was removed and 4 ml of fresh medium was added and incubated at 37°C, 5% CO<sub>2</sub>.

#### **2.2.4 Freezing Cells**

Cells are preserved in Liquid Nitrogen (-196°C) for long time cryo-storage. A freezing medium is required to store the cells in order to prevent cell damage by ice formation around the cells. Freezing medium consists of 10% Dimethyl Sulfoxide (DMSO) in FCS. DMSO is a cryoprotectant but is toxic to cells in room temperature after 15 mins of exposure.

In order to freeze adherent cells, they were washed with X1 PBS, trypsinized and neutralised as per propagating them. They were then combined in a 15 ml falcon tube and centrifuged for 5 mins at 12000 rpm. Supernatant was then aspirated off and the cells were resuspended in 1ml of freezing medium (1ml freezing medium per flask of cells). In under 10 minutes they were transferred to labelled cryo-tubes (Nunc) and stored at -80°C. This will allow the cells to cool at a rate of 103°C per minute. After 24 Hours they were transferred to liquid Nitrogen for long-term cryo storage.

For transfected cell lines the freezing medium consists of 10% DMSO, 30% FCS and 60% selection medium.

## **2.3 Virus Culture**

### **2.3.1 Propagating Viruses**

Prototype strains of viruses (Influenza Virus (H3N2), HRVs, RSV) were propagated on BES cells. 100 µl of virus stock of 50 PFU (Plaque Forming Unit) was added into a Non-treated EasyFlask 25cm<sup>2</sup>, Filter Cap (Nunc) containing BES cells with 1ml of growth medium (75% confluent) and incubated at 37°C, 5% CO<sub>2</sub> for about 24hrs to 36 hrs. Once most of the cells had been killed (the cells start to float up in suspension once killed and looks rounded), the flask was frozen at -20°C and was thawed. It was freeze-thawed for three more times to break the cells and release the virions into the medium. The contents of the flask was centrifuged at 12000 rpm for 2 mins. The supernatant was collected and stored at -80°C in cryotubes.

### **2.3.2 Purifying Viruses using a Sucrose Density Gradient**

All viruses (HRV14, HRV58, HRV5, RSV, Influenza H3N2 and Rotavirus) were purified using a sucrose gradient purification process. The sucrose gradients were prepared in 40ml Beckmann SW28 ultra-centrifuge tubes. The sucrose solutions were layered into the tubes in the following order (with the boundary between them marked): 7ml 60% sucrose in PBS; 6ml 30% sucrose in PBS; and 3ml 10% sucrose in PBS. 15ml virus was gently loaded onto the gradient, and the tubes were centrifuged at 25,000 rpm for 90 minutes at 4°C. The viral load bands at the interface between 30% and 60% sucrose. The top layers of sucrose were carefully removed, and the purified virus was transferred into 15ml Falcon tubes and frozen at -80°C.

### **2.3.3 Isolating Single-Stranded RNA (ssRNA) from Purified viruses**

All procedures were carried out in a sterile environment using sterile equipments and eppendorf tubes. 2µl vanadyl ribonuclease complex (an RNase inhibitor, which stops the breakdown of RNA) was added to each eppendorf, followed by 300µl ultra-pure phenol (the bottom layer). Phenol dissolves any proteins present. After vortexing for 5-10 seconds, the eppendorfs were centrifuged at 13,000 rpm for 10 minutes at RT. The upper layer was then transferred to new eppendorfs. 300µl chloroform / isoamyl alcohol (chloroform dissolves lipids present, and isoamyl alcohol ensures deactivation of RNase) was added to each eppendorf, followed by another round of vortexing and centrifugation. The upper layer was again transferred into new eppendorfs. 15µl (1/20<sup>th</sup>) sodium acetate 2M pH 6.5 and 750µl (2.5x vol) of 95% ethanol were added, mixed, and the eppendorfs were then frozen at -80°C for at least 60 minutes. Afterwards, the eppendorfs (straight from the freezer) were centrifuged at 13,000 rpm for 30 minutes at RT. The excess

supernatant was removed, the eppendorfs were centrifuged at 13,000 rpm for a further minute, and the remaining supernatant was removed, leaving just a pellet of ssRNA. 80µl sterile water (ddH<sub>2</sub>O), or LAL water, was added to each eppendorf, and the ssRNA was frozen at -80°C.

## **2.4 Immunofluorescence**

Immunofluorescence is a technique that is used to detect and quantify an antigen that may be present on the cell surface or inside the cell. A specific antibody to which a fluorophore is attached, is used to bind to the antigen of interest on the cell surface or inside the cell. The amount of fluorescence represent the amount of antigen present. Fluorophores work by absorbing light of a specific wavelength and emitting energy at a different but specific wavelength; FITC (fluorescein isothiocyanate) being the most common fluorophore used. FITC has an excitation wavelength of 495nm (cyan) and an emission wavelength of 519nm (green).

TRITC (tetramethylrhodamine isothiocyanate) is another common fluorophore frequently used, which has an excitation wavelength of 547nm (green) and an emission wavelength of 572nm (yellow). There are two major types of immunofluorescence: primary (direct) and secondary (indirect).

### **2.4.1 Direct Immunofluorescence**

A single antigen specific antibody is used in direct Immunofluorescence which directly conjugates to a fluorophore. The antibody with the fluorophore in turn binds to specific antigens and detection is made possible via microscopy or flow cytometry. (Fig. 2.1).

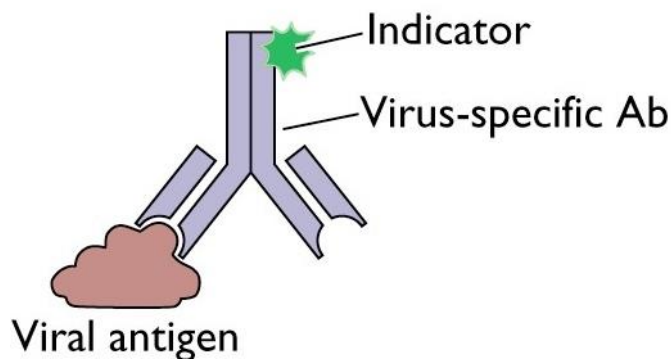


**Figure 2.1: Direct immunofluorescence.** An antigen-specific fluorescently-conjugated antibody binds directly to the antigen.

#### 2.4.2 Indirect Immunofluorescence

There are two antibodies involved in Indirect Immunofluorescence: a primary antibody which is unlabelled and specific for the antigen of interest, the other one being a secondary antibody which is specific for the primary antibody. This secondary antibody is also fluorescently-conjugated.

The structure of an antibody makes this possible, as it has two regions: an Fc region (fragment crystallisable region); and an Fab region (fragment antigen-binding region). The Fab region contains variable sections that determine which antigen is bound, whilst the Fc region is constant in a class of the same species. Antibodies can be designed in such a way that they contain the same Fc region but different Fab regions. In this way, primary antibodies with the same Fc region can be used to detect various antigens (due to differing Fab regions), and still be detected by a single fluorescently-conjugated secondary antibody specific for the Fc region of the primary antibody. Schematic diagram (Figure 2.2) below describes antigen-antibody binding in Indirect Immunofluorescence.

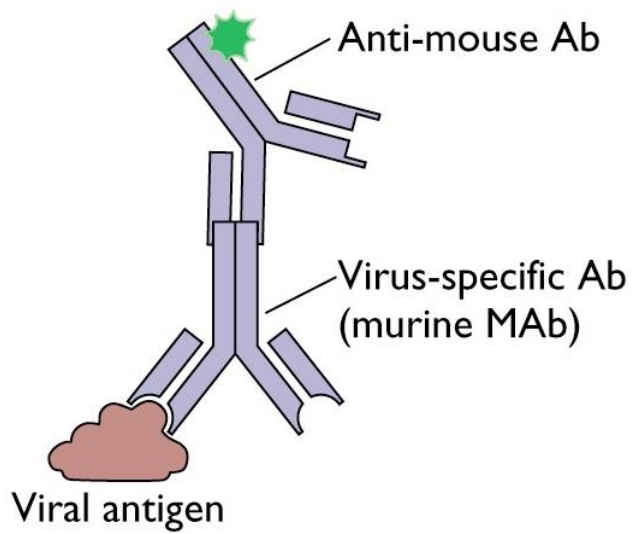


**Figure 2.2:** Indirect immunofluorescence. An antigen-specific primary antibody binds to the antigen, and is itself bound by a fluorescently-conjugated secondary antibody specific to it.

## 2.5 Flow Cytometry

Flow cytometry is a powerful technique used to analyse cellular characteristics of individual cells in a heterogeneous population. In this project, cells were fluorescently tagged via indirect immunofluorescence and passed through the Becton Dickinson (BD) Fluorescence-Activated Cell Sorting (FACSCalibur™) system (Figure 2.3).

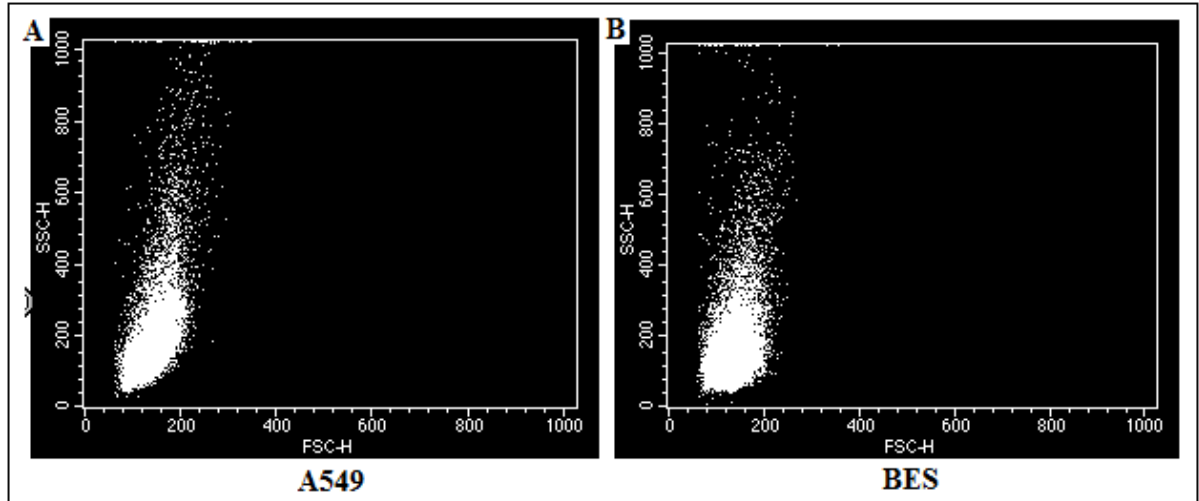


**Figure 2.3** Cell populations of A549 (A) and BES (B) cell types acquired by flow cytometry using CellQuest (BectonDickinson, Oxford, UK). Cells were left unstimulated and receptor expression was determined using the appropriate primary antibody followed by a secondary conjugated to FITC and the Geo.Mean of Fluorescent intensity measured. Fluorescence was detected using a FACS Calibur (BectonDickinson) counting 10,000 cells not gated. The data are a representative scatter chosen from 3 independent experiments.

### 2.5.1 Principles of Flow Cytometry

A flow cytometer works by passing thousands of cells per second through one or more laser beams, scattering the light onto detectors. The cells must be passed through the laser beams in single file to get accurate readings, and this is achieved using hydrodynamic focusing. The sample of cells merges with a flowing stream of sheath fluid and gets funnelled into a smaller orifice, compressing the cells to roughly one cell in diameter. When the laser strikes a cell, two forms of scattered light occur: forward scatter (FSC), which is the amount of light that is scattered in the forward direction, quantifies a cell's size; and side scatter (SCC), which is the rest of the light collected on a detector located 90° from the laser beam, shows the granularity of a cell. Fluorescence can also be detected. Lasers excite the fluorophores, and the subsequent fluorescent emission travels along the same route as the SCC signal. The light is directed through a series of filters

and mirrors, so that the appropriate wavelengths are delivered to the correct detector. All the data is recorded and accessed using the BD CellQuest software.(8,9)

## **2.6 Determining PRR Expression Levels**

In-direct immunofluorescence and flow cytometry were utilised in order to elucidate TLRs and RLRs receptor expression on A549 cells and BES cells.

To perform the indirect immunofluorescence assay, cell samples ( $2 \times 10^6$ ) were either unstimulated, or stimulated with  $20 \mu\text{g}$  of RNA or 100PFU HRV5.14,58 or HRV or H3N2 for different time points (1, 2,4,6, 12 hrs) cells were washed in  $500 \mu\text{l}$  PBS and fixed by adding  $300 \mu\text{l}$  of 4% Paraformaldehyde (PFA {Sigma}) and left to incubate at room temperature for 10 minutes. Cells were then washed two times. The samples were then re-suspended in  $200 \mu\text{l}$  PBS/0.02% BSA/0.02% NaN<sub>3</sub>. 0.02% BSA. To this,  $2 \mu\text{l}$  of primary antibody was added. Cells were then incubated at room temperature for 1 hour, and then washed twice with PBS/0.02% BSA/0.02% NaN<sub>3</sub>. The addition of the appropriate secondary antibody conjugated to FITC was followed. The cells were incubated with secondary antibody for 45 min and then washed twice and re-suspended in  $500 \mu\text{l}$  PBS/0.02% BSA/0.02% NaN<sub>3</sub>. The samples were analysed using a Becton Dickinson Fluorescent Activated Cell Sorter (FACS Calibur) with software supplied by Cell Quest. (10).



## **2.7 Phospho-I $\kappa$ B, IRF3 and Caspase-1 Detection**

### **2.7.1 SDS-PAGE**

SDS-PAGE (Sodium Dodecyl Sulphate Polyacrylamide Gel Electrophoresis) is a technique used to electrophoretically separate proteins according to their Molecular Weight (MW). There are two types of SDS-PAGE; continuous and discontinuous.

#### **2.7.1.1 Continuous SDS-PAGE**

In this method of SDS PAGE the concentration of both the buffers in both the gel and the tank are the same. This is considerably easier to make than the dis-continuous method, providing enough resolutions for electrophoresis of DNA and RNA samples. For observing protein samples a dis-continuous method is often used.

#### **2.7.1.2 Discontinuous SDS-PAGE**

In this method different buffers are used for the gel and the tank. The gel has two parts to it; the upper stacking gel and the lower resolving gel. The 4% stacking gel has larger pores in it (low percentage) and a low pH of 6.8 whereas the lower 10% resolving gel has smaller pores with a higher pH of 8.8. The protein samples are loaded at the interface between the two gel layers in very thin and sharp wells that are made by 1mm combs whilst casting the gels. The proteins whilst travelling through the resolving gel gets separated according to their MW. Proteins with smaller size travel faster and hence

traverses more distance than proteins with higher MW which travel slower and travels less distance. Gels contain Chloride ions which act as the mobile anion. The running buffer (pH 8.8) contains glycine as its anion. Both chloride and glycinate ion migrate through the stacking gel at the beginning of electrophoresis. Chloride ions being smaller and strongly charged move faster than glycinate ions. Due to the low pH in the stacking gel compared to the running buffer, the equilibrium favours the zero net charge zwitterionic form of glycine. The faster  $\text{Cl}^-$  ions leave behind an area of unbalanced, positive counter ions in their wake, creating a steep voltage gradient (the Kohlrausch discontinuity) that pulls the glycinate ions along, resulting in two fronts moving at the same speed. The protein molecules of the sample has an intermediate mobility at this point and gets carried along between these two fronts through large pores of the stacking gel, and deposited in a focused narrow band on top of the resolving gel. When the Kohlrausch discontinuity enters the resolving gel, the pH increases, ionising the glycine and increasing its mobility. The faster running glycinate ions dissipate the discontinuity and run past the protein samples, allowing them to separate themselves through the resolving gel [National Diagnostics, URL]. (7).

### **2.7.2 Western Blot**

This is a standard technique for transferring the proteins that had been electrophoretically separated using SDS-PAGE onto a nitrocellulose membrane. This membrane will be further treated with antibodies for further analysis. The transferring is done using an electroblotting method, where the resolving gel (stacking gel trimmed off) and the nitrocellulose membrane is sandwiched together in between layers of blotting paper and pads soaked in transfer buffer. The sandwich is put in a cassette to hold everything together and then set in a tank filled with transfer buffer, which also contains an ice-pack.

Transferring was done at a constant current of 210 mA applied for 60 mins. This results in the proteins from the gel being transferred to the nitrocellulose membrane. (1,2).

### **2.7.2.1 Probing Membranes with Antibodies**

After the proteins are transferred to the nitrocellulose membrane, the membrane is instantly treated with a blocking reagent. A blocking reagent solution (in this case milk powder dissolved in X1 PBS) contains high amounts of proteins. These prevent the antibodies from binding parts of the membrane which do not have protein bands. A nitrocellulose membrane has very high binding affinity and hence allows all proteins to bind strongly. Antibodies will also bind to it; however bathing the membrane in a blocking solution ensures that the proteins will bind to the rest of the membrane 'blocking' the antibodies from binding. (1).

Post-blocking, the membranes are treated (incubated for 1 hr in room temperature) with primary antibody for the specific protein of interest (protein being detected). Following this the membranes are briefly washed in X1 PBS TWEEN and incubated in secondary antibodies specific to the primary antibody and conjugated to horseradish peroxidase (HRP). Membranes are incubated for 1 hour and washed in X1 PBS TWEEN for 2 hours whilst changing the washing buffer every 20 minutes. The membranes are then treated with an electro-chemiluminescence (ECL) reagent, causing the HRP to emit light only where the protein bands are present. This is done in a dark room, where a photographic film is placed onto the membranes and exposed for a short amount of time (approx 6-8 minutes), depending on the intensity of the luminescence.

### **2.7.3 Stripping and Reprobing Membranes**

After using a nitrocellulose membranes with the bound proteins and the antibodies, it is possible to reprobe the membrane with different antibodies. This is done by incubating the membrane in a stripping buffer at 50 °C, in a shaker incubator for 5-7 minutes. This allows the primary and the secondary antibody to be washed off but having the proteins still bound strongly to the nitrocellulose membrane. After incubation the membrane is washed in X1 PBS-TWEEN for 20 minutes and then blocked for 1 hour in a blocking solution. A complete probing procedure can be done using this membrane at this stage with the same or a different antibody of choice.

### **2.8 Immunoprecipitation**

Immunoprecipitation is a standard immunological procedure that is used to isolate an antigen from a complex, such as a cell lysate. An antibody specific to the antigen of interest is incubated along with the cell lysate. An insoluble support is added to it, in this case is protein-A sepharose beads. This helps to immobilise the antigen-antibody complex. Previous to adding antibodies protein-A sepharose beads and the cell lysate was mixed as a pre-clear. Pre-clearing helps to get rid of unwanted proteins that might possibly bind to the immunoglobulin in a non-specific manner; allowing a reduction in the background and signal to noise ratio (3). The sample is vortexed thoroughly and then centrifuged after which the supernatant is collected in separate tubes and new lysis buffer is added to it. This cycle is repeated. The importance of this step is to get rid of all non-bound proteins and leaving behind only the protein-A sepharose beads that has the antigen-antibody bound to it.

The lysis buffer used has many important functions; it stabilises the native protein conformation. Other functions includes the inhibition of enzymatic activity of the protein.

The lysis buffer also minimises the possibility of the antibody binding site denaturation and increase protein release from the cell lysate (4). The protein of interest is eluted from the protein-A sepharose beads using a reducing buffer (same used in SDS-PAGE). The elute is left for 15 minutes at room temperature after which it can run using SDS-PAGE setup.

Immunoprecipitation experiments were carried out in this study in order to determine whether RIG-I, MDA5 and LGP2 homo-dimerises or hetero-dimerises with each other. This technique exploits the possibility of isolating a particular protein of interest and also determine whether the protein forms a homodimer with itself or forms a heterodimer with any other protein. In this study, antibodies against RIG-I, MDA5 and LGP2 was used to precipitate out the proteins for further study. SDS-PAGE is carried out to detect different proteins, i.e. precipitate out MDA5 and perform SDS-PAGE to detect LGP2.

A549 cells were stimulated with HRV5 and HRV14 on separate occasions and were incubated for the following time points: 1hr, 2hr, 4hr and 6hrs, or left unstimulated (0 hours). Cells were washed at every time point and lysis buffer was subsequently added to them for 2 hours. The lysates were then centrifuged and supernatants were collected in fresh eppendorf tubes. Pre-clearing was done 2 times with protein-A sepharose beads, to prevent non-specific binding of the antibody to undesirable proteins that may be present. More PAS beads were added and incubated with an appropriate primary antibody.

Protein A is used due to the fact that it binds specifically to the heavy chains in the Fc region of the antibody resulting in a favourable orientation of the antibody that allows antigen binding site to face outwards. This also immobilises the antibody so that it can bind to the antigen more effectively. (4).

The pellets are washed in lysis buffer and the samples analysed using SDS-PAGE and western blotting, using X2 SDS-PAGE Non-Reducing Sample Buffer.

## **2.9 Confocal Microscopy**

Confocal microscopy is an optical imaging technique that produces images of high resolution and contrast. It is used to visualise the location of different proteins in a cell. Confocal microscopy creates sharp images of the specimen because it has the ability to exclude out-of-focus light reflecting from the specimen. It does it by using a spatial pinhole, enabling the micrograph to have high contrast and also allowing the reconstruction of three-dimensional images.

This technique was first developed by Minsky in 1955. In his original experiment he focussed a point of light on the specimen, point by point and collected the returning rays. The method by which he reduced background light was by focusing light on a single point and then collecting the light and passing it through a second pinhole aperture that got rid of any unwanted light. The stage on which the specimen sat had to be moved around in order for the specimen to be scanned, instead of moving the light source.

The concept of fluorescence confocal microscopy works by the following principle; a molecule of the specimen absorbs light of a certain frequency however emits light of a different frequency. The sample is treated with a suitable dye and a light of a suitable wavelength is shone on the specimen. The light which the specimen emits as a result is collected and forms an image. Lower wavelength lights are reflected using a dichroic mirror however light of longer wavelength is transmitted. As a result light from the source reflects onto the sample after its passage through the objective. Fluorescent light on the other hand passes through the objective and the mirror since it is of a longer wavelength. This phenomenon is called epifluorescence.

There are two lenses involved in a confocal microscope; light is focused from the focal point of one lens to the focal point of another. The aim is to see only the focal point of

one of the lenses on the specimen so a pinhole is created at the focal point of the other lens stopping light from any other point than the focal point from passing through. A single beam of light illuminates the specimen at the focal point by the use of a pinhole system which reduces the amount of light from out of focus parts. In fluorescent microscopy it is never the case that the entire section of the specimen will be illuminated. An image is formed at the pinhole by the focal point, thus the two points are known as conjugate points. The name 'confocal' is coined since the pinhole is conjugate to the focal point.

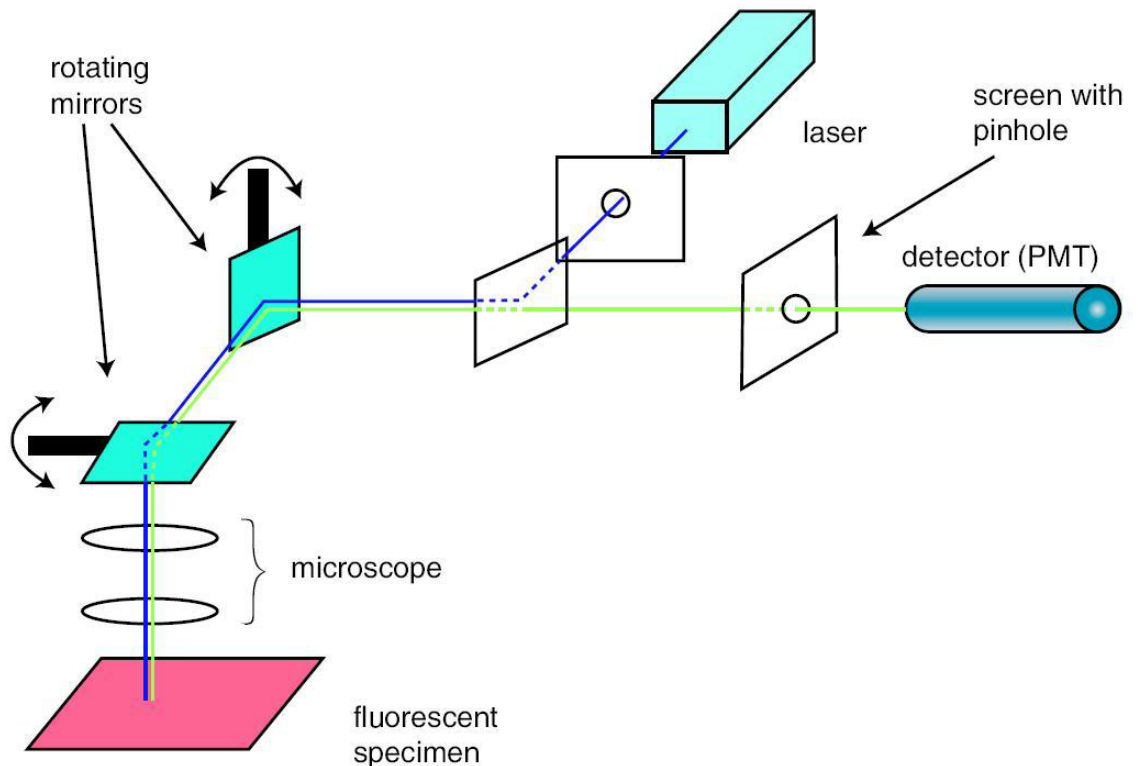


**Figure 2.4. Diagram demonstrating the mechanisms behind confocal microscopy.**

The blue line shows the path of the laser. The laser is reflected off the dichroic mirror and then the rotating (scanning) mirrors. This laser is focused on the specimen after it travels through the microscope lenses. The green light is the path of the emitted light from the specimen containing the fluorescent labels. as it passes back through the microscope and is descanned by the rotating mirrors. It then passes through the dichroic mirror and then the light from the focal plane of the lenses passes through the pinhole and can be detected.

(5).

## **2.10 Plasmid DNA**

### **2.10.1 Plasmid DNA Preparation**

#### **2.10.1.1 Transformation**

All procedures were carried out using sterile tips near a Bunsen burner to ensure sterility. Agar plates previously prepared with 40µl of Ampicillin per 100µl of agar. psiRNA NLRP3 (Invivogen) or psiRNA-NLRC5 (Invivogen) were transformed into a competent *E.coli* strain (*E.coli* GT116). 5µl of the plasmid was added to 100µl of *E.coli* GT116 and incubated on ice for 30 minutes. This was followed by heat shocking the tubes at 42 °C for 45 seconds, then placing them back on ice for 2 minutes. 500µl of Luria Broth (LB) was then added to each tube, and placed on a shaker incubator at 225 rpm at 37°C for 1 hour. 100µl of the transformed *E.coli* in LB was then added to a ampicillin agar plate, evenly spread until absorbed, and placed in a shaker incubator at 225 rpm at 37°C overnight to grow. The plasmids contain a Zeocin-resistance gene, so only the *E.coli* that have taken up the plasmid will survive on the Zeocin agar plates. After growing up the *E.coli* colonies, the transformed *E.coli* and plasmids were expanded. 25µl Ampicillin was added to 25ml LB in bottles, and individual colonies were added to separate bottles, as well as being added to a reference plate, and incubated overnight in a shaker incubator at 225 rpm at 37°C.

#### **2.10.1.2 DNA Isolation**

The luria broth containing the *E Coli* culture was centrifuged at 4000 rpm in 50ml tubes and the supernatant was swiftly discarded without agitating the pellet. After addition of 400µl of STET buffer, the solution was vortexed to lyse the *E.Coli* cell walls and then transferred to sterile eppendorfs. 10µl lysozyme (50mg/ml) was added to each tube. Following this the tubes were put in a waterbath for 1 minute to boil. Samples were placed on ice for 5 minutes and then centrifuged for 30 mins at 13,000 rpm. 5µl of RNase A



(20µg/ml; degrades RNA ) was added to the solution after the pellet was removed using a sterile toothpick. The samples were incubated for at 37°C - 42°C for 30 minutes. 400µl of phenol / chloroform / isoamyl alcohol (bottom layer) was then added, the samples vortexed, and centrifuged for 15 minutes at 13,000 rpm.

The supernatant was transferred to sterile eppendorfs. 400µl of chloroform / isoamyl alcohol was added, the samples vortexed, and centrifuged again for 15 minutes at 13,000 rpm. Supernatants were again collected into sterile eppendorfs. The following was then added to the solution; 20µl (1/20th) sodium acetate 2M pH 6.5 and 1ml (2.5x vol) of 95% ethanol. The solution was mixed and transferred to the freezer (-80°C) for 1 hour/overnight. The samples were afterwards centrifuged at 13,000rpm for 20 minutes from frozen. Supernatant was discarded leaving behind very small pellets which are the purified DNA. Excess supernatant was removed by further centrifuging the tubes for another minute. Pellets were suspended in 80µl sterile water (ddH<sub>2</sub>O), or LAL water, for each tube and stored at -20°C.

### **2.10.1.3 Agarose Gel Electrophoresis**

Agarose gel electrophoresis is a process that utilises a method of gel electrophoresis that separates a mixed population of DNA (or proteins) through a matrix made of agarose. DNA or RNA samples are separated according to the size of the sample fragments; smaller fragments translocate further than the longer fragments, through the agarose gel. An electrical gradient is applied on both ends of the gel, so that the negatively charged molecules translocate, separating the fragments.

To check the purity of the plasmid preparations, the samples were run on an agarose gel. A 1% w/v agarose gel was prepared (1g agarose in 100ml of 1X ELFO), and 10µl of the sample (with 5µl of ELFO Loading Buffer) was run on it at 100V for 45 minutes. A 1kb

DNA ladder was run alongside the samples. Once run, the bands were observed using a Stratagene eagle eye UV imaging system.

### **2.10.2 Silencing**

This technique is used to ‘silence’ or completely or mostly abrogate the production (or downregulate) of a protein in a live cell by suppressing its associated gene. The process involves the introduction of antisense RNA, such as small interfering RNA (siRNA). Once introduced in a cell siRNA binds to and cleaves specific mRNAs and decreasing its activity. RNA interference was used in order to silence the NLRC5, NLRP1, NLRP3 genes.

A psh7SK vector (from Invitrogen) was used to generate different pshRNA clones. Most efficient was against the sequence: for NLRP3 GGAAGTGGACTGCGAGAAGTT, for NLRC5, GAACCTGTGGAGCTGTCTTGT and GCAACAGCATCTGCGTGTC AA.

For NLRP1, GAAGGAGGAGCTGAAGGAGTT and GGCCTGATTATGTGGAGGAGA.

The entire method takes 5 days to complete. Following is an exhaustive protocol of the procedure for transfection.

#### **2.10.2.1 Transfection Procedures**

To begin with a selection medium is made using the following: 200ml of (DMEM), containing GlutaMAX, 10% heat-inactivated Foetal Calf Serum (FCS), and 1% non-essential amino acids (Invitrogen (UK), 1 ml Kanamycin (0.1mg/ml), 1ml Neomycin (0.1 mg/ml). The medium is made in a sterile bottle in sterile conditions.

3, 25 cm<sup>2</sup> Nuclon® TM Surface flasks were chosen with BES cells growing in them with 30-40% confluency. Supernatant was removed and the cell monolayer was washed with

2mls of Opti-MEM® I Reduced Serum Media. Then 1ml of the same medium was added to each flask and set aside.

7 sterile eppendorgs was taken out of which 3 of them was grouped into 'set A' and another 3 was grouped into 'setB'. The last eppendorf had 1 ml of OPTI-MEM and set aside.

35 µl of OPTI-MEM and 15µl of DNA sample was added to each tubes of 'setA'. Tthe mixture was gently flicked and set aside for 5 minutes. To the tubes labelled 'set B', the following was added to each tube; 10µl Lipofectamine2000 and 40µl OPTI-MEM and set aside for 5 minutes.

Contents of each corresponding tubes from 'setA' was mixed with tubes of 'set B' and then incubated for 20 minutes at 37°C. The contents of the tubes were transferred to the 3 flasks prepared before and incubated overnight at 37°C. As a negative control tube containing only OPTIMEM was transferred to a flask containing BES cells.

The next day, the medium was aspirated from the flasks and 5ml of the selection medium containing the antibiotics was added to each flask. The flasks were again left overnight in the incubator at 37°C.

At this point if the transfection is successful, the cells in the flask labelled 'negative control' will die due to the presence of antibiotic in the selection medium. Transfected cells will however thrive well due to the presence of antibiotic resistance gene in the transfected plasmid.

Once the flasks are confluent in the next 2-3 days, they were fixed using 4% PFA, washed in X1 PBS and then treated with appropriate antibodies to confirm whether a protein of interest i.e NLRP3, NLRC5 was silenced, using flow cytometry.

## **2.11 Cytometric Bead Array**

To quantify the inflammatory response of the cells in response to different stimuli the released cytokines were measured. Cytokines are the messengers that co-ordinate inflammation and give a direct representation of cellular response.

In this study the Human Inflammation BD™ Cytometric Bead Array (CBA {BD Biosciences}) kit was used to measure cytokine concentrations

The Human TH1/TH2 CBA kit is capable of detecting six cytokines that play important roles in the human inflammatory response. These are Interleukin-4 (IL-4), Interferon gamma (IFN $\gamma$ ), Interleukin-6 (IL-6), Interleukin-10 (IL-10), Tumor Necrosis Factor (TNF) and Interleukin-2 (IL-2). CBA analysis allows the fast and highly sensitive quantification of an array of cytokines in any one sample.

In order to bind cytokines in a sample the beads are coated with capture antibodies specific for a particular cytokine. In the Human Inflammation BD™ CBA kit there are six bead populations with different fluorescent intensities specific for IL-4, IFN- $\beta$ , IL-6, IL-10, TNF and IL-2. Once the beads have bound to the cytokines a phycoerythrin (PE)-conjugated detection antibody mix is added, this is a mixture of PE-conjugated antibodies specific for each bead.

### **2.11.1 Assay Procedure**

The standards and detection reagents were prepared according to the BD CBA Human Soluble Protein Master Buffer Kit manual. 50 $\mu$ l of the tissue culture supernatant prepared previously was added to flow tubes, followed by the addition of 50 $\mu$ l of the IFN- $\beta$  beads, mixed, and incubated for 1 hour at RT. 50 $\mu$ l of the PE detection reagent was then added

and mixed, followed by a further 2 hour incubation at RT in the dark. 1ml of Wash Buffer was added to each tube, centrifuged at 200g for 5 minutes, and then the supernatant was carefully aspirated off and discarded. The bead pellets were resuspended in 300µl of Wash Buffer, and the samples were analysed using flow cytometry, with the data acquired being analysed using the FCAP Array software (Becton Dickinson).

## **2.12 Statistical Analysis**

Statistical analysis – Data were evaluated by analysis of variance and the Dunnett multiple-comparison test using the InStat program (GraphPad Prism Software, San Diego, CA). Where appropriate (comparison of two groups only), two-tailed t tests were also performed. Statistical differences were considered significant at the level of  $p < 0.05$ . Experiments were performed using triplicate samples and were performed twice or more to verify the results.

**CHAPTER 3:**

**Innate Immune Response to**

**Human Rhinoviruses (HRV5, HRV14, HRV58)**

### **3.1 Introduction**

Human rhinoviruses, the common cold pathogens, are small, non-enveloped single stranded RNA viruses, which affect a significant number of humans during the winter months. Human infection causes severe inflammation mainly in the upper but also lower respiratory system, causing nasal secretions and cough. Although rhinovirus infections are not life-threatening, epidemiological studies have documented their involvement in acute respiratory illness, wheezing and asthma exacerbations in various human populations (Seemungal et al. 2001)(Cox and Le Souef 2014). The role of respiratory infections in asthma has always been of clinical interest and importance, but their overall contribution to this disease has, until recently, been underappreciated. With the use of highly sensitive and specific molecular diagnostic and detection methods, the identification of infectious organisms has increased, and with these findings has come a greater and clearer understanding of the contributions of specific respiratory infections to asthma. From a wide variety of studies, HRVs, have emerged as key and perhaps central microorganisms in many aspects of asthma. For example, studies have pointed to the importance and relevance of symptomatic infections with rhinovirus early in life as a major factor in recurrent wheezing and asthma. Studies by Johnston et al suggests that 80-85% of children (9-11 years of age) who suffer from asthma also suffered from HRV infections. Similar studies show that adults suffer from asthma exacerbations due the HRV infection (Johnston et al. 1995).

Rhinovirus infection induces inflammation and release of cytokines from the respiratory tract thereby attracting inflammatory cells to the airways. Inflammation is the process

aimed at restoring homeostasis after an infection and can be more damaging than the infection itself if uncontrolled, excessive or prolonged.

Our body's innate immune system recognises HRV through a plethora of germ-line encoded PRRs such as the TLRs and RLRs. Antiviral innate immune recognition is mostly sequestered by the active functioning of TLR3, TLR7 and TLR8 (Kawai and Akira 2006, Xagorari and Chlichlia 2008). Also very important are the RLRs called RIG-I and MDA-5 (Slater et al. 2010) which have been shown to play a role in rhinovirus innate recognition.

The aim of this study was to investigate the innate immune responses to Rhinoviral infection and whether different HRV strains contribute differently to the inflammatory response of the host.

### **3.2 Results**

The body's innate immune system responds to RNA virus infection and triggers an antiviral response which results in the production of type I interferons (IFNs). TLRs and RLRs are the two primary pattern recognition receptors that are responsible for the detection of RNA viruses. The RLH (RIG Like Helicase) pathway is very important in the detection of RNA virus invasion in most cell types apart from plasmacytoid dendritic cells. HRV strains are genomically classified in three groups HRV-A, HRV-B and HRV-C (Spyridon Megremis 2012). In this study used HRV-A group strains (HRV5 and 58) as well as HRV-B (HRV14) have been used in order to elucidate the mechanisms of antiviral innate immune response to HRV infection.



### **3.2.1 PRR expression Levels**

Measuring levels of PRR after infecting cells with a pathogen gives a direct understanding of the possible intracellular pathways that might be activated. It also helps us to elucidate what cellular stress responses might be occurring such as interferon and cytokine production, and whether at all these would result in inflammation and necrosis. Here we have measured activation of PRRs such as RIG-I and MDA5 (known to recognise RNA ligands) and also TLRs with special interest to TLR7 and TLR8 which are known to recognise RNA viruses such as HRVs (and viral ssRNA) , and trigger an innate immune response.

#### **3.2.1 .1 PRR expression of A549 cells upon HRV14 infection**

Lung Epithelial cells (A549) which are susceptible to HRV infection were infected with HRV14 (100PFU) in order to determine the upregulation of MDA5 and RIG-I and were monitored at different time points (1h,2h, 4h, 6h, 12hrs). The viral infectious cycle is 6 hours long which is why this is the maximum length of time the cells are left with the virus and an added 6 hours to notice differences in protein expression levels. Unstimulated cells were checked for receptor expression levels at 0hr. Detection of the expression levels were determined by using indirect Immunofluorescence and measuring the Fluorescence intensity (Fig. 3.1). Significant increase in the expression levels of RIG-I and MDA5 were observed when stimulated with the virus showing slight preference for MDA5 expression over RIG-I.

### HRV 14 mediated PRR recognition

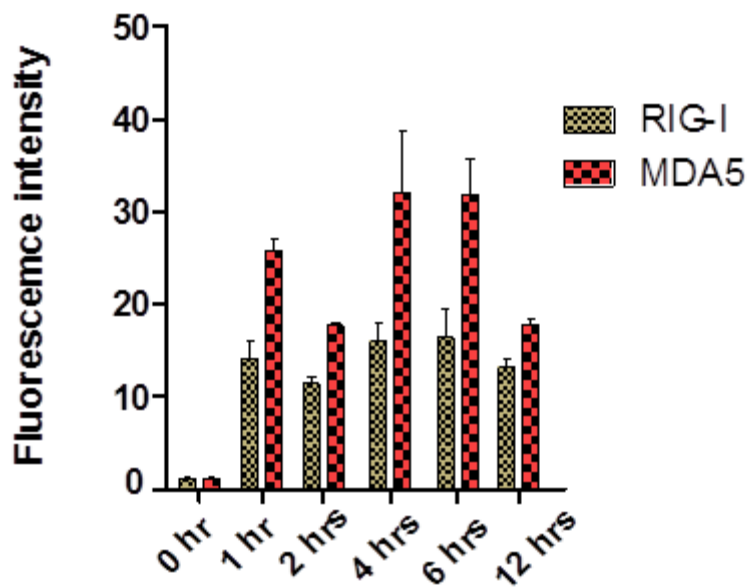


**Figure 3.1 (a) PRR expression levels in cells stimulated with HRV14.** A549 Lung Epithelium Cells were infected with 100 PFU viral stock (HRV14). Following infection PRR expression was tested at different time points using the appropriate primary antibody followed by a secondary conjugated to FITC. Receptor expression was determined as the Geo.Mean of Fluorescent intensity. Fluorescence was detected using a FACSCalibur (Becton Dickinson) The data represent the mean of three independent experiments.

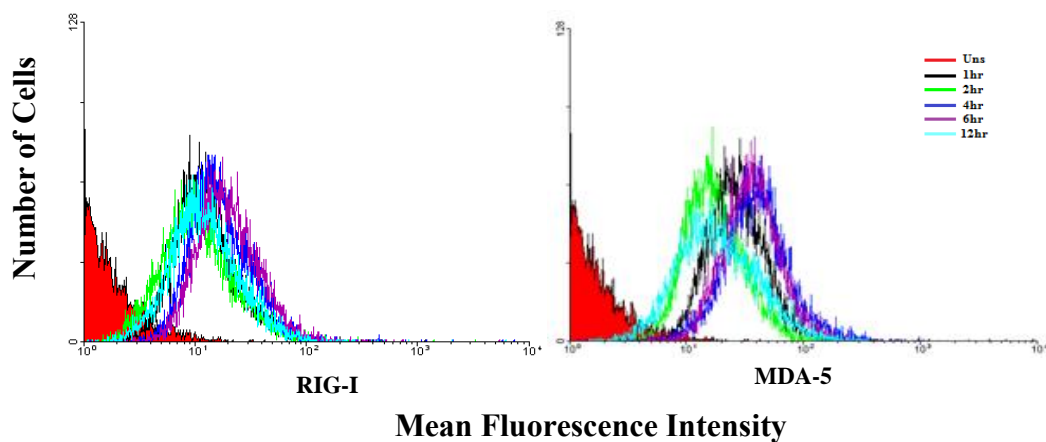


**Figure 3.1 (b) PRR expression levels in cells stimulated with HRV14.** A549 Lung Epithelium Cells were infected with 100 PFU viral stock (HRV14). Following infection PRR expression was tested at different time points using the appropriate primary antibody followed by a secondary conjugated to FITC. Receptor expression was determine as the Geo.Mean of Fluorescent intensity. Fluorescence was detected using a FACS Calibur (BectonDickinson) counting 10,000 cells not gated. Isotype controls were performed, with values similar to unstimulated samples. The data represent the mean SD of 3 independent experiment, indicating statistically significant ( $P < .05$ ) increase in expression compared with corresponding unstimulated controls.

As expected since HRV14 is a positive sense RNA virus and MDA5 has been shown to recognize RNA from positive sense RNA viruses, higher levels of MDA5 were observed as compared to RIG-I.

### 3.2.1.2 PRR expression of A549 cells upon HRV58 infection

Expression levels of PRRs such as the RLR (RIG-I and MDA5) were measured post viral infection of A549 lung epithelial cells by HRV58 (100PFU).

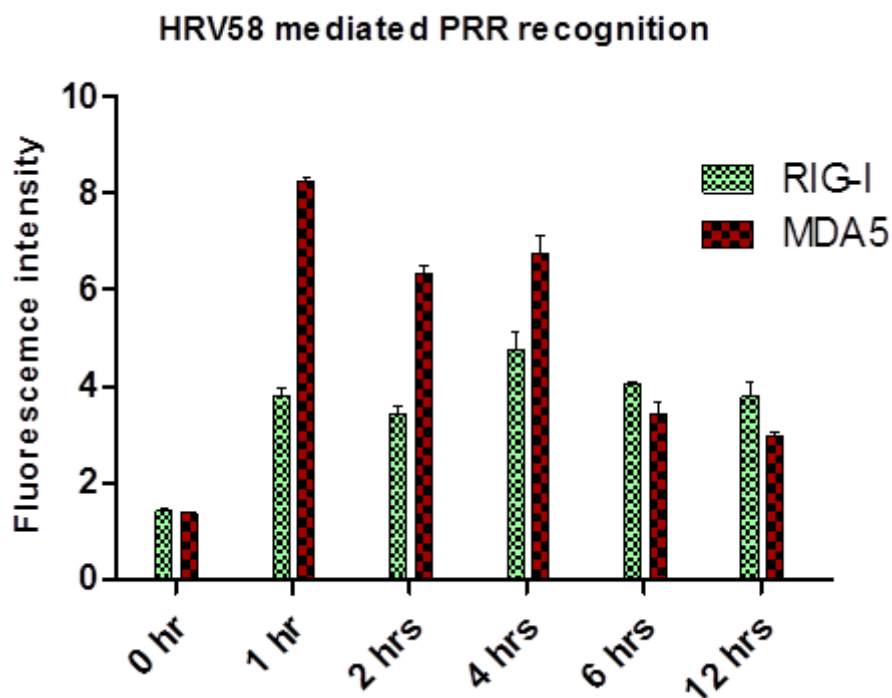


**Figure 3.2 (a) PRR expression levels in cells stimulated with HRV58.** A549 Lung Epithelium Cells were infected with 100 PFU viral stock (HRV58). Following infection PRR expression was tested at different time points using the appropriate primary antibody followed by a secondary conjugated to FITC. Receptor expression was determine as the Geo.Mean of Fluorescent intensity. Fluorescence was detected using a FACSCalibur (BectonDickinson). The data represent the mean of three independent experiments

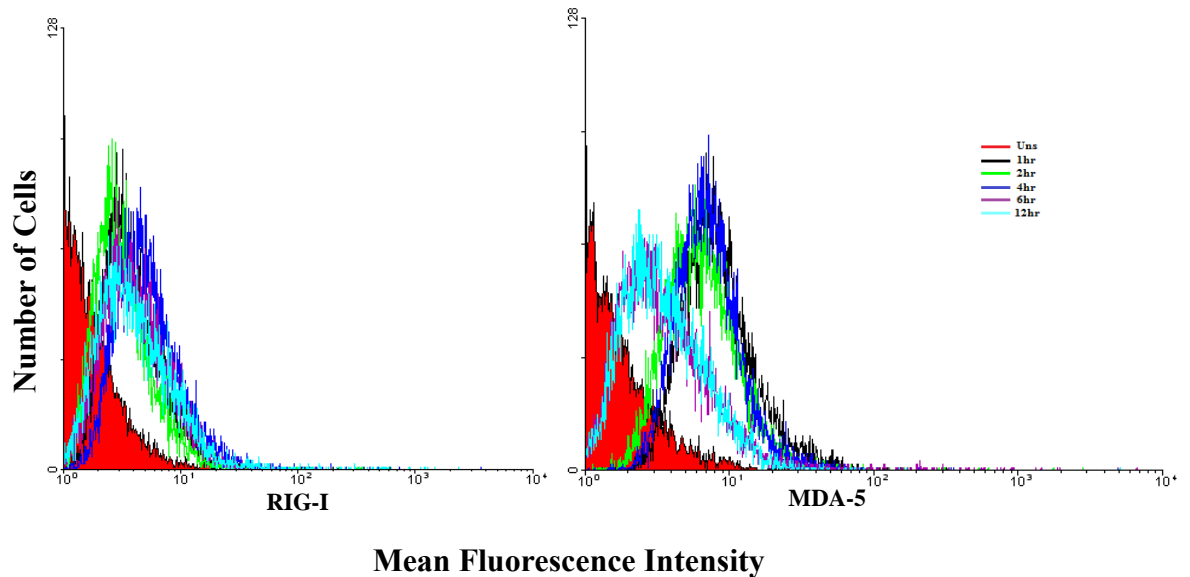


**Figure 3.2 (b) PRR expression levels in cells stimulated with HRV58.** A549 Lung Epithelium Cells were infected with 100 PFU viral stock (HRV58). Following infection PRR expression was tested at different time points using the appropriate primary antibody followed by a secondary conjugated to FITC. Receptor expression was determine as the Geo.Mean of Fluorescent intensity. Fluorescence was detected using a FACSCalibur (BectonDickinson) counting 10,000 cells not gated. Isotype controls were performed, with values similar to unstimulated samples. The data represent the mean SD of 3 independent experiment, indicating statistically significant ( $P < .05$ ) increase in expression compared with corresponding unstimulated controls.

We observe that when A549 cells were infected with HRV58, MDA5 recognises the viral pathogen and is upregulated however RIG-I also detects the virus but to a lesser extent. We suspect from this observation that the RLH pathway is activated. As a result of which we proceeded to investigate signalling pathways to verify RLR involvement. . It was initially believed that RLRs would recognise only one ligand which is dsRNA but studies have shown that RIG-I and MDA5 recognise different viral RNAs from viruses (Kato *et*

*al.*, 2006; Loo *et al.*, 2008). RIG-I recognises single-stranded RNA (ssRNA) containing a terminal 5'-triphosphate (ppp) (Pichlmair *et al.*, 2006), as well as linear dsRNA no longer than 23 nucleotides in length (Kato *et al.*, 2008). MDA5 recognises long strands of dsRNA, but the mechanism by which this occurs is less clear (Kato *et al.*, 2008).

RIG-I recognises negative sense ssRNA viruses, including influenza virus, Newcastle disease virus, Sendai virus, and Hepatitis C virus, whilst positive sense ssRNA viruses, such as picornaviruses, and more specifically encephalomyocarditis virus and Coxsackievirus B3, have been shown to activate MDA5 (Kato *et al.*, 2006; Loo *et al.*, 2008; Wang *et al.*, 2010).

Since HRV is a positive sense ssRNA virus, MDA5 recognition over RIG-I is expected and supported by other studies.

### **3.2.2 Signalling Detection Upon Infection With HRV**

RIG-I and MDA5 are activated by an RNA ligand. A downstream signalling is induced as a result of interaction of IPS-1 via a CARD-CARD interaction. Downstream signalling molecules are recruited and I $\kappa$ B is released from the NF- $\kappa$ B complex and gets phosphorylated. This phosphorylated I $\kappa$ B is ubiquitinated and sent to the proteasome for degradation. NF- $\kappa$ B and IRF3 acts as transcription factors that translocate to the nucleus and upregulate type I IFNs and an eventual innate immune response. In the following experiments the detection of phospho-I $\kappa$ B correlates to the activation of NF- $\kappa$ B.

#### **3.2.2 .1 Signalling detection in HRV5 infected cells**

A549 cells were infected with 100 PFU viral stock (HRV5) for 1hr, 2hr, 4hr and 6hr or left unstimulated (Uns). Cell lysates were collected and analysed for Phospho-I $\kappa$ B and

IRF3 using SDS-PAGE gel electrophoresis and western blot. Primary antibodies specific for IRF3 or phospho-I $\kappa$ B were used followed by the appropriate secondary antibodies conjugated to HRP. The bands were visualised using the ECL procedure.

A slow and gradual increase in the activation of phospho-I $\kappa$ B is observed with the most amounts present after 6 hours of stimulations (fig 3.4). A similar result is noticed in IRF3 production. The commonly known activated IRF3 dimer is seen to form at 2hr and onwards.

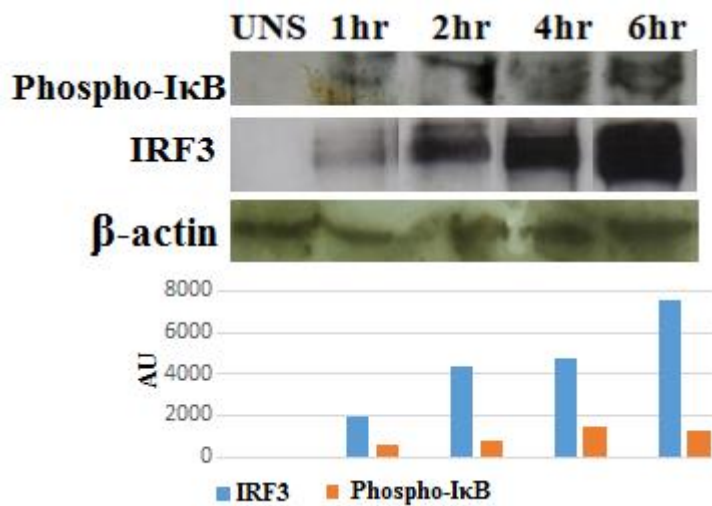


**Figure 3.3 Phospho-I $\kappa$ B and IRF3 detection.** A549 Lung Epithelium Cells were infected with 100 PFU viral stock (HRV5) or left unstimulated (Uns) for 1hr, 2hr, 4hr and 6hr. Cell lysates were collected and analysed for Phospho-I $\kappa$ B and IRF3 using SDS-PAGE gel electrophoresis and western blot. Primary antibodies specific for IRF3 or phospho-I $\kappa$ B were used followed by the appropriate secondary antibodies conjugated to HRP. Loading controls for  $\beta$ -actin are also depicted. The bottom panel shows a quantitative analysis (by densitometry) of Phospho-I $\kappa$ B and IRF3. The bands were visualised using the ECL procedure. Data are representative of experiments done three times.

### 3.2.2 .2 Signalling detection in HRV14 infected cells

A549 cells were infected with 100 PFU viral stock (HRV14) for 1hr, 2hr, 4hr, 6hr and 12 hrs. Cell lysates were collected and analysed for Phospho-I $\kappa$ B and IRF3. A gradual increase in Phospho-I $\kappa$ B production is seen from 1hr through to 12 hrs stimulations (fig. 3.5). IRF3 activation is upregulated at 2hrs, 4hrs and 6rs and seems to dimerise at these timepoints.

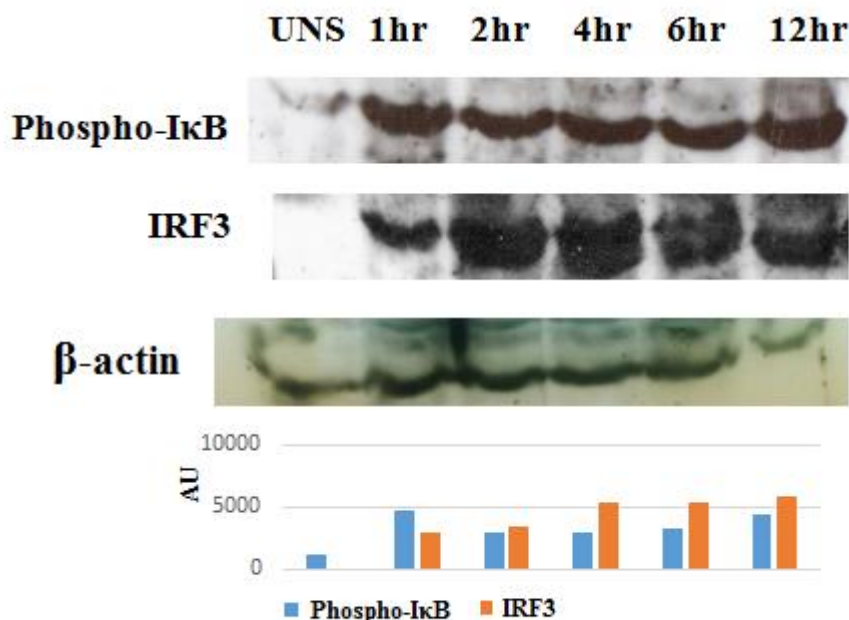


**Figure 3.4 Phospho-I $\kappa$ B and IRF3 detection** A549 cells were infected with 100 PFU viral stock (HRV14) or left unstimulated (Uns) for 1hr, 2hr, 4hr, 6hr and 12 hrs. Cell lysates were collected and analysed for Phospho-I $\kappa$ B and IRF3 using SDS-PAGE gel electrophoresis and western blot. Primary antibodies specific for IRF3 or phospho-I $\kappa$ B were used followed by the appropriate secondary antibodies conjugated to HRP. Loading controls for  $\beta$ -actin are also depicted. The bottom panel shows a quantitative analysis (by densitometry) of Phospho-I $\kappa$ B and IRF3. The bands were visualised using the ECL procedure. Data are representative of experiments done three times.



### 3.2.2 .3 Signalling detection in HRV58 infected cells

A549 cells were infected with 100 PFU viral stock (HRV58) for 1hr, 2hr, 4hr, 6hr and 12 hrs or left unstimulated (Uns). Cell lysates were collected and analysed for Phospho-I $\kappa$ B and IRF3.

Upregulation of Phospho-I $\kappa$ B is observed along with IRF3 and a heightened level is maintained from 1hr through to 12 hrs (Fig 3.6). Dimerisation of IRF3 is also clearly visible through the two bands forming.

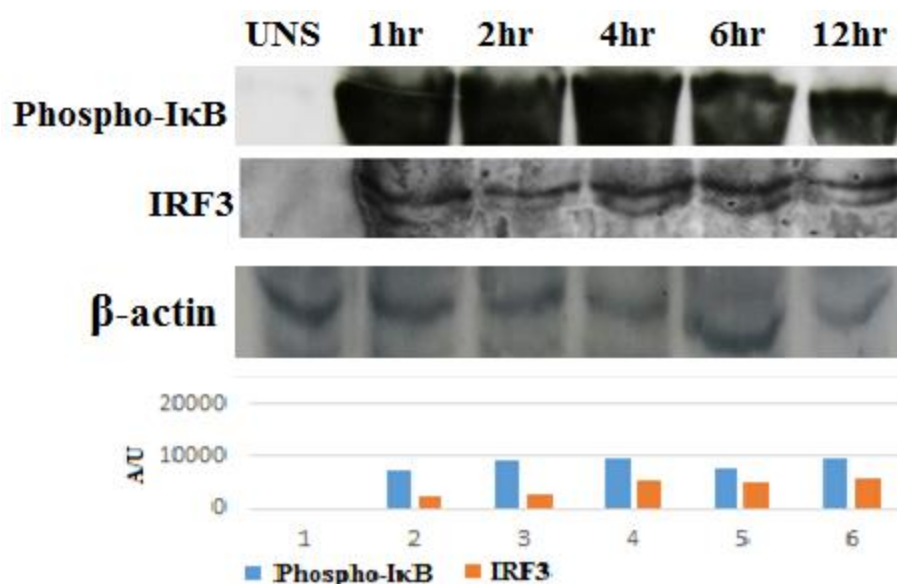


**Figure 3.5 Phospho-I $\kappa$ B and IRF3 detection.** A549 Lung Epithelium Cells were infected with 100 PFU viral stock (HRV58) or left unstimulated (Uns) for 1hr, 2hr, 4hr, 6hr and 12 hrs. Cell lysates were collected and analysed for Phospho-I $\kappa$ B and IRF3 using SDS-PAGE gel electrophoresis and western blot. Primary antibodies specific for IRF3 or phospho-I $\kappa$ B were used followed by the appropriate secondary antibodies conjugated to HRP. Loading controls for  $\beta$ -actin are also depicted. The bottom panel shows a quantitative analysis (by densitometry) of Phospho-I $\kappa$ B and IRF3. The bands were visualised using the ECL procedure. Data are representative of experiments done three times.

Phospho-I $\kappa$ B detection corresponds with NF- $\kappa$ B activation, which, coupled with IRF3 detection, gives an indication of MDA5 and RIG-I activity in response to different stimulations. This is true for all the three strains of HRV used; HRV5, HRV14 and HRV58.

### **3.2.3 IFN- $\beta$ and IL1 $\beta$ Production of HRV infected Cells**

A549 Lung Epithelial cells were infected with 100PFU of HRV14 and left to incubate 1, 2, 4, 6 and 12 hours and then supernatants were collected. The supernatants added to HEK IFN $\beta$  or HEK IL1 $\beta$  reporter cells and incubated for 24 hours. Quanti-Blue was added and the levels of SEAP measured using a spectrophotometer at 630nm. The SEAP levels correspond to the expression levels of IFN $\beta$ / IL1 $\beta$ . The same was repeated with HRV58.

IFN- $\beta$  is a type I IFN, which signals through the IFN- $\alpha$ / $\beta$  receptor and the Jak-STAT pathway to drive interferon stimulated gene (ISG) expression and an innate immune response.

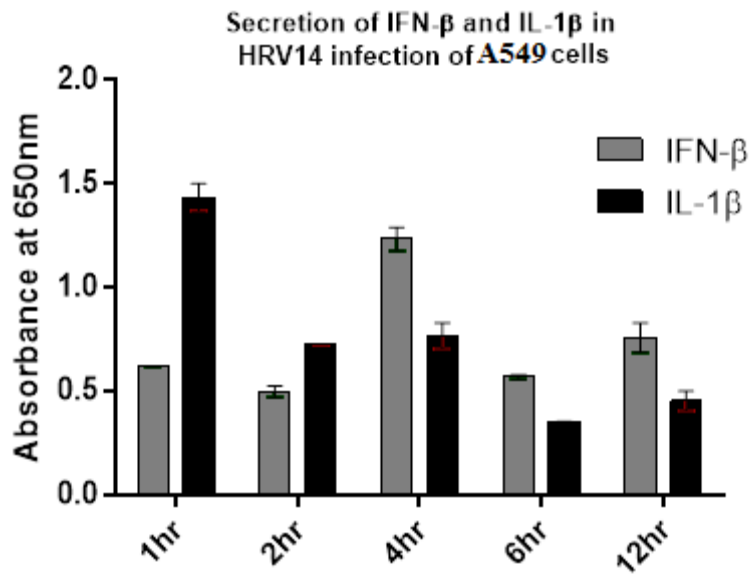


**Figure 3.6 – IFN $\beta$ / IL1 $\beta$  response in HRV14 infections.** Supernatant from A549 cell Infections with 100PFU of HRV14 for 1, 2, 4, 6 and 12 hours was added to HEK IFN $\beta$ / HEK IL1 $\beta$  reporter cells and incubated for 24 hours. Quanti-Blue was added and the levels of SEAP measured using a spectrophotometer at 630nm. The SEAP levels correspond to the expression levels of IFN $\beta$ / IL1 $\beta$ .

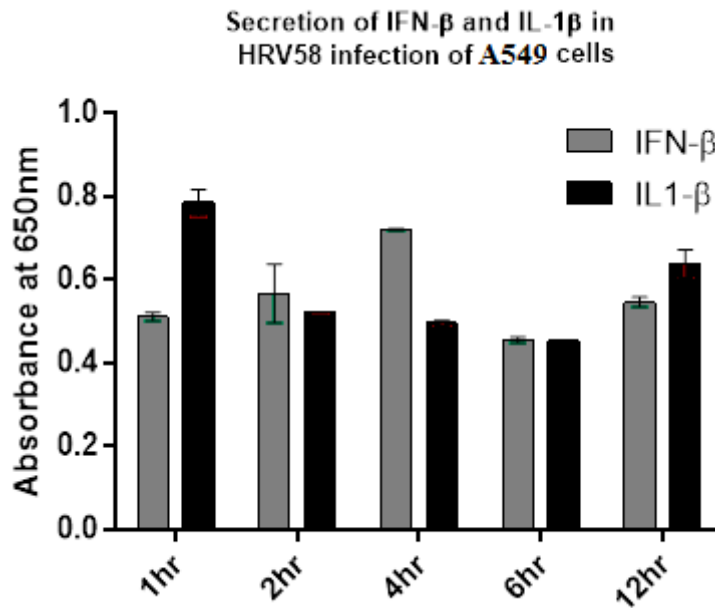


**Figure 3.7 – IFN $\beta$ / IL1 $\beta$  response in HRV58 infections.** Supernatant from A549 cell infections with 100PFU of HRV58 for 1, 2, 4, 6 and 12 hours was added to HEK IFN $\beta$ / HEK IL1 $\beta$  reporter cells and incubated for 24 hours. Quanti-Blue was added and the levels of SEAP was measured using a spectrophotometer at 630nm. The SEAP levels correspond to the expression levels of IFN $\alpha$ / $\beta$ .

In both the stimulations with HRV14 and HRV58, a sharp rise in IL-1 $\beta$  is seen. This suggests that inflammation might occur as a result of HRV infections in lung cells. It could also correspond to the higher level of NLRP3 and whether or not this is a result of an activated NLRP3 inflammasome pathway, will be studied in the following chapter.

However it becomes more apparent that as a result of the RLRs recognising viral invasion eventually stimulates the ISG resulting in the secretion of higher levels of IFN- $\beta$ .

### **3.2.4 HRV5 ssRNA stimulations**

Picornaviruses are positive-sense ssRNA viruses and have a common replication pathway for all viruses in the family. During the viral replication cycle transcription of the viral genome into complementary RNA (negative strand) occurs. This template is used to form new strands of RNA which are double stranded (dsRNA). Other forms of RNA are also formed such as the replicative intermediate form (RF), a partially double stranded form (RI) etc. So, during viral replication a plethora of foreign RNA will be found in the host cell during an infection. These are known to be recognised by RLRs during an infection.

In this study however we have isolated genomic ssRNA from HRV5 and used it to infect lung epithelial cells (A549) to determine which TLRs and RLRs recognise ssRNA and initiates an innate immune response.

### 3.2.4.1 Isolating ssRNA

In order to determine the immunostimulatory effect of viral genomic ssRNA. The viral ssRNA was isolated from purified viral stocks and analysed by agarose gel electrophoresis (Fig 3.8).

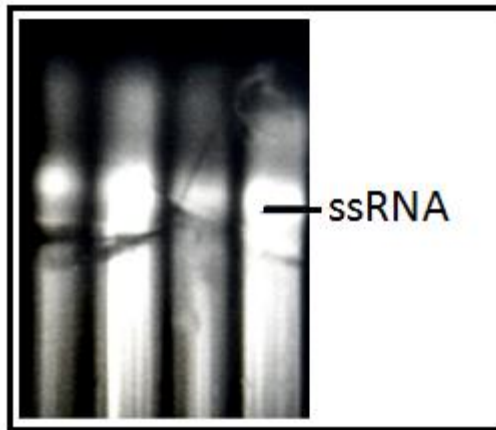


**Figure 3.8 Agarose Gel Electrophoresis of isolated ssRNA from HRV5.** HRV5 RNA was visualized in GelRed-stained gels using a standard UV transilluminator with an ethidium bromide filter. Data are representative of experiments done three times

### 3.2.4.2 ssRNA stimulations and PRR expression levels

Viral RNA mixed with lipofectamine for cell uptake was used to stimulate lung epithelial cells at different time points. The expression level of Pattern recognition receptors that recognize viral RNA such as TLR7, TLR8, MDA5 and RIG-I was determined by Immunofluorescence.(Fig 3.10). A549 cells were stimulated with 20 $\mu$ g of purified ssRNA.

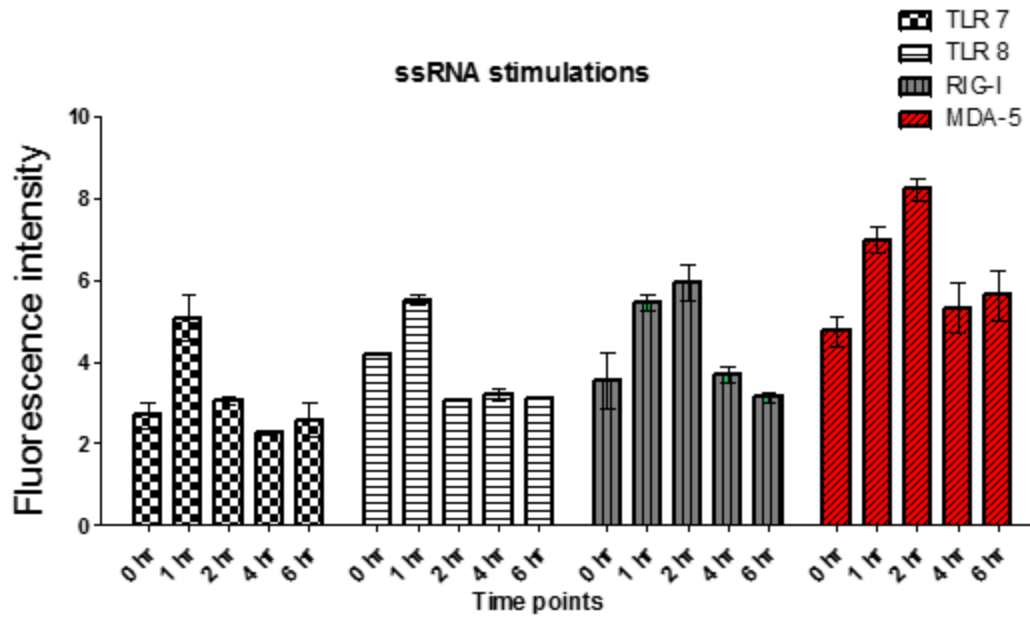


**Figure 3.9 (a) PRR expression levels in cells stimulated with ssRNA.** Following stimulation with ssRNA, PRR expression was examined at different time points using the appropriate primary antibody followed by a secondary conjugated to FITC. Receptor expression was determine as the Geo.Mean of Fluorescent intensity. Fluorescence was detected using a FACSCalibur (BectonDickinson)

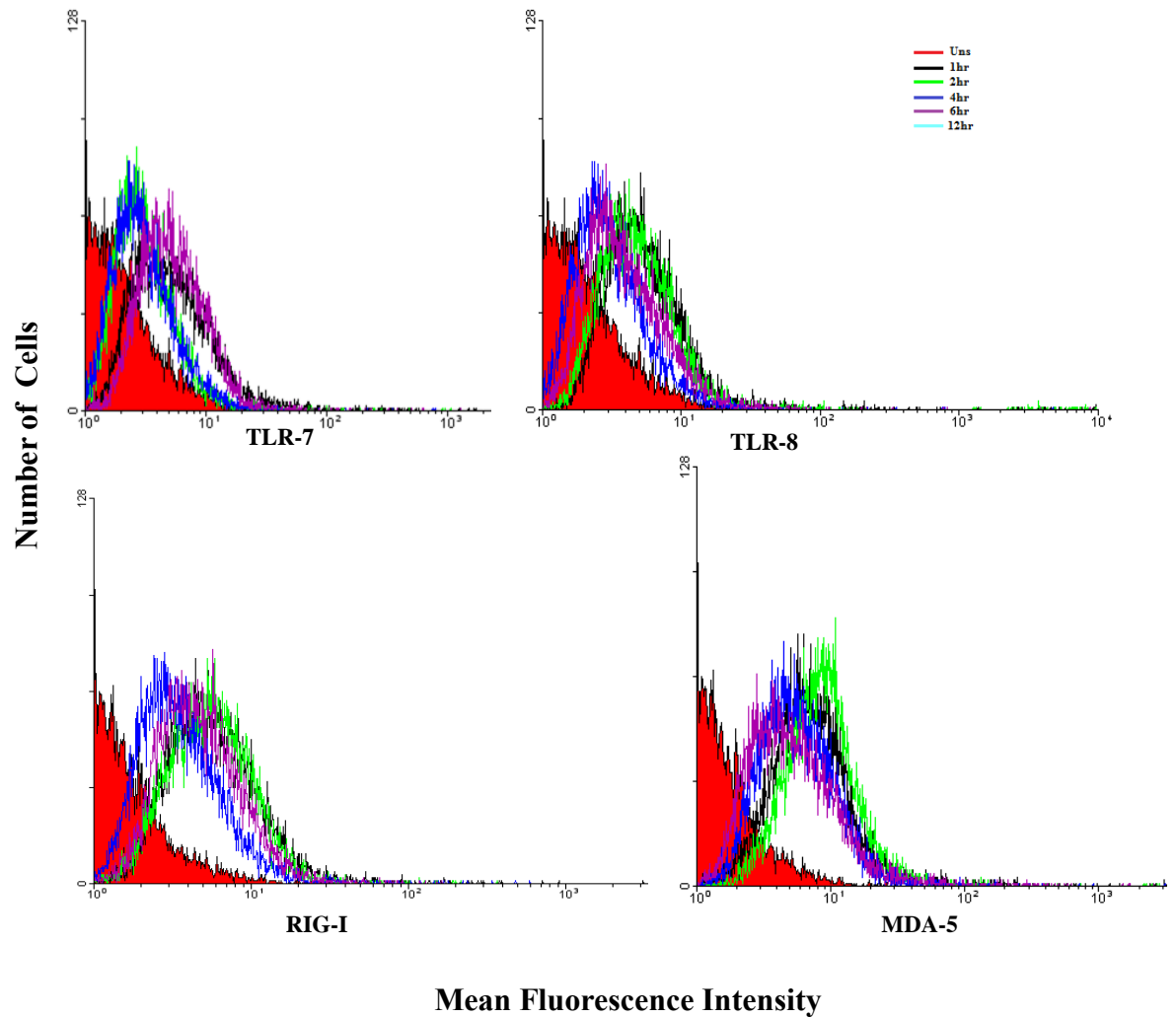


**Figure 3.9 (b) PRR expression levels in cells stimulated with ssRNA.** Following stimulation with ssRNA, PRR expression was examined at different time points using the appropriate primary antibody followed by a secondary conjugated to FITC. Receptor expression was determined as the Geo.Mean of Fluorescent intensity. Fluorescence was detected using a FACSCalibur (Becton Dickinson) counting 10,000 cells not gated. Isotype controls were performed, with values similar to unstimulated samples. The data represent the mean SD of 3 independent experiments, indicating statistically significant ( $P < .05$ ) increase in expression compared with corresponding unstimulated controls.



88From these results we observed upregulation of TLR7 and TLR8 possibly due to the detection of the viral ssRNA genome in the endosomal compartments of the cells by the resident TLR7 and TLR8. These TLRs are seen to be upregulated after stimulating the cells which suggests that they act as host sensors for the HRV5 genome . Both RLHs appear to be upregulated and more specifically MDA5, which is expected since it has been shown to be involved in Picornaviridae recognition.

#### **3.2.4.2 RLH Downstream Signalling and IRF3**

As a response to viral infection mammalian cells elicits both the innate and the adaptive immune system. One of the most efficient antiviral response of the innate immune system is triggered through the production of interferons through IRF3 and IRF7 activation (Kawai et al., 2005). RLHs signalling works through CARD-CARD interactions between the RLH and Interferon Promotor Stimulator 1 (IPS-1) also known as MAVS, Cardif and VISA. IPS-1 contains an N-terminal CARD domain and a C-terminal transmembrane (TM) domain. The TM domain is required for localisation to the mitochondria and allows association and activation of TRAF3. TRAF3 acts as a link between IPS-1 and TBK1/IKKi with TRAF Family Member-Associated NF- $\kappa$ B (TANK) family proteins (TANK, NAP1 and SINTBAD) acting as scaffold proteins. IKKi and TBK1 phosphorylate and activate IRF3 and IRF7 which promote Type IFN production(Kawai T et al., 2005; Kumar H et al., 2006).

In order to confirm the involvement of PRR in HRV5 detection and cytokine release the presence of IRF3 upon stimulation with virus or ssRNA was investigated. The cells were stimulated for different time points and analyzed by SDS-PAGE electrophoresis and western blotting. From the results we observed the presence of IRF3 in lung epithelial cells (A549) when stimulated with live virus and viral ssRNA (3.11).

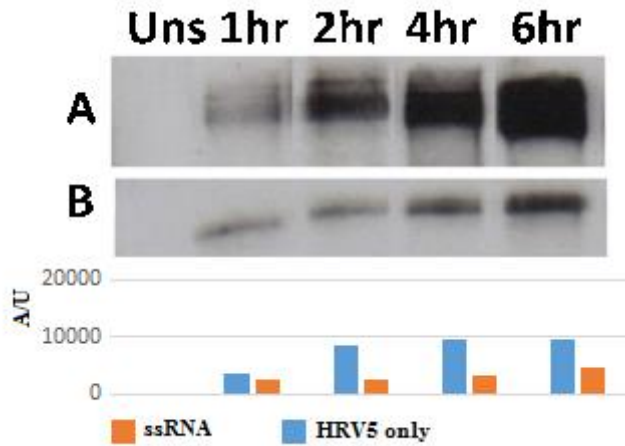


**Figure 3.10 Detection of IRF3 in cells stimulated with HRV5 or ssRNA.**

Western blot of IRF3 from lysates of unstimulated A549 cells and those cells after 1, 2, 4, 6hr stimulation with HRV5 (A) or ssRNA (B). Lysates were separated by sodium dodecyl sulphate polyacrylamide gel electrophoresis and transferred on a nitrocellulose membrane. The membrane was probed for IRF3 specific mAb followed by the appropriate secondary antibody conjugated to HRP and imaged via enhanced chemiluminescence. The bottom panel shows a quantitative analysis (by densitometry) of IRF3. The data represent the mean of three independent experiments

### 3.2.4.3 Cytokine secretions

As mentioned before, TLRs and RLRs engage themselves after recognising virus or viral components in releasing inflammatory cytokines. In this study lung epithelial cells were stimulated with both live virus and viral ssRNA and the inflammatory response produced was measured by investigating cytokine secretion. We observe the secretion of IFN $\gamma$  and IL6 in both stimulations with HRV5 and ssRNA. (Fig 3.12 and Fig3.13) IL6 being more predominant in the ssRNA stimulations.

**Cytokine secretions in response to  
live virus stimulations on A549 cells**

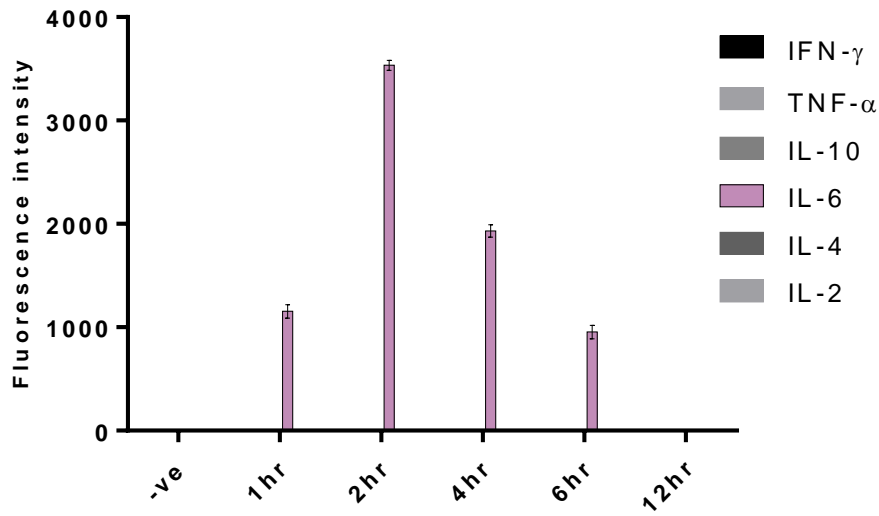


**Figure 3.11 Levels of Cytokine secretions in A549 cells stimulated with 100PFU of live virus (HRV5).** Cells were stimulated at different time points. The supernatants were harvested and assayed for cytokine secretion using the Th1/Th2 CBA kit (Becton Dickinson). Fluorescence was detected using a FACSCalibur (Becton Dickinson)

### Cytokine secretion in response to Viral ssRNA on A549

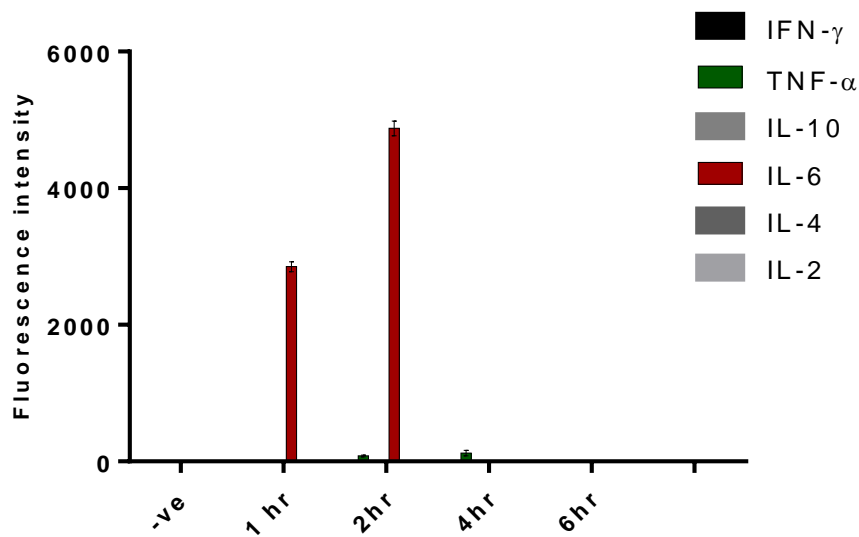


**Figure 3.12 Levels of Cytokine secretions in A549 cells stimulated with 20 $\mu$ g of viral ssRNA** Cells were stimulated at different time points. The supernatants were harvested and assayed for cytokine secretion using the Th1/Th2 CBA kit (Becton Dickinson). Fluorescence was detected using a FACSCalibur (Becton Dickinson).

Secretion of IFN $\beta$  and IL-1 $\beta$  was also measured after infecting A549 cells with 100PFU of HRV5 or 20 $\mu$ g of viral ssRNA, for 1, 2, 4, 6 and 12 hours and supernatant was added to HEK IFN $\beta$ / HEK IL1 $\beta$  reporter cells and incubated for 24 hours. We observe high levels of IFN $\beta$  production for both the stimulations (with live virus and ssRNA), although the response to ssRNA is milder than live virus (fig 3.13). This suggests that although ssRNA has the capability of inducing an acute interferon response, the live virus induces a stronger signal. This might be because of viral proteins that may independently contribute towards signalling for interferon production.

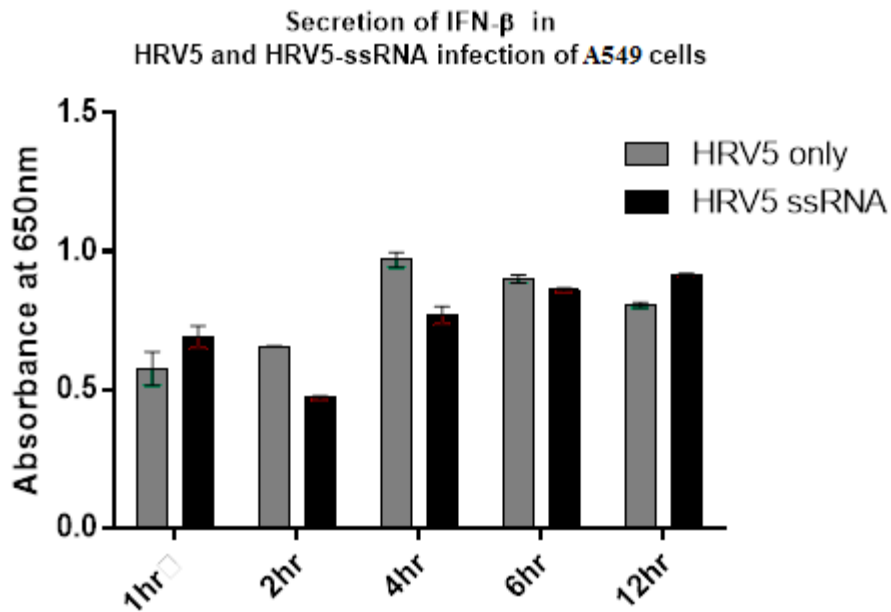


**Figure 3.13 IFN $\beta$  response in HRV5 or HRV5 ssRNA infections.** Supernatant from A549 cell infections with 100PFU of HRV5 or 20 $\mu$ g of viral ssRNA, for 1, 2, 4, 6 and 12 hours was added to HEK IFN $\beta$ / HEK IL1 $\beta$  reporter cells and incubated for 24 hours. Quanti-Blue was added and the levels of SEAP was measured using a spectrophotometer at 630nm. The SEAP levels correspond to the expression levels of IFN $\beta$ .

A similar response is observed with IL-1 $\beta$  production where the live virus stimulations tend to produce more cytokine than the ssRNA itself (Fig 3.14). In the following chapter we describe how HRV has components (viral proteins/ viroporin) has the capacity to independently trigger an inflammatory response.

Secretion of IL1- $\beta$  in  
HRV5 and HRV5-ssRNA infection of A549 cells

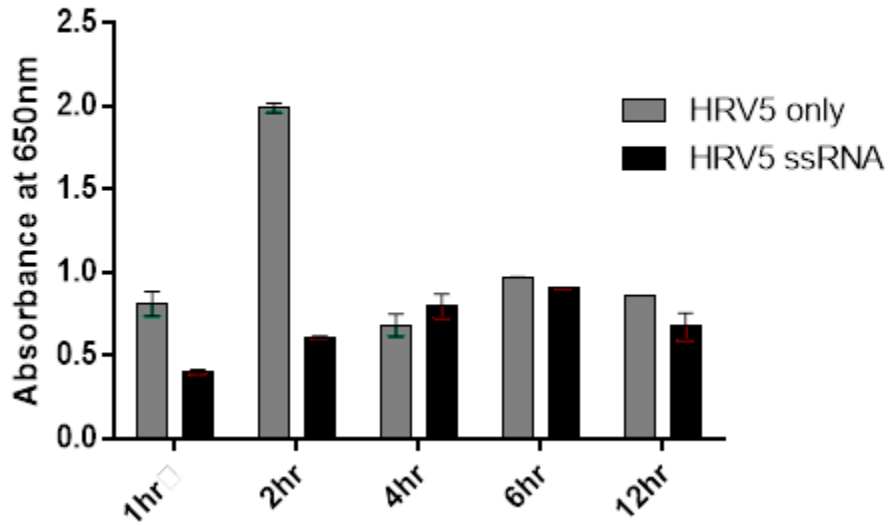


**Figure 3.14 IL1 $\beta$  response in HRV5 or HRV5 ssRNA infections.** Supernatant from A549 cell infections with 100PFU of HRV5 or 20 $\mu$ g of viral ssRNA, for 1, 2, 4, 6 and 12 hours was added to HEK IFN $\beta$ / HEK IL1 $\beta$  reporter cells and incubated for 24 hours. Quanti-Blue was added and the levels of SEAP was measured using a spectrophotometer at 630nm. The SEAP levels correspond to the expression levels of IL1 $\beta$ .

### 3.2.5 RLR Dimerization

RLRs have been shown to recognise viral RNA and stimulate an antiviral response with MAVs which is another RNA helicase used as an adaptor to initiate IFN signalling via phosphorylation of IRF3 and IRF7 (Kawai et al., 2005). It has been shown that activation of RIG-I or MDA5 leads to MAVs dimerisation which is essential for the downstream signal transduction. Since MAVS seems to dimerise upon activation (Yoneyama et al., 2005) we decided to determine whether RIG-I or MDA5 could also dimerise once activated by their viral ligand. As stated in the methods the objective of these experiments was to determine whether these RLRs self dimerise or heterodimerise. RIG-I is 110KDa, MDA5 is 117KDa, while LGP2 is smaller and is around 60KDa. Thus a dimer of RIG-I should be roughly 200KDa, as should an MDA5 dimer, while a RIG-I/MDA5 with LGP2 dimer should be around 170KDa.

Human lung epithelial cells were stimulated with either HRV5 for 1, 2, 4 or 6 hours. Following stimulation with the virus for the different time points, the cells were lysed in lysis buffer (0.5% NP40, 1% CHAPS, 15 mM NaCl, 2mM PMSF, 1mM MgCl<sub>2</sub>) for at least an hour or overnight. The cell lysates were pre-cleared with Protein-A Sepharose beads prior to immunoprecipitations using specific antibodies against MDA5, RIG-I or LGP2. Once the specific antibodies had bound to their cellular target, the complex was precipitated using Protein A Sepharose beads, which have an affinity for the Fc region of the antibody. The pellets were either incubated in SDS-PAGE non-reducing buffer (0.5% SDS, 20% glycerol, 10mM TrisHCl) and incubated at room temperature or incubated in reducing buffer (1.4 M mercaptoethanol, 1% SDS, 20% glycerol, 10mM TrisHCl) and

boiled prior to SDS-PAGE electrophoresis. It was expected that incubation with non-reducing SDS-PAGE buffer at room temperature will retain any associations that might exist between homo and heterodimers.

#### **3.2.5.1 MDA5 and LGP-2 dimerisation**

Cell lysates were pre-cleared and LGP2 was precipitated using LGP2 Goat pAb and PAS beads and analysed by SDS-PAGE electrophoresis. Western blotting was performed using a MDA5 Rabbit pAb followed by a polyclonal Swine anti-Rabbit Ig HRP (Figure 3.15). Dark higher bands approximately 170 kDa can be seen, possibly suggesting the presence of a MDA5- LGP2 dimer. A less strong band of ~110 kDa was also seen, which is most likely the MDA5 monomers.



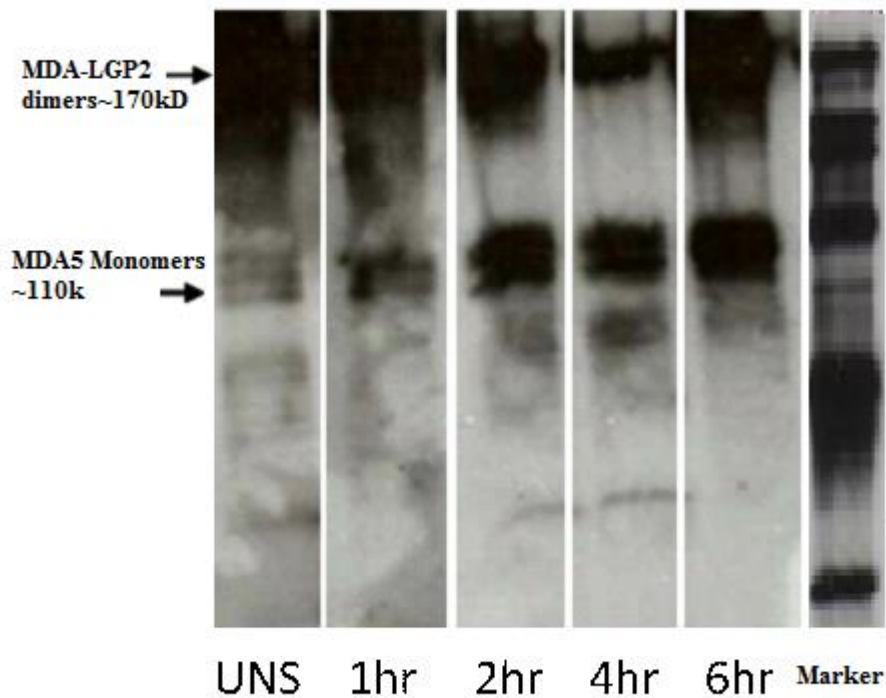


**Figure 3.15 LGP2 and MDA5 heterotypic association.** A549 cells were stimulated with HRV5 for 1, 2, 4, or 6 hours, or left unstimulated. The cell lysates were precleared with PAS beads 2 times. LGP2 was precipitated out of the lysate using LGP2 Goat pAb and PAS beads. Pellets were washed in lysis buffer and analysed using SDS-PAGE (X2 SDS-PAGE Non-Reducing Sample Buffer) and western blotting with MDA5 Rabbit pAb (primary) and followed by polyclonal Swine anti-Rabbit Ig HRP. To visualise the protein bands ECL was performed. Data are representative of experiments done twice

The results showed that there were two bands for each time point, one at around 170KDa which is most likely an LGP2 heterodimer with MDA5. We also notice MDA5 monomers at about 110kDa.

### **3.2.5.2 MDA5 homotypic associations**

To determine MDA5 homotypic interactions, cells were stimulated with HRV5 for 1, 2, 4, or 6 hours, or left unstimulated, and an MDA5 Goat pAb was used to precipitate MDA5 out of the cell lysate and analysed by SDS-PAGE electrophoresis. Western blotting was performed using an MDA5 Rabbit pAb and detected using polyclonal Swine anti-Rabbit Ig HRP are shown in Figure

Initially we investigated MDA5 homo-dimerisation from cell lysates of unstimulated cells as well as cells stimulated with HRV5 at different time points were precipitated with an antibody specific for MDA5. Once the antibody was allowed to bind to its cellular target, the complex was precipitated with Protein A Sepharose beads and analysed by non-reducing SDS-PAGE. It was shown that MDA5 existed as an equilibrium between monomers and dimers 1 and 2 hr post infection, whereas after 4 and 6 hr of infection the whole of the MDA5 cellular pool shifted into homodimers (Fig 3.16).

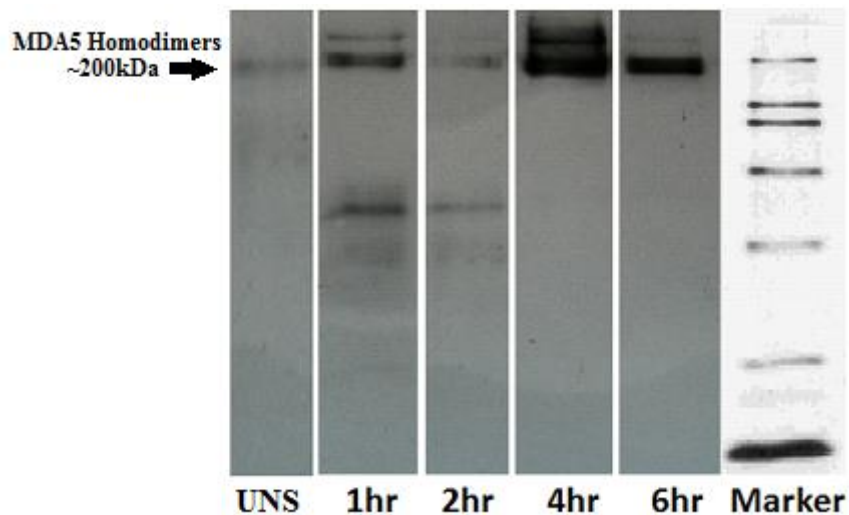


**Figure 3.16 Homotypic associations of MDA5.** The cell lysates (unstimulated and stimulated with HRV5 at different time points) were pre-cleared with Protein-A Sepharose beads prior to immunoprecipitations. Then a specific antibody against MDA5 was used. Once the MDA5 antibody had bound to its cellular target, the complex was precipitated using Protein A Sepharose beads, which have an affinity for the Fc region of the antibody. The pellets were incubated in SDS-PAGE non-reducing buffer and analysed via SDS-PAGE electrophoresis. Western blotting was performed using an MDA5 specific antibody followed by the appropriate secondary conjugated to HRP. The proteins were imaged via enhanced chemiluminescence. Data are representative of experiments done twice.

The MDA5 immunoprecipitations show bands that around 200kDa for all the time points suggesting that MDA5 does indeed form a dimer. There are also bands at around 110kDa which is most likely MDA5 as a monomer. Firstly the heaviest band, at around 200kDa is only present in the later time points, not in the unstimulated. The 120kDa band appears at the unstimulated 1hr and 2 hr time point. This could suggest MDA5 is a monomer in its natural state, but upon infection MDA5 dimerises with itself and thus becomes active.

### 3.2.5.3 RIG-I and LGP-2 dimerisation

To determine RIG-I and LGP2 interactions A549 cells were stimulated with HRV5 for different time points, or left unstimulated. LGP2 was precipitated out of the lysate using LGP2 Goat pAb and PAS beads and analysed by non-reducing SDS-PAGE electrophoresis. Western blotting with RIG-I antibody was used to determine interactions. The association between LGP2 and RIG-I can be seen in (Figure 3.17).

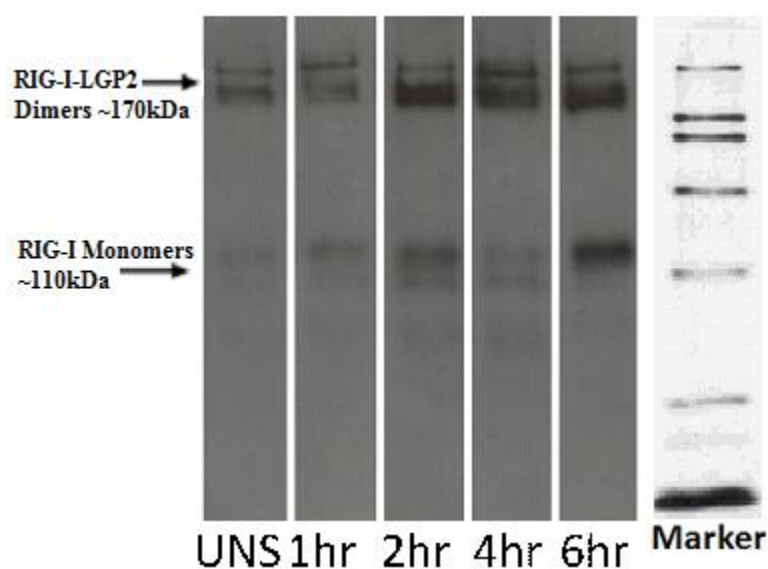


**Figure 3.17 LGP2 and RIG-I heterotypic association.** A549 cells were stimulated with HRV5 for 1, 2, 4, or 6 hours, or left unstimulated. The cell lysates were precleared with PAS beads 2 times. LGP2 was precipitated out of the lysate using LGP2 Goat pAb and PAS beads. Pellets were washed in lysis buffer and analysed using SDS-PAGE (X2 SDS-PAGE Non-Reducing Sample Buffer) and western blotting with RIG-I Rabbit pAb (primary) and followed by polyclonal Swine anti-Rabbit Ig HRP. To visualise the protein bands ECL was performed. Data are representative of experiments done twice.

### 3.2.5.4 LGP2 homotypic associations

In order to determine whether LGP2 also homodimerises, A549 were stimulated with HRV5 for 1, 2, 4, or 6 hours, or left unstimulated, and an LGP2 Goat pAb was used to precipitate LGP2 out of the cell lysate. The western blot results after incubating with LGP2 Rabbit pAb and detecting using polyclonal Swine anti-Rabbit Ig HRP can be seen in Figure 3.18.

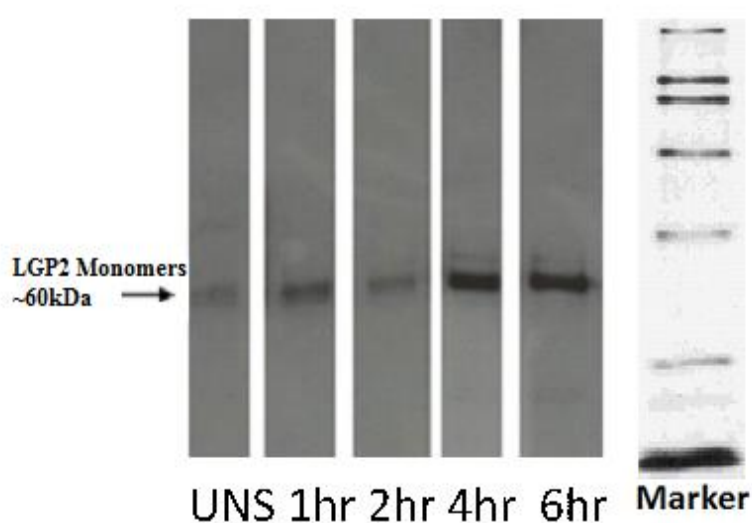


**Figure 3.18 Homotypic associations of LGP2.** The cell lysates (unstimulated and stimulated with HRV5 at different time points) were pre-cleared with Protein-A Sepharose beads prior to immunoprecipitations. Then a specific antibody against LGP2 was used. Once the LGP2 antibody had bound to its cellular target, the complex was precipitated using Protein A Sepharose beads, which have an affinity for the Fc region of the antibody. The pellets were incubated in SDS-PAGE non-reducing buffer and analysed via SDS-PAGE electrophoresis. Western blotting was performed using an LGP2 specific antibody followed by the appropriate secondary conjugated to HRP. The proteins were imaged via enhanced chemiluminescence. Data are representative of experiments done twice.

The bands seen above is around 60KDa showing LGP2 monomers at all time-points. It should be noted that while LGP2 appears to dimerise with RIG-I and MDA5 it clearly does not under these conditions homodimerise.

### 3.2.5.5 RIG-I homotypic associations

To determine RIG I homotypic interactions, cells were stimulated with HRV5 for 1, 2, 4, or 6 hours, or left unstimulated, and an RIG-I Goat pAb was used to precipitate RIG-I out of the cell lysate and analysed by non reducing SDS-PAGE electrophoresis. Western blotting was performed using a RIG-I Rabbit pAb and detected using polyclonal Swine anti-Rabbit Ig HRP are shown in (Figure 3.19).

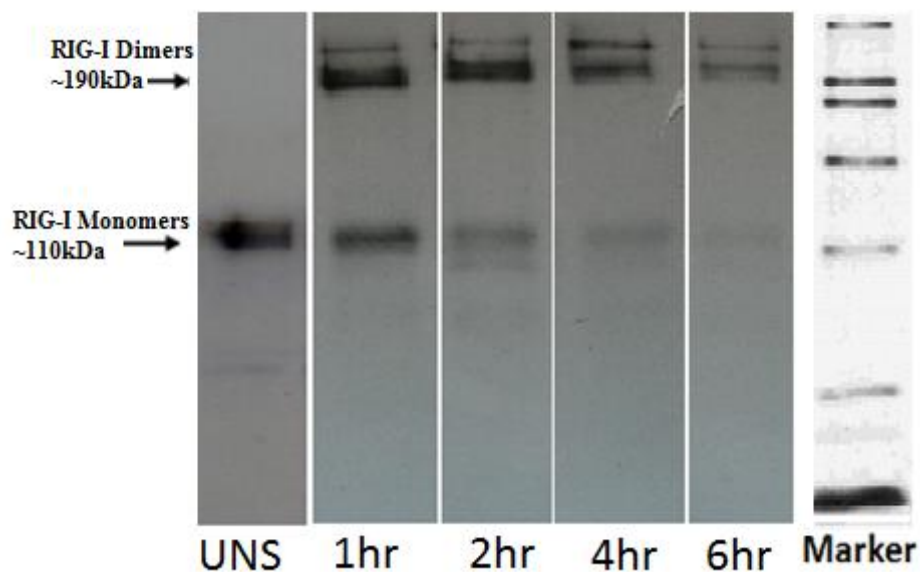


**Figure 3.19 Homotypic associations of RIG-I.** The cell lysates (unstimulated and stimulated with HRV5 at different time points) were pre-cleared with Protein-A Sepharose beads prior to immunoprecipitations. Then a goat anti RIG-I antibody was used. Once the RIG-I antibody had bound to its cellular target, the complex was precipitated using Protein A Sepharose beads, which have an affinity for the Fc region of the antibody. The pellets were incubated in SDS-PAGE non-reducing buffer and analysed via SDS-PAGE electrophoresis. Western blotting was performed using a rabbit anti RIG-

I specific antibody followed by swine anti rabbit Ig secondary conjugated to HPR The proteins were imaged via enhanced chemiluminescence.

The RIG-I immunoprecipitations shows bands at around 190kDa, suggesting the presence of a RIG-I dimer, a band at around 110kDa showing that RIG-I exists as a monomer as well. The monomer exists in the unstimulated state and then upon stimulation with HRV5 dimerises.

### 3.2.5.6 RIG-I and MDA5 under reducing conditions

In order to determine whether the presence of the dimers was specific. The immunoprecipitations were repeated and incubated in reducing buffer and boiled prior to SDS-PAGE electrophoresis to see whether the dimers were specific and whether they could be disrupted (Fig.3.20)

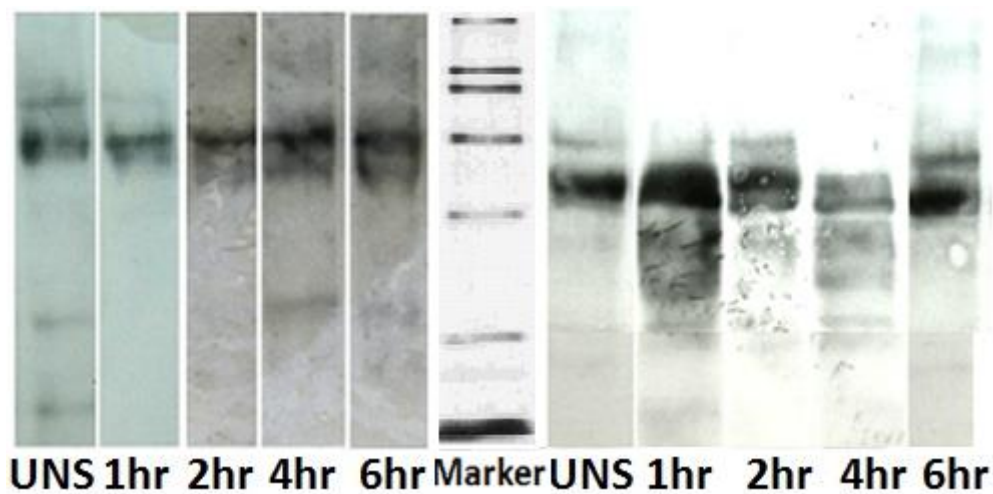


**Figure 3.20 Immunoprecipitation of RIG-I and MDA5 under reducing conditions.**

The cell lysates (unstimulated and stimulated with HRV5 at different time points) were pre-cleared with Protein-A Sepharose beads prior to immunoprecipitations. Then a specific antibody against MDA5 (A) or RIG-I (B) was used. Once the RIG-I antibody had bound to its cellular target, the complex was precipitated using Protein A Sepharose beads, which have an affinity for the Fc region of the antibody. The pellets were incubated in SDS-PAGE -reducing buffer and boiled then analysed via SDS-PAGE electrophoresis. Western blotting was performed using an MDA5 (A) or RIG-I (B)

specific antibody followed by the appropriate secondary conjugated to HRP. The proteins were imaged via enhanced chemiluminescence.

The data showed that the dimers were disrupted, thus the high molecular weight proteins disappeared and only monomers were present after boiling the samples and treating them with reducing agents.

### **3.3 Conclusion**

PRR have been shown to be key components of the innate immune system, creating a hostile environment for viral pathogens by triggering a cytokine and IFN immune response. TLRs as well as RIG-I and MDA5 have been shown to recognise different viruses and target specific viral PAMPs. TLR7 and TLR8 (Triantafyllou et al., 2005) as well as MDA5 has been shown to recognize members of the Picornavirus family (Kato H et al., 2006) (Wang, et. al, 2010). Thus it would seem likely that HRV could be recognized by more than one PRR.

From this study, we can see cytokine secretion as well as IRF3 activation verifying the involvement of PRR in HRV5, 14 and 58 detection. The increased expression of TLR7 and TLR8 when lung cells were stimulated with HRV5 or ssRNA are implicating these TLRs in HRV5 ssRNA detection. Furthermore MDA5 is also shown as up-regulated upon viral infection and IFN secretion is triggered once the virus infects the cells. In addition to identifying the PRR involved in the innate immune response to HRV, RLR dimerisation was also investigated. It has been shown that different PRR can homodimerise upon activation to augment signalling like MAVs the adaptor molecule for RLR signalling or TLR8 which recognizes ss RNA and initiate innate immune responses.



It was shown that upon ligand stimulation, there was a formation of an TLR8 dimer, which enables downstream signalling processes (Tanji et al. 2013).

Therefore it is possible that RLRs could also dimerise. From the immunoprecipitation experiments performed it was evident that like TLR8 and MAVs LGP2, RIG-I and MDA5 exist as monomers in the cell cytoplasm but once activated they form homodimers upon infection, possibly to augment the IFN activation. However it appears that in an uninfected cell both RIG-I and MDA5 forms heterodimers with LGP2, maybe to prevent signalling activities without the presence of a pathogen. However LGP2 exists as a monomer and does not form a homodimer at any point, before or after stimulation. The mechanism by which LGP2 works is very unclear still. These studies have shown that LGP2 seems to form heterodimers with both RIG-I and MDA-5.

## **Chapter 4**

### **Inflammasome activation in HRV infection**

#### **4.1 Introduction**

Human Rhinoviruses have been linked with underlying lung disorders such as asthma and chronic obstructive pulmonary disease in children and adults.

However rhinovirus innate recognition has not been fully elucidated. A study by Stokes et al. shows that epithelial cell responses to rhinovirus are modulated by IL-1 $\beta$  signalling via MyD88 (Stokes et al. 2011). Furthermore there is evidence supporting Rhinoviral infection as a trigger of acute inflammatory exacerbations in patients with underlying airway disease showing that IL-1 $\beta$  levels are enhanced (Hakonarson et al. 1999) within the airways of patients with Chronic obstructive pulmonary disease (COPD) or asthma (de Kluijver et al. 2003, Stokes et al. 2011, Terajima et al. 1997) which can aggravate symptoms. A new study by Dolinay et al. using a mouse model shows that inflammasome-regulated cytokines IL18 and IL-1 $\beta$  are critical mediators of acute lung injury. Their secretion was elevated in the plasma of patients with acute respiratory distress syndrome (ARDS) and served as a novel biomarker of intensive care unit morbidity and mortality (Dolinay et al. 2012). These studies implicate the inflammasome pathway and its downstream cytokines to play critical roles in respiratory inflammation.

Maturation and secretion of interleukins IL-1 $\beta$  and IL-18 is controlled by NOD-like receptors (NLRs) which can be activated by physical damage to the plasma membrane caused by bacterial products and viruses as well as host-derived danger signals (danger associated molecular patterns, DAMPs) and assemble into high-molecular weight, caspase-1-activating platforms called “inflammasomes”. These Inflammasomes play a key role in host defence against bacteria and viruses (Martinon et al. 2002, Yazdi et al. 2010).

This study investigated the contribution of NLR inflammasomes and IL1 $\beta$  secretion in rhinovirus pathogenesis, and the mechanism of inflammasome activation in response to rhinovirus infection.

## **4.2 Results**

### **4.2.1 HRV infection induces inflammasome activation**

A wide variety of danger signals activate inflammasomes. These include pathogen-associated molecular patterns and host-derived molecules that are indicative of cellular damage (danger-associated molecular patterns). In order to determine if HRVs are detected by the inflammasome we infected bronchial cells. The experiments showed that HRV infection induced IL-1 $\beta$  secretion (Fig. 4.1a A) and Caspase-1 cleavage (Fig. 4.1a B).

To define the NLR involvement we knocked down NLRP3, NLRP1, NLRC4 or NLRC5 using shRNA and infected the cells with different HRV strains (HRV14, HRV5, HRV6, HRV58) (shRNA controls in lentivirus constructs were also used) our results were the same for all rhinovirus strains used and showed that the shRNA controls had no effect but IL1 $\beta$  production was impaired when NLRP3 or NLRC5 were knocked down while silencing of NLRP1 or NLRC4 had no effect in IL1 $\beta$  production (Fig. 4.1C). By knocking down both NLRP3 and NLRC5 we completely abrogated IL1 $\beta$  secretion.

IL6 secretion was measured as a control since it is independent of inflammasome activation but is a known marker for NF- $\kappa$ B activation. HRV infected cells with knocked down NLRP3, NLRP1, NLRC4 or NLRC5 had a robust IL6 response (Fig. 4.1D). These

findings suggest that rhinovirus infection activates the NLRP3 and NLRC5 dependent inflammasome.

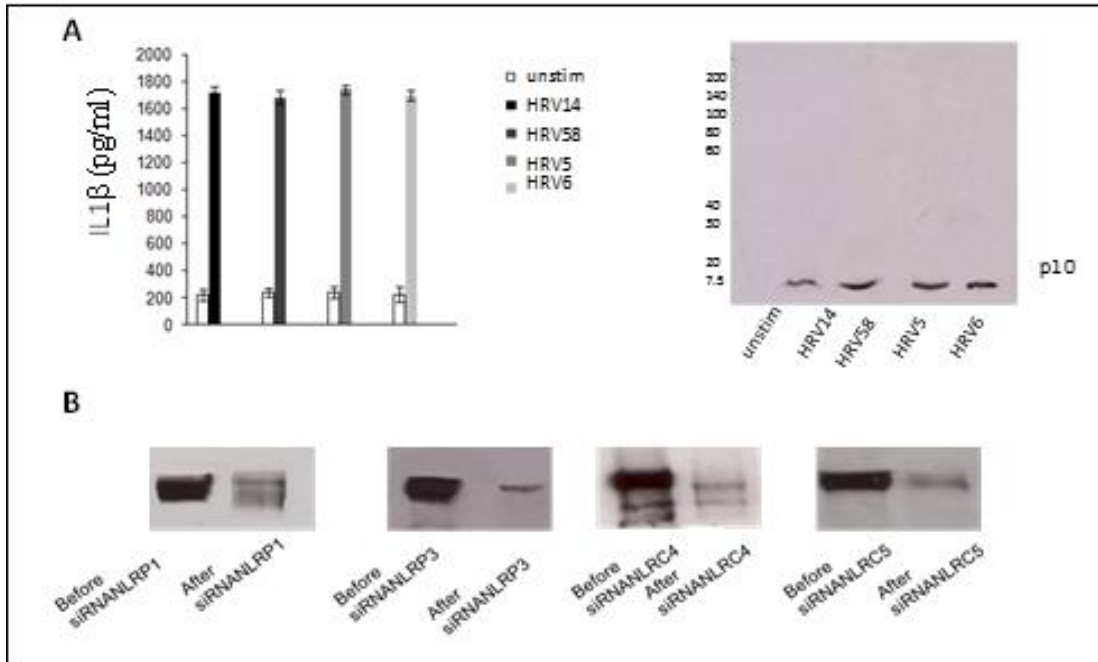


**Figure 4.1 (a) HRV infection activates the NLRP3 and NLRC5 inflammasome.** Bronchial epithelial cells ( $10^6$ ) were infected with 100PFU of HRV14, HRV5, HRV6 and HRV58. Supernatant was collected at 12hr post infection and analysed for IL1 $\beta$  (A) using the CBA bead array system on a FACSCalibur (Becton Dickinson) Cells extracts from infected bronchial epithelial cells were analysed for the presence of caspase p10 by western blotting (B). The data represent the mean of three independent experiments.

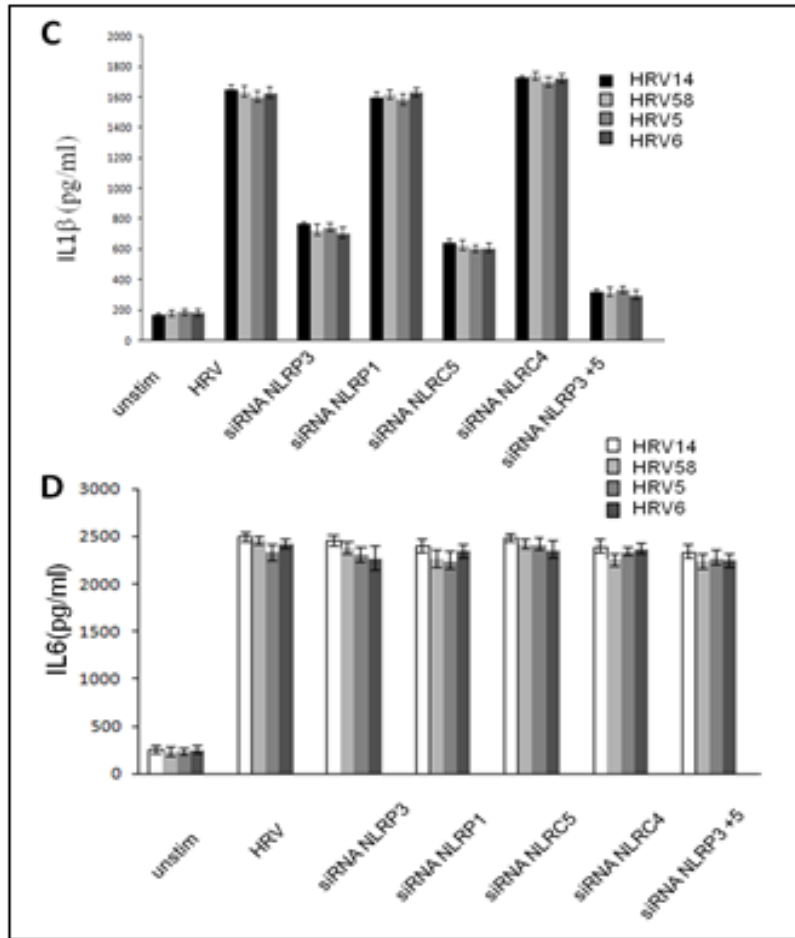


**Figure 4.1(b) HRV infection activates the NLRP3 and NLRC5 inflammasome.** Bronchial epithelial cells ( $10^6$ ) were infected with 100PFU of HRV14, HRV5, HRV6 and HRV58. Supernatant was collected at 12hr post infection and analysed for IL1 $\beta$  NLRP3, NLRP1, NLRC5 or NLRC4 expression was knocked down by siRNA and the cells were again infected with 5moi of HRV14 HRV5, HRV6 and HRV58. Supernatant was collected at 12hr post infection and analysed for IL1 $\beta$  (C) and IL6 using the CBA system (D). The data represent the mean of three independent experiments.

#### **4.2.2 2B ion channel protein triggers inflammasome activation**

To investigate how rhinoviruses stimulate inflammasome activation we looked at rhinovirus proteins that might enhance membrane permeability since it has been shown that membrane perturbations causing potassium efflux by microbial toxins such as aerolysin and nigericin have been shown to activate the NLRP3 inflammasome (Mariathasan et al. 2006). Furthermore the influenza virus M2 proton channel activates the NLRP3 inflammasome pathway by modulating the intracellular  $K^+$  concentration (Ichinohe et al. 2010).

Enteroviruses encode a cytotoxic pore forming protein 2B which changes intracellular  $Ca^{2+}$  homeostasis and interferes with protein trafficking through the secretory pathway (de Jong et al. 2003, van Kuppeveld et al. 1997). Therefore cells were transfected with a plasmid expressing myc-tagged rhinovirus 2B as well as an empty plasmid pEF-myc with a myc tag as a negative control and inflammasome activation was determined by measuring IL1 $\beta$  secretion (Fig. 4.2A) as well as detecting the presence of caspase 1 via western blotting (Fig. 4.2B). The results showed that 2B expression was sufficient to stimulate inflammasome activation.

NLRP3, NLRC4, NLRP1, NLRC5 or NLRP3 and NLRP5 simultaneously were knocked down using siRNA in bronchial cells and cells were transfected with p2B-myc. When IL1 $\beta$  secretion as well as caspase 1 expression was examined the data showed a significant reduction in IL1 $\beta$  secretion (Fig 4.2C) as well as a reduction in caspase 1 expression when NLRP3 or NLRC5 were knocked down while there was no significant change in neither IL1 $\beta$  or caspase 1 when NLRP1 or NLRC4 were knocked down. When both NLRC5 and NLRP3 were silenced IL1 $\beta$  was completely inhibited (Fig. 4.2 b).

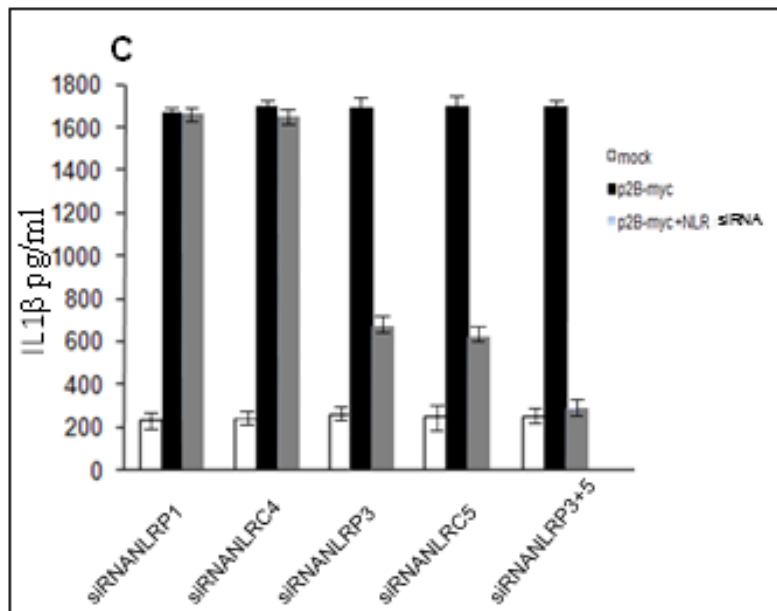
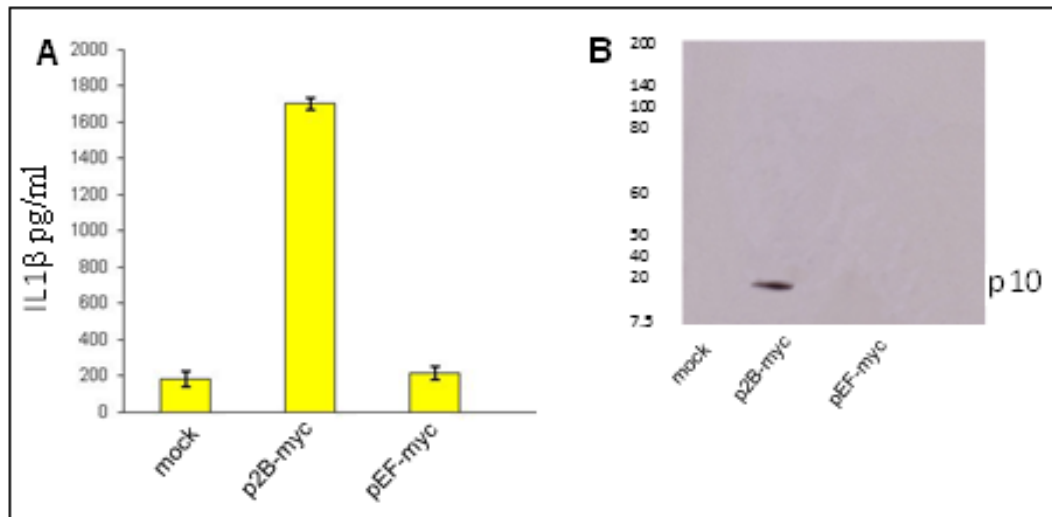


**Figure 4.2 (a) HRV 2B activates inflammasome.** Bronchial epithelial cells were transfected with either 10  $\mu$ g p2B-myc or 10  $\mu$ g pEF-myc an empty plasmid expressing myc as a negative control. Supernatants were collected and tested for IL1 $\beta$  secretion using the CBA bead array system (Becton Dickinson) (A). Cells extracts from mock untransfected and also transfected bronchial cells were analysed for the presence of Caspase p10 by western blotting (B). NLRP3, NLRP1, NLRC4, NLRC5 or NLRP3 and NLRC5 expression was knocked down by psiRNA and the cells were again transfected with p2B-myc and examined for IL1 $\beta$  secretion (C). The data represent the mean of three independent experiments.



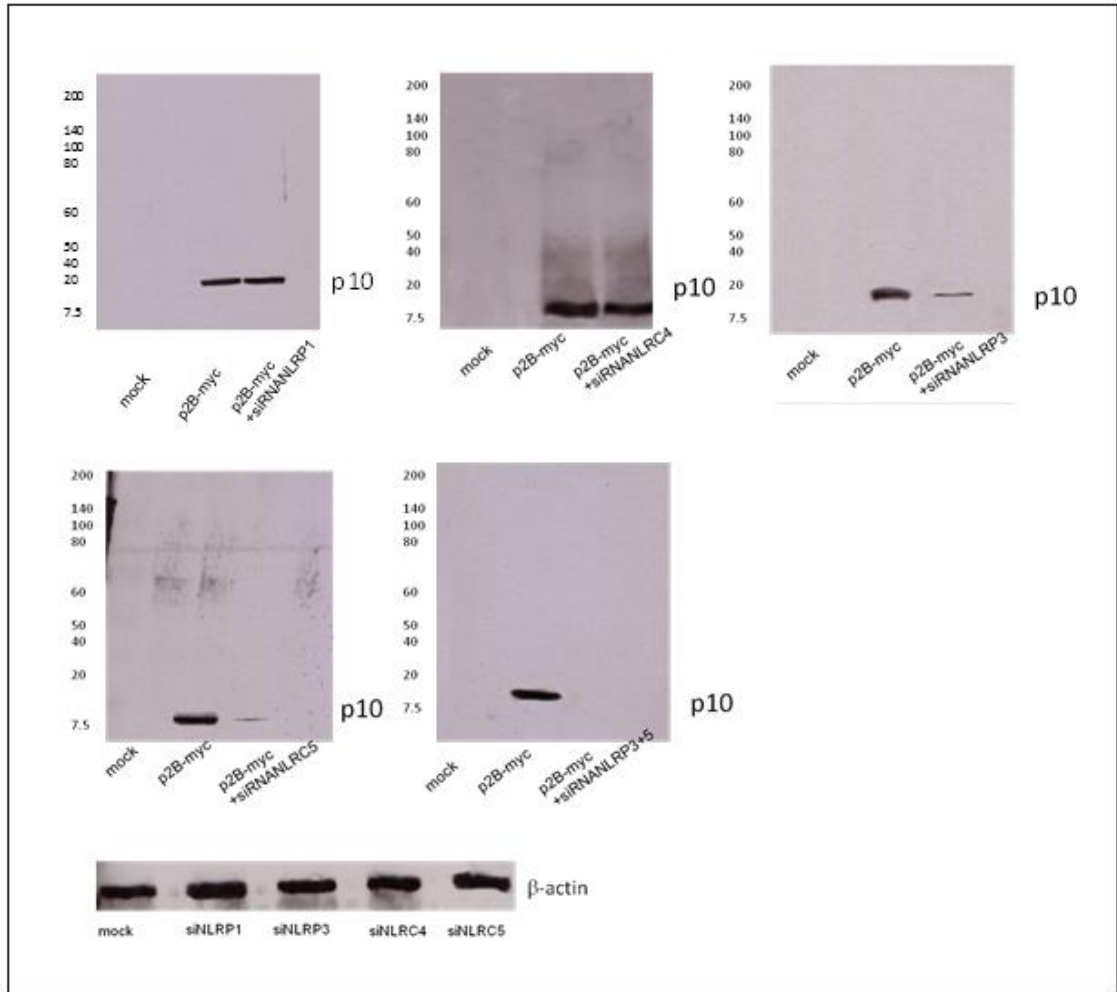


**Figure 4.2 (b) HRV 2B activates inflammasome** Bronchial epithelial cells were transfected with either 10  $\mu$ g p2B-myc or 10  $\mu$ g pEF-myc an empty plasmid expressing myc as a negative control. Cells extracts from mock untransfected and also transfected bronchial cells were analysed for the presence of Caspase p10 by western blotting. NLRP3, NLRP1, NLRC4, NLRC5 or NLRP3 and NLRC5 expression was knocked down by psiRNA and the cells were again transfected with p2B-myc and examined for the presence of Caspase p10 by western blotting (D). The data represent the mean of three independent experiments.

#### **4.2.3 2B protein changes the calcium homeostasis in the cell**

Three mechanisms leading to inflammasome activation had been proposed and studied. Extracellular ATP triggers  $K^+$  efflux (Kanneganti et al. 2007) and induces NLRP3 recruitment, release of lysosomal contents caused by lysosome disruption (Halle et al. 2008, Hornung et al. 2008) or production of ROS (Dostert et al. 2008). Furthermore Murakami et al. also shows that  $Ca^{2+}$  mobilization could be another mechanism of inflammasome activation (Murakami et al. 2012).

Since several studies have identified  $Ca^{2+}$  signalling as a key cellular target for viral infection (Chami et al. 2006) we investigated whether HRV 2B also alters intracellular calcium fluxes, which could trigger NLRP3 and NLRC5 activation.

Bronchial cells were transfected with p2B-myc. Cells transfected with empty plasmid pEF-myc were also used as a control. The  $Ca^{2+}$  sensitive dye FLUO3-AM was used to stain cells for the determination of cytosolic  $Ca^{2+}$  by flow cytometry. Expression of 2B resulted in a significant increase in cytosolic  $Ca^{2+}$  (Fig. 4.3).

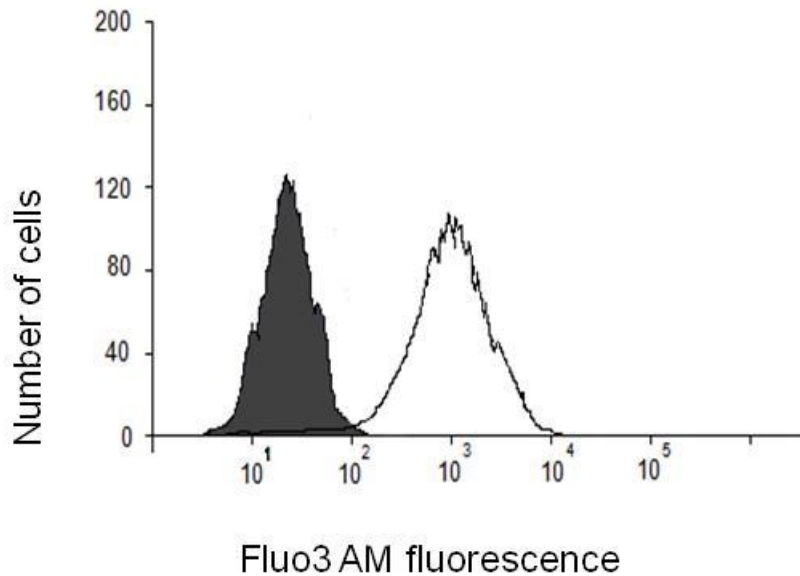


**Fig. 4.3 Cytosolic Ca<sup>2+</sup> measurements**

Bronchial cells were transfected with 10 µg of p2B-myc and the calcium-sensitive dye FLUO3-AM was used to measure the cytosolic calcium level by flow cytometry (white histogram) mock untreated cells are also depicted (grey histogram). This is a representative of four independent experiments

#### **4.2.4 Calcium inhibitors block rhinovirus induced inflammasome activation**

To investigate whether we could inhibit rhinovirus induced inflammasome activation, we used a permeant Ca<sup>2+</sup> chelator, BAPTA-AM as well as ion channel inhibitors: 5-(*N*-ethyl-*N*-isopropyl) amiloride (EIPA) and benzamil, which block Na<sup>+</sup>/H<sup>+</sup> ion channels, and verapamil, which blocks Ca<sup>+</sup> channels (Stuart and Brown 2006). Human bronchial epithelial cells were seeded onto 6-well plates. The following day, cells were infected

with HRV5, HRV6, HRV14 or HRV58 (100PFU) in medium containing the different concentrations of each drug for 60 min (the best working concentration was for BAPTA 15  $\mu$ M, EIPA 25 $\mu$ M, Benzamil 50 $\mu$ M, Verapamil 50  $\mu$ M).

Supernatant containing virus was removed and the cells were washed. Fresh medium containing the drugs was added and the cells were incubated a total of 12 h. (Viability of cells was determined by using 0.2% trypan blue and examining cells under a microscope).

Cell-free supernatant was collected at 12hr post-infection and analyzed by CBA bead array (BD) for IL-1 $\beta$  as well as IL6 as a control since it is a cytokine induced in viral infection but not triggered by inflammasome activation. In some cases, supernatants and cell extracts were collected for Western blot analysis.

To exclude the possibility that the drugs mentioned above affected rhinovirus replication, cells were treated with the optimal concentration of drugs or not treated with drugs and then infected with different strains of rhinoviruses and plaque assay titration was carried out. The results showed that BAPTA-AM, EIPA, benzamil, and verapamil had no effect on viral replication (data not shown).

Our data showed that BAPTA-AM as well as verapamil although to a less degree were able to inhibit IL1 $\beta$  production as well as caspase 1 activation (Fig. 4.4). EIPA or benzamil had no effect in IL1 $\beta$  production and caspase 1 activation. Thus indicating that calcium chelators or calcium inhibitors could be used in the future to control exacerbated IL1 $\beta$  production which is often found in viral inflammatory airway disease.



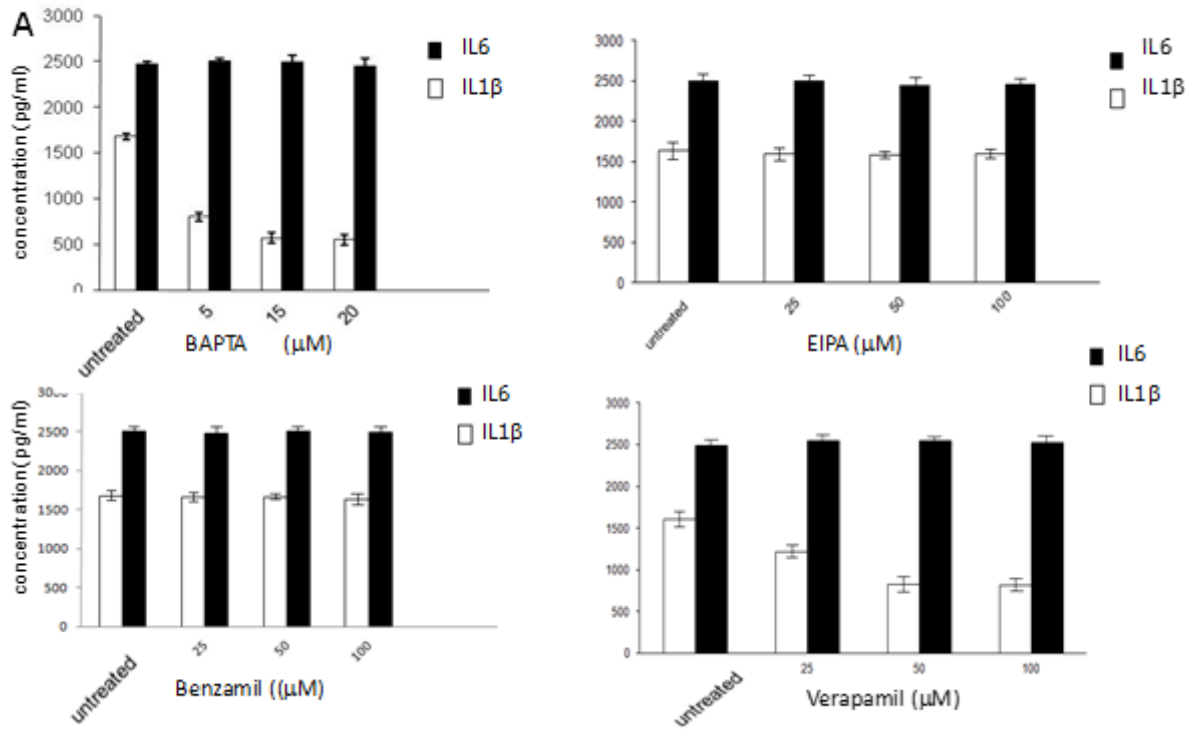


**Figure 4.4 (a) Calcium inhibitors block rhinovirus induced inflammasome activation**

Bronchial cells were infected with HRV14 and cultured in the presence or absence of BAPTA-AM, EIPA, or benzamil or verapamil for 12 hrs. Supernatants were collected and tested for IL1 $\beta$  and IL6 secretion using the CBA bead array system (Becton Dickinson) (A). The data presented is the mean of three independent experiments.

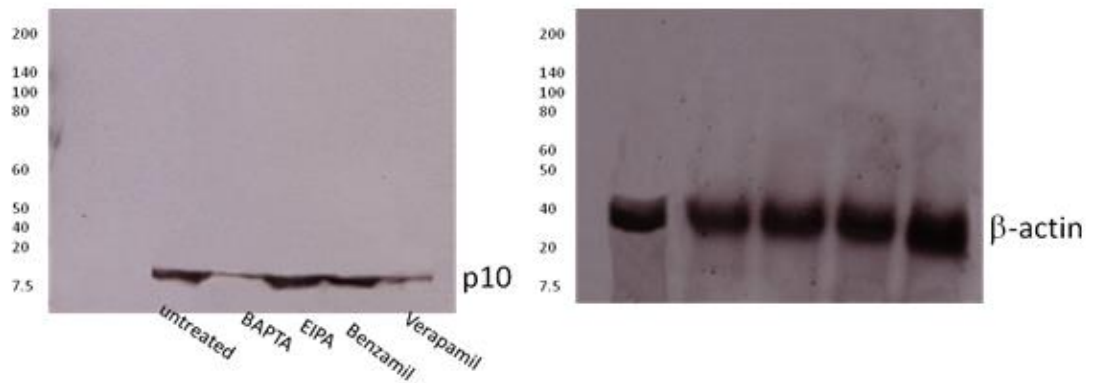


**Figure 4.4 (b) Calcium inhibitors block rhinovirus induced inflammasome activation**  
 Bronchial cells were infected with HRV14 and cultured in the presence or absence of BAPTA-AM, EIPA, or benzamil or verapamil for 12 hrs. Cell lysate was collected and caspase1 expression was investigated by western blotting as well as  $\beta$ -actin as a control (B). The data presented is the mean of three independent experiments.

#### 4.2.5 2B localises with NLRC5 and NLRP3 in the golgi

To elucidate the intracellular interactions of NLRP3 and NLRC5 inflammasome we looked at 2B trafficking in the cell. Previous studies have shown that 2B accumulation occurs at the ER and Golgi (de Jong et al. 2008).

Bronchial cells were transfected with p2B-myc incubated for 24hr and then permeabilised with 0.02% saponin. An anti myc antibody previously conjugated to FITC was used for 2B labelling.

The 2B protein mainly localised at the Golgi complex membranes, whereas NLRP3 and NLRC5 were distributed in the cytoplasm in unstimulated cells. However after 2B transfection there was a percentage of NLRP3 and NLRC5 as well as ASC, which is a

key adaptor to caspase-1 activation (Mariathasan et al. 2004), that partially translocated from the cytoplasm to the Golgi (Fig. 4.5).

In order to investigate the role of the Golgi apparatus in inflammasome activation we utilized Brefeldin A (BFA). The fungal metabolite BFA has been known to induce rapid and reversible disassembly of the Golgi stack into tubules and vesicles, resulting in the redistribution of Golgi-resident enzymes and accumulation of proteins in the ER in a reversible manner (Lippincott-Schwartz et al. 1989, Misumi et al. 1986).

Treatment with BFA disassembled the Golgi and resulted in 2B redistribution (Fig. 4.6) which blocked inflammasome activation by rhinovirus since there was no IL1 $\beta$  production in the supernatant of cells treated with BFA. In order to show that the absence of IL-1 $\beta$  in the supernatant is not due to a transport defect, cells were stimulated with LPS plus ATP and treated with BFA (Fig. 4.6C). The results showed that in these cells inflammasome activation was not blocked by BFA. Thus indicating that localisation of 2B in the Golgi is essential for triggering inflammasome activation.



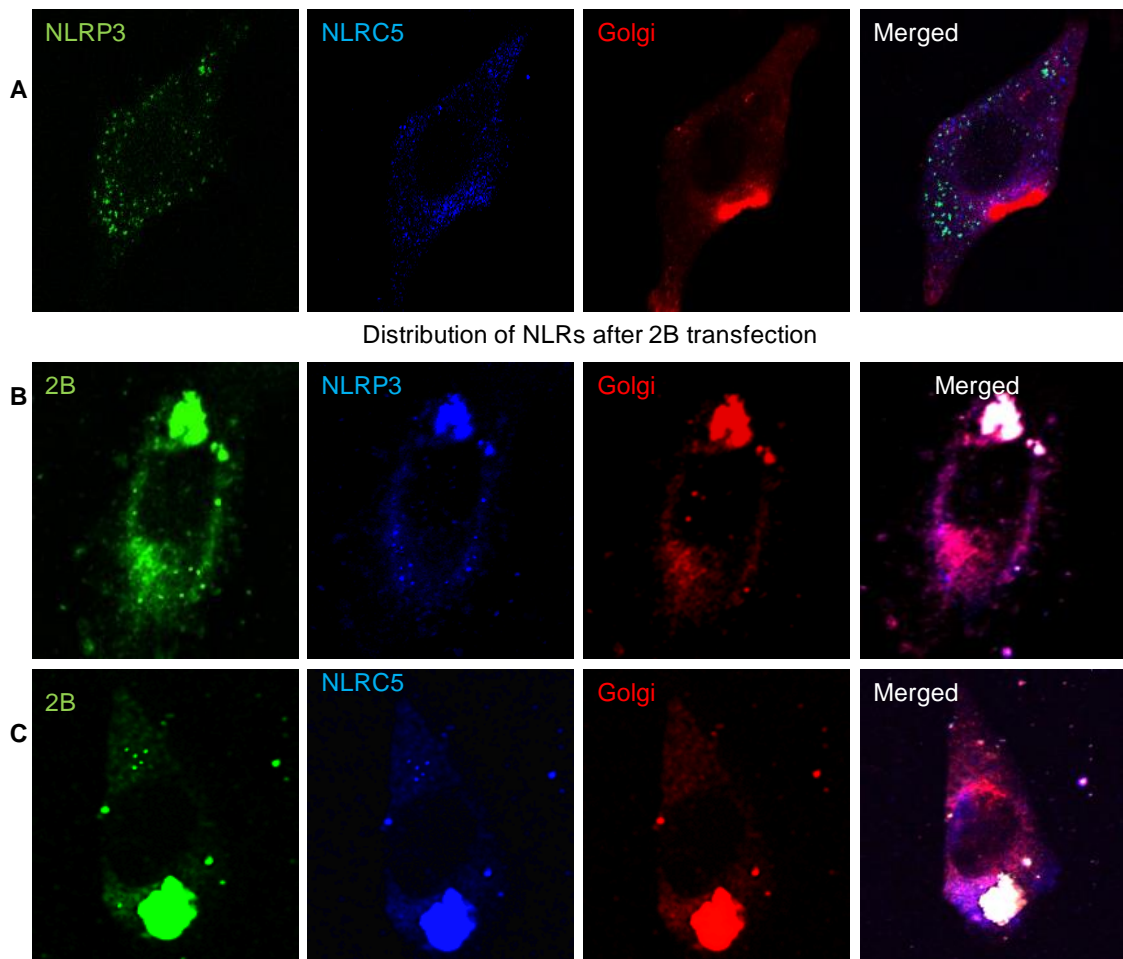


**Figure 4.5 Localisation of 2B, NLRP3 and NLRC5 in the Golgi.** Cells were rinsed twice in PBS/0.02% BSA, prior to fixation with 4% formaldehyde for 15 min. Followed by permeabilisation using PBS/0.02% BSA/0.02% Saponin. and then stained with GM130 mAb followed by Alexa 546-Fab mouse specific Ig to label the golgi system. Anti NLRC5 specific antibody conjugated to Alexa 633 and anti NLRP3 antibody conjugated directly to Alexa 488 were used (A).

Bronchial epithelial cells were transfected with p2B-myc at 24 h post transfection cells were fixed and permeabilised. An anti myc antibody conjugated to FITC was used to label the 2B protein. The golgi sytem was stained with an anti GM130 mAb followed by Alexa 546-Fab mouse specific Ig. Anti NLRP3 antibody conjugated directly to Alexa 633 (B) or anti NLRC5 antibody conjugated to Alexa 633 (C)) were used. Cells were imaged using a Zeiss 510 confocal microscope. Bars 10  $\mu$ m. The data presented is the mean of four independent experiments. The merged images show no apparent localization between NLRP3 and golgi before the presence of 2B, whereas there is extensive colocalisation between NLR3, NLRC5 or ASC and the Golgi when 2B is present.

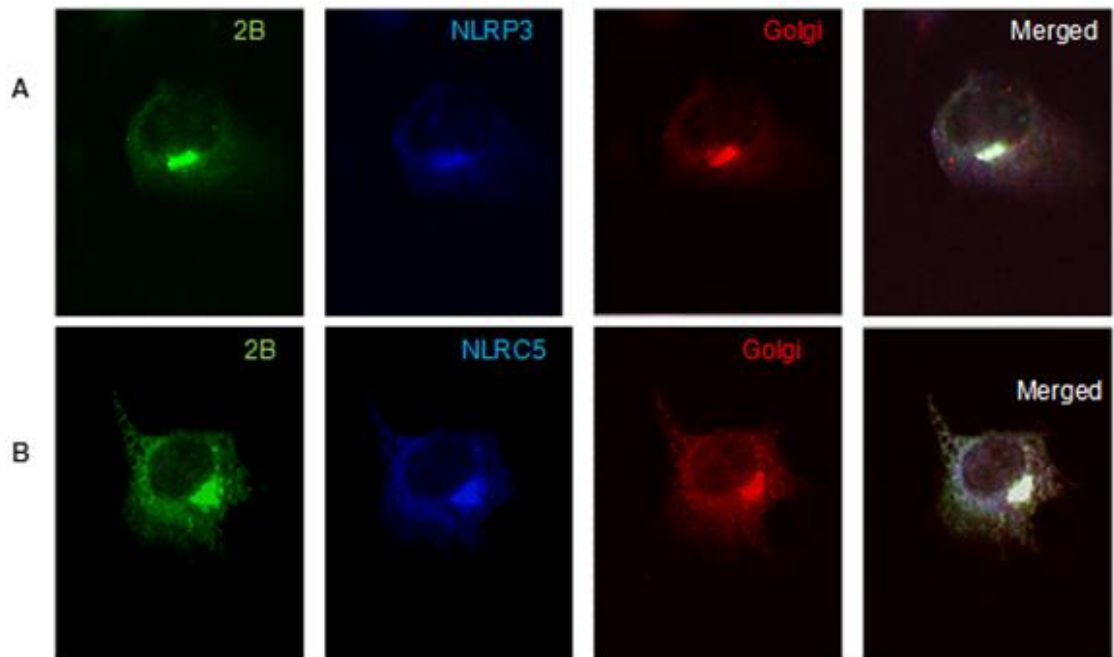


**Figure 4.6 (a) Redistribution of 2B, NLRP3 and NLRC5 prior to Brefeldin A treatment.** Bronchial cells transfected with p2B-myc at 24 h post transfection were used. Golgi was stained with GM130 mAb followed by Alexa 546-Fab mouse specific Ig. An anti myc antibody conjugated to FITC was used to label the 2B protein. Cells were stained for NLRP3 using a rabbit anti NLRP3 Fab conjugated to Alexa 633 or a goat anti NLRC5 conjugated to Alexa 647. The distribution of NLRP3 (A) and NLRC5 (B) in cells transfected with 2B is depicted.

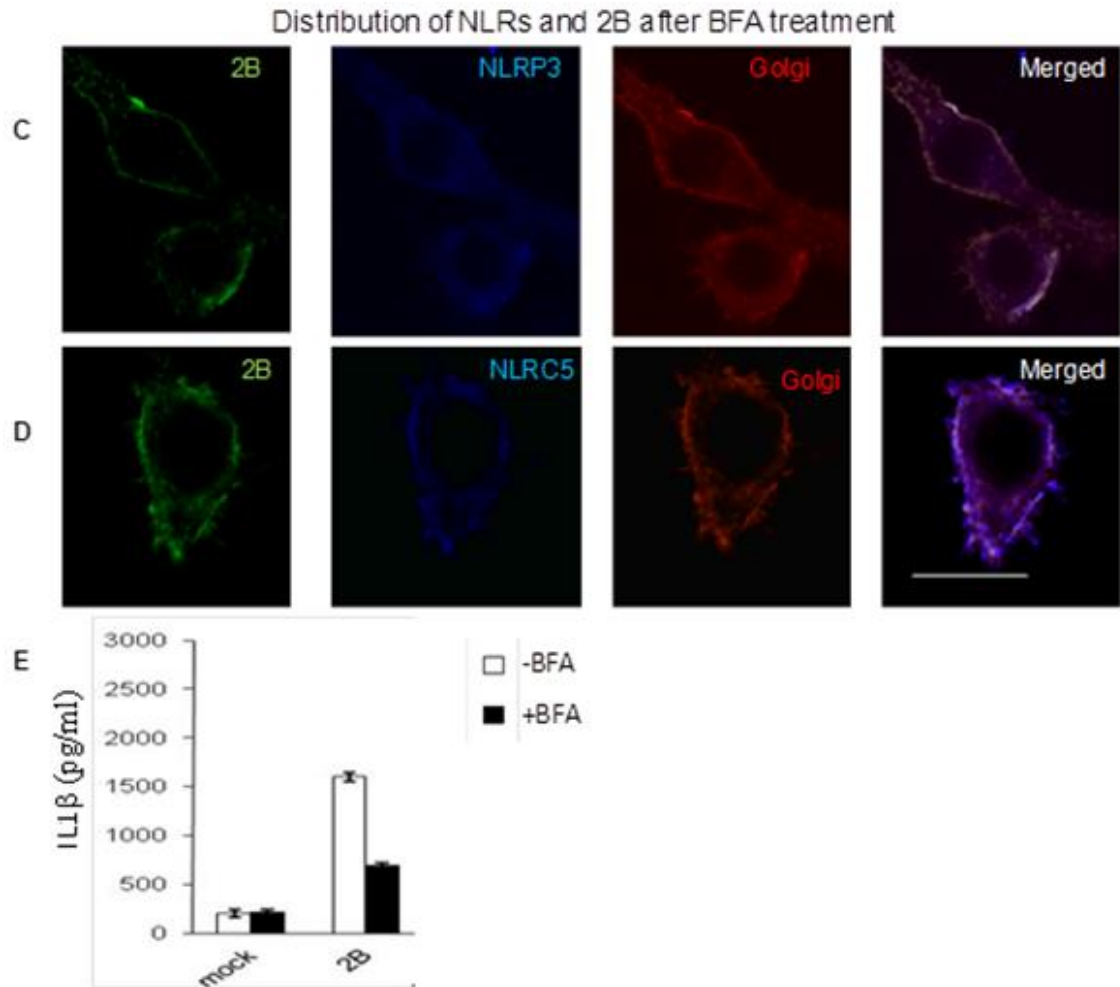


**Figure 4.6 (b)Redistribution of 2B, NLRP3 and NLRC5 post Brefeldin A treatment.**

Bronchial cells transfected with p2B-myc at 24 h post transfection cells were treated with 10 $\mu$ g/ml Brefeldin A. Golgi was stained with GM130 mAb followed by Alexa 546-Fab mouse specific Ig. An anti myc antibody conjugated to FITC was used to label the 2B protein. Cells were stained for NLRP3 using a rabbit anti NLRP3 Fab conjugated to Alexa 633 or a goat anti NLRC5 conjugated to Alexa 647. The distribution of NLRP3 (A) and NLRC5 (B) in cells transfected with 2B is depicted (4.6 A). Following treatment with BFA the distribution of NLRP3 and NLRC5 is shown in panel C and D respectively (The merged images show a reduced degree of colocalisation between 2B and the Golgi). Supernatants were also collected and tested for IL1 $\beta$  secretion using the CBA bead array system (BectonDickinson) from unstimulated (mock) or transfected with 2B (E). The data presented is the mean of three independent experiments.

### 4.3 Discussion

Respiratory viral infections, especially HRV, a member of the Picornaviridae family are a major cause of asthma and COPD, being associated with over 50% of COPD exacerbations (Johnston et al. 1995, Seemungal et al. 2001). The presence of an upper respiratory tract infection leads to a more severe exacerbation and a longer recovery time.

Exacerbations are associated with increased airway inflammation and increased IL6 and TNF $\alpha$  production in addition IL-1 $\beta$  levels are enhanced within the airways of patients with COPD or asthma, with further increases detected during acute exacerbations (de Kluijver et al. 2003, Fleming et al. 1999, Terajima et al. 1997). Furthermore, epithelial and monocytic cells (PBMCs and alveolar macrophages) taken from such patients respond to inflammatory stimuli with greater IL-1 $\beta$  production (Hallsworth et al. 1994).

IL-1 $\beta$  is an important proinflammatory mediator that is generated at sites of injury or immunological challenge to coordinate programs such as cellular recruitment to a site of infection or injury. Proinflammatory stimuli induce expression of the inactive IL-1 $\beta$  precursor but cytokine maturation and release are controlled by inflammasomes.

Several multimolecular proteins complexes comprised of members of the nucleotide binding domain leucine-rich repeat containing (NLR) family referred to as inflammasomes, have been identified as caspase-1 activators. These molecules activate caspase 1 and thus control the second, required step of IL- 1 $\beta$  cytokine activation (Martinon et al. 2002).

In this study we investigated the involvement of inflammasome and IL1 $\beta$  release in human rhinoviruses infection in Primary bronchial cells which is a clinically relevant cell type, for viral respiratory infection. There is an increasing number of studies linking asthma and COPD exacerbations with viral respiratory infections, especially rhinovirus

infections and only by understanding the mechanisms for the persistence of inflammation may lead to new therapeutic approaches.

By silencing different NLRs we discovered that rhinovirus infection activates NLRP3 and NLRC5 which leads to caspase 1 activation and IL1 $\beta$  production. To investigate how rhinoviruses stimulate inflammasome activation we looked at rhinovirus proteins that might enhance membrane permeability since it has been shown that the NLRP3 inflammasome can be activated by pore-forming toxins secreted by bacteria (Koizumi et al. 2012). The rhinovirus 2B protein, one of the nonstructural proteins involved in viral RNA replication, was a possible candidate for inflammasome activation since it has been shown that the 2B protein from Coxsackievirus another member of the Picornaviridae family forms membrane-integral pores, thereby increasing the efflux of Ca<sup>2+</sup> from the stores (van Kuppeveld et al. 1997).

Therefore we transfected a plasmid expressing rhinovirus 2B protein p2B-myc into Primary bronchial cells. Our results showed that 2B protein activates inflammasomes and more specifically NLRP3 and NLRC5. NLRP3 has been shown to recognize a variety of ligands, however NLRC5 role in innate and adaptive immune responses remains controversial. NLRC5 has been implicated in regulating inflammasome signalling (Davis et al. 2011) either as a positive (Neerinx et al. 2010) or negative regulator (Benko et al. 2010). Here we see that NLRC5 like NLRP3 can recognize rhinovirus 2B protein independently and trigger IL1 $\beta$  secretion. To discover the mechanism of inflammasome activation by 2B we looked at Ca<sup>2+</sup> levels using Fluo3-AM. The data revealed an increase in cytosolic Ca<sup>2+</sup> when 2B was transfected.

Tracking rhinovirus 2B protein intracellularly showed that it localised partially in the ER but mainly in the Golgi with NLRP3 and NLRC5. When the Golgi was disrupted using

BFA, caspase 1 activation and IL1 $\beta$  secretion was disrupted verifying that localisation to the Golgi is a prerequisite for inflammasome activation. Furthermore by using 2B ER and Golgi specific targeted constructs we confirmed that Golgi complex localisation of picornavirus 2B but not endoplasmic reticulum localization is a pre-requisite for NLR activation.

The ability of 2B viroporin to localise to the Golgi complex suggests that the NLRP3 and NLRC5 inflammasomes mechanism of activation in rhinovirus infection is by sensing the imbalances in Ca<sup>2+</sup> intracellular homeostasis.

When Ca<sup>2+</sup> inhibitors and chelators were used to inhibit inflammasome activation, it was shown that BAPTA-AM and verapamil were able to inhibit IL1 $\beta$  secretion induced by HRV infection thus indicating that calcium inhibitors could be used in the future to control exacerbated IL1 $\beta$  production which is often found in viral inflammatory airway disease.

NLRs have been shown to have different roles in separate cell types (Ting et al. 2010). There is emerging evidence which suggests that during bacterial infections, multiple NLR inflammasomes have the potential to become activated. For example *Candida albicans* leads to up-regulation of NLRP3 and NLRC4 inflammasome in the oral mucosa (Tomalka et al. 2011). The mechanisms that govern pathogen-induced inflammasome activation remain poorly characterized, and the contribution of individual NLRs has not been fully elucidated. Here we show that infection of primary bronchial cells with HRV leads to NLRP3 and NLRC5 activation and IL1 $\beta$  secretion. The overlapping biologic functions and pathogen specificity of NLRC5 with NLRP3 suggests that these proteins might act in a cooperative manner during the inflammasome assembly.

NLRP3 expression is inducible following several infections of bacteria or viruses (Kanneganti 2010, Kanneganti et al. 2006).

However there could be a tissue specific role for the NLRC5 inflammasome in host sensing and immune defence thus explaining why viral respiratory infections lead to greater airway inflammation and more severe exacerbations since rhinovirus respiratory infections can be detected by both NLRP3 and NLRC5.

## **Chapter 5**

### **Human respiratory syncytial virus viroporin SH signals inflammasome activation**



## 5.1 Introduction

Respiratory syncytial virus (RSV) remains the leading cause of serious viral bronchiolitis and pneumonia in infants and young children throughout the world. The burden of disease is significant, with 70% of all infants being infected with RSV within the first year of their life (Hall 1999). It is the most common cause of hospitalisation in infants and of acute respiratory failure in paediatric intensive care units. 40% of those children discharged from hospital have recurrent, repeated respiratory symptoms and wheezing for at least 10 years (Simoes 1999). The infection is also important in the elderly and immunocompromised individuals. The pathology of the virus is associated with innate immunity and skewed immune responses towards a Th2 phenotype (Becker 2006, Pinto et al. 2006).

One cytokine that is associated with RSV infection is IL-1 $\beta$ . Although this cytokine has been shown to be secreted by RSV-infected airway cells (Schmitz et al. 2005), the question that remains is what the mechanism of inflammasome activation is? It is now emerging that Inflammasomes are multiprotein complexes that act as a platform for the activation of caspase 1 which in turn cleaves pro-IL1 $\beta$  and pro-IL18 resulting into their secretion (Martinon et al. 2009).

Since inflammasomes have been shown to be triggered by diverse ligands, it has been suggested that two or potentially more signals are required for full activation. The first or priming signal can be triggered from a transcriptionally active PRR or cytokine receptor, this leads to transcriptional activation of the genes encoding pro-IL1 $\beta$  and pro-IL18 (Bauernfeind et al. 2009). The second signal is triggered in response to various stress signals associated with damaged self (Martinon et al. 2009).

The question that arises is how is IL-1 $\beta$  triggered in response to RSV infection and which is the “priming” step that leads to IL-1 $\beta$  secretion. A recent study by Segovia et al has

shown that RSV triggers NLRP3 activation via ROS production. Although this study has provided some clues, it hasn't revealed which part of the virus triggers this inflammation and the mechanism of NLRP3 activation remains unknown.

In the current study we have attempted to shed more light into the mechanisms of RSV-induced inflammasome activation.

## **5.2 Results**

### **5.2.1 RSV infection activates the NLRP3 inflammasome**

In order to determine if RSV is detected by the inflammasome, we investigated inflammasome activation by measuring IL1 $\beta$  secretion from primary RSV infected lung epithelial cells. RNA viruses such as vesicular stomatitis virus (VSV), and encephalomyocarditis virus EMCV as well as a DNA virus Herpes simplex virus (HSV1) were also compared to RSV

The data showed that RSV infection resulted in IL1 $\beta$  secretion within 6hr (Figure 5.1a A) IL1 $\beta$  secretion was not observed in infections with the other viruses. To verify if IL1 $\beta$  secretion was NLRP3 specific, NLRP3 expression was knocked down by psiRNA which resulted in a reduction in IL1 $\beta$  secretion (Figure 5.1a B) thus verifying that RSV is detected by the NLRP3 inflammasome. IL-6 secretion was measured as a control for the psiRNA effect since it is independent of inflammasome activation but is a known marker for NF-kB activation. All of the tested viruses triggered IL-6 secretion, but only RSV was detected by the inflammasome in these unprimed cells.

#### **5.2.1.1 RSV triggers pro-IL1 $\beta$ secretion**

IL1 $\beta$  secretion requires two signals: transcription of pro-IL1 $\beta$  (signal 1) and processing by caspase 1 (signal 2). To examine whether RSV infection provides the transcriptional signal, we infected cells with RSV and examined the pro-IL1 $\beta$  response via western

blotting. RSV infection induced a pro-IL1 $\beta$  response while infection by the other viruses did not (Figure 5.1b C).

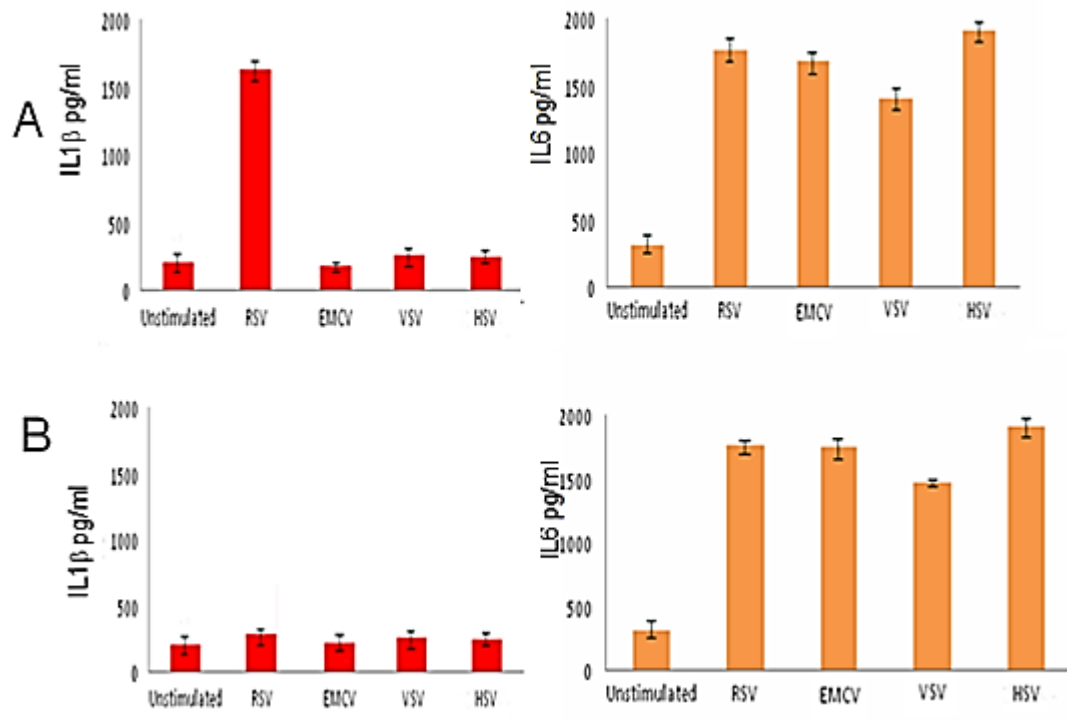


**Figure 5.1 (a) RSV infection activates the NLRP3 inflammasome.** Lung epithelial cells were infected with 100PFU of RSV or EMCV or VSV or HSV1 viruses. Supernatant was collected at 12hr post infection and analysed for IL1 $\beta$  and IL6 using the CBA bead array system on a FACSCalibur (Becton Dickinson) (A).

NLRP3 expression was knocked down by psiRNA and the cells were again infected with 5moi of RSV or EMCV or VSV or HSV1 viruses. Supernatant was collected at 12hr post infection and analysed for IL1 $\beta$  and IL6 using the CBA system (B)

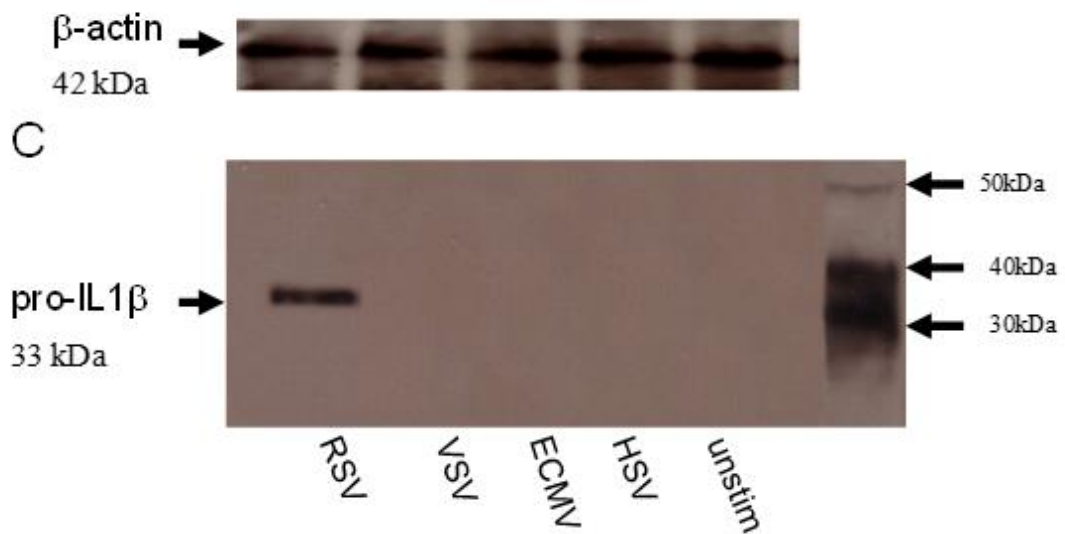


**Figure 5.1(b) RSV infection activates the NLRP3 inflammasome.** Lung epithelial cells were infected with 100PFU of RSV or ECMV or VSV or HSV1 viruses. Cells extracts from infected lung epithelial cells were analysed for the presence of pro-IL1 $\beta$  by western blotting and loading controls for  $\beta$ -actin are also depicted (C). The data represent the mean of three independent experiments.

#### 5.2.1.2 TLR signalling is required for inflammasome activation.

RSV is detected by different PRRs such as TLR4 (Kurt-Jones et al. 2000), TLR7 (Davidson et al. 2011), TLR3 and RIG-I (Liu et al. 2007). To determine if they also play a role in inflammasome activation we individually knocked down RIG-I, TLR3, TLR4, TLR7 or TLR8 in RSV-infected cells as well as TLR2 (Figure 5.2). Only the knocking down of TLR4 resulted in a reduction in expression of pro-IL1 $\beta$  and IL1 $\beta$ . IFN $\beta$  secretion was not reduced by knocking down any of these molecules, showing that the IL1 $\beta$  reduction was specific. TLR4 therefore appears to be required for signal 1, the transcription of pro-IL $\beta$  that results in the subsequent release of mature IL1 $\beta$  by RSV infection.

However some IL1 $\beta$  was still produced leading us to believe that in addition to the established TLR sensors there could yet exist an additional mechanism for triggering IL1 $\beta$  production.

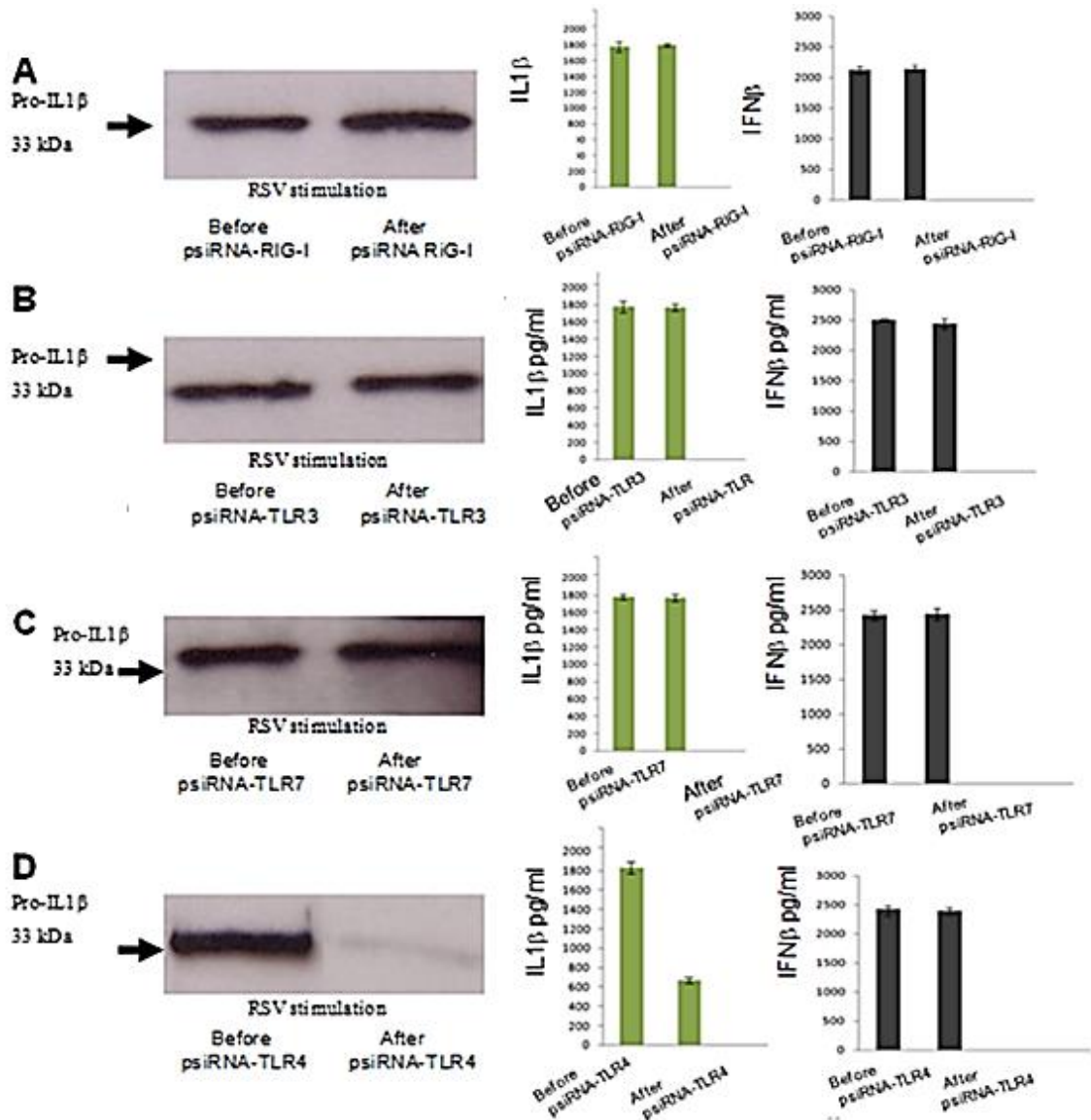


**Figure 5.2 (a) TLR4 provides the first or priming signal of activation.**

Lung epithelial cells were infected with 100PFU of RSV and the presence of pro- IL1 $\beta$  by western blotting was examined as well as the secretion of IL1 $\beta$  and IFN $\beta$  using the CBA system. RIG-I expression was knocked down by psiRNA and the cells were again infected and examined for pro- IL1 $\beta$  as well as IL1 $\beta$  and IFN $\beta$  secretion (A). TLR3 expression was knocked down by psiRNA and the cells were again infected and tested for pro- IL1 $\beta$  as well as IL1 $\beta$  and IFN $\beta$  secretion (B). TLR7 expression was knocked down by psiRNA and the cells were again infected and tested for pro- IL1 $\beta$  as well as IL1 $\beta$  and IFN $\beta$  secretion (C). TLR4 expression was knocked down by psiRNA and the cells were again infected and tested for pro- IL1 $\beta$  as well as IL1 $\beta$  and IFN $\beta$  secretion (D). The data represent the mean of three independent experiments.

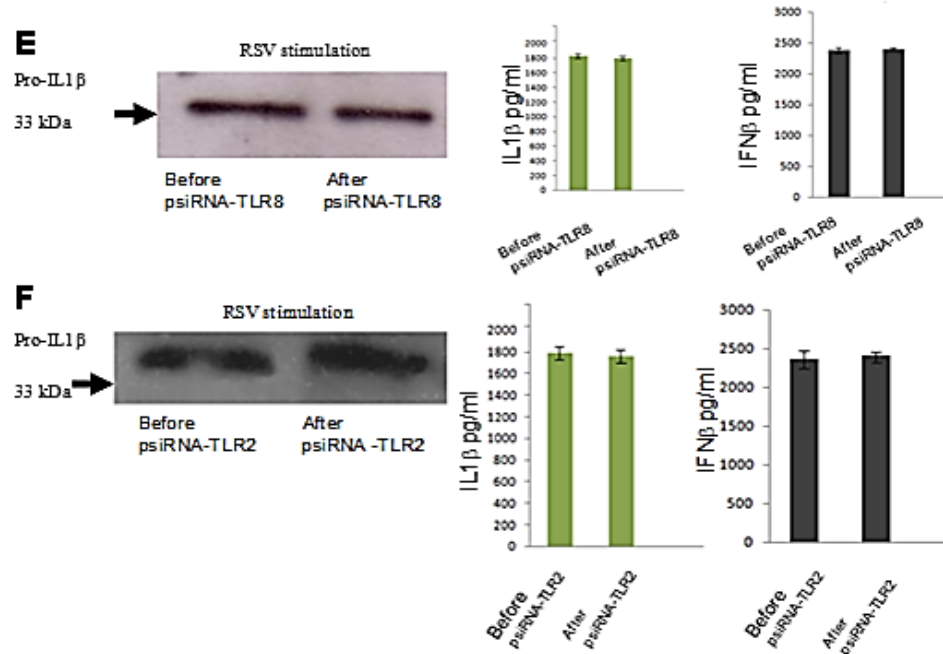


**Figure 5.2 (b) TLR4 provides the first or priming signal of activation.**

Lung epithelial cells were infected with 100PFU of RSV and the presence of pro- IL1 $\beta$  by western blotting was examined as well as the secretion of IL1 $\beta$  and IFN $\beta$  using the CBA system. TLR8 expression was knocked down by psiRNA and the cells were again infected and tested for pro- IL1 $\beta$  as well as IL1 $\beta$  and IFN $\beta$  secretion (E). TLR2 expression was knocked down by psiRNA and the cells were again infected and tested for pro- IL1 $\beta$  as well as IL1 $\beta$  and IFN $\beta$  secretion (F). The data represent the mean of three independent experiments.

### 5.2.1.3 SH mediated mechanism of inflammasome activation

To discover how RSV infection triggers signal 2 we looked at RSV viral proteins which enhance membrane permeability since It has been shown that the influenza M2 ion channel induces inflammasome activation, by modulating the intracellular K<sup>+</sup> concentration (Ichinohe et al. 2010).

The RSV small hydrophobic protein (SH) has been classified as a viroporin. It alters membrane permeability displaying properties of a cation selective ion channel (Gan et al. 2012, Kochva et al. 2003). SH is not essential for viral replication in vitro (Bukreyev et al. 1997). However, deletion of the SH gene leads to attenuation in mouse and chimpanzee models, suggesting it is important for infectivity in vivo (Bukreyev et al. 1997; Whitehead et al. 1999).

To test the role of SH in inflammasome activation an SH deletion mutant RSV rgRSV-GF ( $\Delta$ SHRSV) (Techarpornkul et al. 2001) was used. The  $\Delta$ SHRSV mutant has been shown in previous studies to grow and replicate efficiently in cell culture (Bukreyev et al. 1997). The infection with rgRSV-GF failed to induce caspase activation and release of IL1 $\beta$  (Figure 5.3A). However rgRSV-GF infected cells released IL6 a non-inflammasome cytokine, IFN $\beta$  and pro-IL1 $\beta$ . RSV infection induced caspase 1 production while rgRSV-GF infection did not. Together these results indicate that SH plays an essential role in triggering signal 2 leading to caspase 1 production and inflammasome activation (Figure 5.3).

To investigate the mechanism of SH induced inflammasome activation (Techarpornkul et al. 2001) we infected cells with RSV or with rgRSV-GF and used drugs that block the ion channel of several other viroporins, such as Amantadine, Rimantadine which block the influenza M2 channel and hexamethylene amiloride (HMA) which blocks the HIV Vpu channel as well as the p7 channel of Hepatitis C virus to obtain further understanding of the channel properties of SH protein (Figure 5.4)

HMA was successful in inhibiting IL1 $\beta$  secretion upon RSV infection. However there was no downregulation when amantadine or rimantadine were used. Having observed the effect of HMA, we then examined the effect of other ion channel inhibitors: 5-(*N*-ethyl-*N*-isopropyl)amiloride (EIPA) and benzamil, which also block Na<sup>+</sup>/H<sup>+</sup> ion channels, and



verapamil, which blocks  $\text{Ca}^+$  channels. Verapamil had no effect on  $\text{IL1}\beta$  secretion whereas HMA, EIPA and benzamil reduced  $\text{IL1}\beta$  secretion in RSV infection. These results suggest that SH displays is selective for monovalent cations ( $\text{Na}^+$  and  $\text{K}^+$ ) similar to the HCV p7 protein (Figure 5.4).

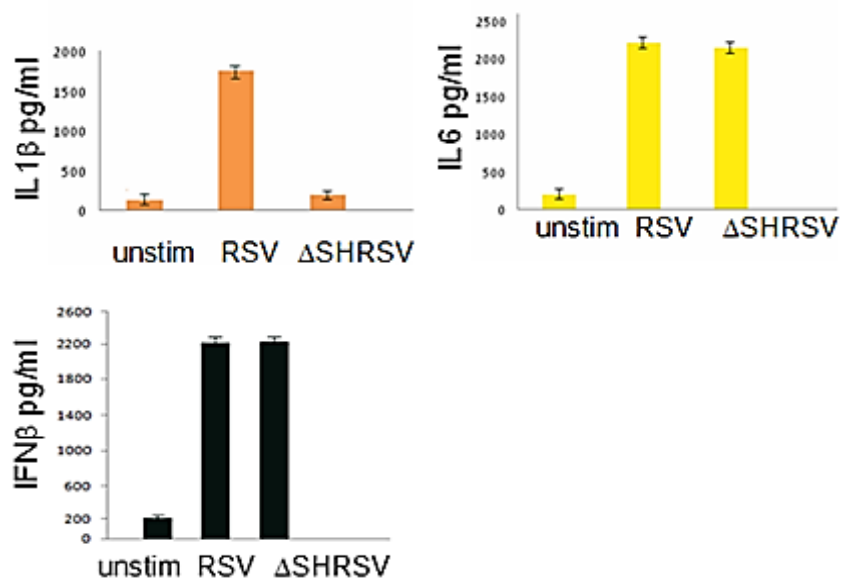


**Figure 5.3 (a) RSV and ΔSHRSV mediated mechanism of inflammasome activation.** Lung epithelial cells were either infected with RSV or ΔSHRSV. Cell supernatant was collected and tested for IL1β, IL6 and IFNβ secretion. The data presented are the mean of three independent experiments.

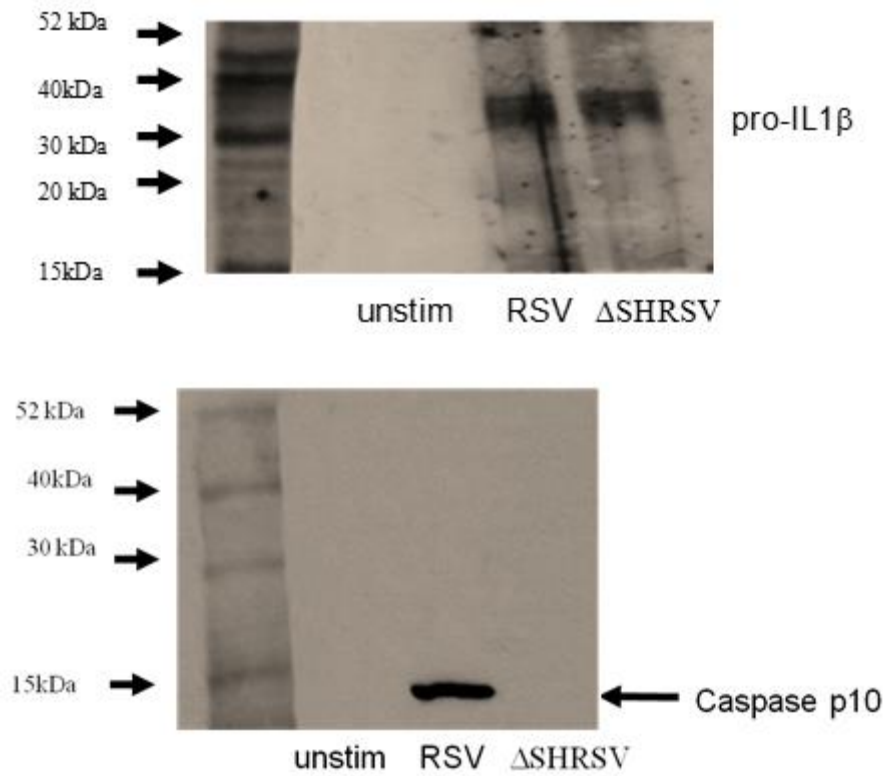


**Figure 5.3 (b) RSV and  $\Delta$ SHRSV mediated mechanism of inflammasome activation.** Cells extracts from infected lung epithelial cells were analysed for the presence of pro-IL1 $\beta$  and Caspase p10 by western blotting. The data presented are the mean of three independent experiments.

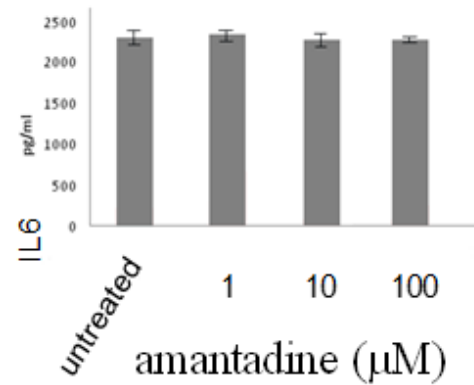
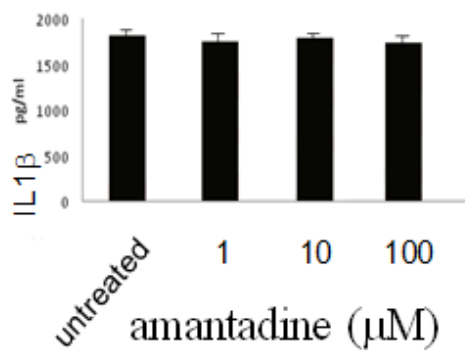
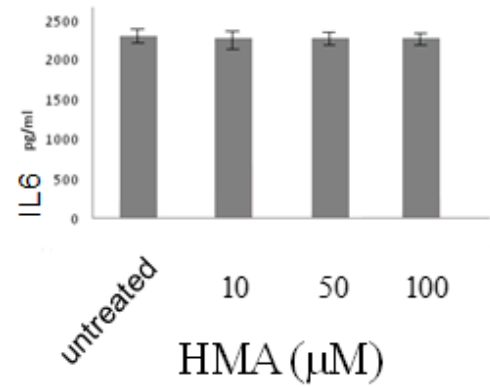
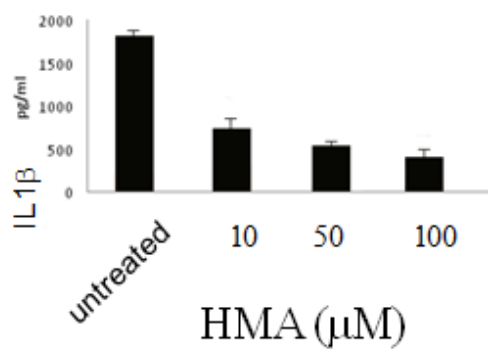


**Figure 5.4 (a) Effects of ion channel inhibitors on inflammasome activation.**

Lung epithelial cells with infected with RSV and cultured in the presence or absence of HMA or amantadine for 12 hrs. Supernatants were collected and tested for IL1 $\beta$  and IL6 secretion using the CBA bead array system (BectonDickinson). Fluorescence was detected using a FACSCalibur(BectonDickinson) The data presented are the mean of three independent experiments.

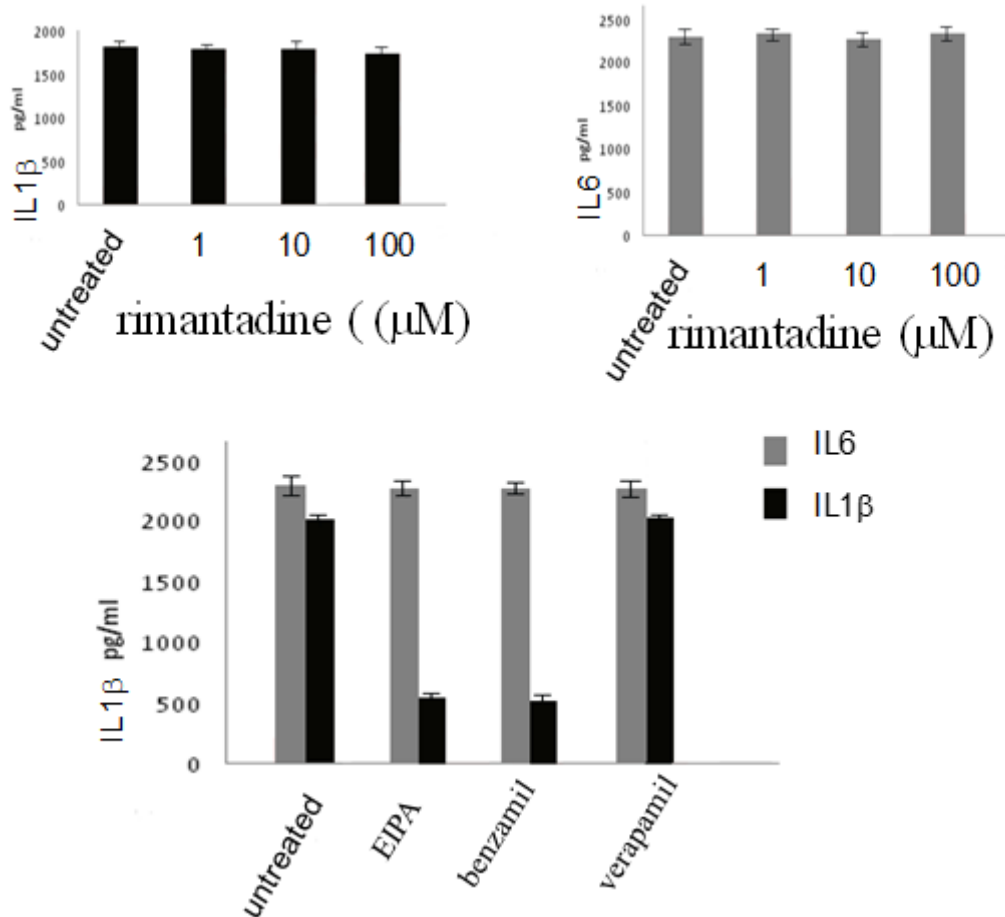


**Figure 5.4 (b) Effects of ion channel inhibitors on inflammasome activation.**

Lung epithelial cells with infected with RSV and cultured in the presence or absence of Rimantadine or EIPA, or benzamil or verapamil for 12 hrs. Supernatants were collected and tested for IL1 $\beta$  and IL6 secretion using the CBA bead array system (BectonDickinson). Fluorescence was detected using a FACSCalibur(BectonDickinson) The data presented are the mean of three independent experiments.

### 5.2.2 SH interactions

To elucidate the intracellular mechanism by which SH activates NLRP3 inflammasome we examined SH trafficking in the cell. Previous studies have shown that RSV assembly and SH accumulation occurs within lipid raft structures on the cell surface and into lipid raft domains in the Golgi network(Rixon et al. 2004).

Lung cells were infected with RSV fixed and permeabilised with 0.2% saponin. An anti-SH antibody previously described was used for SH labelling. The SH protein localised at the endoplasmic reticulum and Golgi complex membranes. Whereas NLRP3 was distributed in the cytoplasm and after RSV infection much of the NLRP3 as well as ASC was found in the Golgi (Figure 5.5).

To analyse the role of lipid raft membranes within the Golgi complex in SH induced inflammasome activation, cells infected with RSV were treated with nystatin which disrupts lipid rafts. The cells were imaged and the images showed that NLRP3 and ASC re-distribution followed nystatin treatment of infected cells, thus showing that lipid raft disruption inhibited inflammasome activation since the re-distribution of NLRP3 and ASC will inhibit their interactions and formation of inflammasome (Figure 5.6A, B). Furthermore, IL1 $\beta$  production in RSV-infected cells was dramatically reduced after nystatin treatment (Figure 5.6D).

To verify the importance of Golgi co-localisation in inflammasome activation we utilized Brefeldin A (BFA). The fungal metabolite BFA has been known to induce rapid and reversible disassembly of the Golgi stack into tubules and vesicles (Lippincott-Schwartz et al. 1989, Misumi et al. 1986).

Treatment with BFA disassembled the Golgi and resulted in NLRP3 and ASC redistribution (Fig. 5.6C) which blocked inflammasome activation by RSV since there was no IL1 $\beta$  production in the supernatant of cells treated with BFA(Fig. 5.6D).

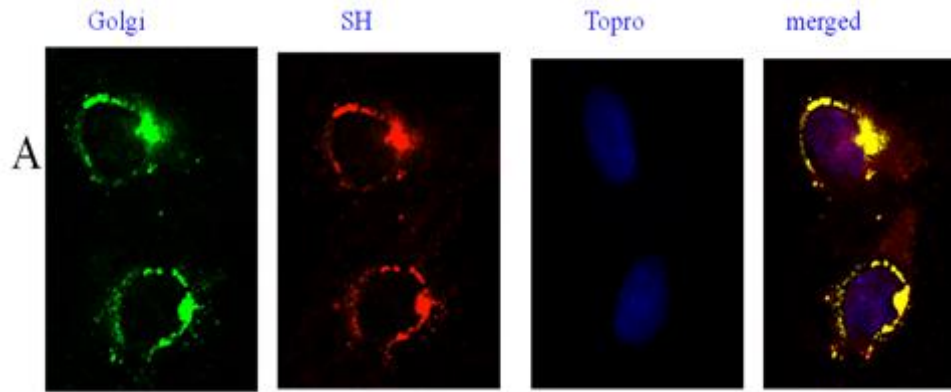


**Figure 5.5 (a) Localisation of SH in the Golgi.** Lung epithelial cells were stimulated with RSV for 6hr and then stained with GM130 mAb followed by Alexa 488-Fab mouse specific Ig to label the Golgi system. An anti SH antibody was used to label the SH RSV protein followed by Alexa 546-Fab mouse specific Ig. The nucleus was labelled using the nuclear stain Topro-3 (A)

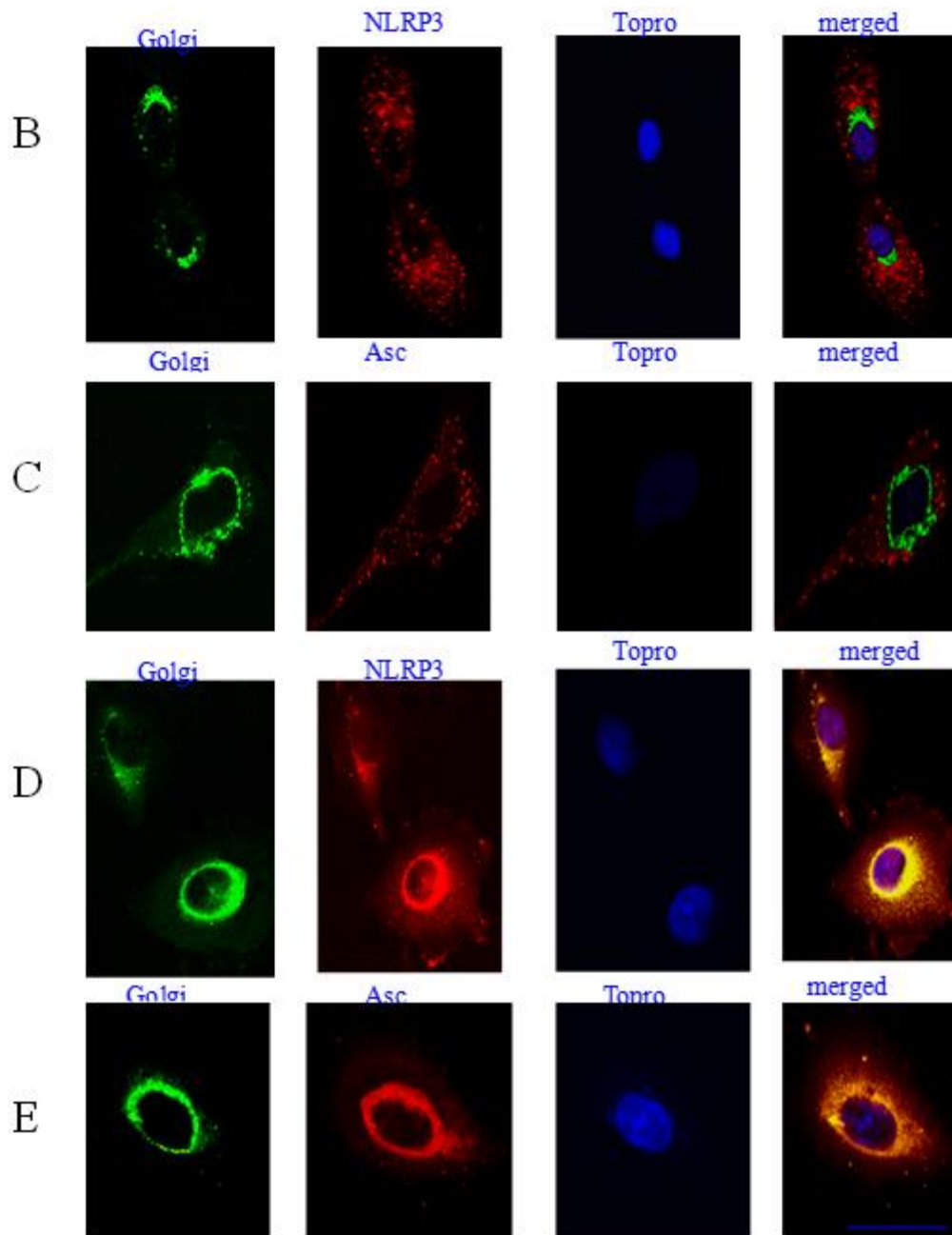


**Figure 5.5 (b) Localisation of SH, NLRP3 and ASC in the Golgi.** Lung epithelial cells were stimulated with RSV for 6hr and then stained with GM130 mAb followed by Alexa 488-Fab mouse specific Ig to label the Golgi system. Ustimulated cells (B, C) or cells stimulated with RSV for 6hrs (D, E) were stained for NLRP3 using a rabbit anti NLRP3 Fab conjugated to Alexa 546 or a goat anti ASC Fab conjugated to Alexa 546. The nucleus was labelled using the nuclear stain Topro-3. Yellow regions indicate localisation of receptors. Cells were imaged using a Zeiss 510 confocal microscope. Bars 10  $\mu$ m. The data are a representative of four independent experiments.



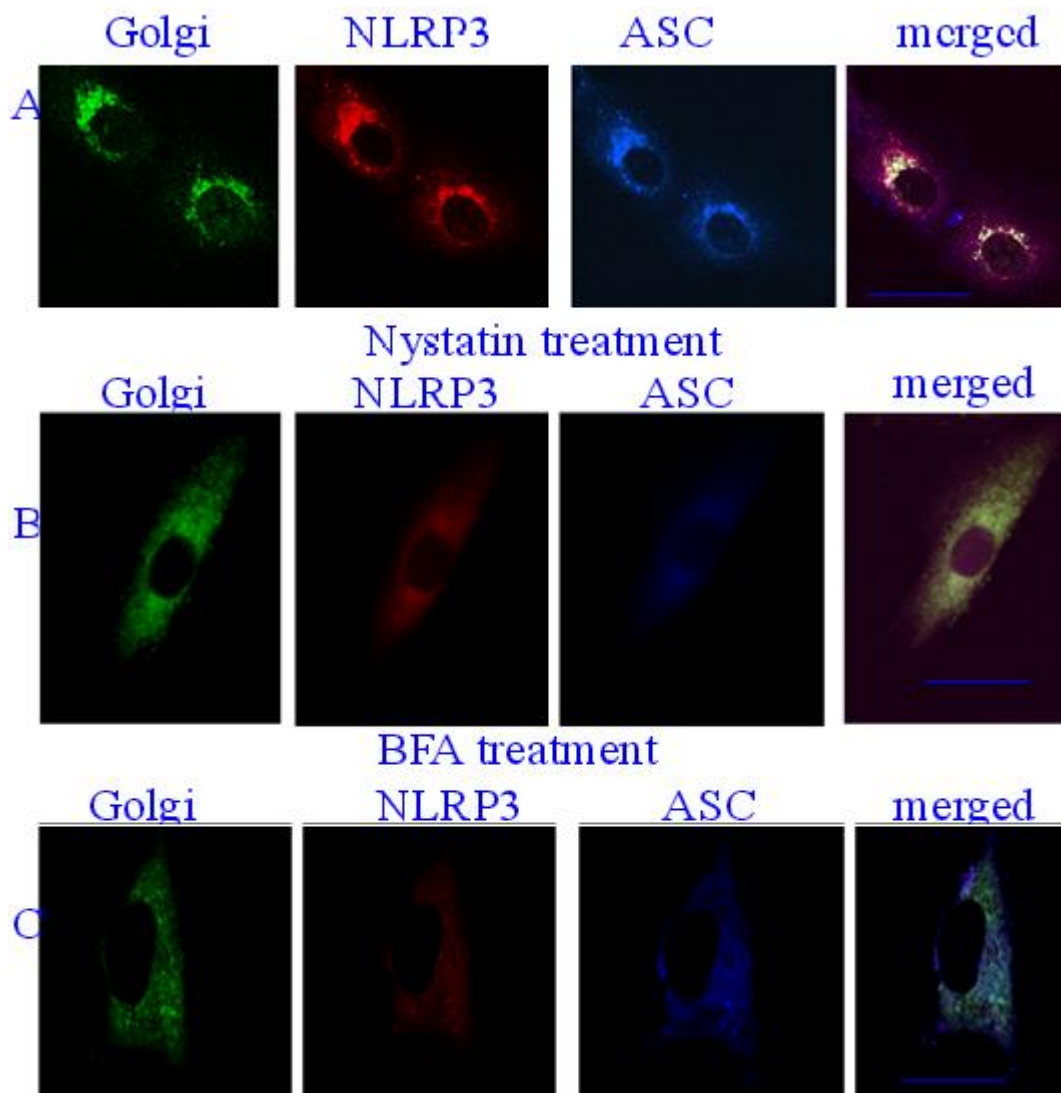


**Figure 5.6 (a) NLRP3, ASC redistribution by nystatin and BFA treatment.** Lung epithelial cells were stimulated with RSV and then either left untreated (A) or cultured with 25 μM nystatin (B) or 10 μM BFA (C). Golgi was stained with GM130 mAb followed by Alexa 488-Fab mouse specific Ig. Cells were stained for NLRP3 using a rabbit anti NLRP3 Fab conjugated to Alexa 546 and a goat anti ASC Fab conjugated to Alexa 647. Cells were imaged using a Zeiss 510 confocal microscope. Bars 10 μm. The data presented are the mean of four independent experiments.

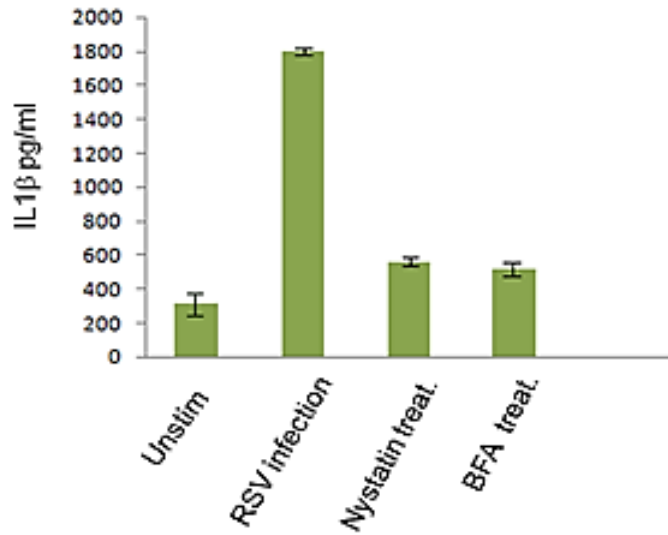


**Figure 5.6 (b)** Supernatants were collected from lung epithelial cells stimulated with RSV (or left unstimulated) and cultured in the absence or presence of 25  $\mu$ M nystatin or 10  $\mu$ M BFA and tested for IL1 $\beta$  secretion using the CBA bead array system (Becton Dickinson). The data presented are the mean of four independent experiments.

### **5.3 Discussion**

In this study it was shown that RSV is capable of triggering NLRP3 activation. This is in agreement with the recent study by (Segovia et al. 2012). The data clearly demonstrates that RSV is able to trigger NLRP3 inflammasome activation on its own, without the need for priming the cells with another PAMP as it has previously been proven necessary for other viruses, such as encephalomyocarditis virus and vesicular stomatitis virus (Rajan et al. 2011). RSV appears to be able on its own to provide both signal 1 and signal 2 for inflammasome activation. The question that remains is how are signal 1 and 2 triggered?

In order to answer this question, the induction of signal 1 in RSV infection was investigated. There are many potential PRRs that might trigger signal 1 in the case of RSV, such as TLR4 (Kurt-Jones et al. 2000), TLR7 (Davidson et al. 2011), TLR3 and RIG-I (Liu et al. 2007). In order to investigate whether one or more of these PRRs trigger signal 1, siRNA was used to knock down their expression and the secretion of IL1 $\beta$  was monitored. Reduction in transcription of IL1 $\beta$  secretion was seen only when TLR4 was knocked down, suggesting that TLR4 is solely responsible for triggering signal 1 of RSV-induced inflammasome activation.

TLR2 knock down had no effect in IL1 $\beta$  secretion. These findings are contrary to those by Segovia et al, who have reported that TLR2 triggers these responses. The differences observed in the two studies, might be due to the different cell types used. The study of Segovia et al. was mainly performed on mouse knockout cells. This study was performed

in human lung epithelial cells. These cells are the main target of human RSV in vivo. In a mouse model, RSV might be detected by different PRRs.

Once it was demonstrated that signal 1 is triggered by TLR4, the mechanism of the induction of signal 2 was also investigated. Three models have been proposed. One model supports that extracellular ATP triggers  $K^+$  efflux (Kanneganti et al. 2007) and induces NLRP3 recruitment, another the release of lysosomal contents caused by lysosome disruption (Halle et al. 2008, Hornung et al. 2008) and NLRP3 activation due to production of ROS (Dostert et al. 2008).

RSV viral proteins that might enhance membrane permeability were also examined since it has been shown that the influenza M2 ion channel induces inflammasome activation, by modulating the intracellular  $K^+$  concentration (Ichinohe et al. 2010). The RSV SH protein has been classified as a viroporin. During the infection of cells by the virus, membrane permeability is modified by the use of viroporins which facilitate virus entry. The main activity of viroporins is to create pores at biological membranes to permit the passage of ions and small molecules, this is useful both in the entry as well as the exit mechanism of the virus.

In order to determine whether RSV SH protein contributes to NLRP3 activation RSV mutants lacking the viroporin SH were used. These mutants have been shown in previous studies to grow and replicate efficiently in cell culture (Bukreyev et al. 1997). The results demonstrated that the RSV mutants lacking the viroporin SH are unable to trigger inflammasome activation, thus suggesting that signal 2 is triggered from the SH protein, possibly by the formation of a pore or channel on the plasma membrane. RSV SH protein joins an increasing list of viral proteins that have been shown to form ion channels in lipid bilayers, including Picornavirus 2B, (Agirre et al. 2002, van Kuppeveld et al. 1997) HIV-1 Vpu (Cohen et al. 1988, Sakai et al. 2003) and HCV p7 which are

permeable to both Na<sup>+</sup> and K<sup>+</sup> ions, and display relatively low ion selectivity (Premkumar et al. 2004), as well as M2 influenza viroporin which exhibits proton conductance and has been shown to activate the NLRP3 inflammasome (Ichinohe et al. 2010).

The use of drugs which block viral ion channels were shown to be able to inhibit IL1 $\beta$  secretion induced by RSV infection suggesting that SH functions similarly to HCV p7 which is selective for monovalent cations (Na<sup>+</sup> and K<sup>+</sup>).

It has previously been shown that SH associates with lipid rafts on the cell surface, but after internalisation it accumulates in the Golgi complex within membrane structures that are enriched with the lipid raft marker, GM1 (Rixon et al. 2004). Our studies confirmed that SH was indeed localised intracellularly in the Golgi membranes. Interestingly, NALP3 was also shown to accumulate in the Golgi apparatus upon RSV infection.

Lipid rafts are specialized membrane microdomains which provide a favourable environment for intra-molecular cross talk but also aid to expedite signal transduction. Several new studies have found accumulation of ion channels and their modulators in lipid rafts (Dart 2010, Martens et al. 2004), which is in agreement with our findings. Lipid rafts are not only on the plasma membrane, but have been shown to accumulate in the Golgi network as well. Their function there is believed to be the sorting of secretory cargo and in the case of RSV, it might be taking advantage of that for its exit mechanism.

The data from this study show that upon infection with RSV, the SH protein is targeted to the Golgi where it must function as an ion channel. In addition, there is trafficking of NLRP3 from the cytoplasm to the Golgi where it localises within lipid rafts structures there. These intracellular raft structures seem to be crucial for the accumulation of ion channels and their modulators. Sensing of cellular stress imposed by imbalances in ionic

concentrations in intracellular vesicles could be a general viral recognition pathway that can be utilised by the infected host cell to signal the activation of NLR inflammasomes.

**CHAPTER 6**  
**INNATE IMMUNE RESPONSE TO INFLUENZA A VIRUS (H3N2)**

## 6.1 Introduction

The Influenza virus (IAV) is a seasonal infection associated with significant morbidity and mortality. IAV causes annual epidemics that affect approximately 5 million people worldwide. It is a negative stranded RNA virus causing severe illness in humans and animals. Until recently, cellular recognition of IAV was thought to be mediated by (TLRs) 3, 7/8, which recognize dsRNA and , ssRNA (Kawai and Akira 2006) and RIG-I (Pichlmair et al. 2006).

More recently, several groups have demonstrated an important role for the inflammasome, in particular NLRP3, in the cellular recognition of IAV and the release of IL1 $\beta$  (Allen et al. 2009, Ichinohe 2009). The activation of the NLRP3 inflammasome and production of IL-1 $\beta$  usually requires two signals (Schroder and Tschopp 2010) . In the case of IAV, viral RNA is a trigger and Toll-like receptor 7 (TLR7) signalling is required for the transcription of pro-IL-1 $\beta$ , while the IAV M2 channel was shown to trigger signal 2 for the activation of NLRP3 inflammasome (Ichinohe et al. 2010). The M2 channel is a viroporin involved in viral genome replication as well as virus particle entry into and release from infected cells

Upon IAV infection, NLRP3 traffics to the Golgi apparatus in primed dendritic cells and macrophages (Ichinohe et al. 2010). Acidification of the Golgi apparatus was essential for influenza-induced activation of inflammasomes, thus showing the importance of intracellular pH in inflammasome activation.

However most of these studies are performed on dendritic cells or mouse models and there is not a lot of information on whether IAV triggers inflammasome assembly in the



lung or respiratory tract. Thus by using a tissue tropic IAV strain I investigated inflammasome activation in human bronchial cells infected by IAV.

### **6.2.1 PRR Expression Levels in IAV infection**

Bronchial Epithelial Cells (BES) were infected with H3N2 (100PFU) in order to determine the regulation of PRRs such as RIG-I, MDA-5 and were monitored at different time points (1h,2h, 4h, 6h,12h). Unstimulated cells were checked for receptor expression levels at 0hr. Detection of the expression levels were determined by using indirect Immunofluorescence and measuring the Fluorescence intensity (Fig. 6.1). Significant increase in the expression levels of RIG-I and MDA5 were observed when stimulated with the virus showing slight preference for RIG-I expression over MDA5. We also observe slight upregulation of NLRP3.

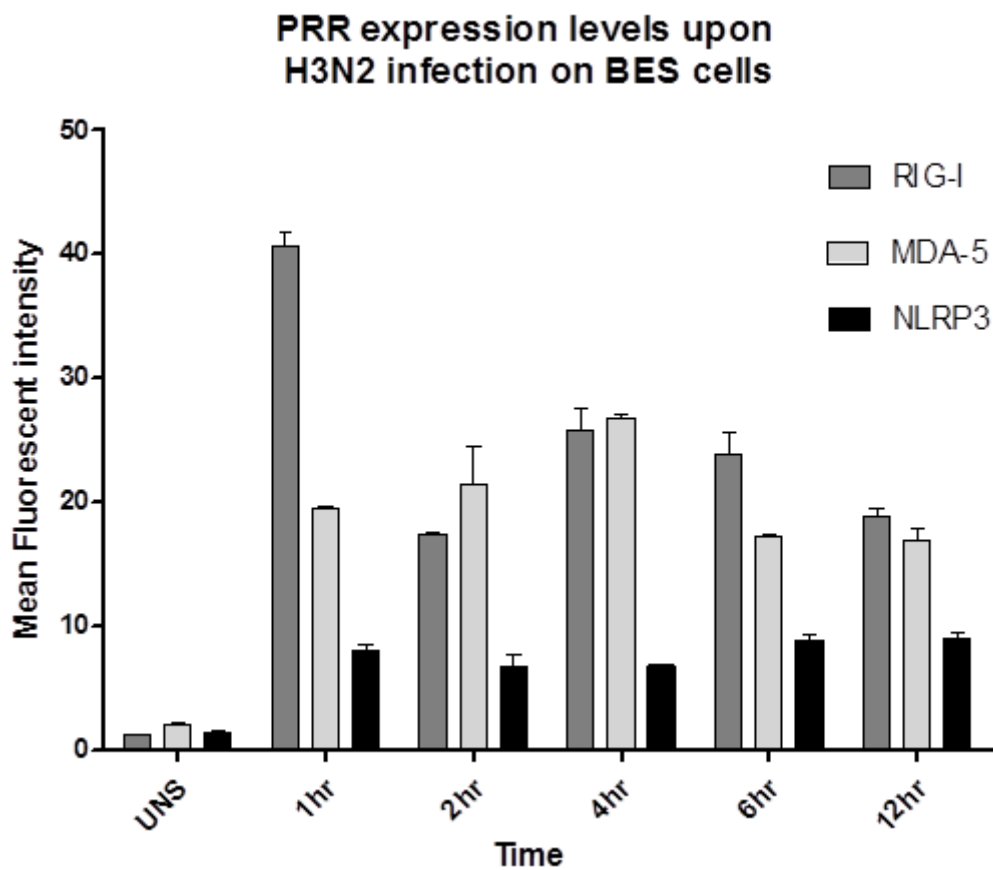


**Figure 6.1 (a)** PRR expression levels in cells stimulated with H3N2. BES were infected with 100 PFU viral stock (H3N2). Following infection PRR expression was tested at different time points using the appropriate primary antibody followed by a secondary conjugated to FITC. Receptor expression was determine as the Geo.Mean of Fluorescent intensity. Fluorescence was detected using a FACSCalibur (BectonDickinson) The data represent the mean of three independent experiments.

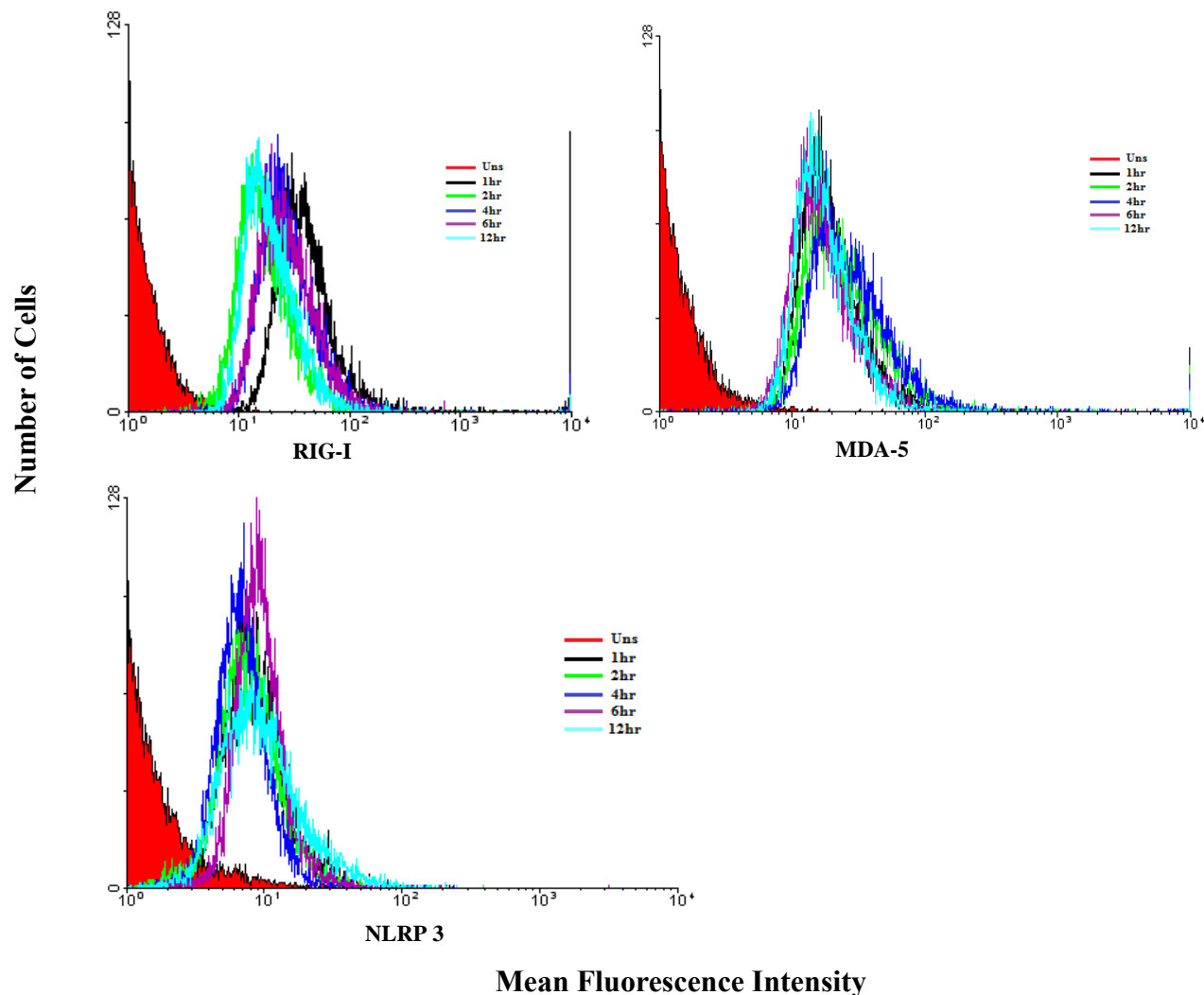


**Figure 6.1 (b)** PRR expression levels in cells stimulated with H3N2. BES were infected with 100 PFU viral stock (H3N2). Following infection PRR expression was tested at different time points using the appropriate primary antibody followed by a secondary conjugated to FITC. Receptor expression was determine as the Geo.Mean of Fluorescent intensity. Fluorescence intensity was detected using a FACSCalibur (Becton Dickinson, Oxford, UK) counting 10,000 cells not gated. Isotype controls were performed, with values similar to unstimulated samples. The data represent the mean SD of 3 independent experiment, indicating statistically significant ( $P < .05$ ) increase in expression compared with corresponding unstimulated controls.

### 6.2.2 Innate immune responses to IAV

To determine whether IAV triggers innate immune responses in the bronchi, BES were infected with 100 PFU viral stock (H3N2) for 1hr, 2hr, 4hr, 6hr and 12 hrs. Cell lysates were collected and analysed for Phospho-I $\kappa$ B and IRF3. A gradual increase in Phospho-I $\kappa$ B production is seen from 1hr through to 12 hrs stimulations (fig 6.2). IRF3 dimerisation is also observed at these timepoints.

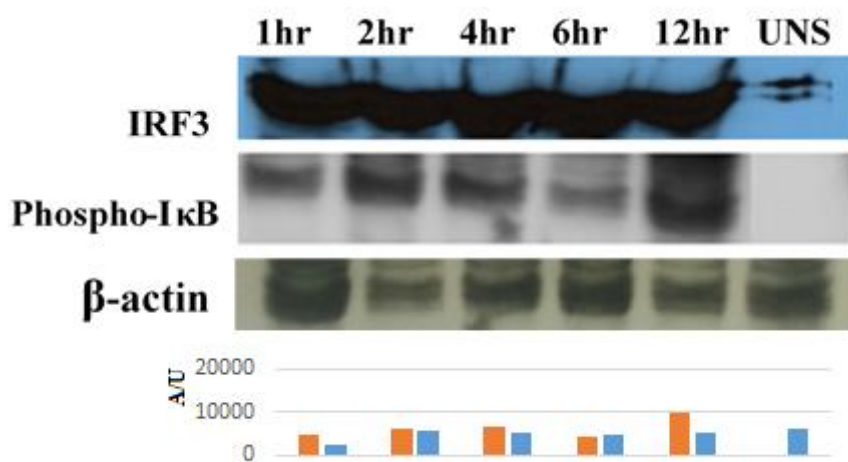


**Figure 6.2 IRF3 and Phospho-I $\kappa$ B detection.** BES were infected with 100 PFU viral stock (H3N2) for 1hr, 2hr, 4hr, 6hr and 12 hrs or left unstimulated (Uns). Cell lysates were collected and analysed for Phospho-I $\kappa$ B and IRF3 using SDS-PAGE gel electrophoresis and western blot. Primary antibodies specific for IRF3 or phospho-I $\kappa$ B were used followed by the appropriate secondary antibodies conjugated to HRP. Loading controls for  $\beta$ -actin are also depicted. The bottom panel shows a quantitative analysis (by densitometry) of IRF3 and Phospho-I $\kappa$ B. The bands were visualised using the ECL procedure. The data is a representative of two independent experiments.

### 6.2.3 IFN- $\beta$ and IL1 $\beta$ Production

Since there was NF $\kappa$ B signalling induced by IAV, I also investigated IFN- $\beta$  and IL1 $\beta$  secretion since both RIG-I and NLRP3 have been shown to be involved in IAV detection by the host. Thus BES cells were infected with 100PFU of H2N2 and left to incubate 1, 2, 4, 6 and 12 hours and then supernatants were collected. The supernatants added to HEK

IFN $\beta$  or HEK IL1 $\beta$  reporter cells and incubated for 24 hours. Quanti-Blue was added and the levels of SEAP measured using a spectrophotometer at 630nm. The SEAP levels correspond to the expression levels of IFN $\beta$ / IL1 $\beta$ .

IFN- $\beta$  is a type I IFN, which signals through the IFN- $\alpha/\beta$  receptor and the Jak-STAT pathway to drive interferon stimulated gene (ISG) expression and an innate immune response.

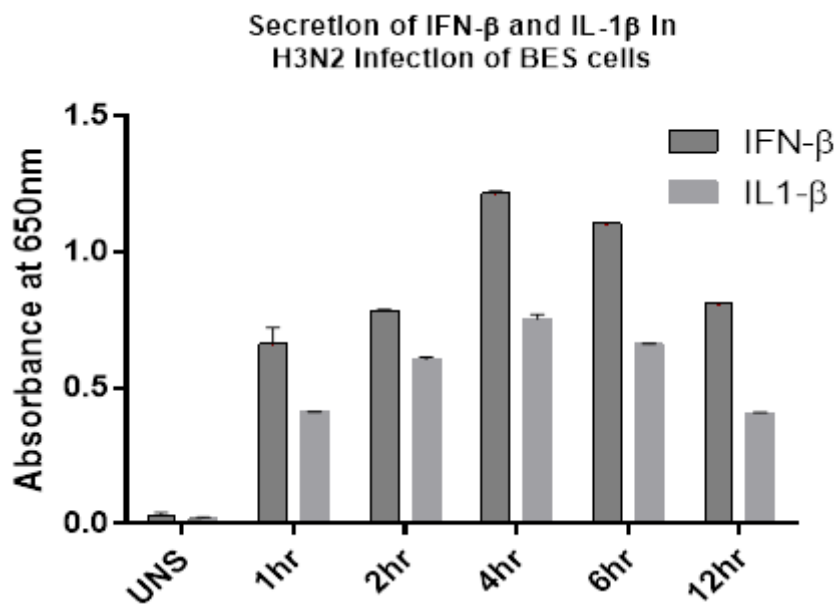


**Figure 6.3 – IFN $\beta$ / IL1 $\beta$  response in H3N2 infections of Bronchial cells.** Supernatant from BES cell infections with 100PFU of H3N2 for 1, 2, 4, 6 and 12 hours was added to HEK IFN $\beta$ / HEK IL1 $\beta$  reporter cells and incubated for 24 hours. Quanti-Blue was added and the levels of SEAP measured using a spectrophotometer at 630nm. The SEAP levels correspond to the expression levels of IFN $\beta$ / IL1 $\beta$ .

An elevated level of IL-1 $\beta$  and IFN- $\beta$  production is observed. This suggests that inflammation occurs as a result of IAV infections of the lung cells. From the IFN $\beta$  response, it seems that RLRs recognise viral invasion as well and stimulate the ISG resulting in the secretion of IFN- $\beta$ .

#### 6.2.4 H3N2 activates the Inflammasome

NLRP3 forms a multiprotein complex with the adaptor protein ASC (pycard) and caspase-1, which leads to the catalytic cleavage of the immature ('pro') forms of interleukin 1 $\beta$  (IL-1 $\beta$ ), IL-18 and IL-33. Inflammasome-mediated cytokine release via NLRP3 requires caspase 1 activation) (Ichinohe et al. 2010). Thus the presence of p10 the active component of caspase 1 was determined in infected cell lysate. The data showed a gradual increase in Caspase-1 p10 production from 1hr through to 12hr timepoints post viral infection. The absence of Caspase-1 p10 in unstimulated cells verifies that viral stimulation is indeed required for inflammasome activation.

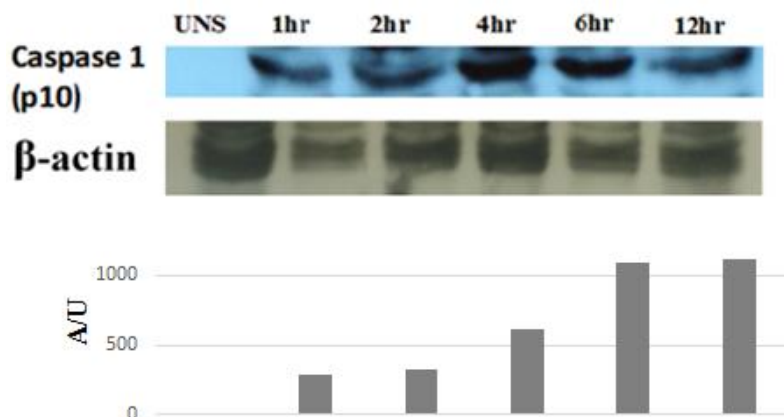


**Figure 6.4 Caspase-1 (p10).** Bronchial Cells (BES) were infected with 100 PFU viral stock (H3N2) for 1hr, 2hr, 4hr, 6hr and 12 hrs or left unstimulated (Uns). Cell lysates were collected and analysed for Caspase 1 (p10) using SDS-PAGE gel electrophoresis and western blot. Primary antibodies specific for Caspase-1(p10) or ASC were used followed by the appropriate secondary antibodies conjugated to HRP. Loading controls for  $\beta$ -actin are also depicted. The bottom panel shows a quantitative analysis (by densitometry) of Caspase-1 (p10). The bands were visualised using the ECL procedure. This data is a representative of two independent experiments.

#### 6.2.4 .1 NLRP3 inflammasome activation

In order to determine which NLR is activated, Different NLRs (NLRP3, NLRC5 and NALP1) were silenced using shRNA. The silenced cells were then infected with H3N2 (100PFU). The presence of Caspase-1 in the transfected cells was investigated via western blotting (figure 6.5).



**Figure 6.5** Bronchial epithelial cells were transfected with shRNA to knock down the levels of NLRC5, NLRP3 and NALP1. The transfected cells were then infected with H2N2. The cells were analysed for the presence of Caspase-1(p10) by western blotting. Primary antibodies specific for Caspase 1 (p10) were used followed by the appropriate secondary antibodies conjugated to HRP. The bands were visualised using the ECL procedure. This data is a representative of two independent experiments

It is observed that silencing NLRP1 and NLRC5 did not abrogate Caspase-1p10 production. Hence NLRC5 and NLRP1 are not involved in IAV detection. However on the contrary knocking down NLRP3 had a dramatic effect on Caspase-1 p10 production by completely abrogating it. Since Caspase-1 production directly correlates with inflammasome activation, NLRP3 inflammasome is the main sensor of IAV in BES cells

### **6.2.5 Effects of different Inhibitors in IAV infection**

In order to determine the mechanism of NLRP3 activation, different ion channel inhibitors were used since it has been shown that M2 plays a role in inflammasome recruitment. BES cells were treated with Adamantanes which are a class of known antiviral drugs that has been used in the past and still currently in use, to treat Influenza virus A infections (Jing et al. 2008). Adamantanes have two derivatives: Rimantadine and Amantadine which in this experiment has been used to treat bronchial cells post infection with H3N2.

ROS inhibitor N-acetyl-L-cysteine was also used (Halasi et al. 2013) in order to study the effect it might cause on inflammasome production. A calcium inhibitor such as Verapamil was also used.

The best working concentrations for the drugs were ROS inhibitor N-acetyl-L-cysteine (10 $\mu$ M), Verapamil (50 $\mu$ M), Rimantadine (10 $\mu$ M) and Amantadine (10 $\mu$ M). Supernatants containing the virus was removed and the cells were washed. The drugs were added along with fresh medium and incubated for 12 hours. Viability assays prior to infection were performed to verify that the drugs had no lethal effect on the cells.

The supernatant was collected for cytokine analysis. The cells were lysed and analysed for the presence of Caspase 1 (p10) via Western Blotting.



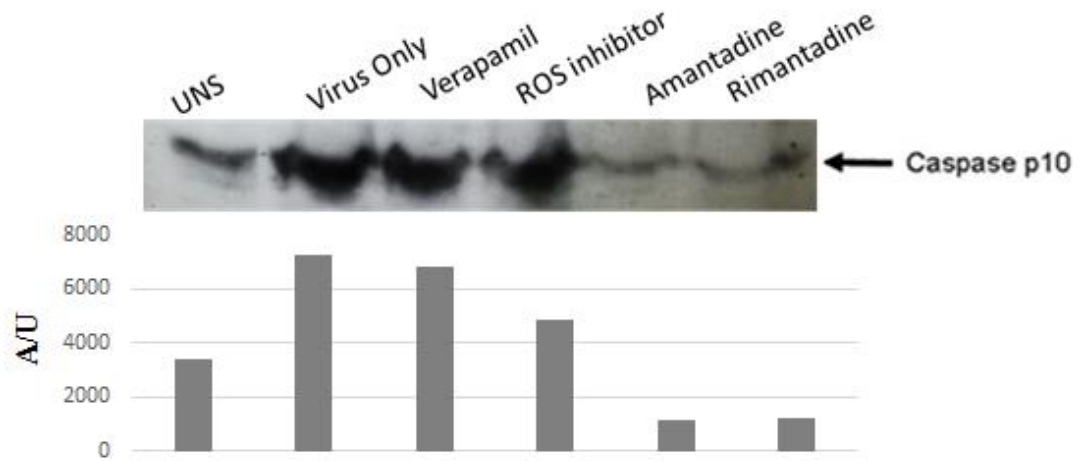


**Figure 6.6 Effects of drugs on H3N2 induced Inflammasome activation.** BES cells were first infected with H3N2 for 12 hours and then treated with different inhibitors and left to incubate for a further of 12 hours. As controls cells were either left unstimulated or treated with virus but no inhibitors. All cells were lysed in X2 reducing buffer and analysed for the presence of Caspase-1 (p10). Primary antibodies specific for Caspase-1(p10) were used followed by the appropriate secondary antibodies conjugated to HRP. The bottom panel shows a quantitative analysis (by densitometry) of Caspase-1 (p10). The bands were visualised using the ECL procedure.

The data showed that in the unstimulated cell there is no production of Caspase-1 p10 whereas in the Virus Only stimulation, there is considerable amount of Caspase-1 p10 present. Cells treated with drugs Verapamil and ROS inhibitor has no effect on Caspase-1 p10. However cells treated with Amantadine and Rimantadine has a reduction in Caspase-1 p10 suggesting that by blocking  $K^+$  channels there is a direct effect on inflammasome activation (Leonov et al. 2011). The anti-flu amino adamantyls

(Amantadine and Rimantadine) are known to block the influenza M2 channel, they specifically inhibit the H<sup>+</sup> of the Influenza M2. The positive charge of the amino group in the adamantyls cause an electrostatic hindrance to the M2 H<sup>+</sup> (Leonov et al. 2011). Functional studies indicate that amantadine binds to the pore of the IAV M2 proton-selective ion channel (Jing et al. 2008). Unwarranted NLRP3 inflammasome activation causes inflammatory disease and it is vastly demonstrated that potassium efflux could lead to engaging this inflammasome (Kanneganti and Lamkanfi 2013) (Munoz-Planillo et al. 2013). Blocking K<sup>+</sup> channels through the use of adamantyls can prevent the assembly of the NLRP3 inflammasome and the resultant Caspase-1 secretion.

### **6.3 Discussion**

It has been previously demonstrated that IAV initiates an innate immune response through the recognition of viral RNA that results in the activation of the NLRP3 inflammasome, *in vivo* (Allen et al. 2009). A plethora of PRRs such as the RLHs, TLRs and NLRs have been identified and shown to be activated in response to IAV in dendritic cells, macrophages and also demonstrated *in vivo*. Also the Influenza viral ion channel protein M2 is involved in inflammasome activation in dendritic cells and macrophages (Ichinohe et al. 2010). In this study we demonstrate that infection of bronchial cells can elicit an innate immune response and viral invasion is recognised by RIG-I and MDA-5, the latter being less expressed in the infected cells. NLRP3 also senses IAV infection of BES and triggers the assembly of the NLRP3 inflammasome and cause the release of IL-1 $\beta$ . Using drugs such and Amantadine and Rimantadine which are K<sup>+</sup> channel blockers we propose that the M2 ion channel is involved the NLRP3 inflammasome activation in bronchial cells.

**CHAPTER 7**  
**DISCUSSION**

The cells and organs of the human body require a constant stream of oxygen to stay alive. The respiratory system provides oxygen to the body's cells while removing carbon dioxide, a waste product that can be lethal if allowed to accumulate. Like other organs, such as the skin and gastrointestinal tract, the respiratory tract is constantly exposed to microbes and particles by inhalation. It contains both mechanical (ie, ciliated epithelial movement and mucus production) and biochemical (ie, antimicrobial enzymes/ peptides) barriers that inhibit colonization of the lungs by most microorganisms. However, many respiratory pathogens, including viruses, have evolved to successfully colonize and replicate on or within the lung epithelial cells, occasionally causing life-threatening diseases. Viral infections of the respiratory tract are the most common triggers of bronchiolitis, wheezing and acute asthma exacerbations. Previous studies have shown that respiratory syncytial virus (RSV), human rhinovirus (HRV), (Johnston et al. 1995, Seemungal et al. 2001) human influenza virus (IAV), and human parainfluenza virus (HPIV) are detected in the acute exacerbation of asthma and chronic obstructive pulmonary disease (COPD), leading to rapid decline in lung function and increased mortality (Kurai et al. 2013). However, the relationships between viral infections, host immune response, and host factors in the pathophysiology of chronic bronchitis, chronic obstructive pulmonary disease, and bronchial asthma remains unclear.

The increased airway inflammation is caused by the excessive production of cytokines such as Il-6 and TNF $\alpha$ . In this study we have also noticed an over-secretion of IL-1 $\beta$  in respiratory viral infections which causes inflammation of the lung tissue. The conglomeration of all these cytokines leads to COPD and asthma. A further increment of these pro-inflammatory cytokines are observed in acute exacerbations (de Kluijver et al. 2003, Fleming et al. 1999, Terajima et al. 1997). Epithelial cells and monocytes (PBMCs and alveolar macrophages) collected from COPD and asthma patients secrete greater

amounts of IL-1 $\beta$ , responding vigorously to inflammatory stimulus (Hallsworth et al. 1994).

IL-1 $\beta$  is an important pro-inflammatory mediator and is generally produced at a site of injury/ damage or a site of infections (or immunological challenge). This happens, in order to recruit cells (immune cells/ immune receptors) to the site of damage to combat pathogen entry. Pathogen induced stimulus prompts the production of inactive IL-1 $\beta$  which is converted to the active form by multi-molecular protein complexes termed as inflammasomes. Mature cytokines are then released from the cells onto the site of infection causing inflammation and tissue damage. Inflammasomes contain members of the nucleotide binding domain leucine-rich repeat containing (NLR) family. These are identified as caspase-1 activators and thus controlling the second step required for the maturation and release of IL-1 $\beta$ .

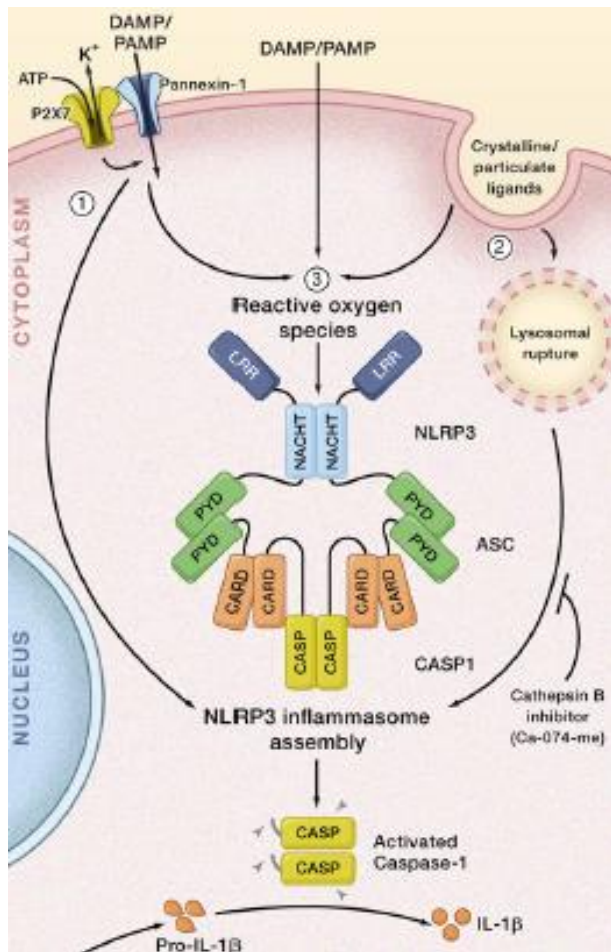


**Figure 7.1 NLRP3 Inflammasome activation.** Three major models are proposed for the inflammasome activation which makes the signal 2 for activation. 1.) ATP acts as an NLRP3 agonist resulting in its activation and inflammasome assemblage 2.) Crystal and particles act as an NLRP3 agonist, which are engulfed and result in lysosomal rupture 3.) DAMPs or Danger Associate Molecular Patterns and also PAMPs trigger the formation of ROS (Reactive Oxygen Species). A ROS dependent pathway triggers the inflammasome activation after engaging NLRP3. Diagram modified from (Tschopp et al. 2003).

In this study IL-1 $\beta$  production was investigated in response to inflammasome activation induced by various respiratory viruses such as RSV, HRVs and IAV in primary bronchial epithelial cells which is a clinically relevant cell type for viral respiratory infections. Silencing different NLRs allowed us to discover their involvement in inflammasome activation. These experiments confirmed that NLRP3 plays a major role in RSV, HRV

and IAV infections in addition NLRC5 inflammasomes was also involved in Caspase-1 activation and the subsequent production of IL-1 $\beta$  in HRV infections. NLRs have been shown to have different roles in separate cell types (Ting et al. 2010).

There is emerging evidence which suggests that during bacterial infections, multiple NLR inflammasomes have the potential to become activated. For example *Candida albicans* leads to up-regulation of NLRP3 and NLRC4 inflammasome in the oral mucosa (Tomalka et al. 2011) Here we show that infection of primary bronchial cells with HRV leads to NLRP3 and NLRC5 activation and IL1 $\beta$  secretion. The overlapping biologic functions and pathogen specificity of NLRC5 with NLRP3 suggests that these proteins might act in a cooperative manner during inflammasome assembly and that the host immune response has evolved to use both NLRC5 and NLRP3 in case one of them stops functioning the other can compensate.

To determine the mechanism of inflammasome activation by these viruses we studied viral proteins that affect ion homeostasis in the cell since inflammasome has been shown to be triggered by K<sup>+</sup>/Na<sup>+</sup> fluxes as well as Ca<sup>2+</sup> imbalances (Chami et al. 2006). The 2B protein encoded by the Rhinovirus genome is a non-structural protein which also enhances membrane permeability. 2B protein forms integral pores in the membranes which could be a mechanism of inflammasome activation since bacterial pore forming toxins activate the NLRP3 inflammasome (Koizumi et al. 2012). These pores allow Calcium ion efflux (van Kuppeveld et al. 1997).

Tracking 2B protein intracellularly via confocal microscopy and the use of calcium inhibitors revealed that 2B viroporin localises to the Golgi complex and reduces ER and Golgi Ca<sup>2+</sup> levels thus triggering NLRP3 and NLRC5 inflammasome activation.

For RSV our experiments showed that the small hydrophobic (SH) viroporin, which forms channels in the plasma membrane, is essential in triggering the NLRP3 inflammasome in RSV infections of lung epithelial cells. Furthermore, RSV mutants lacking the viroporin SH were unable to trigger inflammasome activation and IL-1 $\beta$  secretion. Pharmacological treatment of RSV-infected cells with drugs that inhibited viral ion channels blocked inflammasome activation. Upon RSV infection, the RSV SH viroporin accumulates in the Golgi within lipid raft structures which are specialised membrane microdomain which form favourable conditions for intra-molecular cross-talks and also facilitate signal transduction. Recent studies have reported that several ion channels as well as their modulators accumulate in lipid rafts (Dart 2010, Martens et al. 2004). Lipid rafts are found in the Golgi network as well as the plasma membrane. They are positioned at the Golgi network possibly for sorting secretory cargo (Klemm et al. 2009). In the case of RSV, the virus might be using lipid rafts as its exit mechanism by forming ion channels selective for monovalent cations (Na<sup>+</sup> and K<sup>+</sup>), RSV triggers the translocation of NLRP3 from the cytoplasm to the Golgi and its activation.

In conclusion our data reveals that during an RSV infection, its SH protein localises at the Golgi network and there it acts as an ion channel protein causing ionic flux across internal vesicular membranes. NLRP3 is observed to translocate from the cytosol of the



cell to the Golgi and localise with the lipid raft structures present there. These intracellular raft structures are crucial for ion channel accumulation. When cells are imposed with stress caused by viral invasion, ionic concentration imbalance occurs within intracellular vesicles and the cytosol mediated by viral pore forming proteins such as the SH protein. This could be a possible mechanism of viral recognition and an induction of an innate immune response through the activation of the NLR inflammasomes.

Influenza virus like the other respiratory viruses discussed above has the same delirious effect on the human body and cause annual epidemics and more than ~5 million people suffer from it every year. Although a great deal of study has been made on trying to elucidate how the Influenza virus works there are still unknown areas in human knowledge regarding its exact function during infection. The scope of this study was to provide a glimpse into how the body innate immunity detects the invading pathogen and triggers an inflammatory response in order to combat the situation. Bronchial epithelial cells which are a suitable candidate for such viral infections were used and we infer from this study that PRRs such as the RIG-I and MDA-5 play a key role in recognising the invading pathogen and trigger the first line of defence. The NLRs such as the NLRP3 in particular engages itself in forming a very typical macromolecular complex triggered by  $K^+$  imbalances caused by IAV, which lead to NLRP3 inflammasome activation and the production of inflammatory cytokines. Thus we propose that using ion channel inhibitors such as Adamantyls will help prevent inflammatory signals and greatly reduce the production of  $IL1\beta$  from lung cells. These data demonstrate that the Influenza M2 ion channel is highly involved in the NLRP3 assemblage and using  $K^+$  channel blockers can reduce the production of  $IL-1\beta$ . Ichinohe et al has demonstrated similar findings but in dendritic cells and macrophages. Our data is in agreement with Ichinohe et. al. however they are based on lung tissue, which is more relevant to IAV infections.

In conclusion it is observed that most respiratory viruses encode ion channel proteins called viroporins including HRV, RSV and IAV. These small ion channel proteins change intracellular ion homeostasis which triggers the innate immune system and one of the main responses is the activation of the inflammasome. A disruption of the permeability barrier is observed in most respiratory viral infections across intracellular compartments (For example the Golgi and the trans-Golgi network) and also the plasma membrane. Viroporins trigger ion flux across these cellular compartments/membranes (such as Na<sup>+</sup>/K<sup>+</sup> and Ca<sup>2+</sup>) and this ionic imbalance across the membranes causes the inflammasome activation and IL-1 $\beta$  secretion. This is the body's natural defence against combating invading pathogens however repeated infections can cause damage to the lung tissues and cytokine secretion seems to do more harm than just controlling pathogen invasion. Therefore by blocking the ion channels could prove therapeutically beneficial in antiviral therapy.

## REFERENCES

- Agostini L, Martinon F, Burns K, McDermott MF, Hawkins PN, Tschopp J. 2004. NALP3 forms an IL-1beta-processing inflammasome with increased activity in Muckle-Wells autoinflammatory disorder. *Immunity* 20: 319-325.
- Ahlquist P, Kaesberg P. 1979. Determination of the length distribution of poly(A) at the 3' terminus of the virion RNAs of EMC virus, poliovirus, rhinovirus, RAV-61 and CPMV and of mouse globin mRNA. *Nucleic Acids Res* 7: 1195-1204.
- Agirre A, Barco A, Carrasco L, Nieva JL. 2002. Viroporin-mediated membrane permeabilization. Pore formation by nonstructural poliovirus 2B protein. *J Biol Chem* 277: 40434-40441.
- Allen IC, Scull MA, Moore CB, Holl EK, McElvania-TeKippe E, Taxman DJ, Guthrie EH, Pickles RJ, Ting JP. 2009. The NLRP3 inflammasome mediates in vivo innate immunity to influenza A virus through recognition of viral RNA. *Immunity* 30: 556-565.
- Allen IC, Scull MA, Moore CB, Holl EK, McElvania-TeKippe E, Taxman DJ, Guthrie EH, Pickles RJ, Ting JP. 2009. The NLRP3 inflammasome mediates in vivo innate immunity to influenza A virus through recognition of viral RNA. *Immunity* 30: 556-565.
- Akira S. 2003. Mammalian Toll-like receptors. *Curr Opin Immunol* 15: 5-11.
- —. 2009. Pathogen recognition by innate immunity and its signaling. *Proc Jpn Acad Ser B Phys Biol Sci* 85: 143-156.
- Akira S, Takeuchi O. 2010. LGP2 is a positive regulator of RIG-I- and MDA5-mediated antiviral responses. *Proc Natl Acad Sci U S A* 107: 1512-1517.

- Akira S, Uematsu S, Takeuchi O. 2006. Pathogen recognition and innate immunity. *Cell* 124: 783-801.
- Alexopoulou,L., Holt,A.C., Medzhitov,R., and Flavell,R.A. (2001). Recognition of double-stranded RNA and activation of NF-kappaB by Toll-like receptor 3. *Nature* 413, 732-738.
- Andino R, Boddeker N, Silvera D, Gamarnik AV. 1999. Intracellular determinants of picornavirus replication. *Trends Microbiol* 7: 76-82.
- Barik S. 1992. Transcription of human respiratory syncytial virus genome RNA in vitro: requirement of cellular factor(s). *J Virol* 66: 6813-6818.
- Barton DJ, Black EP, Flanagan JB. 1995. Complete replication of poliovirus in vitro: preinitiation RNA replication complexes require soluble cellular factors for the synthesis of VPg-linked RNA. *J Virol* 69: 5516-5527.
- Batonick M, Wertz GW. 2011. Requirements for Human Respiratory Syncytial Virus Glycoproteins in Assembly and Egress from Infected Cells. *Adv Virol* 2011.
- Bauernfeind FG, et al. 2009. Cutting edge: NF-kappaB activating pattern recognition and cytokine receptors license NLRP3 inflammasome activation by regulating NLRP3 expression. *J Immunol* 183: 787-791.
- Becker Y. 2006. Respiratory syncytial virus (RSV) evades the human adaptive immune system by skewing the Th1/Th2 cytokine balance toward increased levels of Th2 cytokines and IgE, markers of allergy--a review. *Virus Genes* 33: 235-252.
- Belsham GJ, Sonenberg N. 1996. RNA-protein interactions in regulation of picornavirus RNA translation. *Microbiol Rev* 60: 499-511.
- Beutler BA. 2009. TLRs and innate immunity. *Blood* 113: 1399-1407.

- Blyn LB, Towner JS, Semler BL, Ehrenfeld E. 1997. Requirement of poly(rC) binding protein 2 for translation of poliovirus RNA. *J Virol* 71: 6243-6246.
- Boukhvalova MS, Prince GA, Soroush L, Harrigan DC, Vogel SN, Blanco JC. 2006. The TLR4 agonist, monophosphoryl lipid A, attenuates the cytokine storm associated with respiratory syncytial virus vaccine-enhanced disease. *Vaccine* 24: 5027-5035.
- Burckstummer T, et al. 2009. An orthogonal proteomic-genomic screen identifies AIM2 as a cytoplasmic DNA sensor for the inflammasome. *Nat Immunol* 10: 266-272.
- Bukreyev A, Whitehead SS, Murphy BR, Collins PL. 1997. Recombinant respiratory syncytial virus from which the entire SH gene has been deleted grows efficiently in cell culture and exhibits site-specific attenuation in the respiratory tract of the mouse. *J Virol* 71: 8973-8982.
- Carter SD, et al. 2010. Direct visualization of the small hydrophobic protein of human respiratory syncytial virus reveals the structural basis for membrane permeability. *FEBS Lett* 584: 2786-2790.
- Ciampor F. 2003. The ion channels coded by viruses. *Acta Microbiol Immunol Hung* 50: 433-442.
- Collins PL, Mottet G. 1993. Membrane orientation and oligomerization of the small hydrophobic protein of human respiratory syncytial virus. *J Gen Virol* 74 ( Pt 7): 1445-1450.
- Cohen EA, Terwilliger EF, Sodroski JG, Haseltine WA. 1988. Identification of a protein encoded by the vpu gene of HIV-1. *Nature* 334: 532-534.
- Collins PL, Graham BS. 2008. Viral and host factors in human respiratory syncytial virus pathogenesis. *J Virol* 82: 2040-2055.

- Contoli M, et al. 2006. Role of deficient type III interferon-lambda production in asthma exacerbations. *Nat Med* 12: 1023-1026.
- Cox DW, Le Souef PN. 2014a. Rhinovirus and the developing lung. *Paediatr Respir Rev*.— 2014b. Rhinovirus and the developing lung. *Paediatr Respir Rev* 15: 268-274.
- Cui S, Eisenacher K, Kirchhofer A, Brzozka K, Lammens A, Lammens K, Fujita T, Conzelmann KK, Krug A, Hopfner KP. 2008. The C-terminal regulatory domain is the RNA 5'-triphosphate sensor of RIG-I. *Mol Cell* 29: 169-179.
- Dart C. 2010. Lipid microdomains and the regulation of ion channel function. *J Physiol* 588: 3169-3178.
- Dasgupta A, Baron MH, Baltimore D. 1979. Poliovirus replicase: a soluble enzyme able to initiate copying of poliovirus RNA. *Proc Natl Acad Sci U S A* 76: 2679-2683.
- Davidson S, et al. 2011. Plasmacytoid dendritic cells promote host defense against acute pneumovirus infection via the TLR7-MyD88-dependent signaling pathway. *J Immunol* 186: 5938-5948.
- Davis BK, Wen H, Ting JP. 2011. The inflammasome NLRs in immunity, inflammation, and associated diseases. *Annu Rev Immunol* 29: 707-735.
- de Jong AS, de Mattia F, Van Dommelen MM, Lanke K, Melchers WJ, Willems PH, van Kuppeveld FJ. 2008. Functional analysis of picornavirus 2B proteins: effects on calcium homeostasis and intracellular protein trafficking. *J Virol* 82: 3782-3790.

- Diebold,S.S., Kaisho,T., Hemmi,H., Akira,S., and Reis e Sousa,C. (2004). Innate antiviral responses by means of TLR7-mediated recognition of single-stranded RNA. *Science* 303, 1529-1531.
- Dostert C, Petrilli V, Van Bruggen R, Steele C, Mossman BT, Tschopp J. 2008. Innate immune activation through Nalp3 inflammasome sensing of asbestos and silica. *Science* 320: 674-677.
- Faustin B, Lartigue L, Bruey JM, Luciano F, Sergienko E, Bailly-Maitre B, Volkmann N, Hanein D, Rouiller I, Reed JC. 2007. Reconstituted NALP1 inflammasome reveals two-step mechanism of caspase-1 activation. *Mol Cell* 25: 713-724.
- Fernie BF, Gerin JL. 1982. Immunochemical identification of viral and nonviral proteins of the respiratory syncytial virus virion. *Infect Immun* 37: 243-249.
- Fitzgerald KA, McWhirter SM, Faia KL, Rowe DC, Latz E, Golenbock DT, Coyle AJ, Liao SM, Maniatis T. 2003. IKKepsilon and TBK1 are essential components of the IRF3 signaling pathway. *Nat Immunol* 4: 491-496.
- Flanagan JB, Baltimore D. 1977. Poliovirus-specific primer-dependent RNA polymerase able to copy poly(A). *Proc Natl Acad Sci U S A* 74: 3677-3680.
- Fredericksen BL, Gale M, Jr. 2006. West Nile virus evades activation of interferon regulatory factor 3 through RIG-I-dependent and -independent pathways without antagonizing host defense signaling. *J Virol* 80: 2913-2923.
- Gamarnik AV, Andino R. 1996. Replication of poliovirus in *Xenopus* oocytes requires two human factors. *EMBO J* 15: 5988-5998.

- Gamarnik AV, Boddeker N, Andino R. 2000. Translation and replication of human rhinovirus type 14 and mengovirus in *Xenopus* oocytes. *J Virol* 74: 11983-11987.
- Gan SW, et al. 2012. The small hydrophobic protein of the human respiratory syncytial virus forms pentameric ion channels. *J Biol Chem* 287: 24671-24689.
- Gantner BN, Simmons RM, Canavera SJ, Akira S, Underhill DM. 2003. Collaborative induction of inflammatory responses by dectin-1 and Toll-like receptor 2. *J Exp Med* 197: 1107-1117.
- Gern JE. 2010. The ABCs of rhinoviruses, wheezing, and asthma. *J Virol* 84: 7418-7426.
- Gielen V, Johnston SL, Edwards MR. 2010. Azithromycin induces anti-viral responses in bronchial epithelial cells. *Eur Respir J* 36: 646-654.
- Gonzalez ME, Carrasco L. 2003. Viroporins. *FEBS Lett* 552: 28-34.
- Gorbalenya AE, Koonin EV, Donchenko AP, Blinov VM. 1988. A novel superfamily of nucleoside triphosphate-binding motif containing proteins which are probably involved in duplex unwinding in DNA and RNA replication and recombination. *FEBS Lett* 235: 16-24.
- Greene CM, McElvaney NG. 2005. Toll-like receptor expression and function in airway epithelial cells. *Arch Immunol Ther Exp (Warsz)* 53: 418-427.
- Groskreutz DJ, Monick MM, Powers LS, Yarovinsky TO, Look DC, Hunninghake GW. 2006. Respiratory syncytial virus induces TLR3 protein and protein kinase R, leading to increased double-stranded RNA responsiveness in airway epithelial cells. *J Immunol* 176: 1733-1740.
- Guillot L, Le Goffic R, Bloch S, Escriou N, Akira S, Chignard M, Si-Tahar M. 2005. Involvement of toll-like receptor 3 in the immune response of lung



epithelial cells to double-stranded RNA and influenza A virus. *J Biol Chem* 280: 5571-5580.

- Haeberle HA, Takizawa R, Casola A, Brasier AR, Dieterich HJ, Van Rooijen N, Gatalica Z, Garofalo RP. 2002. Respiratory syncytial virus-induced activation of nuclear factor-kappaB in the lung involves alveolar macrophages and toll-like receptor 4-dependent pathways. *J Infect Dis* 186: 1199-1206.
- Halasi M, Wang M, Chavan TS, Gaponenko V, Hay N, Gartel AL. 2013. ROS inhibitor N-acetyl-L-cysteine antagonizes the activity of proteasome inhibitors. *Biochem J* 454: 201-208.
- Hall CB. 1999. Respiratory syncytial virus: A continuing culprit and conundrum. *J Pediatr* 135: 2-7.
- Halle A, Hornung V, Petzold GC, Stewart CR, Monks BG, Reinheckel T, Fitzgerald KA, Latz E, Moore KJ, Golenbock DT. 2008. The NALP3 inflammasome is involved in the innate immune response to amyloid-beta. *Nat Immunol* 9: 857-865.
- Harada T, Tautz N, Thiel HJ. 2000. E2-p7 region of the bovine viral diarrhea virus polyprotein: processing and functional studies. *J Virol* 74: 9498-9506.
- Harutyunyan S, Kumar M, Sedivy A, Subirats X, Kowalski H, Kohler G, Blaas D. 2013. Viral uncoating is directional: exit of the genomic RNA in a common cold virus starts with the poly-(A) tail at the 3'-end. *PLoS Pathog* 9: e1003270.
- Heil,F., Hemmi,H., Hochrein,H., Ampenberger,F., Kirschning,C., Akira,S., Lipford,G., Wagner,H., and Bauer,S. (2004). Species-specific recognition of single-stranded RNA via Toll-like receptor 7 and 8. *Science* 303, 1526-1529.
- Hiscott J, Lin R, Nakhaei P, Paz S. 2006. MasterCARD: a priceless link to innate immunity. *Trends Mol Med* 12: 53-56.

- Hlaing T, Guo RF, Dilley KA, Loussia JM, Morrish TA, Shi MM, Vincenz C, Ward PA. 2001. Molecular cloning and characterization of DEFCAP-L and -S, two isoforms of a novel member of the mammalian Ced-4 family of apoptosis proteins. *J Biol Chem* 276: 9230-9238.
- Hoebe K, et al. 2005. CD36 is a sensor of diacylglycerides. *Nature* 433: 523-527.
- Hoffman HM, Mueller JL, Broide DH, Wanderer AA, Kolodner RD. 2001. Mutation of a new gene encoding a putative pyrin-like protein causes familial cold autoinflammatory syndrome and Muckle-Wells syndrome. *Nat Genet* 29: 301-305.
- Hoffmann JA. 2003. The immune response of *Drosophila*. *Nature* 426: 33-38.
- Hornung V, Ablasser A, Charrel-Dennis M, Bauernfeind F, Horvath G, Caffrey DR, Latz E, Fitzgerald KA. 2009. AIM2 recognizes cytosolic dsDNA and forms a caspase-1-activating inflammasome with ASC. *Nature* 458: 514-518.
- Hornung V, et al. 2006. 5'-Triphosphate RNA is the ligand for RIG-I. *Science* 314: 994-997.
- Hornung, V., Ellegast, J., Kim, S., Brzozka, K., Jung, A., Kato, H., Poeck, H., Akira, S., Conzelmann, K.K., Schlee, M., Endres, S., and Hartmann, G. (2006). 5'-Triphosphate RNA is the ligand for RIG-I. *Science* 314, 994-997.
- Hornung V, Bauernfeind F, Halle A, Samstad EO, Kono H, Rock KL, Fitzgerald KA, Latz E. 2008. Silica crystals and aluminum salts activate the NALP3 inflammasome through phagosomal destabilization. *Nat Immunol* 9: 847-856.
- Hoebe, K., Du, X., Georgel, P., Janssen, E., Tabet, K., Kim, S.O., Goode, J., Lin, P., Mann, N., Mudd, S., Crozat, K., Sovath, S., Han, J., and Beutler, B. (2003). Identification of Lps2 as a key transducer of MyD88-independent TIR signalling. *Nature* 424, 743-748.

- Huhn MH, McCartney SA, Lind K, Svedin E, Colonna M, Flodstrom-Tullberg M. 2010. Melanoma differentiation-associated protein-5 (MDA-5) limits early viral replication but is not essential for the induction of type 1 interferons after Coxsackievirus infection. *Virology* 401: 42-48.
- Hunt M. April 26, 2010. RNA VIRUS REPLICATION STRATEGIES. (2/2/2013 2013; <http://pathmicro.med.sc.edu/mhunt/rna-ho.htm>)
- Ichinohe T, Pang IK, Iwasaki A. 2010. Influenza virus activates inflammasomes via its intracellular M2 ion channel. *Nat Immunol* 11: 404-410.
- Ichinohe T, Pang IK, Iwasaki A. 2010. Influenza virus activates inflammasomes via its intracellular M2 ion channel. *Nat Immunol* 11: 404-410.
- Ichinohe T, Lee HK, Ogura Y, Flavell R, Iwasaki A. 2009. Inflammasome recognition of influenza virus is essential for adaptive immune responses. *J Exp Med* 206: 79-87.
- Ikegame S, Takeda M, Ohno S, Nakatsu Y, Nakanishi Y, Yanagi Y. 2010. Both RIG-I and MDA5 RNA helicases contribute to the induction of alpha/beta interferon in measles virus-infected human cells. *J Virol* 84: 372-379.
- Invitrogen.
- Ito M, Yanagi Y, Ichinohe T. 2012. Encephalomyocarditis virus viroporin 2B activates NLRP3 inflammasome. *PLoS Pathog* 8: e1002857.
- Iwamura C, Nakayama T. 2008. Toll-like receptors in the respiratory system: their roles in inflammation. *Curr Allergy Asthma Rep* 8: 7-13.
- Jackson RJ, Kaminski A. 1995. Internal initiation of translation in eukaryotes: the picornavirus paradigm and beyond. *RNA* 1: 985-1000.

- Janeway CA, Jr. 1989. Approaching the asymptote? Evolution and revolution in immunology. *Cold Spring Harb Symp Quant Biol* 54 Pt 1: 1-13.
- Jing X, Ma C, Ohigashi Y, Oliveira FA, Jardetzky TS, Pinto LH, Lamb RA. 2008. Functional studies indicate amantadine binds to the pore of the influenza A virus M2 proton-selective ion channel. *Proc Natl Acad Sci U S A* 105: 10967-10972.
- Jin MS, Lee JO. 2008. Structures of the toll-like receptor family and its ligand complexes. *Immunity* 29: 182-191.
- Johnson CL, Gale M, Jr. 2006. CARD games between virus and host get a new player. *Trends Immunol* 27: 1-4.
- Johnston SL, et al. 1995. Community study of role of viral infections in exacerbations of asthma in 9-11 year old children. *BMJ* 310: 1225-1229.
- Kang DC, Gopalkrishnan RV, Wu Q, Jankowsky E, Pyle AM, Fisher PB. 2002. mda-5: An interferon-inducible putative RNA helicase with double-stranded RNA-dependent ATPase activity and melanoma growth-suppressive properties. *Proc Natl Acad Sci U S A* 99: 637-642.
- Kang JY, Nan X, Jin MS, Youn SJ, Ryu YH, Mah S, Han SH, Lee H, Paik SG, Lee JO. 2009. Recognition of lipopeptide patterns by Toll-like receptor 2-Toll-like receptor 6 heterodimer. *Immunity* 31: 873-884.
- Kanneganti TD. 2010. Central roles of NLRs and inflammasomes in viral infection. *Nat Rev Immunol* 10: 688-698.
- Kanneganti TD, Lamkanfi M. 2013. K(+) drops tilt the NLRP3 inflammasome. *Immunity* 38: 1085-1088.

- Kanneganti TD, Lamkanfi M, Kim YG, Chen G, Park JH, Franchi L, Vandenberghe P, Nunez G. 2007. Pannexin-1-mediated recognition of bacterial molecules activates the cryopyrin inflammasome independent of Toll-like receptor signaling. *Immunity* 26: 433-443.
- Kanneganti TD, et al. 2006. Critical role for Cryopyrin/Nalp3 in activation of caspase-1 in response to viral infection and double-stranded RNA. *J Biol Chem* 281: 36560-36568.
- Karin M, Ben-Neriah Y. 2000. Phosphorylation meets ubiquitination: the control of NF- $\kappa$ B activity. *Annu Rev Immunol* 18: 621-663.
- Kato, H., Takeuchi, O., Mikamo-Satoh, E., Hirai, R., Kawai, T., Matsushita, K., Hiiragi, A., Dermody, T. S., Fujita, T., and Akira, S. Length-dependent recognition of double-stranded ribonucleic acids by retinoic acid-inducible gene-I and melanoma differentiation-associated gene 5. *J. Exp Med* 205, 1601-1610. 2008.
- Kato H, Takeuchi O, Sato S, Yoneyama M, Yamamoto M, Matsui K, Uematsu S, Jung A, Kawai T, Ishii KJ, Yamaguchi O, Otsu K, Tsujimura T, Koh CS, Reis e Sousa C, Matsuura Y, Fujita T, and Akira S. Differential roles of MDA5 and RIG-I helicases in the recognition of RNA viruses. *Nature* 441, 101-105. 2006.
- Kato H, Takeuchi O, Mikamo-Satoh E, Hirai R, Kawai T, Matsushita K, Hiiragi A, Dermody TS, Fujita T, Akira S. 2008. Length-dependent recognition of double-stranded ribonucleic acids by retinoic acid-inducible gene-I and melanoma differentiation-associated gene 5. *J Exp Med* 205: 1601-1610.
- Kato H, et al. 2006. Differential roles of MDA5 and RIG-I helicases in the recognition of RNA viruses. *Nature* 441: 101-105.

—. 2008. Toll-like receptor and RIG-I-like receptor signaling. *Ann N Y Acad Sci* 1143: 1-20.

—. 2010. The role of pattern-recognition receptors in innate immunity: update on Toll-like receptors. *Nat Immunol* 11: 373-384.

- Kawai T, Akira S. 2007. TLR signaling. *Semin Immunol* 19: 24-32.
- Kawai T, Akira S. 2006. Innate immune recognition of viral infection. *Nat Immunol* 7: 131-137.
- Kawai,T., Takahashi,K., Sato,S., Coban,C., Kumar,H., Kato,H., Ishii,K.J., Takeuchi,O., and Akira,S. (2005). IPS-1, an adaptor triggering RIG-I- and Mda5-mediated type I interferon induction. *Nat. Immunol* 6, 981-988.
- Kim HM, et al. 2007. Crystal structure of the TLR4-MD-2 complex with bound endotoxin antagonist Eritoran. *Cell* 130: 906-917.
- Kitchens RL. 2000. Role of CD14 in cellular recognition of bacterial lipopolysaccharides. *Chem Immunol* 74: 61-82.
- Kochva U, Leonov H, Arkin IT. 2003. Modeling the structure of the respiratory syncytial virus small hydrophobic protein by silent-mutation analysis of global searching molecular dynamics. *Protein Sci* 12: 2668-2674.
- Komuro A, Horvath CM. 2006. RNA- and virus-independent inhibition of antiviral signaling by RNA helicase LGP2. *J Virol* 80: 12332-12342.
- Krusat T, Streckert HJ. 1997. Heparin-dependent attachment of respiratory syncytial virus (RSV) to host cells. *Arch Virol* 142: 1247-1254.
- Kumar H, et al. 2006. Essential role of IPS-1 in innate immune responses against RNA viruses. *J Exp Med* 203: 1795-1803.

- Kumar H, Kawai T, Kato H, Sato S, Takahashi K, Coban C, Yamamoto M, Uematsu S, Ishii KJ, Takeuchi O, and Akira S. 107. Essential role of IPS-1 in innate immune responses against RNA viruses. *J. Exp Med* 203, 1795-1803. 2006.
- Kurt-Jones EA, et al. 2000. Pattern recognition receptors TLR4 and CD14 mediate response to respiratory syncytial virus. *Nat Immunol* 1: 398-401.
- Lamb RA, Pinto LH. 1997. Do Vpu and Vpr of human immunodeficiency virus type 1 and NB of influenza B virus have ion channel activities in the viral life cycles? *Virology* 229: 1-11.
- Latz E. 2010. The inflammasomes: mechanisms of activation and function. *Curr Opin Immunol* 22: 28-33.
- Lei Y, Moore CB, Liesman RM, O'Connor BP, Bergstralh DT, Chen ZJ, Pickles RJ, Ting JP. 2009. MAVS-mediated apoptosis and its inhibition by viral proteins. *PLoS One* 4: e5466.
- Lencer WI, Hirst TR, Holmes RK. 1999. Membrane traffic and the cellular uptake of cholera toxin. *Biochim Biophys Acta* 1450: 177-190.
- Leonov H, Astrahan P, Krugliak M, Arkin IT. 2011. How do aminoadamantanes block the influenza M2 channel, and how does resistance develop? *J Am Chem Soc* 133: 9903-9911.
- Li X, Ranjith-Kumar CT, Brooks MT, Dharmiah S, Herr AB, Kao C, Li P. 2009. The RIG-I-like receptor LGP2 recognizes the termini of double-stranded RNA. *J Biol Chem* 284: 13881-13891.
- Lippincott-Schwartz J, Yuan LC, Bonifacino JS, Klausner RD. 1989. Rapid redistribution of Golgi proteins into the ER in cells treated with brefeldin A: evidence for membrane cycling from Golgi to ER. *Cell* 56: 801-813.

- Liu P, Jamaluddin M, Li K, Garofalo RP, Casola A, Brasier AR. 2007. Retinoic acid-inducible gene I mediates early antiviral response and Toll-like receptor 3 expression in respiratory syncytial virus-infected airway epithelial cells. *J Virol* 81: 1401-1411.
- Loo YM, et al. 2008. Distinct RIG-I and MDA5 signaling by RNA viruses in innate immunity. *J Virol* 82: 335-345.
- Lund JM, Alexopoulou L, Sato A, Karow M, Adams NC, Gale NW, Iwasaki A, Flavell RA. 2004. Recognition of single-stranded RNA viruses by Toll-like receptor 7. *Proc Natl Acad Sci U S A* 101: 5598-5603.
- Madan V, Redondo N, Carrasco L. 2010. Cell permeabilization by poliovirus 2B viroporin triggers bystander permeabilization in neighbouring cells through a mechanism involving gap junctions. *Cell Microbiol* 12: 1144-1157.
- Malathi K, Dong B, Gale M, Jr., Silverman RH. 2007. Small self-RNA generated by RNase L amplifies antiviral innate immunity. *Nature* 448: 816-819.
- Mariathasan S, Newton K, Monack DM, Vucic D, French DM, Lee WP, Roose-Girma M, Erickson S, Dixit VM. 2004. Differential activation of the inflammasome by caspase-1 adaptors ASC and Ipaf. *Nature* 430: 213-218.
- Mariathasan S, Weiss DS, Newton K, McBride J, O'Rourke K, Roose-Girma M, Lee WP, Weinrauch Y, Monack DM, Dixit VM. 2006. Cryopyrin activates the inflammasome in response to toxins and ATP. *Nature* 440: 228-232.
- Martens JR, O'Connell K, Tamkun M. 2004. Targeting of ion channels to membrane microdomains: localization of KV channels to lipid rafts. *Trends Pharmacol Sci* 25: 16-21.
- Martinon F, Mayor A, Tschopp J. 2009. The inflammasomes: guardians of the body. *Annu Rev Immunol* 27: 229-265.



- Martinon F, Burns K, Tschopp J. 2002. The inflammasome: a molecular platform triggering activation of inflammatory caspases and processing of proIL-beta. *Mol Cell* 10: 417-426.
- Martinon F, Tschopp J. 2007. Inflammatory caspases and inflammasomes: master switches of inflammation. *Cell Death Differ* 14: 10-22.
- McCartney SA, Thackray LB, Gitlin L, Gilfillan S, Virgin HW, Colonna M. 2008. MDA-5 recognition of a murine norovirus. *PLoS Pathog* 4: e1000108.
- Megremis S, Demetriou P, Makrinioti H, Manoussaki AE, Papadopoulos NG. 2012. The genomic signature of human rhinoviruses A, B and C. *PLoS One* 7: e44557.
- Medzhitov R. 2007. Recognition of microorganisms and activation of the immune response. *Nature* 449: 819-826.
- Meissner F, Molawi K, Zychlinsky A. 2008. Superoxide dismutase 1 regulates caspase-1 and endotoxic shock. *Nat Immunol* 9: 866-872.
- Meylan E, Curran J, Hofmann K, Moradpour D, Binder M, Bartenschlager R, Tschopp J. 2005. Cardif is an adaptor protein in the RIG-I antiviral pathway and is targeted by hepatitis C virus. *Nature* 437: 1167-1172.
- Misumi Y, Misumi Y, Miki K, Takatsuki A, Tamura G, Ikehara Y. 1986. Novel blockade by brefeldin A of intracellular transport of secretory proteins in cultured rat hepatocytes. *J Biol Chem* 261: 11398-11403.

- Mittmann C, et al. 2002. Expression of ten RGS proteins in human myocardium: functional characterization of an upregulation of RGS4 in heart failure. *Cardiovasc Res* 55: 778-786.
- Munoz-Planillo R, Kuffa P, Martinez-Colon G, Smith BL, Rajendiran TM, Nunez G. 2013. K(+) efflux is the common trigger of NLRP3 inflammasome activation by bacterial toxins and particulate matter. *Immunity* 38: 1142-1153.
- Muir A, Soong G, Sokol S, Reddy B, Gomez MI, Van Heeckeren A, Prince A. 2004. Toll-like receptors in normal and cystic fibrosis airway epithelial cells. *Am J Respir Cell Mol Biol* 30: 777-783.
- Mukherjee A, Morosky SA, Shen L, Weber CR, Turner JR, Kim KS, Wang T, Coyne CB. 2009. Retinoic acid-induced gene-1 (RIG-I) associates with the actin cytoskeleton via caspase activation and recruitment domain-dependent interactions. *J Biol Chem* 284: 6486-6494.
- Nair CN, Panicali DL. 1976. Polyadenylate sequences of human rhinovirus and poliovirus RNA and cordycepin sensitivity of virus replication. *J Virol* 20: 170-176.
- Nieva JL, Madan V, Carrasco L. 2012. Viroporins: structure and biological functions. *Nat Rev Microbiol* 10: 563-574.
- O'Connor W, Jr., Harton JA, Zhu X, Linhoff MW, Ting JP. 2003. Cutting edge: CIAS1/cryopyrin/PYPAF1/NALP3/CATERPILLER 1.1 is an inducible inflammatory mediator with NF-kappa B suppressive properties. *J Immunol* 171: 6329-6333.

Oganesyan G, Saha SK, Guo B, He JQ, Shahangian A, Zarnegar B, Perry A, Cheng G. 2006. Critical role of TRAF3 in the Toll-like receptor-dependent and -independent antiviral response. *Nature* 439: 208-211.

- Peeples M, Levine S. 1979. Respiratory syncytial virus polypeptides: their location in the virion. *Virology* 95: 137-145.
- Pichlmair A, Schulz O, Tan CP, Näslund TI, Liljeström P, Weber F, and Reis e Sousa C. RIG-I-mediated antiviral responses to single-stranded RNA bearing 5'-phosphates. *Science* 314, 997-1001. 2007.
- Pichlmair A, Schulz O, Tan CP, Naslund TI, Liljestrom P, Weber F, Reis e Sousa C. 2006. RIG-I-mediated antiviral responses to single-stranded RNA bearing 5'-phosphates. *Science* 314: 997-1001.
- Pichlmair, A., Schulz, O., Tan, C. P, Rehwinkel, J., , Kato H., Takeuchi, O., Akira, S., Way, M., Schiavo, G., and Reis e Sousa C. Activation of MDA5 requires higher-order RNA structures generated during virus infection. *J.Virol* 83, 10761-10769. 2009.
- Pichlmair A, Schulz O, Tan CP, Naslund TI, Liljestrom P, Weber F, Reis e Sousa C. 2006. RIG-I-mediated antiviral responses to single-stranded RNA bearing 5'-phosphates. *Science* 314: 997-1001.
- Pinto LH, Holsinger LJ, Lamb RA. 1992. Influenza virus M2 protein has ion channel activity. *Cell* 69: 517-528.
- Pinto RA, Arredondo SM, Bono MR, Gaggero AA, Diaz PV. 2006. T helper 1/T helper 2 cytokine imbalance in respiratory syncytial virus infection is associated with increased endogenous plasma cortisol. *Pediatrics* 117: e878-886.

- Pippig DA, Hellmuth JC, Cui S, Kirchhofer A, Lammens K, Lammens A, Schmidt A, Rothenfusser S, Hopfner KP. 2009. The regulatory domain of the RIG-I family ATPase LGP2 senses double-stranded RNA. *Nucleic Acids Res* 37: 2014-2025.
- Poeck H, et al. 2010. Recognition of RNA virus by RIG-I results in activation of CARD9 and inflammasome signaling for interleukin 1 beta production. *Nat Immunol* 11: 63-69.
- Pringle CR, Shirodaria PV, Gimenez HB, Levine S. 1981. Antigen and polypeptide synthesis by temperature-sensitive mutants of respiratory syncytial virus. *J Gen Virol* 54: 173-183.
- Premkumar A, Wilson L, Ewart GD, Gage PW. 2004. Cation-selective ion channels formed by p7 of hepatitis C virus are blocked by hexamethylene amiloride. *FEBS Lett* 557: 99-103.
- Rajan JV, Rodriguez D, Miao EA, Aderem A. 2011. The NLRP3 inflammasome detects encephalomyocarditis virus and vesicular stomatitis virus infection. *J Virol* 85: 4167-4172.
- Rehwinkel J. 2010. Exposing viruses: RNA patterns sensed by RIG-I-like receptors. *J Clin Immunol* 30: 491-495.
- Rehwinkel J, Reis e Sousa C. 2010. RIGorous detection: exposing virus through RNA sensing. *Science* 327: 284-286.
- Reibman J, Hsu Y, Chen LC, Bleck B, Gordon T. 2003. Airway epithelial cells release MIP-3alpha/CCL20 in response to cytokines and ambient particulate matter. *Am J Respir Cell Mol Biol* 28: 648-654.

- Rixon HW, Brown G, Aitken J, McDonald T, Graham S, Sugrue RJ. 2004. The small hydrophobic (SH) protein accumulates within lipid-raft structures of the Golgi complex during respiratory syncytial virus infection. *J Gen Virol* 85: 1153-1165.
- Rixon HW, Brown G, Aitken J, McDonald T, Graham S, Sugrue RJ. 2004. The small hydrophobic (SH) protein accumulates within lipid-raft structures of the Golgi complex during respiratory syncytial virus infection. *J Gen Virol* 85: 1153-1165.
- Roche WR, Montefort S, Baker J, Holgate ST. 1993. Cell adhesion molecules and the bronchial epithelium. *Am Rev Respir Dis* 148: S79-82.
- Rohll JB, Percy N, Ley R, Evans DJ, Almond JW, Barclay WS. 1994. The 5'-untranslated regions of picornavirus RNAs contain independent functional domains essential for RNA replication and translation. *J Virol* 68: 4384-4391.
- Rothenfusser S, Goutagny N, DiPerna G, Gong M, Monks BG, Schoenemeyer A, Yamamoto M, Akira S, Fitzgerald KA. 2005. The RNA helicase Lgp2 inhibits TLR-independent sensing of viral replication by retinoic acid-inducible gene-I. *J Immunol* 175: 5260-5268.
- Saha SK, et al. 2006. Regulation of antiviral responses by a direct and specific interaction between TRAF3 and Cardif. *EMBO J* 25: 3257-3263.
- Saito T, Owen DM, Jiang F, Marcotrigiano J, Gale M, Jr. 2008. Innate immunity induced by composition-dependent RIG-I recognition of hepatitis C virus RNA. *Nature* 454: 523-527.
- Saito T, Hirai R, Loo YM, Owen D, Johnson CL, Sinha SC, Akira S, Fujita T, Gale M, Jr. 2007. Regulation of innate antiviral defenses through a shared repressor domain in RIG-I and LGP2. *Proc Natl Acad Sci U S A* 104: 582-587.

- Samji T. 2009. Influenza A: understanding the viral life cycle. *Yale J Biol Med* 82: 153-159.
- Satoh T, Kato H, Kumagai Y, Yoneyama M, Sato S, Matsushita K, Tsujimura T, Fujita T, Schlee M, Hartmann G. 2010. The chase for the RIG-I ligand--recent advances. *Mol Ther* 18: 1254-1262.
- Schmidt A, et al. 2009. 5'-triphosphate RNA requires base-paired structures to activate antiviral signaling via RIG-I. *Proc Natl Acad Sci U S A* 106: 12067-12072.
- Schroder K, Tschopp J. 2010. The inflammasomes. *Cell* 140: 821-832.
- Schwarze J, Mackenzie KJ. 2013. Republished: novel insights into immune and inflammatory responses to respiratory viruses. *Postgrad Med J* 89: 516-518.
- Seemungal T, et al. 2001. Respiratory viruses, symptoms, and inflammatory markers in acute exacerbations and stable chronic obstructive pulmonary disease. *Am J Respir Crit Care Med* 164: 1618-1623.
- Seth RB, Sun L, Ea CK, Chen ZJ. 2005. Identification and characterization of MAVS, a mitochondrial antiviral signaling protein that activates NF-kappaB and IRF 3. *Cell* 122: 669-682.
- Sha Q, Truong-Tran AQ, Plitt JR, Beck LA, Schleimer RP. 2004. Activation of airway epithelial cells by toll-like receptor agonists. *Am J Respir Cell Mol Biol* 31: 358-364.
- Sharma S, tenOever BR, Grandvaux N, Zhou GP, Lin R, Hiscott J. 2003. Triggering the interferon antiviral response through an IKK-related pathway. *Science* 300: 1148-1151.

- Shimazu R, Akashi S, Ogata H, Nagai Y, Fukudome K, Miyake K, Kimoto M. 1999. MD-2, a molecule that confers lipopolysaccharide responsiveness on Toll-like receptor 4. *J Exp Med* 189: 1777-1782.
- Stec DS, Hill MG, 3rd, Collins PL. 1991. Sequence analysis of the polymerase L gene of human respiratory syncytial virus and predicted phylogeny of nonsegmented negative-strand viruses. *Virology* 183: 273-287.
- Sun Q, Sun L, Liu HH, Chen X, Seth RB, Forman J, Chen ZJ. 2006. The specific and essential role of MAVS in antiviral innate immune responses. *Immunity* 24: 633-642.
- Sen, G.C. (2001). Viruses and interferons. *Annu. Rev. Microbiol.* 55, 255-281.
- Stark, G.R., Kerr, I.M., Williams, B.R., Silverman, R.H., and Schreiber, R.D. (1998). How cells respond to interferons. *Annu. Rev. Biochem.* 67, 227-264.
- Sakai A, Claire MS, Faulk K, Govindarajan S, Emerson SU, Purcell RH, Bukh J. 2003. The p7 polypeptide of hepatitis C virus is critical for infectivity and contains functionally important genotype-specific sequences. *Proc Natl Acad Sci U S A* 100: 11646-11651.
- Schmitz N, Kurrer M, Bachmann MF, Kopf M. 2005. Interleukin-1 is responsible for acute lung immunopathology but increases survival of respiratory influenza virus infection. *J Virol* 79: 6441-6448.
- Schroder K, Tschopp J. 2010. The inflammasomes. *Cell* 140: 821-832.
- Segovia J, Sabbah A, Mgbemena V, Tsai SY, Chang TH, Berton MT, Morris IR, Allen IC, Ting JP, Bose S. 2012. TLR2/MyD88/NF-kappaB pathway, reactive oxygen species, potassium efflux activates NLRP3/ASC inflammasome during respiratory syncytial virus infection. *PLoS One* 7: e29695.
- Simoes EA. 1999. Respiratory syncytial virus infection. *Lancet* 354: 847-852.

- Spyridon Megremis PD, Heidi Makrinioti, Alkistis E Manoussaki, Nikolaos G Papadopoulos. 2012. The Genomic Signature of Human Rhinoviruses A, B and C. *PLoS ONE* 13;7(9): e44557.
- Tabeta,K., Georgel,P., Janssen,E., Du,X., Hoebe,K., Crozat,K., Mudd,S., Shamel,L., Sovath,S., Goode,J., Alexopoulou,L., Flavell,R.A., and Beutler,B. (2004). Toll-like receptors 9 and 3 as essential components of innate immune defense against mouse cytomegalovirus infection. *Proc. Natl. Acad. Sc. USA* 101, 3516-3521.
- Takahasi K, Yoneyama M, Nishihori T, Hirai R, Kumeta H, Narita R, Gale M, Jr., Inagaki F, Fujita T. 2008. Nonsel self RNA-sensing mechanism of RIG-I helicase and activation of antiviral immune responses. *Mol Cell* 29: 428-440.
- Takahasi K, et al. 2009. Solution structures of cytosolic RNA sensor MDA5 and LGP2 C-terminal domains: identification of the RNA recognition loop in RIG-I-like receptors. *J Biol Chem* 284: 17465-17474.
- Takeda K, Akira S. 2004. TLR signaling pathways. *Semin Immunol* 16: 3-9.
- Takeuchi O, Akira S. 2007. Recognition of viruses by innate immunity. *Immunol Rev* 220: 214-224.
- Takeuchi O and Akira S. MDA5/RIG-I and virus recognition. *Curr Opin Immunol.* 20, 17-22. 2008.
- Takeuchi, O. and Akira, S. Innate immunity to virus infection. *Immunol Rev* 227, 75-86. 2009.
- Takeuchi,O., Hoshino,K., and Akira,S. (2000). TLR2-deficient and MyD88-deficient mice are highly susceptible to *Staphylococcus aureus* infection. *J Immunol* 165, 5392-5396.



- Tanji H, Ohto U, Shibata T, Miyake K, Shimizu T. 2013. Structural reorganization of the Toll-like receptor 8 dimer induced by agonistic ligands. *Science* 339: 1426-1429.
- Triantafilou K, Kar S, van Kuppeveld FJ, Triantafilou M. 2013a. Rhinovirus-Induced Calcium Flux Triggers NLRP3 and NLRC5 Activation in Bronchial Cells. *Am J Respir Cell Mol Biol*.
- Triantafilou K, Kar S, Vakakis E, Kotecha S, Triantafilou M. 2013b. Human respiratory syncytial virus viroporin SH: a viral recognition pathway used by the host to signal inflammasome activation. *Thorax* 68: 66-75.
- Triantafilou K, Kar S, van Kuppeveld FJ, Triantafilou M. 2013a. Rhinovirus-Induced Calcium Flux Triggers NLRP3 and NLRC5 Activation in Bronchial Cells. *Am J Respir Cell Mol Biol*.
- Triantafilou,K., Vakakis,E., Orthopoulos,G., Ahmed,M.A.E., Schumann,C., Lepper,P.M., and Triantafilou,M. (2005). TLR8 and TLR7 are involved in the host's immune response to Human Parechovirus 1. *Eur J Immunol* 35, 2416-2423.
- Triantafilou K, Triantafilou M. 2014. Ion flux in the lung: virus-induced inflammasome activation. *Trends Microbiol*.
- Triantafilou K, Kar S, van Kuppeveld FJ, Triantafilou M. 2013. Rhinovirus-Induced Calcium Flux Triggers NLRP3 and NLRC5 Activation in Bronchial Cells. *Am J Respir Cell Mol Biol* 49: 923-934.
- Tschopp J, Martinon F, Burns K. 2003. NALPs: a novel protein family involved in inflammation. *Nat Rev Mol Cell Biol* 4: 95-104.

- Techaarpornkul S, Barretto N, Peeples ME. 2001. Functional analysis of recombinant respiratory syncytial virus deletion mutants lacking the small hydrophobic and/or attachment glycoprotein gene. *J Virol* 75: 6825-6834.
- Thomas PG, et al. 2009. The intracellular sensor NLRP3 mediates key innate and healing responses to influenza A virus via the regulation of caspase-1. *Immunity* 30: 566-575.
- Uzri D, Gehrke L. 2009. Nucleotide sequences and modifications that determine RIG-I/RNA binding and signaling activities. *J Virol* 83: 4174-4184.
- van Kuppeveld FJ, Hoenderop JG, Smeets RL, Willems PH, Dijkman HB, Galama JM, Melchers WJ. 1997. Coxsackievirus protein 2B modifies endoplasmic reticulum membrane and plasma membrane permeability and facilitates virus release. *EMBO J* 16: 3519-3532.
- Vareille M, Kieninger E, Edwards MR, Regamey N. 2011. The airway epithelium: soldier in the fight against respiratory viruses. *Clin Microbiol Rev* 24: 210-229.
- Venkataraman T, Valdes M, Elsby R, Kakuta S, Caceres G, Saijo S, Iwakura Y, Barber GN. 2007. Loss of DExD/H box RNA helicase LGP2 manifests disparate antiviral responses. *J Immunol* 178: 6444-6455.
- von Itzstein M. 2007. The war against influenza: discovery and development of sialidase inhibitors. *Nat Rev Drug Discov* 6: 967-974.
- Voynow JA, Rubin BK. 2009. Mucins, mucus, and sputum. *Chest* 135: 505-512.
- Wang K, Xie S, Sun B. 2011. Viral proteins function as ion channels. *Biochim Biophys Acta* 1808: 510-515.

- Wang Q, et al. 2009. Role of double-stranded RNA pattern recognition receptors in rhinovirus-induced airway epithelial cell responses. *J Immunol* 183: 6989-6997.
- Wang, J. P, Cerny, A., Asher, D. R, Kurt-Jones, E. A, Bronson, R. T., and Finberg, R. W. MDA5 and MAVS mediate type I interferon responses to coxsackie B virus. *J.Virol* 84, 254-260. 2010.
- Wilkins C, Gale M, Jr. 2010. Recognition of viruses by cytoplasmic sensors. *Curr Opin Immunol* 22: 41-47.
- Wunner WH, Pringle CR. 1976. Respiratory syncytial virus proteins. *Virology* 73: 228-243.
- Xagorari A, Chlichlia K. 2008. Toll-like receptors and viruses: induction of innate antiviral immune responses. *Open Microbiol J* 2: 49-59.
- Xu LG, Wang YY, Han KJ, Li LY, Zhai Z, Shu HB. 2005. VISA is an adapter protein required for virus-triggered IFN-beta signaling. *Mol Cell* 19: 727-740.
- Yamamoto M, Akira S. 2004. [TIR domain--containing adaptors regulate TLR-mediated signaling pathways]. *Nihon Rinsho* 62: 2197-2203.
- Yamamoto M, Takeda K. 2010. Current views of toll-like receptor signaling pathways. *Gastroenterol Res Pract* 2010: 240365.
- Yao Y, Qian Y. 2013. Expression regulation and function of NLRC5. *Protein Cell* 4: 168-175.
- Yoneyama M, Fujita T. 2009. RNA recognition and signal transduction by RIG-I-like receptors. *Immunol Rev* 227: 54-65.
- Yoneyama,M., Kikuchi,M., Matsumoto,K., Imaizumi,T., Miyagishi,M., Taira,K., Foy,E., Loo,Y.M., Gale,M., Jr., Akira,S., Yonehara,S., Kato,A., and Fujita,T.

- (2005). Shared and unique functions of the DExD/H-box helicases RIG-I, MDA5, and LGP2 in antiviral innate immunity. *J Immunol* 175, 2851-2858.
- Yoneyama M, Kikuchi M, Natsukawa T, Shinobu N, Imaizumi T, Miyagishi M, Taira K, Akira S, Fujita T. 2004. The RNA helicase RIG-I has an essential function in double-stranded RNA-induced innate antiviral responses. *Nat Immunol* 5: 730-737.
  - Yoneyama M, et al. 2005. Shared and unique functions of the DExD/H-box helicases RIG-I, MDA5, and LGP2 in antiviral innate immunity. *J Immunol* 175: 2851-2858.
  - Zhao T, Yang L, Sun Q, Arguello M, Ballard DW, Hiscott J, Lin R. 2007. The NEMO adaptor bridges the nuclear factor-kappaB and interferon regulatory factor signaling pathways. *Nat Immunol* 8: 592-600.
  - Zhou R, Tardivel A, Thorens B, Choi I, Tschopp J. 2010. Thioredoxin-interacting protein links oxidative stress to inflammasome activation. *Nat Immunol* 11: 136-140.

## **WEB REFERENCES**

1. abcam. WESTERN BLOTTING - A BEGINNER'S GUIDE.  
<http://www.abcam.com/ps/pdf/protocols/WB-beginner.pdf> .
2. Campbell, M. A. Western Blot Procedure. Department of Biology, Davidson College.  
<http://www.bio.davidson.edu/courses/genomics/method/Westernblot.html> . 2001.

3. abcam. IMMUNOPRECIPITATION (IP) PROTOCOL.

[http://www.abcam.com/ps/pdf/protocols/Immunoprecipitation%20protocol%20\(IP\).pdf](http://www.abcam.com/ps/pdf/protocols/Immunoprecipitation%20protocol%20(IP).pdf)  
. 2011.

4 Thermo Scientific. Immunoprecipitation (IP).

<http://www.piercenet.com/browse.cfm?fldID=E5049863-D59D-B7A5-D057-E23F7B22AD44> . 2011. 20-2-2013

5. Cox,G. (2002) Biological Confocal Microscopy *Materials Today* **5**, 34-41.

6. Invitrogen. Introduction to Flow Cytometry.

[http://probes.invitrogen.com/resources/education/tutorials/4Intro\\_Flow/player.html](http://probes.invitrogen.com/resources/education/tutorials/4Intro_Flow/player.html) . 8-8-2011. 16-3-2013.

7. Caprette, D. R. Introduction to SDS-PAGE. Department of Biochemistry and Cell Biology, Rice University. <http://www.ruf.rice.edu/~bioslabs/studies/sds-page/gellab2.html> . 2011. 16-4-2013.

8.Campbell, M. A. SDS-PAGE (PolyAcrylamide Gel Electrophoresis). Department of Biology, Davidson College.

<http://www.bio.davidson.edu/courses/genomics/method/SDSPAGE/SDSPAGE.html> . 2001. 02-2-2013.

9. Protocol Online. Flow Cytometry (FCM). [http://www.protocol-online.org/prot/Cell\\_Biology/Flow\\_Cytometry\\_\\_FCM\\_/index.html](http://www.protocol-online.org/prot/Cell_Biology/Flow_Cytometry__FCM_/index.html) . 30-7-2011. 22-3-2013

10. Flow Cytometry Facility, UC Berkeley. Introduction.

[http://biology.berkeley.edu/crl/flow\\_cytometry\\_basic.html](http://biology.berkeley.edu/crl/flow_cytometry_basic.html) . 2011. 22-3-2013

